

**MOLECULAR CONTROL OF
THE DIFFERENTIATION-
MITOSIS CHECKPOINT OF
KERATINOCYTES IN
RESPONSE TO DNA DAMAGE.**



IDIVAL

Instituto de Investigación Sanitaria de Valdecilla
Laboratorio Ciclo Celular, Células Madre y
Cáncer

UNIVERSIDAD DE CANTABRIA

Facultad de Medicina
Departamento de Biología Molecular

Rut Molinuevo Llaría

Memoria presentada para la obtención del grado de doctor.

Santander, 2018

**REGULACIÓN MOLECULAR
DEL PUNTO DE CONTROL
EPIDÉRMICO MITOSIS-
DIFERENCIACIÓN EN
RESPUESTA AL DAÑO EN EL
ADN.**



IDIVAL

**Instituto de Investigación Sanitaria de Valdecilla
Laboratorio Ciclo Celular, Células Madre y
Cáncer**

UNIVERSIDAD DE CANTABRIA

**Facultad de Medicina
Departamento de Biología Molecular**

Rut Molinuevo Llaría

Memoria presentada para la obtención del grado de doctor.

Santander, 2018

El Dr. Albero Gandarillas Solinís, investigador principal del grupo Ciclo Celular, Células Madre y Cáncer del Instituto de Investigación Sanitaria de Valdecilla.

CERTIFICA:

Que la licenciada Rut Molinuevo Llaría ha realizado bajo su dirección el presente trabajo de Tesis Doctoral titulado:

Molecular control of the differentiation-mitosis checkpoint of epidermal keratinocytes in response to DNA damage.

Regulación molecular del punto de control epidérmico mitosis-diferenciación en respuesta al daño en el ADN.

Que considera que este trabajo reúne los requisitos de originalidad y calidad científica necesarios para su presentación como Memoria de Doctorado por el interesado, al objeto de poder optar al grado de Doctor por la Universidad de Cantabria.

Y para que conste y surta los efectos oportunos, firma el presente certificado.

Santander, Marzo 2018.

Fdo. Alberto Gandarillas

Esta Tesis ha sido financiada con las siguientes ayudas:

This Thesis has been founded by:

- The Cell Cycle, Stem Cell Fate and Cancer Laboratory and Instituto de Salud Carlos III-FIS/CIBER (PI14/09000).
- The Department of Dermatology, University of Michigan.
- EMBO short-term fellowship (ASTF 226-2016).

A mis padres.

*La vida cobra sentido cuando se hace de ella una aspiración a no
renunciar a nada.*

José Ortega y Gasset (1883-1995)

*The greater the circle of light, the greater the boundary of darkness by
which it is surrounded.*

Humphry Davy (1778-1829)

AGRADECIMIENTOS

En primer lugar, agradezco al doctor Alberto Gandarillas la oportunidad de trabajar con él. Soy de la opinión de que una gran parte del éxito depende de estar en el momento y en el lugar adecuado. Creo que eso es lo que me ocurrió cuando llegué a Santander. Alberto me permitió desde el principio ser parte activa del día a día del laboratorio, y sumergirme rápidamente en el mundo de la investigación. Gracias por eso, Alberto. Aprendí más durante las prácticas de máster contigo que en 4 años de carrera. La otra parte del éxito depende, sin duda, del trabajo. Gracias también Alberto por motivarme a no conformarme. Gracias por enseñarme siempre intentando promover mi pensamiento crítico. Por tu apoyo y tus consejos. Incluso en los momentos en los que tuvimos diferentes opiniones, he aprendido. Gracias.

En segundo lugar, tengo que agradecer a mis compañeras de laboratorio. Gracias a Laura Ceballos, por su apoyo técnico y por su disponibilidad para echar una mano siempre que me hacía falta. Gracias Laura. A Pilar Molinedo, porque aunque no fueras miembro oficial del laboratorio, llegaste a serlo. Gracias Pilar. A Ana Freije, gracias por enseñarme todo casi desde cero. Sin duda, esta tesis hubiese sido muchísimo más difícil sin ti. Gracias Ana por tu paciencia, por tus tirones de oreja que me ayudaron a adquirir sentido de la responsabilidad, por los consejos, por las risas, las confianzas, el apoyo, el cariño... Siento que no tendría páginas para terminar de agradecerte. A Isabel de Pedro, gracias. Porque para mí hubo un antes y un después cuando llegaste al laboratorio. A Natalia Sanz, porque eras la que faltaba. Gracias Natalia. Ana, Isa, Natalia, más que compañeras sois amigas. Lo mejor de estos años ha sido compartirlos con vosotras. Os quiero.

I would also like to thank my supervisor Professor JT Elder during my placement at Ann Arbor. Thank you JT for your guidance and patience, I am tremendously grateful for the opportunity I had in your lab. Finally, thanks to my mates there in Ann Arbor. You all truly made me feel at home. To Alex Tsoi, for your technical support. To Stefan Stoll and Sylviane Lambert for your support on the professional and personal side during those months. To Zhaolin, for your smile every single morning. To Nancy Vanderkuyl, for your welcoming and your help. Without that, my placement in Ann Arbor would have been much harder. Thank you all.

Tengo que agradecer también a toda esa gente que me ha acompañado durante estos años. A mi familia en Ann Arbor: Germán, María, Carlos y Juan. Gracias por acogerme tan bien desde el principio. Mención especial al núcleo duro: Juan y Carlos, gracias por todas las fiestas, los viajes, las charlas, las cervezas... A Isa e Itziar, corto pero intenso. A Carlos, otra vez: *the best is yet to come*. A Mirari, por todos los vinos y tés que te has tomado aguantándome. Gracias. A mis amigas Laura y Bea, y a mi prima Eva, por los fines de semana de fiesta después de estar toda la semana trabajando. Gracias chicas. Así era más fácil volver los lunes al laboratorio. A Ángel, gracias por todos los viajes de ida y de vuelta. Por respetar y apoyar todas mis decisiones, aunque no fuesen lo que tú querías. Gracias, contigo todo ha sido más fácil.

Por último, a mi familia. Sé que soy afortunada de teneros a todos conmigo. A mi abuelo Alejandro, porque estaría orgulloso. A mis padres, Jesús y Raquel, y a mi hermano Borja. Gracias por vuestro apoyo y amor incondicional, ahora y siempre. Sé que no he sido fácil. Sin vosotros no lo hubiese conseguido y la verdad es que esta tesis es también vuestra. Os quiero.

Table of Contents

List of Figures and Tables	i
List of Acronyms	v
PUBLICATIONS	vii
RESUMEN	1
PAPEL DE p53 EN EL PUNTO DE CONTROL DE MITOSIS- DIFERENCIACIÓN DE QUERATINOCITOS HUMANOS.....	3
EL EQUILIBRIO ENTRE PROLIFERACIÓN Y DIFERENCIACIÓN EN LA EPIDERMIS PUEDE DEPENDER DEL PUNTO DE CONTROL MITOSIS-DIFERENCIACIÓN.....	6
IMPLICACIONES DEL PUNTO DE CONTROL MITOSIS- DIFERENCIACIÓN EN LA CARCINOGENESIS EPIDÉRMICA.....	9
PAPEL DEL DAÑO EN EL ADN EN EL PROGRAMA NATURAL DE DIFERENCIACIÓN DE LOS QUERATINOCITOS EPIDÉRMICOS.....	10
CONCLUSIONES	16
INTRODUCTION	18
HOMEOSTASIS CONTROL IN DEVELOPING TISSUES.....	21
THE CELL CYCLE	23
1. Phases of the cell cycle.....	23
1.1. Molecular regulation of the cell cycle.....	25
2. The mitosis master gene FOXM1.....	29
2.1. FOXM1 target genes.....	30
2.2. FOXM1 regulation during the cell cycle.....	32
THE DNA DAMAGE RESPONSE.....	35
3. Sources of DNA damage.....	35
4. The cell cycle checkpoints.....	37
4.1. The intra-S checkpoint.....	38
4.2. The G1 and G2 checkpoints.....	39
4.3. The spindle assembly checkpoint.....	40
5. The DNA damage repair pathways.....	41

5.1.	Excision-based repair pathways.	42
5.2.	DSB repair pathways.	43
5.3.	DNA-PK regulates NHEJ repair.	44
5.4.	ATM activates the cellular response to DSBs.	45
5.5.	ATR coordinates the DDR to replication stress.....	46
6.	Chromatin based DDR- signaling.	47
7.	DDR and cell fate.	49
EPIDERMIS AS AN ADULT DEVELOPING TISSUE.....		53
8.	Structure and function of the skin.....	53
9.	Structure of the epidermis.	54
9.1.	Basal keratinocytes.....	55
9.2.	The differentiation program of keratinocytes.	56
10.	The epidermis: an endoreplicative tissue.	57
10.1.	The differentiation-mitosis checkpoint.	59
OBJECTIVES		63
MATERIALS & METHODS		67
1.	Cell cultures.....	67
1.1.	Primary cell culture	67
1.2.	Cell lines.	68
2.	Treatment with chemical inhibitors.	69
3.	Cell infections.	69
3.1.	Retroviral infections.	69
3.2.	Lentiviral infections.	70
4.	Clonogenicity assays.	71
5.	Flow cytometry.....	72
5.1.	DNA content.....	72
5.2.	DNA synthesis.	72
5.3.	Protein expression.	73
6.	Immunofluorescence.....	74
6.1.	Immunofluorescence on cultured cells.....	74
6.2.	Immunofluorescence on frozen tissue.	74
6.3.	Immunofluorescence on paraffin-embedded tissue.....	76

6.4. Run-on transcription assay.....	77
7. Protein analysis by Western Blotting.....	78
8. mRNA analysis by Quantitative Real-Time PCR (Q-RT-PCR) ...	80
9. Comet assay.....	81
10. Transcriptome analysis	82
RESULTS.....	85
ROLE OF p53 IN THE DIFFERENTIATION-MITOSIS CHECKPOINT OF HUMAN KERATINOCYTES.....	87
1. Inactivation of a temperature-sensitive p53 mutant protein promotes differentiation, whereas its inactivation attenuates it.....	87
2. The differentiation response induced by loss of p53 is unaffected by ectopic AREG expression.....	91
ROLE OF FOXM1 OVEREXPRESSION IN THE DIFFERENTIATION-MITOSIS CHECKPOINT OF HUMAN KERATINOCYTES.....	95
3. FOXM1 rescues the proliferative block and attenuates the squamous differentiation response caused by inactivation of p53.....	95
4. FOXM1 allows keratinocytes to proliferate in spite of genomic instability.....	101
5. Overexpression of FOXM1 drives MYC-induced differentiation into proliferation.....	107
CHARACTERIZATION OF THE DIFFERENTIATION-MITOSIS CHECKPOINT IN IMMORTALIZED NTERT KERATINOCYTES.....	111
6. The immortalized cell line NTERT presents defects in the differentiation-mitosis checkpoint.....	111
DNA DAMAGE AS PART OF THE NATURAL SQUAMOUS DIFFERENTIATION PROGRAM OF KERATINOCYTES.....	119
7. DNA damage signaling is detected in normal keratinocytes.....	119
8. ATR signaling activates the squamous differentiation program of primary keratinocytes.....	122
9. ATR inactivation leads to DNA damage accumulation and differentiation.....	126
10. Inhibition of the DDR impairs terminal differentiation of keratinocytes.....	128
11. Inhibition of the γ H2AX signal impairs squamous differentiation and induces an epidermal to mesenchymal transition.	135

12.	DNA damage signaling is detected in the epidermis <i>in situ</i>	140
	SEARCH FOR NOVEL MOLECULES POTENTIALLY INVOLVED IN THE DIFFERENTIATION RESPONSE TO DNA DAMAGE..	143
13.	Transcriptome analyses reveal a list of genes potentially involved in the activation of the differentiation-mitosis checkpoint of keratinocytes.....	145
	DISCUSSION	153
	p53 PLAYS A DUAL ROLE IN EPIDERMAL HOMEOSTASIS.....	155
	A DIFFERENTIATION-MITOSIS CHECKPOINT MIGHT MAINTAIN THE BALANCE BETWEEN PROLIFERATION AND DIFFERENTIATION OF EPIDERMAL KERATINOCYTES.	157
	IMPLICATIONS OF THE DIFFERENTIATION-MITOSIS CHECKPOINT INTO EPIDERMAL CARCINOGENESIS.....	159
	DNA DAMAGE AS PART OF THE NATURAL DIFFERENTIATION PROGRAM OF EPIDERMAL KERATINOCYTES.....	163
	THE DNA DAMAGE-INDUCED DIFFERENTIATION RESPONSE AS AN AUTOMATIC CELL-AUTONOMOUS LIMIT TO PROLIFERATION IN MORPHOGENESIS.	165
	CONCLUSIONS.....	169
	REFERENCES.....	173
	ANNEX.....	199

List of Figures and Tables

INTRODUCTION

Figure 1 | Phases of the cell cycle.

Figure 2 | Regulation of the cell cycle by cyclin/Cdk complexes.

Figure 3 | Regulation of cyclin/Cdk complexes.

Figure 4 | FOXM1 regulates the transcription of genes involved in mitosis progression.

Figure 5 | Repression of origin firing by the intra-S checkpoint.

Figure 6 | Activation of the G1 and G2 checkpoints in response to DNA damage.

Figure 7 | The spindle assembly checkpoint (SAC) prevents aberrant chromosome segregation.

Figure 8 | DNA-PK promotes DNA repair via NHEJ.

Figure 9 | Activation of ATM and ATR in response to DNA damage.

Figure 10 | γ H2AX promotes DNA damage signal amplification.

Figure 11 | Structure of the epidermis.

Figure 12 | A prolonged mitotic arrest activates the differentiation-mitosis checkpoint (DMC) and triggers terminal differentiation.

MATERIALS & METHODS

Table I | Chemical inhibitors and used concentrations.

Table II | Primary antibodies.

Table III | Secondary antibodies.

RESULTS

Figure 13 | p53 is efficiently overexpressed and inactivated in primary keratinocytes at 39°C.

Figure 14 | Inactivation of p53 induces terminal differentiation of primary keratinocytes.

Figure 15 | Inactivation of p53 irreversibly inhibits the colony forming potential of primary keratinocytes.

Figure 16 | AREG silencing induces terminal differentiation of primary keratinocytes.

Figure 17 | AREG does not inhibit the DMC in the absence of p53.

Figure 18 | Inhibition of p53 and overexpression of FOXM1 in primary keratinocytes.

Figure 19 | FOXM1 rescues the proliferative capacity of human epidermal keratinocytes lacking p53.

Figure 20 | FOXM1 inhibits the expression of differentiation markers induced by p53 loss.

- Figure 21 | FOXM1 inhibits the differentiation response to p53 loss.
- Figure 22 | FOXM1 inhibits cell shedding in the absence of p53.
- Figure 23 | FOXM1 is expressed in mitotic keratinocytes in the epidermis.
- Figure 24 | FOXM1 suppresses the mitotic block caused by loss of p53 in primary keratinocytes.
- Figure 25 | FOXM1 might play a role in global transcription regulation.
- Figure 26 | Keratinocytes overexpressing FOXM1 displayed a lower optical density.
- Figure 27 | FOXM1 allows accumulation of DNA damage in proliferative keratinocytes upon p53 inactivation.
- Figure 28 | FOXM1 increases the proliferative capacity of MYCER keratinocytes and inhibits squamous differentiation.
- Figure 29 | FOXM1 alleviates the mitotic arrest induced by MYC.
- Figure 30 | FOXM1 allows MYC overexpressing keratinocytes to proliferate in spite of genomic instability.
- Figure 31 | NTERT increase cell size and become polyploid in response to Nocodazol.
- Figure 32 | NTERT continue proliferating after Nocodazol treatment.
- Figure 33 | Proliferating NTERT-R1 undergo morphological changes.
- Figure 34 | NTERT-R1 proliferate in spite of becoming polyploid.
- Figure 35 | Inhibition of Aurora B or Polo-like kinases induce morphological changes in NTERT.
- Figure 36 | Inhibition of anaphase progression induces terminal differentiation of NTERT.
- Figure 37 | DNA damage signaling is detected in primary keratinocytes *in vitro*.
- Figure 38 | The DDR is active in primary keratinocytes *in vitro*.
- Figure 39 | TopBPER translocates to the nucleus in response to OHT.
- Figure 40 | TopBPER nuclear translocation increases γ H2AX signal.
- Figure 41 | TopBPER activates ATR in the absence of DNA damage.
- Figure 42 | ATR promotes squamous differentiation in primary keratinocytes.
- Figure 43 | shATR induces the accumulation of γ H2AX.
- Figure 44 | shATR triggers squamous differentiation of primary keratinocytes
- Figure 45 | ATM or DNA-PK inhibition does not affect the differentiation response of primary keratinocytes.
- Figure 46 | ATR inhibition drastically induces H2AX phosphorylation.
- Figure 47 | Effect of ATR, ATM and DNA-PK inhibition in the DNA damage response.
- Figure 48 | Inhibition of the DNA damage response impairs the squamous differentiation program.

Figure 49 | Inhibition of ATR, ATM and DNA-PK impairs DDR in the presence of increased DNA damage.

Figure 50 | Inhibition of H2AX expression in primary keratinocytes.

Figure 51 | shH2AX induces DNA damage.

Figure 52 | shH2AX impairs the differentiation response of keratinocytes.

Figure 53 | shH2AX inhibits the squamous phenotype.

Figure 54 | shH2AX induces an epithelia to mesenchyma transition.

Figure 55 | DNA damage signaling is detected in the epidermis *in situ*.

Figure 56 | Identification of differentially expressed genes.

Figure 57 | GO enrichment analysis of DEGs identified after p53 silencing.

Figure 58 | GO enrichment analysis of DEGs identified after Polo-like kinase inhibition.

Figure 59 | GO enrichment analysis of DEGs identified after DOXO treatment.

Figure 60 | GO enrichment analysis of DEGs identified after Aurora B inhibition.

Figure 61 | GO enrichment analysis of common DEGs.

DISCUSSION

Figure 62 | Model for the role of p53 in proliferation and differentiation of human epidermal keratinocytes.

Figure 63 | Model of the action of mitotic FOXM1 in p53- or MYC- mutant keratinocytes.

Figure 64 | Model for the role of the DDR in the natural differentiation program of epidermal keratinocytes.

Figure 65 | The DNA damage differentiation response (DDDR) might link proliferation with differentiation in endoreplicating tissues.

List of Acronyms

5'-Fu	5'-fluorouridine
53BP1	p53-binding protein 1
9-1-1 complex	Rad9-Hus1-Rad1 complex
AP	Apurinic/apyrimidinic abasic sites
APC	Anaphase promoting complex
AREG	Amphiregulin
ARF	Alternative reading frame
ATM	Ataxia-Telangiectasia mutated kinase
ATMi	ATM inhibitor
ATR	ATM and Rad3 related kinase
ATRi	ATR inhibitor
ATRIP	ATR interaction protein
AurB	Aurora B kinase
BCC	Basal cell carcinoma
BER	Base excision repair
BM	Basement membrane
BRCA	Breast cancer protein
BrdU	Bromodesoxyuridine
BUB3	Mitotic checkpoint protein BUB3
Cdk	Cyclin-dependent kinase
cDNA	Complementary DNA
Cenp	Centromere protein
CKI	Cdk inhibitor
CPD	Cyclobutane pyrimidine dimmers
CtIP	C-terminal binding protein 1 (CtBP1) interacting protein

DDB	DNA damage binding protein
DDR	DNA damage response
DMC	Differentiation-Mitosis Checkpoint
DNA	Deoxyribonucleic acid
DNA-PK	DNA-protein kinase complex
DNA-PKi	DNA-PK inhibitor
dNTP	Deoxynucleotide
DOXO	Doxorubicin
DSB	Double strand break
EDTA	Ethylenediaminetetraacetic acid
EGF	Epidermal growth factor
EGFP	Epidermal growth factor protein
EMT	Ephitelia to mesenchyma transition
ETAA1	Ewings tumor-associated antigen 1
ETOH	Ethanol
FACS	Fluorescence-activated cell sorting
FBS	Fetal bovin serum
FEN1	Flap 1 endonuclease
FHO	Formaldehyde
FOXM1	Forkhead box protein M1
H2AX	Histone H2A variant X
HR	Homologous recombination
IDL	Insertion-deletion loop
IF	Immunofluorescence
IgG	Immunoglobulin
IR	Ionizing radiation
IRIF	Ionizing radiation induced foci

K1	Keratin 1
K10	Keratin 10
K14	Keratin 14
K16	Keratin 16
K5	Keratin 5
K8	Keratin 8
LMA	Low-melting agarose
MCC	Mitotic checkpoint complex
MDC	Mediator of DNA damage checkpoint
MDM2	Mouse double minute 2 homolog
MeOH	Methanol
MLH	Mul homolog
MMR	Mismatch repair
MRN	MRE11, RAD50 and NBS1 complex
mRNA	Messenger RNA
MSH	Mus homolog
NB	Nuclear body
NER	Nucleotide excision repair
NHEJ	Non-homologous end joining
NOCO	Nocodazol
OHT	4-hydroxytamoxifen
OID	Oncogen-induced differentiation
PBS	Phosphate-buffered saline
PCNA	Proliferating cell nuclear antigen
PDDF	Persistent DNA damage foci
PFA	Paraformaldehyde
PI	Propidium iodide

PI3K	Phosphoinositol 3-kinase
Plk	Polo-like kinase
PURO	Puromycin
Rb	Retinoblastoma protein
RNA	Ribonucleic acid
RNA-seq	RNA sequencing
RNS	Reactive nitrogen specie
ROS	Reactive oxygen specie
RPA	Replication protein A
RS	Replication stress
RT-PCR	Real-time PCR
SAC	Spindle assembly checkpoint
SC	Stem cell
SCC12F	Squamous cell carcinoma cell line 12F
SCF	Skp/Cullin-1/F-box complex
SDS	Sodium dodecyl sulphate
shRNA	Short hairpin RNA
SSB	Single strand break
TAC	Transient amplifying cell
TAD	Trans-activating domain
TBE	Tris-borate-EDTA
TC-NER	Transcription-coupled NER
TET	Tetracyclin
TopBP1	Topoisomerase binding protein 1
Tris	Tris (hydroxymethyl) aminomethane
TTBS	Tween tris-buffered saline
UV	Ultraviolet

WB	Western blot
XLF	XRCC4-like factor
XP	Xeroderma pigmentosum
XRCC4/LigIV	DNA repair protein XRCC4/Ligase IV complex
γH2AX	Phosphorylated H2AX

PUBLICATIONS

The results obtained from this Thesis have been published as follows:

Los resultados obtenidos de esta Tesis han sido publicados como se indica:

- FREIJE, A., MOLINUEVO, R., CEBALLOS, L., CAGIGAS, M., ALONSO-LECUE, P., RODRIGUEZ, R., MENENDEZ, P., ABERDAM, D., DE DIEGO, E. & GANDARILLAS, A. 2014. Inactivation of p53 in Human Keratinocytes Leads to Squamous Differentiation and Shedding via Replication Stress and Mitotic Slippage. *Cell Rep*, 9, 1349-60.
- MOLINUEVO, R., FREIJE, A., DE PEDRO, I., STOLL, S. W., ELDER, J. T. & GANDARILLAS, A. 2017. FOXM1 allows human keratinocytes to bypass the oncogene-induced differentiation checkpoint in response to gain of MYC or loss of p53. *Oncogene*, 36,956-965.

RESUMEN

Durante la expansión y la regeneración de un tejido en desarrollo tiene lugar una fase de rápida multiplicación celular (Slack, 2013). Llegado el momento, ésta debe cesar para evitar una proliferación descontrolada que pueda poner en peligro la integridad y homeostasis del tejido. La apoptosis, senescencia o diferenciación terminal son procesos que limitan la proliferación. La entrada en senescencia, aunque está implicada en la remodelación de tejidos durante el desarrollo (Muñoz-Espin et al., 2013; Storer et al., 2013), se encuentra asociada con algunos efectos perjudiciales como el fomento de desarrollo de tumores y fenotipos degenerativos relacionados con el envejecimiento (Krtolica et al., 2001; Liu y Hornsby, 2007; Baker, et al., 2011; Perrigue et al., 2015). Por otro lado, la apoptosis permite la eliminación física de poblaciones de células durante el desarrollo (Glucksmann, 1965; Chen y Zhao, 1998; Pampfer y Donnay, 1999). En algunos tejidos en desarrollo autorrenovables, como la epidermis, la proliferación celular se controla mediante la diferenciación terminal. La diferenciación es el proceso por el cual una célula madre pierde la capacidad de dividirse y se convierte en un tipo celular más especializado, mediante modificaciones de la expresión génica altamente controladas (Slack, 2013). A pesar de su relevancia en la homeostasis de tejidos que se expanden para desarrollar una función específica, los mecanismos moleculares que coordinan la proliferación y la diferenciación son todavía poco conocidos. En esta Tesis se han estudiado estos mecanismos de regulación tomando como modelo de tejido autorrenovable la epidermis.

La epidermis es un epitelio estratificado escamoso que presenta una alta capacidad de auto-regeneración durante toda la vida de los individuos (OpenStax, 2016). Compone la capa mas externa de la piel y su

unidad celular básica es el queratinocito. Los queratinocitos proliferan adheridos a la membrana basal en la capa más interna de la epidermis, conocida como capa basal. Tras una fase inicial de rápida expansión clonal, los queratinocitos pierden adhesión a la membrana basal y comienzan el proceso de diferenciación terminal a la vez que migran por las diferentes capas de la epidermis, hasta que finalmente son eliminados por descamación (Watt, 2014). El proceso de diferenciación está precedido de un bloqueo mitótico que se vuelve irreversible e impide que los queratinocitos continúen dividiéndose (Gandarillas y Freije, 2014). Los queratinocitos en diferenciación son incapaces de mantener el bloqueo mitótico de manera efectiva y llevan a cabo varias rondas de replicación del ADN en ausencia de división celular, proceso conocido como endoreplicación. De esta manera, los queratinocitos se vuelven poliploides durante el proceso de diferenciación (Zanet et al., 2010). Nuestro laboratorio ha demostrado que la desregulación del ciclo celular por alteraciones oncogénicas induce un bloqueo mitótico y la diferenciación escamosa (Freije et al., 2012; Freije et al., 2014). Esta observación sugiere que los queratinocitos presentan un punto de control de mitosis-diferenciación (DMC, del inglés *differentiation-mitosis checkpoint*) que protege a la epidermis de alteraciones oncogénicas. Dada la importancia del DMC en la homeostasis epidérmica, en esta Tesis se han estudiado los procesos moleculares implicados. Se ha analizado con especial atención el papel del daño en el ADN y de su señalización en el proceso de diferenciación natural de la epidermis.

PAPEL DE p53 EN EL PUNTO DE CONTROL DE MITOSIS-DIFERENCIACIÓN DE QUERATINOCITOS HUMANOS.

Con el objetivo de dilucidar los mecanismos implicados en la activación del DMC en queratinocitos humanos epidérmicos decidimos estudiar el papel de p53, una proteína supresora de tumores. Los resultados derivados de este estudio se publicaron en *Cell Reports* en 2017 (Freije et al., 2014). p53 es un factor de transcripción con un importante papel en la regulación del ciclo celular (Lane, 1992). p53 responde al daño en el ADN con la activación de los puntos de control del ciclo celular mediante sus dianas transcripcionales (Giono y Manfredi, 2006). También es capaz de inducir la apoptosis cuando el daño en el ADN no puede ser reparado (Canman et al., 1994). Por estas razones, hipotetizamos que p53 podría estar mediando la respuesta de diferenciación de los queratinocitos. Para estudiar esta hipótesis, decidimos introducir en queratinocitos primarios una construcción retroviral que sobre-expresaba una proteína p53 mutante termo-sensible (p53ts). Esta proteína presenta su forma activa cuando las células son cultivadas a 32°C, pero se inactiva mediante un cambio conformacional a 39°C, comportándose como un mutante dominante negativo (Michalovitz et al., 1990). Para introducir esta construcción en queratinocitos primarios, estos fueron cultivados con el sobrenadante de células AM12productoras de retrovirus. Este método se utilizó para todas las infecciones retrovirales realizadas en esta Tesis.

La proteína exógena p53ts fue eficazmente expresada por los queratinocitos, como se detectó mediante inmunofluorescencia (IF) y western blot (WB). p53ts a 39°C no era capaz de inducir su diana transcripcional p21^{Cip}, ni siquiera en respuesta al daño en el ADN producido por Doxorubicina (DOXO). Además la p53ts se acumulaba a esta temperatura, como sucede con la proteína mutante inactiva pues deja de ser degradada (Lane, 1992).

Estos resultados confirmaron la inactivación de la proteína exógena a 39°C. Mediante citometría de flujo se observó que a 32°C en los cultivos que expresaban p53ts se reducía el porcentaje de células con alto tamaño y complejidad. Se sabe que estos parámetros aumentan en queratinocitos durante la diferenciación (Jones y Watt, 1993). También se observó una reducción en la expresión de los marcadores de diferenciación Involucrina y queratina K16 (K16). Por el contrario, la inactivación de p53ts a 39°C, aumentaba el porcentaje de células en diferenciación. Los resultados mostraban que la inactivación de p53 inducía diferenciación mientras que su activación la inhibía. Además, observamos que tras el tratamiento a 39°C durante 5 días disminuía la capacidad clonogénica de los queratinocitos, incluso cuando eran relanzados a las condiciones óptimas de cultivo a 37°C, confirmando que la inducción de diferenciación era irreversible. Estos resultados eran opuestos a lo esperado y mostraban un papel para p53 protector de la capacidad proliferativa de los queratinocitos.

AREG es una proteína de la familia del factor de crecimiento epidérmico EGF. Se ha demostrado que su inhibición activa la diferenciación terminal a través de un bloqueo mitótico (Stoll et al., 2016). Se sabe que AREG se activa transcripcionalmente por p53 en respuesta al daño en el ADN (Taira et al., 2014). Por esta razón decidimos analizar si la sobreexpresión de AREG inhibía la respuesta de diferenciación inducida por la pérdida de p53. Con este objetivo, infectamos queratinocitos primarios con una construcción lentiviral que sobreexpresa AREG o el correspondiente vector vacío. A continuación, los queratinocitos se infectaron con una construcción lentiviral que expresa un *short-hairpin* ARN (del inglés, shRNA) contra p53 (shp53) o su correspondiente vector vacío. Para ello, se utilizó el sobrenadante de células productoras de lentivirus 293T. Este método se utilizó en todas las infecciones lentivirales descritas en esta Tesis. La sobreexpresión de AREG no fue capaz de rescatar el potencial proliferativo de los queratinocitos

perdido por la inhibición de p53. De hecho, mediante PCR cuantitativa (Q-RT-PCR) y citometría de flujo se detectó un aumento del marcador de diferenciación queratina K1. Concluimos que AREG no inhibía la diferenciación inducida por la inhibición de p53.

En conjunto, nuestros resultados sugieren que el papel de p53 en queratinocitos humanos consiste en proteger el potencial proliferativo de estas células. En este sentido, se sabe que la expresión de p53 se pierde al inicio de la diferenciación (Dazard et al., 2000) y que su sobreexpresión inhibe la de marcadores de diferenciación en cultivos organotípicos (Woodworth et al., 1993). Además, los resultados demuestran que la pérdida de p53 induce el programa de diferenciación de los queratinocitos y que esta proteína no es necesaria para la activación del DMC. De hecho, la pérdida de p53 acelera el proceso de diferenciación inducido por la sobreexpresión de MYC (Freije, et al., 2014), sugiriendo que ambas funciones son opuestas. p53 también es capaz de inducir apoptosis en queratinocitos tras la exposición a la luz ultravioleta (Ziegler et al., 1994). Estas observaciones sugieren que p53 tiene un papel dual en el mantenimiento de la epidermis. Por un lado, protegería el potencial proliferativo de las células madre al favorecer la reparación del daño en el ADN mediante la activación de los puntos de control del ciclo celular. Por otro lado, induciría la muerte celular en presencia de un daño tan severo que no pudiese ser reparado.

EL EQUILIBRIO ENTRE PROLIFERACIÓN Y DIFERENCIACIÓN EN LA EPIDERMIS PUEDE DEPENDER DEL PUNTO DE CONTROL MITOSIS-DIFERENCIACIÓN.

Dado que el bloqueo mitótico impuesto por el DMC limita la proliferación de los queratinocitos epidérmicos, sugerimos que alteraciones directamente implicadas en favorecer la mitosis podrían debilitar esta regulación. Para estudiar esta hipótesis, decidimos promover la división celular en queratinocitos que carecían de p53 o sobreexpresaban MYC. Se ha demostrado que ambas alteraciones inducen la diferenciación terminal a partir de un bloqueo mitótico (Gandarillas y Watt, 1997; Gandarillas y Freije, 2014). Con el fin de forzar la división celular a pesar del DMC, sobreexpresamos FOXM1 en estas células. FOXM1 es un factor de transcripción que se expresa en células proliferativas en organismos adultos y se pierde en células quiescentes o en diferenciación (Wierstra y Alves, 2007). Su principal función es promover la mitosis y citoquinesis mediante la transcripción de moléculas directamente implicadas en estos procesos (Costa, 2005). Se considera un oncogén puesto que se encuentra sobreexpresado en diferentes tipos de cánceres humanos, entre ellos los carcinomas epidermoides de piel y de cabeza y cuello (Laoukili et al., 2007; Teh et al., 2013).

Los queratinocitos fueron infectados con una construcción lentiviral que sobreexpresa FOXM1 o su correspondiente vector vacío. A continuación, las células fueron infectadas con una construcción lentiviral que expresa un shp53 o su correspondiente vector vacío, o con una construcción retroviral que sobreexpresa MYC inducible por OHT o el correspondiente vector vacío. Las infecciones se realizaron de manera eficaz, y la sobreexpresión de FOXM1 y MYC o la inhibición de p53 se comprobaron mediante Q-RT-PCR, IF o WB. Es importante que la sobreexpresión de FOXM1 en

ausencia de p53 o tras la sobreexpresión de MYC fue capaz de inhibir el bloqueo en G2/M y de reducir el porcentaje de células poliploides, como se detectó por citometría de flujo. Curiosamente, observamos que FOXM1 inhibía el inicio de la transcripción, que se cuantificó mediante la incorporación de 5'-fluorouridina. Se sabe que la transcripción se produce en interfase y se inhibe durante la mitosis. Sin embargo FOXM1 inhibía la transcripción tanto en células mitóticas que expresaban ciclina A, como en células interfásicas. El gen de FOXM1 codifica para tres isoformas (FOXM1a, b y c), que fueron detectadas en las células mediante WB. Mientras que las isoformas FOXM1b y FOXM1c estimulan la transcripción de sus dianas, la isoforma FOXM1a presenta actividad inhibitoria (Song et al., 2017). Consideramos que la correcta expresión de estas tres isoformas podría ser necesaria para la regulación de la mitosis. Es la primera vez que se propone esta función de FOXM1.

Además de inhibir el bloqueo mitótico, FOXM1 fue capaz de recuperar el potencial proliferativo de los queratinocitos, así como su potencial clonogénico. Mediante IF, Q-RT-PCR y citometría de flujo comprobamos que FOXM1 inhibía la respuesta de diferenciación inducida por la pérdida de p53 o la sobreexpresión de MYC. Este efecto se midió en base a la expresión de marcadores de diferenciación (Involucrina, K1 o Filagrina), los cambios en el aumento en tamaño y complejidad de las células y la pérdida de adhesión celular. Los resultados sugieren que FOXM1 mantiene el potencial proliferativo de los queratinocitos mediante la superación del bloqueo mitótico que da lugar a la diferenciación escamosa.

Los experimentos realizados utilizando la línea celular inmortalizada NTERT confirmaron el papel del DMC en la regulación de la expansión de queratinocitos. Esta línea celular epidérmica presenta expresión ectópica de la subunidad catalítica de la telomerasa humana y de manera espontánea es deficiente en la expresión del inhibidor del ciclo celular p16^{INK4a} (Dickson et al., 2000). Aunque los queratinocitos NTERT no entran en senescencia, sí

presentan expresión de marcadores de diferenciación en cultivos organotípicos. Los NTERT fueron tratados durante tres días con inhibidores químicos específicos de las quinasas mitóticas Aurora B y Polo-like 1. Estas quinasas están implicadas en la segregación cromosómica y en la entrada en anafase (Hansen et al., 2004; Ditchfield et al. 2003). Estos tratamientos inducen el programa de diferenciación terminal en queratinocitos primarios a partir del bloqueo mitótico (Freije et al., 2012). Como se observó por citometría de flujo, estos tratamientos indujeron una parada mitótica y un aumento del porcentaje de NTERT poliploides. Además, se indujo la expresión del marcador de diferenciación Involucrina. Mediante ensayos de clonogenicidad, se comprobó que la inducción de la diferenciación producía una pérdida irreversible del potencial proliferativo. A continuación, decidimos tratar los NTERT con el inhibidor de la polimerización de microtúbulos Nocodazol (NOCO). Este tratamiento induce el programa de diferenciación terminal en queratinocitos primarios a partir del bloqueo mitótico (Gandarillas et al., 2000). Por el contrario, en NTERT esta respuesta se inducía de manera parcial. Por citometría de flujo, observamos un aumento de poliploidía y de tamaño, consistente con la diferenciación epidérmica. Sin embargo, no se detectó aumento en la expresión de Involucrina y los ensayos de clonogenicidad demostraron que estas células eran capaces de seguir proliferando a pesar de ser poliploides. De esta manera, concluimos que los NTERT presentan una respuesta parcial al bloqueo mitótico y defectos en el DMC que podrían colaborar en su inmortalización. Esta misma respuesta parcial se ha observado en la línea celular derivada de un carcinoma escamoso SCC12F (Alonso-Lecue et al. 2017), indicando que defectos en el DMC podrían estar implicados en la carcinogénesis.

IMPLICACIONES DEL PUNTO DE CONTROL MITOSIS-DIFERENCIACIÓN EN LA CARCINOGENESIS EPIDÉRMICA.

Nuestros resultados demostraron que la pérdida de p53 induce la diferenciación escamosa. Se conoce que la mutación de p53 no es un evento iniciador del cáncer de piel, a pesar de que se encuentra frecuentemente mutado en este tipo de cáncer. De hecho, en la piel humana sana se encuentran parches de células con p53 mutada que no dan lugar a carcinogénesis (Jonason, et al., 1996; Ren, et al., 1997; le Pelletier, et al., 2001). Sin embargo, mutaciones en p53 aceleran el desarrollo de cáncer de piel (Kemp, et al., 1993). Nuestros resultados explican esta aparente paradoja. Proponemos que el DMC actúa como un mecanismo de protección contra alteraciones oncogénicas en la epidermis (Gandarillas y Watt, 1997; Freije et al., 2012; Gandarillas y Freije, 2014). Las células con mutaciones en p53 debido a su inactivación, serían expulsadas de la piel por diferenciación y descamación.

Los resultados obtenidos tras la sobreexpresión de FOXM1 apoyan este modelo. FOXM1 permitía la proliferación de células dañadas por la inhibición de p53 o la sobreexpresión de MYC. El nivel de daño fue analizado mediante la cuantificación por citometría de flujo del marcador γ H2AX y de las roturas en las hebras de ADN mediante ensayos *cometa*. En conclusión, ante alteraciones moleculares que desregulan el ciclo celular, el DMC actuaría como una barrera anti-oncogénica disparando la diferenciación terminal. En presencia de alteraciones adicionales que promueven la división celular, como FOXM1, las células mutadas serían capaces de seguir dividiéndose, creando una población de células proliferativas genómicamente inestables que podrían dar lugar al desarrollo del cáncer. FOXM1 también podría tener un papel en el desarrollo de la

carcinogénesis independiente del DMC, mediante la inducción de la expresión de β 1-integrinas, como se detectó por WB. Puesto que los queratinocitos diferencian al perder adhesión a la membrana basal (Adams y Watt, 1989), el aumento de estas moléculas mantendría su potencial proliferativo.

PAPEL DEL DAÑO EN EL ADN EN EL PROGRAMA NATURAL DE DIFERENCIACIÓN DE LOS QUERATINOCITOS EPIDÉRMICOS.

Los queratinocitos de la capa basal de la epidermis pueden encontrarse en dos estados proliferativos (Watt et al., 2006). Por un lado, las células madre presentan una alta capacidad proliferativa pero se mantiene quiescentes y se dividen infrecuentemente. Por otro lado, las células de amplificación transitoria (del inglés, TACs) proliferan activamente pero están determinadas a diferenciar tras 4-5 ciclos de división celular. La transición de una célula madre a una célula TAC se caracteriza por la activación y posterior desregulación del ciclo celular (Dazard et al., 2000; Zanet et al., 2010; Freije et al., 2102). Sin embargo, que determina las células TAC a diferenciar, es desconocido. Nosotros planteamos que el daño en el ADN que se estaría acumulando en las TAC por la desregulación del ciclo, podría formar parte del programa natural de diferenciación en la epidermis y establecer el balance entre proliferación y diferenciación. Los resultados obtenidos en esta Tesis apoyan este modelo.

Mediante IF comprobamos que los queratinocitos primarios cultivados *in vitro* expresan proteínas implicadas en la señalización y reparación del daño en el ADN, γ H2AX y 53BP. El marcador de daño γ H2AX también se detectó mediante IF en la epidermis *in situ*. La acumulación de daño en el ADN activa una respuesta celular (*DNA damage response* en inglés, DDR),

que consiste en la detección y señalización del daño, la activación de los puntos de control del ciclo celular y de proteínas implicadas en reparación. En el caso de que el daño no pueda ser reparado, la DDR activa los programas de apoptosis o senescencia (López-Contreras y Fernández-Capetillo, 2012). Se conocen tres quinasas implicadas en la activación de la DDR: ATM, ATR y DNA-PK. Mientras que ATM y DNA-PK responden principalmente a roturas de la doble cadena del ADN, ATR reconoce y se activa por todo un abanico de lesiones típicamente producidas por el estrés del ciclo celular o estrés de replicación (del inglés, RS). Se ha demostrado que la activación de ATR en ausencia de daño en el ADN es suficiente para inducir senescencia (Toledo et al., 2008). Por ello, hipotetizamos que en queratinocitos ATR podría estar mediando la diferenciación escamosa. Infectamos queratinocitos primarios con una construcción retroviral que sobreexpresa la subunidad catalítica de la proteína TopBP1 inducible por OHT (TopBPER a partir de ahora), o su correspondiente vector vacío. TopBP1 es una proteína necesaria para la activación de ATR (Kumagai et al., 2006). Comprobamos por IF y WB que TopBPER se expresaba eficazmente en los queratinocitos y que el tratamiento con OHT inducía su translocación al núcleo. Para comprobar que la activación de ATR era efectiva estudiamos el marcador γ H2AX, una de las primeras moléculas fosforiladas por ATR en respuesta al daño (Fernández-Capetillo et al., 2004). Por WB y citometría de flujo comprobamos que el tratamiento con OHT aumentaba la señal de γ H2AX. Mediante ensayos *cometa* confirmamos que el aumento de la señal se debía a la hiperactivación de ATR y no a un aumento real del daño en el ADN. A continuación, analizamos el efecto de la activación de ATR en la diferenciación de los queratinocitos y, por citometría de flujo, observamos que se producía un aumento del tamaño y complejidad celular y de la expresión de Involucrina. También detectamos una importante pérdida de clonogenicidad. Concluimos que la activación de ATR es suficiente para inducir la diferenciación escamosa de los queratinocitos.

En base a nuestros resultados, dedujimos que la inhibición de ATR podría impedir la respuesta a diferenciación de los queratinocitos. Para comprobarlo, infectamos las células con una construcción lentiviral que portaba un shRNA contra la expresión de ATR (shATR) o su correspondiente vector vacío. Mediante Q-RT-PCR comprobamos que la expresión de ATR se inhibió eficazmente. Esta inhibición fue acompañada por un aumento de la señal de γ H2AX, que se detectó por IF. Además, por citometría de flujo observamos que la inhibición de ATR activaba los puntos de control de G2/M e inducía un aumento del porcentaje de células poliploides, del tamaño celular y de la expresión de K1. Contrariando nuestra hipótesis, los resultados demostraron que la pérdida de ATR activaba el programa de diferenciación de los queratinocitos. Al mismo tiempo se producía un aumento de la señal γ H2AX. En presencia de daño en el ADN, γ H2AX es también fosforilada por ATM y DNA-PK (López-Contreras y Fernández-Capetillo, 2012). De manera que interpretamos que probablemente las otras quinasas estaban supliendo la falta de ATR. Por tanto concluimos que existe una relación directa entre la señal DDR y la diferenciación de los queratinocitos, aunque ATR es dispensable para la activación de última.

Con el fin de inhibir completamente la DDR utilizamos inhibidores químicos para las actividades quinasas de ATM, ATR y DNA-PK. Mediante citometría de flujo, observamos que la inhibición de ATM o DNA-PK no influían en la señal de γ H2AX. Sin embargo, la inhibición de ATR sí disminuyó γ H2AX tras un tratamiento de 5 horas e indujo un drástico incremento de la señal cuando el tratamiento se prolongó hasta tres días como habíamos observado mediante shRNA para ATR. Puesto que ATR es responsable de la reparación de lesiones producidas durante la replicación, su inhibición impide la reparación de este daño. Por tanto, el aumento de γ H2AX (señal

daño en el ADN) al inhibir ATR (la reparación) sugiere que el RS es una importante fuente de daño endógeno en los queratinocitos en proliferación.

La inhibición conjunta de ATR y ATM aumentó aún más la señal de γ H2AX. Además, mediante ensayo *cometa* se observó un incremento de las roturas en el ADN, lo que sugiere que ATM participa en la reparación de lesiones producidas por RS en ausencia de ATR. Esta respuesta fue de nuevo acompañada por un aumento de la diferenciación terminal, según la expresión de marcadores de diferenciación Involucrina y K1 y el aumento del tamaño y complejidad celulares. Sin embargo, la inhibición simultánea de ATR, ATM y DNA-PK atenuó la señal de γ H2AX, como se detectó por IF y citometría de flujo. Esta disminución se produjo en ausencia de un descenso de la fragmentación del ADN en ensayos *cometa*. Tanto IF como citometría de flujo, mostraron una inhibición de la expresión de Involucrina y K1. Mediante ensayos de clonogenicidad, también se observó una recuperación parcial de la capacidad clonogénica. Por lo tanto, la entrada en diferenciación parece estar mediada por la señal de γ H2AX.

Para confirmar esta hipótesis, inhibimos la señal γ H2AX. Utilizamos una construcción lentiviral que expresa un shRNA contra H2AX, o su correspondiente vector vacío. La inhibición de H2AX se realizó eficazmente, como pudimos comprobar mediante IF, WB y Q-RT-PCR. Como esperábamos, al silenciar H2AX inhibimos la señal de γ H2AX, según se detectó por WB y citometría de flujo. La inhibición de γ H2AX no solo fue acompañada de una disminución de los marcadores de diferenciación escamosa, sino también de la del marcador de epitelio escamoso queratina K5. Además, aumento la expresión del marcador de epitelio simple queratina K8. La bajada de K5 y el aumento de K8 están asociados con la transición epitelio-mesénquima (TEM, Caulin et al., 1993). Estos resultados apoyan la

hipótesis de que γ H2AX media la diferenciación escamosa en respuesta al daño en el ADN.

Basándonos en el conjunto de resultados obtenidos, proponemos un modelo que explicaría la relación entre la proliferación y la diferenciación normal de los queratinocitos epidérmicos. Los queratinocitos basales proliferando activamente estarían determinados a diferenciar debido a la acumulación de daño en el ADN por el estrés del ciclo celular. Este modelo sugiere que existe una respuesta diferenciación al daño en el ADN (*DNA damage-differentiation response* en inglés, DDDR). La DDDR establecería un mecanismo automático auto-limitante de la proliferación y de la iniciación de la diferenciación. Además, proponemos que este modelo podría funcionar en otros tejidos que proliferan activamente durante el desarrollo o la regeneración.

Nuestros resultados sugieren que la entrada en diferenciación en respuesta al daño en el ADN es dependiente de la señal de γ H2AX. Sin embargo, esta relación parece ser parcial, puesto que la inhibición de γ H2AX no inhibe completamente la diferenciación escamosa. Con el fin de identificar nuevas moléculas involucradas en la DDDR, que responden a γ H2AX o que son independientes de esa señal, secuenciamos el transcriptoma de queratinocitos primarios tras activar el DMC utilizando cuatro tratamientos diferentes. Estos experimentos se realizaron con la colaboración del Centro Nacional de Análisis Genómico (CNAG) y del laboratorio del Dr. JT Elder en la Universidad de Michigan, dónde realicé una estancia financiada por la Organización Europea de Biología Molecular (EMBO). Una vez identificados los genes diferencialmente expresados en cada tratamiento en base a su significancia estadística, los comparamos y seleccionamos aquellos cuya expresión aumentaba o disminuía comúnmente en los cuatro tratamientos. Se identificaron 40 genes cuya expresión disminuía y 15 cuya

expresión aumentaba. En futuros estudios se validarán estos resultados y se estudiará el papel de estos genes en la DDDR de queratinocitos

CONCLUSIONES

1. p53 protege el potencial proliferativo de los queratinocitos epidérmicos.
2. p53 es dispensable para la activación del punto de control mitosis-diferenciación (DMC).
3. AREG no suprime el DMC inducido por la pérdida de p53.
4. FOXM1 aumenta la capacidad proliferativa de los queratinocitos humanos e inhibe el DMC en presencia de alteraciones oncogénicas, como la pérdida de p53 o la sobreexpresión de MYC.
5. FOXM1 permite la proliferación de los queratinocitos que acumulan daño en el ADN inducido por alteraciones oncogénicas, aumentando su inestabilidad genómica.
6. La línea celular inmortalizada NTERT presenta defectos en el DMC.
7. La señal de daño en el ADN se detecta en queratinocitos epidérmicos en condiciones normales de proliferación.
8. La respuesta al daño en el ADN controla la diferenciación de los queratinocitos mediante la señal de γ H2AX.
9. La pérdida de H2AX favorece en queratinocitos la conversión fenotípica epitelial-mesenquimal típica de la carcinogénesis epidermoide.

INTRODUCTION

HOMEOSTASIS CONTROL IN DEVELOPING TISSUES

Developing tissues undergo a phase of rapid cell proliferation during both expansion and regeneration (Slack, 2013). In order to control tissue size and homeostasis, cell multiplication needs to stop at some point given that uncontrolled proliferation might lead to loss of tissue integrity and carcinogenesis. Limits to cell proliferation during tissue development are senescence, apoptosis and terminal differentiation. Senescence implies a permanent growth arrest and the secretion of numerous biologically active factors, mainly proinflammatory cytokines that affect the surrounding cells (Tominaga, 2015). Although senescent cells are involved in tissue remodeling during development (Storer et al., 2013, Munoz-Espin et al., 2013), some detrimental effects such as tumor promotion and age-related degenerative phenotypes are associated with this cellular state (Liu and Hornsby, 2007, Krtolica et al., 2001, Perrigue et al., 2015, Baker et al., 2011). Apoptosis or programmed cell death regulates the elimination of specific undesired cells during embryogenesis and adult tissues development, and plays an important role in sculpting the overall shape or organization of organs (Chen and Zhao, 1998, Glucksmann, 1965, Pampfer and Donnay, 1999). However, apoptosis is not a suitable option when tissues expand to accomplish a specialized function. Differentiation is the process by which a stem cell changes into a more specialized cell type and lose the capacity of dividing, due to highly controlled modifications in gene expression (Slack, 2013). The molecular mechanisms that coordinate proliferation with differentiation in developing tissues are not yet understood.

The epidermis, the outermost layer of the skin, is a developing tissue that undergoes self-renewal during the whole lifespan of organisms. This tissue presents a dynamic equilibrium which ensures that the number of cells

generated in the basal proliferative layer equals the number of cells detached from the surface via shedding. This equilibrium between proliferation and differentiation is maintained even under hyperproliferative conditions and its disruption can lead to cancer development. Despite its importance the mechanisms maintaining this homeostatic balance are poorly understood, although they must depend on the regulation of cell cycle. Unraveling the link between cell proliferation and differentiation in the epidermis might help elucidating how homeostasis is maintained in other developing tissues.

THE CELL CYCLE

1. Phases of the cell cycle.

The cell cycle consists in a series of cellular events leading to the duplication of the DNA and cell division, in order to produce two identical daughter cells (Figure 1). The cell cycle is divided into four well defined phases: G1 (gap 1), S (DNA synthesis), G2 (gap 2) and M [mitosis; (Alberts B. et al., 2007, Morgan, 2007)]. The G1 phase immediately follows cytokinesis and is mainly a period of growth after cell division. In addition, mRNA synthesis takes place and histone proteins and enzymes needed by the DNA replication machinery of the next phase are generated. Alternatively to G1, post-mitotic cells under unfavorable or stress conditions can exit cell cycle and are maintained in a quiescent state referred to as G0. G0 cells re-enter G1 upon stimulation.

Following G1, cells enter into S phase where the DNA is faithfully duplicated in order to produce two identical copies, one for each of the two daughter cells. The centrosomes, organelles that nucleate microtubules of the mitotic spindle during mitosis, are also duplicated during the S phase. G2 is a relative short phase where the cell builds up energy and material stores for cell division, as well as RNA and proteins needed for mitosis. During this gap, the cell also checks that the DNA has been replicated properly. Finally, in the M or mitosis phase cell division occurs. The doubled DNA organized in chromosomes is separated and the cellular nucleus divides (karyokinesis) as does the rest of the cell (cytokinesis). The M phase can itself be divided into six phases: prophase, prometaphase, metaphase, anaphase, telophase and cytokinesis (Alberts B. et al., 2007, Morgan, 2007).

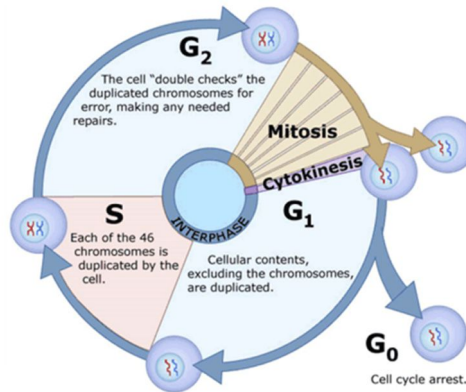


Figure 1 | Phases of the cell cycle. The eukaryotic cell cycle consists in four well differentiated phases. G₁ (synthesis of cellular components), S (synthesis of DNA), G₂ (synthesis of cellular components and DNA integrity testing) compose the interphase. During M (mitosis) chromosomes are segregated. Cell division takes place in cytokinesis. Under unfavorable conditions, the cell can exit cell cycle and maintain a quiescent state (G₀; www.le.ac.uk).

- In prophase the DNA condense and most of it becomes transcriptionally inactive. The Golgi bodies and the endoplasmatic reticulum begin to break apart into membranous vesicles that can be more easily distributed between the two daughter cells. The centrosomes, duplicated during the S phase, move to opposite sides of the cell to establish the poles from which the microtubules are nucleated to form the mitotic spindle.

- The prometaphase is defined by the breakup of the nuclear envelope produced by phosphorylation of the nuclear lamins. The microtubules of the mitotic spindle attach to the centromeric regions of the chromosomes via the kinetochore proteins.

- Unlike the other phases, metaphase is relatively static. The sister chromatids are pushed and pulled by the spindle microtubules organized by

the centrosomes until they are all lined up along the midline of the mitotic spindle. Once they are lined up, the cell is considered to have reached the metaphase.

- Anaphase is reached only if all chromosomes are lined up at the metaphase plate. During this phase, the sister chromatids separate and are pulled toward opposite poles of the mitotic spindle. Separation of sister chromatids requires their dissociation from the cohesin proteins. Cohesins bind to both molecules of DNA shortly after replication in S phase and hold them together until they are inactivated by the action of the enzyme separase.

- Telophase begins when both sets of chromosomes arrive at their respective poles. Nuclear lamina and nuclear envelope are re-constructed. Endoplasmic reticulum and Golgi also start to re-form. By the end of telophase, the product is a single large cell with two complete nuclei on opposite sides.

- The next and last step, cytokinesis, splits the cell in two separate and independent daughter cells. A contractile ring composed by actin and myosin is formed in the middle of the cell, just beneath the plasma membrane in a plane perpendicular to the axis of the spindle. Using ATP the ring contracts and pulls the membrane inward so as to divide the cell in two, thereby ensuring that each daughter cell receives not only one complete set of chromosomes but also half of the cytoplasmic constituents in the parental cell.

1.1. Molecular regulation of the cell cycle.

The regulation of the cell cycle is very complex. Progression through the cell cycle depends on the activity of complexes formed by two types of

regulatory proteins: cyclins and cyclin-dependen kinases [Cdks; Figure 2. (Murray, 2004)]. Cdks are serine/threonine kinases that phosphorylate different substrates inducing changes in their enzymatic activity or in their interaction with other proteins. So far, 20 different Cdks have been identified in human cells although only four are known to participate in the regulation of cell cycle (Cao et al., 2014). Cdk2, Cdk4 and Cdk6 act during interphase (G1, S and G2 phases of the cell cycle) while Cdk1 activity is restricted to mitosis (Malumbres and Barbacid, 2009). Cyclins act as regulatory subunits that activate Cdks, and their expression varies with progression through the cell cycle. 29 different cyclins have been identified, but only 10 of them are known to play a role in cell cycle progression. These 10 cyclins are classified in 4 sub-groups: type D, E, B and A cyclins. Regulated degradation of the cyclins is essential for proper cell cycle progression (Nakayama et al., 2001, Fung et al., 2005).

In response to extracellular proliferative signals, such as growth factors or cytokines, cells in early G1 activate the expression of the D-type cyclins [D1, D2 and D3; (Matsushime et al., 1991, Won et al., 1992, Sherr, 1995)]. D-type cyclins bind to Cdk4 and Cdk6, and the activated complex induces the phosphorylation of the retinoblastoma tumor suppressor protein [Rb; (Sherr and Roberts, 1999, Sherr and Roberts, 2004)]. Phosphorylation of Rb inhibits its binding to the transcription factor E2F which, once released, initiates the transcription of cyclin E (Johnson and Schneider-Broussard, 1998, Geng et al., 1996, Ohtani et al., 1995). Cyclin E associates with Cdk2 and this complex induces the transition from G1 to S phase (DeGregori et al., 1995). Cyclin E/Cdk2 complex participates in maintaining Rb in the hyperphosphorylated state (Hinds et al., 1992) and, thus, orchestrate a positive feedback loop for the accumulation of active E2F.

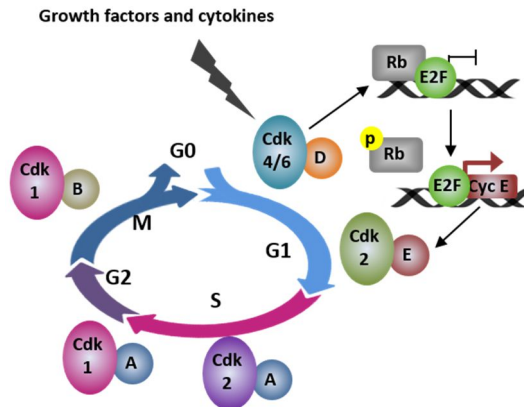


Figure 2 | Regulation of the cell cycle by cyclin/Cdk complexes. Transition from G1 to S phase is dependent on the action of the complexes cyclin D/Cdk4-6 and cyclin E/Cdk2, which phosphorylates Rb and subsequently activates the transcription factor E2F. Progression from S to G2 depends on the complexes cyclin A/Cdk1-2. Finally, activation of the cyclin B/Cdk1 complex is needed for the entry into mitosis.

E2F also regulates the transcription of cyclin A at G1, whose expression persists through the S and G2 phases (Schulze et al., 1995). Cyclin E-A/Cdk2 complexes participate in DNA replication during the S phase by phosphorylating proteins directly involved in the process (Woo and Poon, 2003, Petersen et al., 1999, Coverley et al., 2000). Cyclin A/Cdk2 promotes completion of the S phase and progression to G2 (Lehner and O'Farrell, 1989). Progression from S to G2 also requires cyclin E degradation by the SCF ubiquitin ligase complex (Nakayama et al., 2001). Then, G2/M transition is promoted by cyclin A association with Cdk1 (Gong and Ferrell, 2010). Activation of this complex is required for the initiation of the prophase (Gadea and Ruderman, 2005). Cyclin A is finally degraded in prometaphase by the ubiquitin ligase Anaphase-promoting complex [APC; (Fung et al., 2005)]. Completion of mitosis is regulated by cyclin B/Cdk1 complex by phosphorylation of different substrates that include cytoskeleton proteins such as lamins, histone H1, and possibly components of the mitotic spindle (Arellano and Moreno, 1997, Pines and Hunter,

1991). Mitosis progression is indirectly regulated by Wee1, a kinase that inactivates the cyclin B/Cdk1 complex in response to DNA damage [Figure 3; (Schmidt et al., 2017)]. Anaphase initiates only when cyclin B is degraded during metaphase by the APC (Harper et al., 2002). Progression through the cell cycle also requires the dephosphorylation and activation of the cyclin/Cdk complexes by the Cdc25 phosphatases [Figure 3; (Aressy and Ducommun, 2008)]. While G1/S progression is mainly controlled by dephosphorylation and activation of cyclin E/Cdk2 and cyclin A/Cdk2 by Cdc25A, entry into mitosis requires cyclin B/Cdk1 phosphorylation by Cdc25B and C. Cdc25 phosphatases, cyclin/Cdk complexes and Wee1 are all regulated by the activity of the 14-3-3 proteins [Figure 3; (Khorrami et al., 2017)]. 14-3-3 associates with Cdc25 proteins and sequester them in the cytoplasm, hence inhibiting cyclin/Cdk complexes activation. In addition, binding of 14-3-3 to Wee1 leads to its activation and the inhibition of cyclin B/Cdk1 complex.

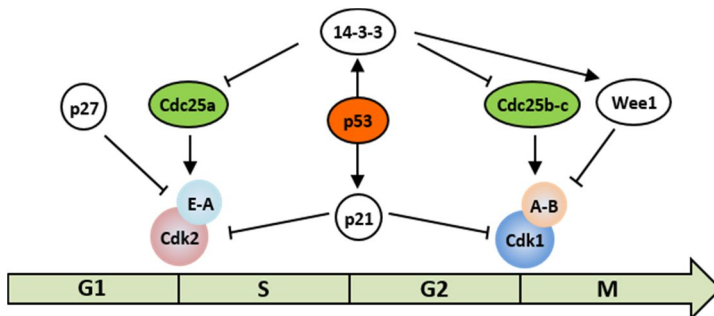


Figure 3 | Regulation of cyclin/Cdk complexes. Progression through the cell cycle requires cyclin/Cdk complexes activation by the Cdc25 family proteins. The repressors p21^{Cip} and 14-3-3 are activated by p53 in response to DNA damage. 14-3-3 in turn inactivates Cdc25 and activates the inhibitor Wee1. p27 directly inhibits the cyclin/Cdk complexes and prevent cell cycle entry.

The activity of Cdks is also modulated by different Cdk inhibitor proteins (CKIs). Two types of CKIs are known: INK4 and Cip/Kip family proteins. INK4 family includes p16^{INK4A}, p15^{INK4B}, p18^{INK4C} and p19^{INK4D}. These

proteins are potent inhibitors of Cdk4 and Cdk6 (Sherr and Roberts, 1995). In late G1 phase, the INK4 proteins compete with cyclin D for Cdk4/Cdk6 to prevent the formation of the activated complex. The Cip/Kip family of CKIs includes p21^{Cip1}, p27^{Kip1} and p57^{Kip2} control cell cycle progression by regulating the activity of cyclin-Cdk complexes [Figure 3; (Sherr and Roberts, 1999, Besson et al., 2008)]. Cip/Kip inhibitors play important roles in restraining proliferation during development, differentiation and in the response to cellular stress. Each of them has specific biological functions that distinguish it from the other family members. p21^{Cip1} is an important transcriptional target of p53 and mediates DNA-damage induced cell cycle arrest in G1 and G2 (Gartel and Tyner, 1999, el-Deiry et al., 1993). In contrast, p27^{Kip1} expression is usually elevated in quiescent cells and the protein is rapidly downregulated as cells enter the cell cycle (Besson et al., 2008, Coats et al., 1996). Finally, p57^{Kip2} has an important role in the regulation of the cell cycle during embryonic development (Besson et al., 2008).

2. The mitosis master gene FOXM1.

FOXM1 is a transcription factor of the forkhead superfamily, which is identified by an evolutionarily conserved winged helix DNA-binding region (Song et al., 2017). The human FOXM1 gene is mapped to chromosome 12p13–3 which consists of ten exons. Two of the exons, Va and VIIa, can be alternatively spliced and give rise to three different isoforms named FOXM1a, FOXM1b and FOXM1c. The splice variant FOXM1a is transcriptionally inactive (Wierstra and Alves, 2007). Both FOXM1b and FOXM1c are transcriptionally active. The FOXM1 protein consists of 3 functional regions including an N-terminal autorepressor domain (NRD), a conserved forkhead DNA binding domain (DBD) and a transactivation domain (TAD) at the C-terminal end

FOXM1 is a typical proliferation-associated transcription factor. It stimulates M-phase entry and is involved in proper execution of mitosis. FOXM1 displays a proliferation-specific expression pattern (Laoukili et al., 2007a): it is ubiquitously expressed during embryo development but is barely detectable in quiescent and terminally differentiated cells (Kalin et al., 2011, Korver et al., 1997a). In adult organisms its expression is restricted to a few proliferating cell types and self-renewing tissues (Korver et al., 1997b, Ye et al., 1997). However, its expression is reactivated after organ injury or cancer formation (Wierstra and Alves, 2007). As not unexpected for a proliferation-stimulating transcription factor, FOXM1 is implicated in tumorigenesis, as it is frequently up-regulated in human non-small cell lung cancers, head and neck squamous carcinoma, hepatocellular carcinomas, colon carcinomas, basal cell carcinomas, ductal breast carcinomas, glioblastomas, pancreatic carcinomas, gastric cancer, among others (Laoukili et al., 2007b).

2.1. FOXM1 target genes.

According to its role in cell cycle progression, FOXM1 regulates genes that control G1/S-transition, S-phase progression, G2/M-transition and M-phase progression. FOXM1 induces expression of cyclin D, cyclin E, cyclin A and Cdc25A phosphatase, which are critical for G1/S transition, DNA replication and G2 progression (Wierstra and Alves, 2007, Costa, 2005, Wang et al., 2005). In addition, FOXM1 induces transcription of *Skp2* and *Cks1* which encode subunits of the SCF complex, required for the degradation of p21^{Cip1} and p27^{Kip1} during G1 phase of the cell cycle (Wang et al., 2005). Thus, FOXM1 negatively regulates the stability of p21^{Cip1} and p27^{Kip1} proteins, leading to increased Cdk2 activity and promoting G1/S transition. FOXM1 also transactivates the oncogene MYC (Wierstra and Alves, 2006). Both Cdc25B and cyclin B1 are also direct transcriptional

targets of FOXM1, which are required for mitosis progression (Leung et al., 2001, Wang et al., 2002). In addition, FOXM1 is a transcriptional activator of various genes critical for chromosome segregation and cytokinesis, such as Aurora B, Polo-like kinase 1 (Plk1), Survivin and Cenp A, B and F isoforms [Figure 4; (Kalin et al., 2011)]. Although FOXM1 activates the transcription of genes involved in S-phase progression, its main role seems to be the promotion of mitosis. Depletion of FOXM1 caused chromosome instability and frequent failure of cytokinesis (Laoukili et al., 2005). In addition, FOXM1 knockout mice died *in utero* due to multiple abnormalities in various organ systems, including liver, lungs, blood vessels and heart (Kalin et al., 2011). Interestingly, these mice presented abnormal accumulation of polyploid cardiomyocytes and hepatoblasts resulting from failure to complete mitosis. Hence, FOXM1 seems essential for mitosis progression but not for DNA replication.

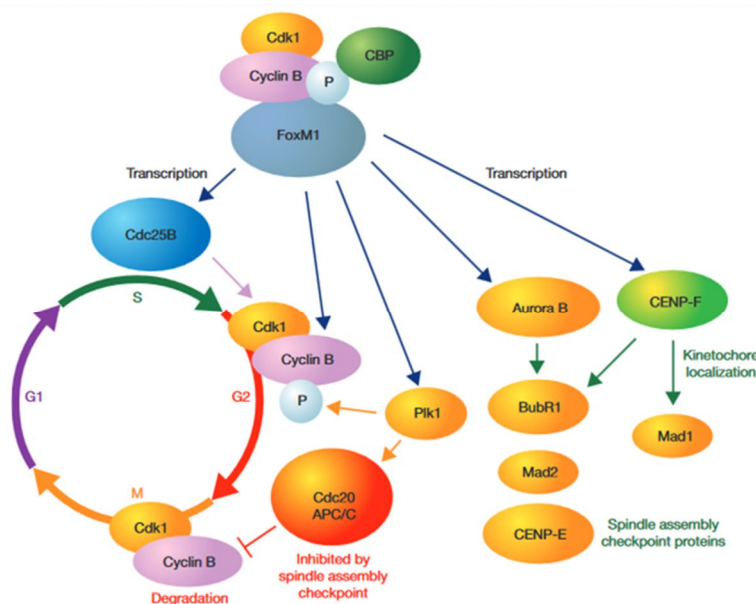


Figure 4 | FOXM1 regulates the transcription of genes involved in mitosis progression. FOXM1 transactivates a set of genes needed for G2/M transition,

chromosome segregation and cytokinesis. These genes include cyclin B, Polo-like kinase, Aurora B or CENP (Costa 2005).

2.2. FOXM1 regulation during the cell cycle.

FOXM1 regulates cell cycle progression by the transactivation of different genes needed for each of the phases. At the same time, FOXM1 protein activity is controlled to ensure the coordinated progression through the different phases of the cell cycle. It has been found that phosphorylation by cyclin/Cdk complexes plays an important role its activation state, cellular localization and stability (Song et al., 2017). FOXM1 activation is increased progressively during cell cycle and reaches its maximum at the G2/M transition.

During the G1/S phase, the presence of FOXM1 in the nucleus is low. It is mainly localized in the cytoplasm as a dimmer and its activity is repressed by its own N-terminal domain. Cyclin D/Cdk4-6 initiates FOXM1 phosphorylation at the C-terminal region of the TAD domain and the N-terminal autorepressor domain during G1 (Song et al., 2017). This phosphorylation makes it more stable, causing its accumulation along with an increased transcriptional activity. With the progression of the cell cycle, cyclin A/Cdk2 and cyclin B/Cdk1 are responsible of FOXM1 further phosphorylation and complete activation (Lim and Kaldis, 2013). Translocation of FOXM1 to the nucleus occurs in late S-phase due to phosphorylation on two ERK1/2 target sites by Raf/MEK/MAPK (Ma et al., 2005). The coexistence of these two regulatory mechanisms (stabilization and nuclear translocation) causes a peak of FOXM1 activity in the G2/M phase of the cell cycle (Song et al., 2017). Once in the nucleus, FOXM1 phosphorylates Plk1 which subsequently binds and phosphorylates FOXM1, enhancing its transcriptional activity (Fu et al., 2008). Later during G2/M, FOXM1 is further activated by Cdc25 phosphorylation (Sullivan et

al., 2012). Cyclin B, Cdc25 and Plk1 in turn generate a positive feedback loop, leading to further increase in FOXM1 activity and therefore also cyclin B and Plk1 levels. As the major transcription factor during cell cycle transition, full activation of FOXM1 ensures the coordinated expression of transcriptional networks essential for timely entry into mitosis. For this reason it has been proposed as a mitosis master gene (Costa, 2005).

Finally, in order to avoid uncontrolled cell proliferation, FOXM1 expression must be decreased at some point during the cell cycle. The tumor suppressor ARF protein is known to repress FOXM1 activity by sequestering it into the nucleolus (Kalinichenko et al., 2004, Gusarova et al., 2007). In addition, FOXM is indirectly inhibited by p21^{Cip1} and p27^{Kip1}. These inhibitors repress the activity of FOXM1 by targeting the cyclin/Cdk complexes (Wierstra and Alves, 2007).

THE DNA DAMAGE RESPONSE

DNA is continuously being damaged in many ways. Both endogenous and exogenous agents are causes of multiple types of DNA lesions. These lesions interfere with DNA replication, transcription, and genome integrity. Therefore, the damage must be repaired to ensure homeostasis and prevention of disease. The organisms have developed an integrative network of pathways to repair DNA damage faithfully, which is known as DNA damage response [DDR; (Lopez-Contreras and Fernandez-Capetillo, 2012)]. In general, DDR involves DNA lesion recognition and a signaling cascade that arrests the cell cycle and promotes DNA repair. DDR is also responsible for the induction of senescence or apoptosis in cells with extensive irreparable DNA damage, limiting the propagation of mutated cells. Activation of the DDR depends on three serine/threonine protein kinases of the PI3K-related kinase family: Ataxia-Telangiectasia mutated (ATM), ATM and Rad3-related (ATR) and DNA-protein kinase complex (DNA-PK). While ATM and DNA-PK respond primarily to double strand breaks (DSBs), ATR is activated by a much wider range of DNA lesions produced during DNA replication, including DSB and single strand breaks [SSBs; (Zou and Elledge, 2003)].

3. Sources of DNA damage.

As mentioned, sources of DNA damage can be endogenous or exogenous. Exogenous damage can be produced by physical or chemical sources. Examples of physical genotoxic agents are IR and UV radiation. IR can generate SSBs, DSBs and base modifications such as oxidation, alkylation, deamination, loss of base residues that produce apurinic or apyrimidinic sites (AP sites). All of them can indirectly lead to SSBs and/or DSBs. There are also cross-links formed involving DNA-DNA or DNA-protein

interactions (Ciccia and Elledge, 2010). UV radiation, through direct excitation of pyrimidine bases, induces two main classes of bipyrimidine photoproducts: cyclobutane pyrimidine dimers (CPDs) and pyrimidine (6-4) pyrimidone (6-4PPs) photoproducts (Mitchell et al., 1990). In addition, UV radiation also gives rise to reactive oxygen and nitrogen species (ROS and RNS, respectively) which are also DNA damage agents (Halliday, 2005). Lastly, chemical exogenous sources of DNA damage can produce different DNA lesions, such as attachment of alkyl groups to DNA bases, cross-links, SSB and DSB or DNA adducts.

Endogenous sources of DNA damage are mainly ROS and DNA replication errors produced by replication stress (RS). ROS can be generated by UV radiation as explained, but endogenous ROS arise from metabolism or inflammatory response involving the immune system (Cooke et al., 2003, Kohchi et al., 2009). DNA lesions produced by ROS include abasic (AP) sites, SSB, sugar moiety modifications and deaminated and adducted bases. Finally, replication stress (RS) refers to errors generated during DNA replication due to replication fork collapse. RS typically produces SSBs that become DSBs if the damage persists (Ward and Chen, 2001). RS is commonly induced by DNA fragile sites, which are loci in the genome that are particularly difficult to replicate, hence rendering it prone to fragility (Durkin and Glover, 2007). Another source of RS is the replication-transcription complex collision. Although transcription and replication machineries are known to be spatially and temporally separated, it has been reported that large genes, often located at fragile sites, are transcribed more than once per cell cycle. This increases the probability of collision between replication and transcription complexes and the formation of DNA-RNA hybrids (Helmrich et al., 2011). Shortage of the dNTP pool during replication is another cause of genetic damage. Small variations in dNTP pool size substantially affect fork progression (Bester et al., 2011, Gay et al.,

2010). Finally, base insertions, deletions and substitutions can be produced by polymerase errors during DNA replication, with a mutation rate per base pair ranging from 10^{-9} to 10^{-10} (Mertz et al., 2017).

Cell cycle deregulation by oncogenic alterations promotes RS and induces the DDR during tumorigenesis (Macheret and Halazonetis, 2015). Oncogene-induced RS seems to be produced by direct or indirect Cdk activity deregulation, which in turn results in the uncoupling of the phases of the cell cycle. Coordinated activation of Cdks is essential for replication origin licensing and firing during G1 and S phases respectively. Hence, oncogenes can influence the timing of DNA replication initiation. Oncogenes can also induce RS at the level of replication fork progression by decreasing the dNTP pool due to upregulation of origin licensing and firing. Fork progression can also be affected by the accelerated entry into S: shortened of G1 results in the decrease of replisome and chromatin associated components synthesis, which are needed for DNA replication. In concordance, overexpression of the oncogenic MYC or cyclin E is associated with increased firing of replication origin, impaired of replication fork progression and DNA damage (Bartkova et al., 2006, Rohban and Campaner, 2015). Finally, uncoupling of G1 and S phases increases the probability of genomic loci to be transcribed and replicated simultaneously increasing the chance of DNA-RNA hybrids formation.

4. The cell cycle checkpoints.

The cell cycle possesses protective mechanisms that monitor the order, integrity and fidelity of the major events: DNA replication and mitosis. These mechanisms of control are known as cell cycle checkpoints.

4.1. The intra-S checkpoint.

DNA replication errors produced by RS are detected by the intra-S checkpoint, which activates a cascade of events that slow down replication and stabilize replisomes at stalled forks (Nyberg et al., 2002). Of the DDR kinases, ATR is the most crucial mediator of the intra-S checkpoint (Blackford and Jackson, 2017). ATR also functions in unperturbed S phase, where it regulates firing of replication origins (Sorensen et al., 2004, Shechter et al., 2004, Petermann and Helleday, 2010). Upon RS, ATR inhibits replication origin firing by phosphorylating and activating Chk1 (Blackford and Jackson, 2017). Chk1 subsequently phosphorylates Cdc25A, targeting it for ubiquitin mediated degradation. Inactivation of Cdc25A reduces Cdk2 activity and results in cell cycle arrest and inhibition of replication origin firing by Cdc45 [Figure 5; (Sorensen et al., 2003, Zou and Stillman, 1998)].

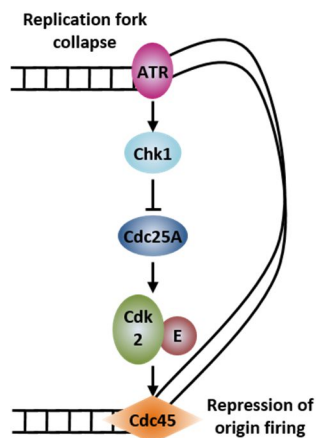


Figure 5| Repression of origin firing by the intra-S checkpoint. In response to replication fork collapse ATR activates its target Chk1. Chk1 inhibits Cdc25A by phosphorylation, which results in the inactivation of cyclin E/Cdk2 complex needed for replication origin firing by Cdc45.

Inhibition of origin firing prevents new forks from encountering damage and stalling. Despite the global inhibition of replication origins, the intra-S checkpoint activates the firing of dormant origins that are passively

replicated under normal conditions (Yekezare et al., 2013). Firing of dormant origins help to complete replication in the vicinity of stalled forks and thereby mitigate the consequence of fork stalling.

4.2. The G1 and G2 checkpoints.

During interphase DNA damage activates the G1 or G2 checkpoints by inhibiting Cdk2 or Cdk1 prior to commitment to subsequent S- or M-phases of the cell cycle (Figure 6). Cell cycle arrest allows DNA repair.

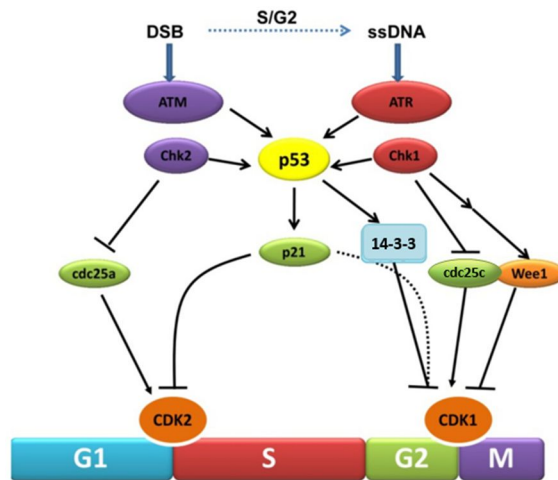


Figure 6 | Activation of the G1 and G2 checkpoints in response to DNA damage. ATM and ATR kinases orchestrate the activation of a molecular pathway that induces cell cycle arrest in response to DNA damage (Lopez-Contreras & Fernandez-Capetillo, 2012).

Activation of these checkpoints depends on ATM and ATR signal transduction by Chk2 and Chk1 respectively, although there is some overlap and redundancy between the functions of these two proteins (Lopez-Contreras and Fernandez-Capetillo, 2012). Active Chk2 and Chk1 phosphorylate the Cdk2 activator Cdc25A and promote its degradation, arresting the cell cycle at G1. ATM and ATR also induce stabilization of the transcription factor p53 by direct phosphorylation or by the mediation of Chk2 and Chk1. p53 activates the transcription of *p21^{Cip1}*, maintaining an

effective cell cycle arrest. The role of DNA-PK in checkpoint activation is controversial, although it has been found to participate in cell cycle arrest in the absence of ATM (Callen et al., 2009).

During the activation of the G2/M checkpoint, Chk2 and Chk1 phosphorylate and inhibit the Cdk1 activator Cdc25C. This phosphorylation creates a binding site for the repressor 14-3-3, which sequesters Cdc25C in the cytoplasm and inhibits its activity (Zeng and Piwnicka-Worms, 1999). In addition, Chk1 and Chk2 activate Wee1, which promotes the G2 arrest by inhibiting the cyclin B/Cdk1 complex (Lopez-Contreras and Fernandez-Capetillo, 2012). p53 participates in the activation of the G2/M checkpoint by transactivating p21^{Cip1} and 14-3-3 σ , which prevents nuclear localization of cyclin B/Cdk1 after DNA damage (Hermeking et al., 1997).

4.3. The spindle assembly checkpoint.

The segregation of sister chromatids at anaphase is under the mechanical control of the mitotic spindle. Progression through anaphase is promoted by the APC, which targets a number of proteins for degradation. The spindle assembly checkpoint (SAC) prevents activation of the APC when kinetochores are not occupied by spindle microtubules, or are attached but not under tension (Figure 7). Binding of the substrates to the APC during mitosis depends on Cdc20, responsible for APC activation (Chang et al., 2014). Therefore, by targeting Cdc20, the SAC efficiently inhibits the APC. The proteins responsible for Cdc20 inhibition form the mitotic checkpoint complex (MCC), which includes MAD and BUB3 proteins (De Antoni et al., 2005). Once the SAC is satisfied, Cdc20 is released from MCC inhibition and allows active APC^{Cdc20} to degrade securin and cyclin B (Manchado et al., 2010). Degradation of securin releases the enzyme separase, which cleaves cohesin complexes at the kinetochores and permits chromatid arm separation. Destruction of cyclin B inhibits Cdk1 activity. Loss of Cdk1

activity in turn allows another APC activator, Cdh1, to bind and activate APC. APC^{Cdh1} targets further proteins (Peters, 2006).

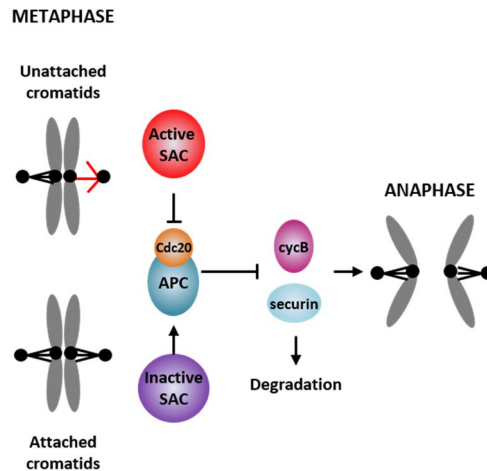


Figure 7 |The spindle assembly checkpoint (SAC) prevents aberrant chromosome segregation. During metaphase the SAC detects errors in chromatid attachment to kinetochores and inhibits the anaphase promoting complex (APC). When the SAC is satisfied, activation of the APC by Cdc20 degrades cyclin B and securin and allows entry into anaphase and chromosome segregation.

5. The DNA damage repair pathways.

As described, the sources of DNA damage are many and diverse. In addition, the type of lesion that is produced depends on the damaging source, and the molecular mechanism for repair is very specific of the type of lesion. As a consequence, cells possess a broad variety of DNA repair pathways to manage the different types of damage. The cellular repair pathways can be classified into two subtypes. On the one hand, excision-based repair pathways involve lesions in which the bases are damaged or mismatched but the sugar-phosphate backbone is intact. On the other hand, homologous recombination (HR) and non-homologous end joining (NHEJ) are responsible of the repair of DSBs.

5.1. Excision-based repair pathways.

Excision-based pathways repair damaged or mismatched DNA by resynthesis of new DNA using the complementary strand as a template. For this reason, it can occur in any phase of the cell cycle (Barnum and O'Connell, 2014). It is unclear whether this type of lesion activates the cell cycle checkpoints. It seems more likely that checkpoints are activated by the indirect effect of the lesion during DNA replication (Callegari and Kelly, 2006).

- Mismatch repair (MMR) removes mismatched bases incorrectly incorporated to the DNA sequence by the DNA polymerase. It also removes chemically modified bases and mono-, di-, and trinucleotide insertion/deletion loops (IDLs). Distortion of the DNA helix resulting from mismatches and IDLs are detected by members of the MutS homologs MSH protein family, which bind to the DNA as heterodimers. The MutL homolog (MLH) complex, which presents endonucleolytic activity, is recruited by the MSH complex and generates nicks in the DNA. The exonuclease EXO1 resects the damaged strand, and polymerases and ligases synthesize new DNA and close the nick respectively (Jiricny, 2013).

- Base excision repair (BER) removes modified bases and repair apurinic/apyrimidinic (AP) abasic sites. The first event in BER consists on the recognition and cleavage of the modified base from the sugar by a DNA glycosylase. This is followed by excision of the backbone by short-patch or long-patch repair (Krokan and Bjoras, 2013). In short-patch repair, a single nucleotide is removed, and the gap is filled by DNA polymerase β and ligated by ligase 1 or 3. In long-patch repair, 2 to 10 nucleotides are removed, and the process requires FEN1, PCNA, DNA polymerase β , σ or ϵ , and ligase 1.

- Nucleotide excision repair (NER) removes bases modified by products of metabolism, UV light and environmental mutagens. It plays a critical role in the repair of UV-damaged bases. CPDs and 6-4PPs typically produced by UV light disturb the double helix and are a physical impediment to DNA and RNA polymerases. These lesions are recognized via the XPC-RAD23 or DDB complexes. They then recruit other XP proteins that promote unwinding of the DNA, excision of the damaged strand and resynthesis (Scharer, 2013). Transcription-coupled NER (TC-NER) is activated when the RNA polymerase stalls during transcription. In TC-NER is the RNA polymerase II itself, and not XPC-RAD23 or DDB1-DDB2 complexes, which recognize the damage (Hanawalt and Spivak, 2008).

5.2. DSB repair pathways.

DSBs are the most catastrophic DNA lesions and their inefficient repair might result in cell death or cellular transformation. DSBs can be produced directly by ROS, IR and chemicals, or indirectly by SSBs produced during replication (Barnum and O'Connell, 2014). During HR, DNA is resynthesized using the sister chromatid as a template and because of this, it is restricted to the S and G2 phases of the cell cycle. In G1, DSBs are repaired via NHEJ. NHEJ does not require activation of the cell cycle checkpoints, although they can be activated by ATM if the DNA damage persists (Lopez-Contreras and Fernandez-Capetillo, 2012). Repair by any of these pathways leads to the formation of intermediate structures different from double-stranded DNA that can be recognized as damage and activate a different repair pathway. Hence, repair can begin through a pathway and be shunted into another via a common intermediate (Barnum and O'Connell, 2014).

5.3. DNA-PK regulates NHEJ repair.

DNA-PK promotes DSB repair by NHEJ, which involves ligation of two broken DNA ends without needing a sister chromatid as template. For this reason, it can be active at any phase of the cell cycle (Lopez-Contreras and Fernandez-Capetillo, 2012). DNA-PK is activated when recruited to DSBs by Ku70/80 [Figure 8; (Gell and Jackson, 1999, Singleton et al., 1999)].

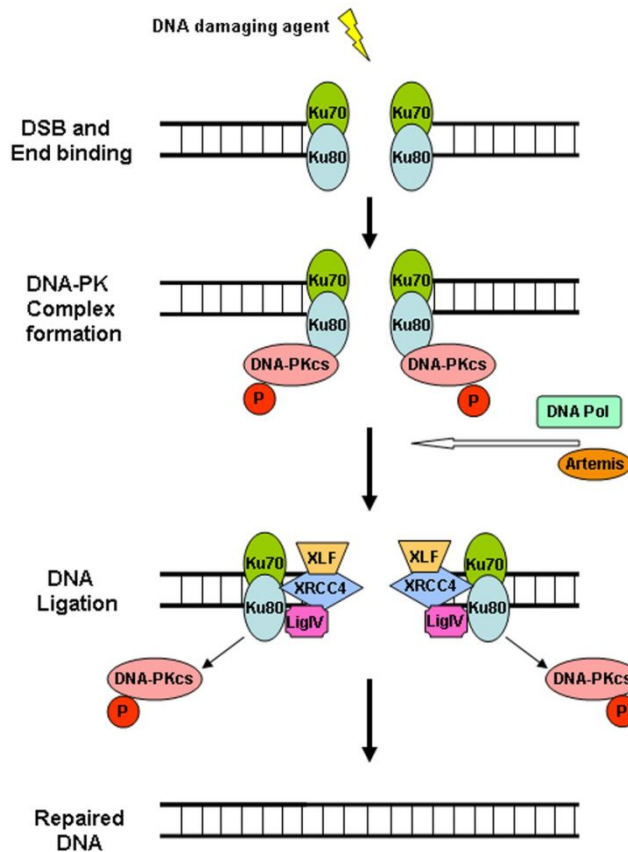


Figure 8 | DNA-PK promotes DNA repair via NHEJ. DNA-PK is activated in response to DSB. Its recruitment and activation depends on the interaction with Ku70/80. DNA ends are processed by ARTEMIS and DNA polymerase, and ligated by the action of XRCC4/LigIV with the help of the stimulatory factor XLF (Kanungo, 2013).

DNA-PK plays a critical role in stabilizing DSB ends and preventing end resection through a series of phosphorylation reactions (Meek et al., 2008). Following DNA binding DNA-PK is autophosphorylated, which results in the destabilization of its interaction with DNA ends. This provides access of processing proteins. At this point, XRCC4/LigIV is recruited and promotes the re-ligation of the broken ends with the help of the stimulatory factor XLF (Mahaney et al., 2009). DNA termini that contain non-ligable end groups are processed by ARTEMIS prior to DNA ligation (Ma et al., 2002).

5.4. ATM activates the cellular response to DSBs.

ATM is responsible of promoting DSBs repair via HR and the activation of the cell cycle checkpoints through the mechanisms previously explained. The mechanism for ATM activation is not completely understood yet. It has been proposed that ATM activation in response to DSBs includes a dimer to monomer dissociation and recruitment to the damage site. Dissociation is produced by ATM autophosphorylation in response to DNA lesions (Bakkenist and Kastan, 2003, Kozlov et al., 2006). Recruitment of ATM to DSBs depends on the assembly of the MRN complex, comprising MRE11, Rad50 and NBS1 [Figure 9; (Lee and Paull, 2005)]. Rad50 associates to the DSB ends and recruits MRE11 via its ATPase containing domain. Then, NBS1 associates with ATM and promotes its recruitment to DSBs by interacting with MRE11.

Once activated, ATM promotes HR. Repair is initiated by nucleolytic resection of the two 5' strands from the DSBs (Symington, 2014). DNA end resection is regulated by ATM through CtIP, which interacts with BRCA1 and MRN in the BRCA1-C complex. The resection reaction helps to commit the DSB to be repaired by HR and eliminates the possibility of NHEJ (Daley and Wilson, 2005). After resection, the 3' tails are bound by

Replication Protein A [RPA; (Raderschall et al., 1999)]. Then, several recombination mediator proteins, such as BRCA2, facilitate the replacement of RPA by Rad51 recombinase. This Rad51-ssDNA complex is required for homology identification in the sister chromatid. Once homology is located, the 3' end of the complex invade the sister chromatid producing a DNA joint known as displacement loop. Finally, the new DNA is synthesized using the invading strand as primer.

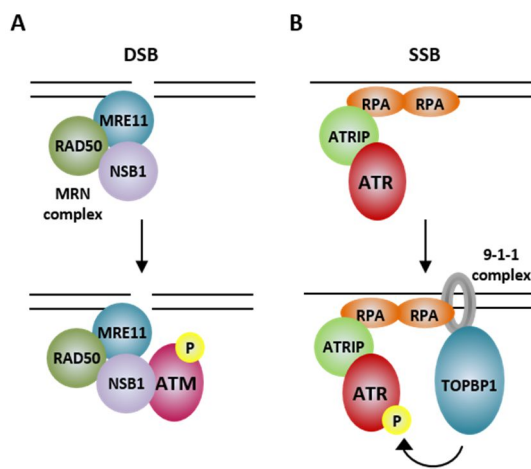


Figure 9 | Activation of ATM and ATR in response to DNA damage. A) ATM is activated by DSB. The MRN complex, composed by MRE11, RAD50 and Nsb1, recruits ATM to the sites of damage and activates it by phosphorylation. **B)** ATR is activated in response to SSB. RPA-ssDNA recruits ATR to the lesion interacting with ATRIP. Activation of ATR depends on its phosphorylation by TOPBP1, which is recruited independently by the 9-1-1 complex.

5.5. ATR coordinates the DDR to replication stress.

ATR activates the DDR in response to RS and, unlike ATM and DNA-PK, it is essential in proliferating cells (Brown and Baltimore, 2000). ATR participates in HR repair after resection of DSB ends via phosphorylation of Rad51 and BRCA2 (Lopez-Contreras and Fernandez-Capetillo, 2012). In

addition, ATR prevents replication fork collapse and participates in the stabilization of replisomes.

ATR activation is promoted by RPA-coated single stranded DNA (ssDNA) typically generated by collapsed replication forks (Byun et al., 2005) or during DSB ends resection during HR promoted by ATM (Raderschall et al., 1999). Activation of ATR by ATM-dependent resection is an example of ATM and ATR signaling pathways overlapping at some point during DDR activation (Cuadrado et al., 2006). The opposite case occurs when a replication fork collapse at a SSB, resulting in the formation of a DSB and the activation of the ATM pathway (Ward and Chen, 2001). RPA-ssDNA recruits ATR to DNA lesions via direct interaction with the ATR interacting protein (ATRIP), which forms a complex with ATR [ATR/ATRIP complex. Figure 9; (Zou and Elledge, 2003)]. ATR/ATRIP complex recruitment to RPA-ssDNA is not sufficient for ATR activation. The best known activator of ATR is the topoisomerase binding protein 1 (TopBP1), which contains an ATR-activation domain that stimulates ATR kinase activity (Kumagai et al., 2006). TopBP1 is recruited to RPA-ssDNA by the 9-1-1 complex independently of ATR (Delacroix et al., 2007, Lee et al., 2007). Recently, a second ATR-activator protein, ETAA1, was identified and found to contain an ATR-activation domain similar to that of TopBP1 (Haahr et al., 2016). Unlike TopBP1, ETAA1 is recruited to RPA-ssDNA via direct binding to RPA.

6. Chromatin based DDR- signaling.

One of the first proteins phosphorylated by ATM, ATR and DNA-PK in response to DSBs is H2AX, a histone H2A variant, on serine 139 [γ H2AX; (Fernandez-Capetillo et al., 2004)]. γ H2AX spreads for distance up to 1-2 megabases around DSBs and is required for DNA damage signal

amplification and subsequent accumulation of numerous DDR proteins at DSB sites, to form so called ionizing radiation induced foci [IRIF; (Ciccia and Elledge, 2010)]. γ H2AX signal intensity increases as cells progress through the cell cycle, reaching maximal levels at metaphase (McManus and Hendzel, 2005). In addition, γ H2AX is needed for proper chromosome segregation during mitosis (Eliezer et al., 2014). H2AX signal amplification starts with the binding of MDC (Stucki et al., 2005). Then Nsb1 promotes MDC1-MRN retention on γ H2AX-chromatin containing sites (Spycher et al., 2008). MDC1-MRN recruits and phosphorylates ATM, leading to further γ H2AX formation and MDC1-MRN-ATM recruitment, thus spreading the assembly along chromatin and amplifying DDR signal [Figure 10, (Stucki and Jackson, 2006, Blackford and Jackson, 2017)]. In turn this results in the increasing accumulation of repair factors to the site of DNA damage, including BRCA1 and 53BP1 (Sobhian et al., 2007, Bekker-Jensen et al., 2005). BRCA1 and 53BP1 proteins present antagonist functions and compete at the DSB sites to promote DNA repair via HR or NHEJ during S/G2 (Shibata, 2017). 53BP1 promotes NHEJ by preventing end resection. However, BRCA1 promotes HR by relocating 53BP1 from the foci center to the periphery. 53BP1 is also involved in maintain γ H2AX marked chromatin transcriptionally inactive by retained damaged DNA in the so called 53BP1 nuclear bodies [NBs; (Fernandez-Vidal et al., 2017)]. 53BP1 NBs are formed in G1 phase around DNA lesions produced in the previous cell cycle due to RS and disappear as cells enter into the S phase. Interestingly, the presence of 53BP1 NBs has been shown to be associated with G1 arrest and cellular senescence (Feng and Jasin, 2017).

Finally, γ H2AX also plays an important role in chromatin remodeling in response to DNA damage. DDR factor recruitment by γ H2AX is influenced by the action of a network of chromatin modifying enzymes regulating ubiquitination, sumoylation, acetylation and methylation (Bekker-

Jensen and Mailand, 2010). In addition, chromatin remodeling enzymes recruited by γ H2AX stimulate chromatin relaxation at DSB sites to facilitate the interaction of DDR proteins with the lesion, thus promoting its repair (Lee et al., 2010, van Attikum and Gasser, 2009).

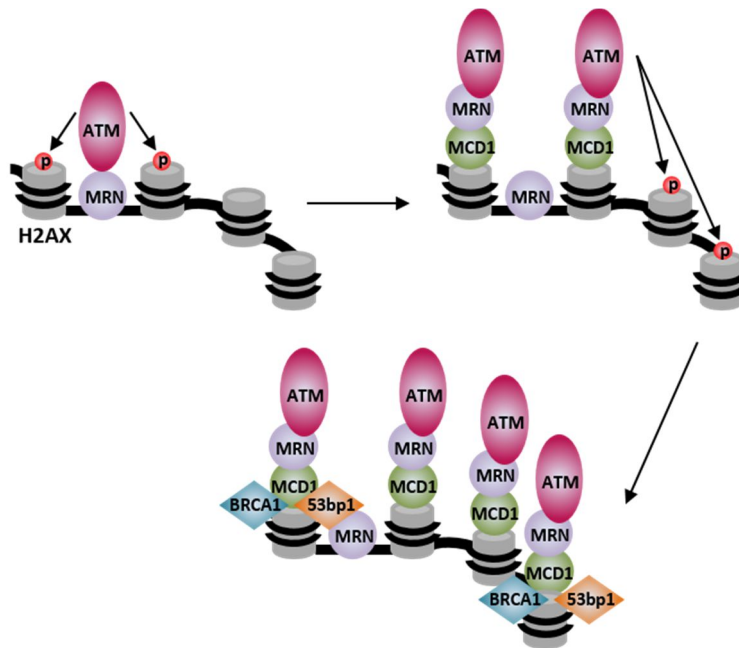


Figure 10 γ H2AX promotes DNA damage signal amplification. ATM phosphorylates H2AX at the sites of DNA damage. γ H2AX leads to further recruitment of MRN-ATM via interaction with MCD1, and this in turn spreads the γ H2AX signal. Finally, repairing proteins such as BRCA1 and 53BP1 are also recruited and complete the formation of the IRIF.

7. DDR and cell fate.

As explained in this section, cells have developed a DDR to manage with DNA lesions in order to avoid propagation of mutations to the next generation that could lead to genomic instability, disruption of homeostasis and disease. DDR includes cell cycle checkpoints and mechanisms to repair DNA lesions. Finally, in response to permanent DNA damage, DDR is known to end in apoptosis, senescence or differentiation in order to avoid

proliferation of damaged cells (Lopez-Contreras and Fernandez-Capetillo, 2012).

Apoptosis or programmed cell death is an irreversible and highly regulated process that results in the physical loss of the damaged cells (Matt and Hofmann, 2016). The most important regulator of DNA damage-induced apoptosis is p53, which transactivate the expression of pro-apoptotic factors such as Puma, Noxa and Bax (Miyashita and Reed, 1995, Nakano and Vousden, 2001, Oda et al., 2000). These factors promote the permeabilization of the mitochondrial membrane and allow the release of cytochrome c, Smad and HtrA2/Omi to the cytosol (Chinnaiyan, 1999). These proteins activate the caspase cascade, which results in fragmentation of the cellular components, including nuclear membrane. Apoptosis is essential in some developing tissues to maintain homeostasis and cell population balance (Abud, 2004). Very interestingly, it has been shown that DDR activation precedes regression of the inter-digital tissue in vertebrate embryos (Montero et al., 2016) and during postnatal development of retina (Martin-Oliva et al., 2015).

An alternative outcome for cells with irreparable DNA damage is senescence. Cellular senescence is a permanent cell-cycle arrest that participates both in the developmental program and in normal ageing and age-related disease (McHugh and Gil, 2018). Senescence is accompanied by altered gene expression and morphological changes that distinguish it from terminal differentiation (Gandarillas, 2000). p53 is responsible of the activation of the DNA-damage induced senescence via its target p21^{Cip1}. Increased p21^{Cip1} expression inhibits the cyclin/Cdk complexes causing a permanent G1 arrest (Tonnessen-Murray et al., 2017). p16^{INK4A} is also responsible for inhibition of the cyclin/Cdk complexes, preventing the

phosphorylation of Rb (Sherr and Roberts, 1995). This allows the Rb family of proteins to recruit chromatin modifiers that silence expression of genes driving cell cycle progression, thus turning cell cycle arrest irreversible (Narita et al., 2003). Different cellular stresses can induce DDR-mediated senescence. Telomere shortening was the first identified cause of the senescence response (Harley et al., 1990). ROS also promote the activation of the DDR and senescence (Parrinello et al., 2003). Finally, oncogene-induced replication stress is another important cause of cellular senescence, which acts as a barrier against cellular transformation and prevents tumor formation (Serrano et al., 1997).

Recently, DDR activation in response to extensive DNA damage has been related to the activation of the differentiation program in melanocytes, neurons and keratinocytes (Inomata et al., 2009, Tedeschi and Di Giovanni, 2009, Zanet et al., 2010, Freije et al., 2012). The mechanism by which DDR triggers differentiation has not been elucidated. It has been proposed to be mediated by p53-dependent promotion of stem cell asymmetric division (Lopez-Contreras and Fernandez-Capetillo, 2012). Despite its importance in genome stability and tissue homeostasis maintenance, the mechanism by which the DDR and p53 decides between apoptosis, senescence or differentiation is unknown. However, this might depend on the cellular context and the source or type of the DNA lesion (Sherman et al., 2011).

EPIDERMIS AS AN ADULT DEVELOPING TISSUE

8. Structure and function of the skin.

The skin constitutes a barrier that covers the external surface of the organism. Its main function is to act as first line of defense of the body against environmental aggressions; mainly UV radiation but also toxic chemicals, microorganism and mechanical trauma. It plays an important role in the prevention of water and electrolytes loss and is a sensitive and secretory organ directly involved in body temperature regulation. The skin is composed by three layers: the epidermis, the dermis and the hypodermis (OpenStax, 2016).

The epidermis is a squamous stratified epithelium that constitutes the outermost layer of the skin. The cellular unit of the epidermis is the keratinocyte but other cellular types are also found: melanocytes, Langerhans cells and Merkel cells. Keratinocytes are cells characterized by the production and storage of keratins. Keratins are intracellular proteins that provide skin its harness and water-resistant properties and compose accessory structures, such as hair and nails. The function of melanocytes is the production of melanin, the pigment responsible of blocking UV radiation. Merkel cells are mechanoreceptors that confers the sensation of touch and Langerhans cells are involved in the immunological response (Leigh et al., 1994). The epidermis acts as a protective interface with the external environment and also maintains the lubrication of the skin with lipids and thermoregulation by hairs and sweat.

The dermis is placed immediately below the epidermis and its function is to provide mechanical strength, elasticity and nutrient supply (OpenStax,

2016). It is composed by connective tissue enriched with elastin and collagen fibers produced by fibroblasts. The epidermis and the dermis are separated by the basement membrane (BM), an extracellular matrix mainly composed by laminins and type IV collagens, which ensure firm adhesion between dermis and epidermis. It also controls the traffic of cells and bioactive molecules in both directions and is able to bind a variety of cytokines and growth factors (Breitkreutz et al., 2009). The hypodermis or subcutaneous tissue is the innermost layer of the skin composed by connective and adipose tissue, and connects to the underlying fascia of the bones and muscles (OpenStax, 2016). It provides anchorage and lipid storage.

9. Structure of the epidermis.

The epidermis is composed by keratinocytes at different stages of differentiation distributed in different layers (Figure 11). Keratinocytes at the innermost layer of the epidermis, the basal layer or *stratum basale*, proliferate attached to the BM. During the differentiation process keratinocytes modify their biochemical characteristics, migrate throughout the different layers of the epidermis and are finally eliminated from the tissue via shedding (OpenStax, 2016). Terminally differentiated cells must be replaced by new cells produced in the basal layer, which means that the epidermis is a tissue that presents high self-renewal capacity (Watt et al., 2006). During this process the balance between keratinocyte proliferation in the basal layer and differentiation is essential for the maintenance of epidermal homeostasis. This is the reason why the epidermis is considered as an adult developing tissue and a good model for the study of the mechanisms that regulates proliferation and differentiation.

9.1. Basal keratinocytes.

Within the basal layer of the epidermis, keratinocytes can be distinguished in two different proliferative states. On the one hand, we found the stem cells (SC) which possess self-renewal unlimited proliferative capacities. However, epidermal SCs are mainly quiescent and very rarely divide (Niemann and Watt, 2002). On the other hand, we found the transient amplifying cells (also known as TACs) in an active proliferative state. Transition from SC to TAC implies commitment to differentiation. TACs block mitosis after 4 or 5 rounds of fast cell division, loss attachment to the BM and initiate the process of terminal differentiation (Gandarillas and Freije, 2014). Adhesion of keratinocytes to the BM is mediated by integrins, which play an important role in the regulation of differentiation (Adams and Watt, 1989, Watt et al., 1993). Epidermal SCs and TACs can be distinguished by their expression of β 1-integrins (Watt and Jones, 1993), given that SCs express higher levels.

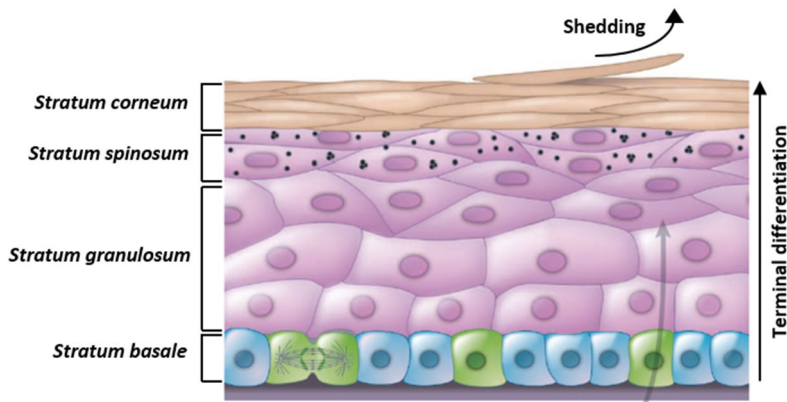


Figure 11 | Structure of the epidermis. Keratinocytes proliferate within the basal layer of the epidermis and migrate throughout the *strata granulosum*, *spinosum* and *corneum* during the process of terminal differentiation. They are finally eliminated from the tissue via shedding (Watt 2014).

9.2. The differentiation program of keratinocytes.

Once keratinocytes in the basal layer of the epidermis lose the attachment to the BM, they activate the differentiation program. During differentiation keratinocytes migrate throughout the different layers and undergo profound morphological and biochemical changes, which mainly consist on changes in the expression of keratins (OpenStax, 2016). Within the basal layer, keratinocytes express keratin K5 (K5) and keratin K14 (K14). However, as the differentiation initiates they switch on the expression of keratin K1 (K1) and keratin K10 [K10; (Fuchs and Green, 1980)]. Keratin filaments composed by K1/K10 form thicker bundles than those formed by basal keratins and provide mechanical integrity to the epidermis (Moll et al., 2008). K1 and K10 are also known as anti-proliferative keratins because they physically prevent proliferation of keratinocytes (Kartasova et al., 1992).

Differentiating keratinocytes from the basal layer are pushed to stratify by the newly proliferating cells and migrate throughout the more superficial layers of the epidermis [Figure 11; (OpenStax, 2016)]. First, keratinocytes enter into the spinous layer or *stratum spinosum* which is immediately above the basal layer. Terminal differentiation is accompanied by an increase in cell size that correlates with the expression of Involucrin, a precursor of the cornified envelope (Sun and Green, 1976, Watt and Green, 1981). Then, keratinocytes continue migration to the granular layer or *stratum granulosum*. In this layer, keratinization continues and keratinocytes present keratohyalin granules mainly containing Involucrin, profilaggrin and loricrin. Finally, as keratinocytes migrate to the outermost layer of the epidermis, the horny layer or *stratum corneum*, keratohyalin granules break up. Their contents are processed to form the cornified envelope just inside the plasma membrane. Keratinocytes in the horny layer are known as corneocytes and become

flatten and polygonal, and lack nuclei and cellular organelles. In this layer, keratinocytes are released from the epidermis via shedding.

10. The epidermis: an endoreplicative tissue.

It has been demonstrated that keratinocytes differentiate in the presence of an active cell cycle (Zanet et al., 2010). Keratinocytes continue DNA synthesis in suprabasal layers of the epidermis (Penneys et al., 1970, Lavker and Sun, 1983, Weinstein et al., 1984, Pierard-Franchimont and Pierard, 1989). While basal keratinocytes are mostly found in G0/G1, suprabasal keratinocytes can be found in any phase of the cell cycle. Notably an increased proportion of differentiating cell is found displaying 4N DNA content, characteristic of the G2 or M phases (Zanet et al., 2010). In addition, mitotic cells are frequently found in suprabasal epidermis. Given that keratinocyte proliferation is restricted to the basal layer of the epidermis, the presence of an active cell cycle in differentiating cell is only explained by endoreplication (Gandarillas and Freije, 2014). Endoreplication consists in DNA re-replication in the absence of cell division (Fox and Duronio, 2013). This can occur via mitosis bypass or mitosis slippage. In the case of mitosis bypass, cell cycle is arrested by the G2 checkpoint and the cell skips mitosis, re-entering in a new phase of DNA synthesis. Mitosis bypass occurs when Cdk1 is inhibited in G2, and requires Cdk2 activity (Kim et al., 2010). During mitosis slippage, however, the cell cycle is arrested at mitosis and exit of mitosis and completion of cytokinesis are inhibited (Andreassen and Margolis, 1994). Progression to anaphase by cyclin B degradation in the presence of an active SAC that impedes chromosome segregation and cytokinesis is necessary for mitotic slippage to occur (Brito and Rieder, 2006). After mitotic slippage, cells do not re-enter into G1 but are maintained in a special G2/M state (Zanet et al., 2010, Mantel et al., 2008). Regardless of the occurring mechanism, endoreplication

arises from the incapability of the cell to maintain an effective G2/M arrest and results in increased DNA content and polyploidy. Although the exact mechanisms triggering endoreplication has not been elucidated yet, turning from a proliferative to an endoreplicative cell cycle seems to rely on a switch in the expression of cell cycle regulators. Endoreplicating cells that do not express Cdk1 or its activators, cyclin B, cyclin A and Cdc25C, but exhibit expression of Cdk2, cyclin E and p-Rb (Edgar and Orr-Weaver, 2001). In concordance, expression of mitotic regulators is loss in suprabasal layer, while expression of S phase regulators is maintained (Zanet et al., 2010). Expression of cyclin E occurs in all the layers of the epidermis but while in the basal layer it is moderate and patchy, it increases and spreads in differentiated layers. Regarding mitotic cyclins A and B, the most positive cells are detected within the first suprabasal layer. Here, cyclins A and B are co-expressed with the terminal differentiation keratins K1 and K10, known anti-proliferative keratins (Kartasova et al., 1992). No cyclin A or B is detected in more superficial layers that markedly express cyclin E.

Endoreplication in the skin might play relevant biological functions and collaborate in the maintenance of tissue homeostasis in many ways (Freije et al., 2012). Indeed, it has been proposed that mitotic slippage is an alternative to apoptosis induced by a prolonged mitotic arrest (Blagosklonny, 2007). Endoreplication allows keratinocytes to increase in size, improving the resistance of skin to mechanical tension. The larger size reduces the number of cells that are needed for a given body surface, limiting the number of cell division within the basal layer and thus the probability of gene mutations due to environmental hazard such as UV light. In addition, amplifying gene copy number renders more efficient the production of mRNA and proteins. Finally, endoreplication acts as an anti-oncogenic barrier that allows proliferating keratinocytes to differentiate when the mitosis checkpoints are activated.

10.1. The differentiation-mitosis checkpoint.

In the epidermis, active proliferation and terminal differentiation are linked by a molecular mechanism that is essential for the maintenance of tissue homeostasis. However, this mechanism is not completely understood yet. Our laboratory has described that keratinocytes possess a checkpoint that activates the differentiation program in response to a prolonged G2/M arrest: the differentiation mitosis checkpoint [DMC; Figure 12; (Gandarillas and Freije, 2014)]. Blocking mitosis by inhibiting Cdk1 or components of the spindle checkpoint, such as Aurora B or Polo-like kinases, activates the DMC and triggers a rapid increase in cell size and expression of differentiation markers (Freije et al., 2012). Activation of the G2/M checkpoints by causing genotoxic insult by doxorubicin or bleomycin also induces this response (Zanet et al., 2010).

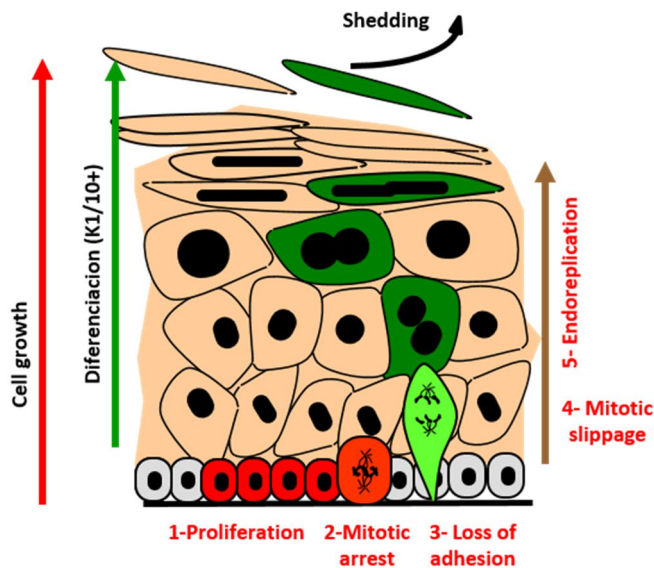


Figure 12 | A prolonged mitotic arrest activates the differentiation-mitosis checkpoint (DMC) and triggers terminal differentiation. Active proliferating keratinocytes suffer a mitotic arrest that results in the loss of adhesion to the BM. As a consequence keratinocytes undergo mitotic slippage, endoreplication and terminal differentiation (Gandarillas & Freije, 2014).

The DMC is also activated in response to S phase deregulation by oncogenic alterations, such as MYC or cyclin E overexpression (Gandarillas and Watt, 1997, Freije et al., 2012). The transcription factor MYC is an oncogene found upregulated in many types of human cancer. Its oncogenic activity relies on its capacity of promote cell cycle entry and progression. MYC activates the expression of essential proteins for G1/S progression such as E2F, Cdk2, Cdk4, Cdk6, cyclin D and cyclin E (Bretones et al., 2015). MYC also represses the expression of the Cdk inhibitors p21^{Cip1} and p27^{Kip1} (Claassen and Hann, 2000, Yang et al., 2001). Due to the DMC, overexpression of MYC or cyclin E in keratinocytes does not lead to uncontrolled proliferation, but to terminal differentiation (Gandarillas and Watt, 1997, Freije et al., 2012). These alterations produce the deregulation of cell cycle and the accumulation of DNA damage due to RS, and activate the G2/M checkpoints (Gorgoulis et al., 2005, Hills and Diffley, 2014). A prolonged G2/M arrest brings about the activation of the DMC, and keratinocytes undergo endoreplication and differentiation (Figure 12). Hence, the DMC contributes to maintain homeostasis by linking proliferation with differentiation and is part of an oncogene-induced differentiation response (OID) that protects the epidermis from oncogenic alterations (Gandarillas, 2012). The OID ensures that dangerous DNA mutations do no longer have undesirable effects, given that cell division is irreversibly blocked. Thus, additional alterations directly involved in mitosis control disrupting the DMC might be needed for carcinogenesis. Indeed, defects in the DMC has been shown to increase genomic instability and malignant progression of squamous cell carcinoma (Alonso-Lecue et al., 2017). Thus, the role of OID in the epidermis might be similar to that of apoptosis or senescence in other systems (Evan and Littlewood, 1998, Halazonetis et al., 2008).

OBJECTIVES

OBJECTIVES

The objectives established in this Thesis were directed to the study of the molecular regulation of the Differentiation-Mitosis Checkpoint of epidermal keratinocytes in response to DNA damage. The specific objectives were:

1. To study the role of tumour suppressor p53 in the Differentiation-Mitosis Checkpoint of human primary keratinocytes.
2. To determine if a cell division block is responsible for squamous terminal differentiation.
3. To analyze the role of the DNA damage response in the normal program of squamous differentiation.
4. To search for the molecular signals that triggers squamous differentiation in response to DNA damage.

MATERIALS & METHODS

MATERIALS & METHODS

1. Cell cultures

Ethical permission for this study was requested, approved and obtained from the Ethical Committee for Clinical Research of Cantabria Council, Spain. In all cases, human tissue material discarded after surgery was obtained with written consent presented by clinicians to the patients, and it was treated anonymously.

1.1. Primary cell culture

Primary human keratinocytes were cultured under high or low calcium concentration conditions. For high calcium concentration (1.2 mM Ca^{2+}) keratinocytes were cultured in the presence of a mouse fibroblast feeder layer J2-3T3 containing the pBabe-PURO plasmid, which confers resistance to puromycin (Rheinwald and Beckett, 1980, Rheinwald, 1989, Gandarillas and Watt, 1997). J2-3T3 cells were inactivated by mitomycin C (*feeders*, 6 $\mu\text{g}/\text{ml}$. Sigma-Aldrich; ref. M0503). Keratinocytes and *feeders* were co-cultured in Rheinwald FAD medium: DMEM/Ham's F12 (3:1 v/v, DMEM: Dulbecco's Modified Eagle Medium. Lonza; ref. BE12-604F. Ham's F12: Lonza; ref. BE12-615F) containing 10% of fetal bovine serum (FBS. Lonza; ref. DE14-8001F), 0.5ng/ml hydrocortisone (Sigma-Aldrich; ref. H0888), 0.01 ng/ml epidermal growth factor (EGF. Sigma-Aldrich; ref. E9644), 0.08 ng/ml cholera toxin (Sigma-Aldrich; ref. C8052), 1.8×10^{-4} M adenine (Sigma-Aldrich; ref. A2786), 5 $\mu\text{g}/\text{ml}$ insulin (Sigma-Aldrich; ref. I5500), 2 mM L-glutamine (Lonza; ref. BE17-605E), 0.75 mM sodium pyruvate (Lonza; ref. BE13-115E) and 100 U/ml penicillin-streptomycin (PenStrep. Lonza; ref. BE17-602E). For low calcium concentration (< 0.1 mM Ca^{2+}) keratinocytes were cultured on Keratinocyte Growth Medium 2 (Promocell; ref. C-20111) or Defined Keratinocyte-SFM (Thermo-Fisher; ref. 10744019). Cells were

cultured at 37°C and 5% CO₂. Culture medium was replaced three times per week.

Before keratinocyte harvesting, dishes were washed with PBS-EDTA (250uM. EDTA: Sigma-Aldrich; ref: E7889; PBS: Lonza; ref. BE17-517Q). In high-calcium cultures, the *feeders* were first removed by pipetting PBS-EDTA insisently. Keratinocytes were detached with PBS-EDTA and trypsin (2:1 v/v, 0.25% Trypsin-EDTA. Thermo-Fisher; ref. 25200-056). Keratinocytes were resuspended and disaggregated by pipetting the cell suspension in Rheinwald FAD medium insisently. Cells harvested were counted using a Neubauer counting chamber and centrifuged at 1,000 rpm for 5 minutes. The supernatant was discharged and the cellular pellet resuspended in FAD medium at a density of 1×10^6 cells per milliliter. When replated under high calcium conditions 4×10^5 keratinocytes in 100 mm dishes were plated. Under low calcium conditions, this number was raised up to 2×10^6 keratinocytes in 100 mm dishes. In this project three strains of keratinocytes from different individual were used: KSH, KSJ and KSP.

1.2. Cell lines.

In addition to primary cells, cell lines used in this project were 3T3-J2, HEK293T and AM12. All of them were cultured in DMEM medium supplemented with 10% donor bovine serum (DONOR. Thermo-Fisher: ref. 16030074), PenStrep and L-glutamine. Telomerase-immortalized N/TERT-2G keratinocytes (Dickson et al., 2000) were grown in Rheinwald FAD medium as primary keratinocytes above.

2. Treatment with chemical inhibitors.

Primary human keratinocytes grown under high calcium conditions were treated with chemical inhibitors for different aims (Table 1). After treatment, keratinocytes were harvested at the lengths of times and the analyses indicated in the assays.

Table II Chemical inhibitors and used concentrations.

Compound	Effect	Company	Reference	Concentration
AZ20	ATR inhibition	Selleckchem	S7050	3 μ M
BI 2536	Plk inhibition	Axon Medchem	1129	10 nM
Doxorubicin	Massive DNA damage	Sigma-Aldrich	D1515	0.5 μ M 0.1 μ M
KU 5593	ATM inhibition	Tocris	3544	1 μ M
Nocodazol	Inhibition of microtubules polymerization	Sigma-Aldrich	M1404	20 μ M
NU 7441	DNA-PK inhibition	Selleckchem	S2638	1 μ M
ZM 44739	AurB inhibition	Tocris	2458	2 μ M

3. Cell infections.

For gene delivery in primary human keratinocytes two different methods were used.

3.1. Retroviral infections.

This method was chosen for stable expression in primary human keratinocytes of the retroviral vectors pBabe-empty, pBabe-MYCER (MYC fusion protein containing the ligand binding domain of a mutant estrogen receptor that responds to 4-OH-hydroxytamoxifen (Freije et al., 2014,

Gandarillas et al., 2000, Gandarillas and Watt, 1997), pMXPIE-empty and pMXPIE-TopBPER [TopBP1 activating domain fused to a mutant estrogen receptor that responds to 4-OH-hydroxytamoxifen (Toledo et al., 2008)]. AM12 producer cells were grown to confluence and treated with mitomycin C for 2 hours. AM12 cells and primary keratinocytes were co-cultured under high calcium conditions for 2 days. AM12 cells were then removed from the cultures by pipetting PBS-EDTA and *feeders* were added to the keratinocyte culture. Puromycin (1 μ g/ml. Sigma-Aldrich; ref. P8833) was added for selection of vector expressing keratinocytes.

3.2. Lentiviral infections.

The following lentiviral vectors were expressed in primary human keratinocytes: pLKO1-empty, pLKO1-shp53-427, pLKO1-shH2AX, pLKO1-shATR, pLVHTM-GFP, pLVHTM-shp53-GFP, pLVX-empty, pLVX-proAREG, pLVX-FOXM1, pLenti4/Block-iT-DEST-shEGFP and pLenti4/Block-iT-DEST-shAREG (constructs expressing shEGFP or shAREG under the control of a tetracycline (TET)-regulated histone H1 promoter). Lentiviral production was performed by transient transfection of HEK293T cells. HEK293T cells were transfected at 70% percent of confluence with a plasmid expressing the protein envelope of the virus pCl-VSVG (3 μ g. Addgene; ref. 11653), the packing plasmid psPAX2 (7.5 μ g. Addgene; ref. 12260) and the plasmid of interest (10 μ g). jetPEI (VWR, ref. 101-01) was used as transfection reagent. 5×10^8 HEK293T cells were plated in 100 mm dishes the day before transfection. 90 μ l of jetPEI were diluted in 660 μ l of NaCl 150 mM. The three plasmids described above were resuspended in a final volume of 750 μ l of NaCl 150 mM. JetPEI and plasmid solutions were mixed and incubated for 20 minutes at room temperature. The mix was then added to the HEK293T cultures.

For keratinocyte infection under high calcium concentration conditions, HEK293T cells were incubated with the transfection mix for 8 hours and fresh medium was added (DMEM 10% DONOR serum). 8 hours before keratinocyte infection HEK293T cells medium was replaced by Rheinwald FAD medium for keratinocytes. 5×10^5 primary human keratinocytes were plated in 10 mm dishes in the presence of *feeders* and Rheinwald FAD medium. 6 hours later HEK293T supernatant was collected and filtered through 22 μm filters (Merk-Millipore; ref. SLGP033RB). Polybrene infection reagent (8 $\mu\text{g}/\text{ml}$, Sigma-Aldrich; ref. H9268) was added to the filtered supernatant. The supernatant was added to keratinocyte cultures. The infection was performed at 37°C and 5% CO₂ overnight. Supernatant was removed and fresh Rheinwald FAD medium was added to the cultures.

For keratinocyte infection under low calcium concentration conditions 2×10^6 primary human keratinocytes were plated in 10 mm dishes the day before infection in Keratinocyte Growth Medium 2. HEK293T cells were incubated with the transfection mix overnight and then fresh medium was added (DMEM 10% DONOR serum). 8 hours later, Keratinocyte Growth Medium 2 was added to the HEK293T cultures and cells were incubated overnight. Supernatant was collected, filtered and supplemented with polybrene infection reagent. Keratinocytes were incubated with supernatant for 8 hours at 37°C and 5% CO₂. Supernatant was removed and Defined Keratinocyte-DSF medium was added.

4. Clonogenicity assays.

For clonogenicity assays keratinocytes were plated at low densities (5,000 cells per well) with *feeders* and Rheinwald FAD medium in 6 well plates. After 12-14 days, wells were washed with cold PBS and fixed with formaldehyde (3.7%, Sigma-Aldrich; ref. F8775) for 10 minutes. Wells were

then washed again with cold PBS and stained with Rodamine-Nile Blue solution (Rodanile: 1% Rodamine B, Sigma-Aldrich; ref. R6626, 1% NileBlue. Sigma-Aldrich; ref. N5632) in distilled water (Watt and Jones, 1993). Wells were washed with distilled water three times.

5. Flow cytometry

Flow cytometry was performed on a Becton Dickinson BD FACS Canto™ cytometer (Franklin Lakes, NJ, USA) and analyzed by BD FACS Canto software. To minimize the presence of aggregated cells each sample was resuspended and filtered through 70 µm filters. For each sample a total of 10,000 events were acquired excluding cell debris. Specifications about primary and secondary antibodies can be found in Table 2 and 3.

5.1. DNA content.

DNA content analysis was performed as described (Freije et al., 2012). Harvested cells were washed with cold PBS and centrifuged twice at 1,000 rpm for 5 minutes at 4°C. Cells were then fixed in 1 ml 70% cold ethanol (ETOH. Sigma-Aldrich; ref. 02860) and vortexed vigorously for 1 minute. Fixed cells were maintained at 4°C for at least 30 minutes. Cells were washed with 2 mL PBS 0.5% FBS and centrifuged 5 minutes at 2,000 rpm at 4°C. Cells were then resuspended in 500 µl of the solution RNAsa (100 µg/ml, Thermo-Fisher; ref. 12091-021), propidium iodide (PI. 25 µg/ml, Thermo-Fisher; ref. P3566) and PBS. Cells were incubated overnight at 4°C.

5.2. DNA synthesis.

Cells were treated with Bromodesoxyuridine (BrdU. 10 uM, Sigma-Aldrich; ref. B5002) for 1.5 hours before harvest. BrdU untreated negative controls were also carried out. Once harvest cells were washed twice, centrifuged and

fixed in 70% cold ethanol. Cells were then washed with washing buffer, PBS 5% FBS and 0.5% Tween 20 (Sigma-Aldrich; ref. P1379) and centrifuged 5 minutes at 2,000 rpm at 4°C (Zanet et al., 2010). The supernatant was removed and cells were treated with 2 M HCl (Merk-Millipore; ref. 100319) at room temperature for 20 minutes. Cells were washed twice with 0.1 M sodium tetraborate (NaB_4O_7 , Sigma-Aldrich; ref. 221732) and once with the washing buffer described above. Cells were incubated with primary antibody anti-BrdU for 1 hour at room temperature. Cells were washed twice with washing buffer and incubated with the secondary antibody AlexaFluor[®] 488 anti-mouse IgG for 1 hour at room temperature in darkness. Cells were washed twice with washing buffer and stained with PI as described above.

5.3. Protein expression.

The expression of the epidermal differentiation markers Involucrin, K1 and K16 and the DNA damage marker γH2AX was analyzed by flow cytometry.

For Involucrin expression analyses cells were harvested and fixed in 3.7% paraformaldehyde (PFA, Sigma-Aldrich; ref: STBB5309) for 10 minutes. Cells were then washed twice with PBS containing 0.5% FBS and permeabilized with 0.3% saponin (Sigma-Aldrich; ref. S4521) for 20 minutes at room temperature. Samples were washed twice with washing buffer PBS containing 5% FBS and 0.1% saponin and centrifuged at 2,000 rpm. Cells were incubated for 1 hour at room temperature with primary antibody anti-Involucrin. After washed twice, cells were incubated for 1 hour at room temperature with corresponding secondary antibody.

For keratins K1, K16 and γH2AX cells were harvest, fixed with 70% cold ethanol and vortex vigorously for 1 minute. Cells were washed twice with washing buffer PBS, 5% FBS and 0.5% Tween 20 and centrifuged at 2,000 rpm. Cells were incubated for 1 hour with primary antibody at room

temperature. After washed twice, cells were incubated for 1 hour at room temperature with corresponding secondary antibody.

6. Immunofluorescence.

6.1. Immunofluorescence on cultured cells.

Cells were cultured on round glass coverslips and fixed with methanol (MeOH) at -20°C for 10 minutes. For Involucrin detection cells were fixed with 3.7% formaldehyde (FHO) for 10 minutes and permeabilized with -20°C MeOH for 5 minutes. After fixation, samples were washed with PBS twice and for the last wash with PBS 0.05% Tween 20 (PBS-Tween). Samples were incubated with the primary antibody (Table 2) for 1 hour at room temperature. Samples were washed twice with PBS and once with PSB-Tween, and incubated with the corresponding anti-mouse or anti-rabbit secondary antibody for 1 hour in darkness at room temperature (Table 3). Nuclear DNA was stained with DAPI (0.2 µg/ml. Sigma-Aldrich; ref. D9542) for 10 minutes. Coverslips were mounted using Prolong Gold antifade mountant reagent (Thermo-Fisher; ref. P36934) and visualized with the fluorescence microscope Zeiss Imager D2 with Axio Cam MRm camera and light source for fluorescence illumination HXP 120C Ku;bler codex.

6.2. Immunofluorescence on frozen tissue.

Fat and connective tissue were removed from neonatal foreskin samples before their inclusion in O.C.T. compound (Sakura Tissue-TEK; ref. 4583). After inclusion samples were frozen in isopentane (ITW; ref. 123501) and submerged in liquid nitrogen. Frozen samples were stored at -80°C. Samples were sectioned with a cryostat in 10-12 µm sections, which were collected in Superfrost Plus microscope slides (Thermo-Fisher; ref. J1800AMNZ). For immunofluorescence detection sections were fixed 10 minutes with

MeOH -20°C, or 10 minutes with 3,7% FHO and permeabilized with MeOH -20°C for 5 minutes or 0.5% Triton X-100 (Sigma-Aldrich; ref: 9002-93-1). Samples were then washed and incubated with primary and secondary antibodies as described in section 6.1. Nuclear DNA was stained with DAPI. Slides were mounted using Prolong Gold antifade mountant reagent. Specifications about primary and secondary antibodies can be found in Table 2 and 3.

Table III Primary antibodies used by flow cytometry (FACS), immunofluorescence (IF) or western blot (WB). *IgG used as negative controls. ** Negative controls are used at the same concentration of the corresponding primary antibody. *** Unknown. **** Provided by Oskar Fernandez-Capetillo.

Primary antibodies						
Antibody	Host	Company	Reference	Dilution		
				FACS	IF	WB
* IgG	Mouse	Sigma-Aldrich	I-5381	**	-	-
* IgG	Rabbit	Sigma-Aldrich	R9133	**	-	-
53BP1	Rabbit	Bethyl	A300-272A	-	1:200	-
β1-integrin (P5D2)	Mouse	***	***	-	1:50	-
BrdU	Mouse	Benton-Dickinson	347580	4μ	-	-
BrdU	Mouse	Sigma	B8434	-	1:50	-
Cyclin A (H-432)	Mouse	Santa Cruz	sc-751	-	1:50	1:500
Cyclin B (GNS1)	Mouse	Santa Cruz	sc-245	-	1:100	1:500
Cyclin E (HE12)	Mouse	Santa Cruz	sc-247	-	1:50	1:100
ER (MC20)	Rabbit	Santa Cruz	sc-542	-	-	1:500
ER (Mouse Estrogen cret94D:H9)	Mouse	****	****	-	Pure	1:10
FOXM1	Rabbit	Santa Cruz	sc-502	-	1:100	1:500
GAPDH (0411)	Mouse	Santa Cruz	sc-47724	-	-	1:200

γ H2AX	Mouse	Merk-Millipore	05-636	1:250	1:1000	1:500
γ -tubulin (GTU-88)	Mouse	Sigma-Aldrich	T 6557	-	1:300	-
H2AX (C20)	Mouse	Santa Cruz	sc-54606	-	1:1000	1:500
Involucrin (SY5)	Mouse	Sigma-Aldrich	I-9018	1:50	1:100	1:5000
Keratin 1 (AF87)	Rabbit	BioLegend	PRB-149P	1:60	1:100	-
Keratin 5 (C-terminal)	Rabbit	Sigma-Aldrich	ESAB4501651	-	1:100	-
Keratin 8 (M20)	Mouse	Sigma-Aldrich	C5301	-	1:100	1:500
Keratin 16	Mouse	Santa Cruz	sc-53255	1:100	-	-
p21 (CP47)	Mouse	Sigma-Aldrich	P1484	-	-	1:1000
p53 (FL393)	Mouse	Santa Cruz	sc-6243	-	1:100	1:1000
p-ATM:ATR substrates	Rabbit	Cell Signalling	2851S	-	1:100	-
p-H3 (Ser10)	Rabbit	Santa Cruz	sc-8656-R	-	-	1:500

6.3. Immunofluorescence on paraffin-embedded tissue

Paraffin-embedded skin sections on Superfrost Plus microscope slides were deparaffinated by incubation at 55°C during 15 minutes. For rehydration prior to staining, samples were immersed 3 times in xylol for 5 minutes each time, 3 times in pure ethanol for 5 minutes each time, 5 minutes in 90% ethanol, 5 minutes in 50% ethanol and washed 5 minutes with distilled water. For antigen retrieval, samples were immersed in retrieval buffer (distilled water containing 1.8% of 100 mM monohydrate citric acid and 8.2% of 100 mM dehydrate sodium citrate) and boiled in a microwave at 900 W. Then, samples were incubated at 150 W for 15 minutes and chilled at room temperature for 20 minutes. Samples were next washed with distilled water.

For autofluorescence blocking, sections were incubated for 30 minutes at room temperature in 100 mM NH₄Cl and washed with PBS 3 times for 5 minutes each time. Samples were then incubated for 1 hour in PBS containing 8% of goat serum (Thermo-Fisher; ref. 16210064) and 1% bovine albumin serum (BSA, Sigma-Aldrich; ref. A6003). Samples were washed twice with PBS and once with PBS 0.05% Tween 20, and incubated with primary antibodies diluted in 2% BSA over night at 4°C. Samples were then washed twice with PBS and once with PBS 0.05% Tween 20, and incubated with secondary antibodies diluted in 2% BSA 1 hour at room temperature in darkness. After washing 3 times with PBS, samples were incubated 10 minutes with DAPI as in section 6.1. Slides were mounted using Prolong Gold antifade mountant reagent. Specifications about primary and secondary antibodies can be found in Table 2 and 3.

6.4. Run-on transcription assay.

For detection of nascent RNA *in cellula*, primary human keratinocytes were cultured on coverslips and incubated for 20 minutes with 5'-fluorouridine (5-FU, Sigma-Aldrich; ref. F5130) to a final concentration of 2 mM. Cells were then washed with HEPES buffer (30 mM Hepes, 65 mM Pipes, 2 mM EGTA and 2 mM MgCl₂) and fixed with 3.7% PFA in HEPES buffer containing 0.5% Triton X-100 for 10 minutes. The incorporation of 5'-FU into nascent RNA was detected with an antibody against halogenated UTP for 1 hour at room temperature. Samples were washed twice with 0.05% Tween 20 in PBS and incubated with corresponding secondary antibody (Table 3) for 1 hour at room temperature.

For double detection of nascent RNA and cyclin A expression, samples were co-incubated for 1 hour at room temperature with anti-BrdU and anti-cyclin A primary antibodies. After washing, samples were co-incubated for 1

hour at room temperature with corresponding secondary antibodies. DNA was stained with DAPI as described in section 6.1. Specifications about primary and secondary antibodies can be found in Table 2 and 3.

7. Protein analysis by Western Blotting.

Cells were harvested by PBS-EDTA and trypsin and were centrifuged at 12,000 rpm for 30 seconds. Cell pellets were stored at -20°C until the moment of lysis. Lysis buffer [150 mM NaCl 4M, 50 mM Tris 1M pH 8, 20 mM NaF 1M, 1% Np40, 1 mM EDTA 0.5M pH 8, 0.2% SDS 10%, 1X phosphatases inhibitor (Thermo-Fisher; ref. 88667)] and protease inhibitor (1:100. Merck-Millipore; ref. 539131) were added directly to the cell pellets and mixed by pipetting. Cells were incubated with lysis buffer for 10 minutes on ice and mechanical lysis was performed by pipetting. This process was repeated three times, up to 30 minutes. Lysates were centrifuged at 12,000 rpm for 15 minutes at 4°C, supernatants were collected and stored at -80°C. Protein quantification was performed using the fluorometric system Qubit 4.0 (Life Technologies).

Samples (50-80 µg of protein) were mixed with loading buffer [4X Laemli buffer (BioRad; ref. 1610747), 100 nM Tris-HCl 1M pH 6.8, 4% SDS, 20% glycerol, 8% B-mercaptoethanol and 0.1% blue bromophenol] and heated at 95°C for 5 minutes. Samples were then loaded into polyacrylamide-SDS gels. The percent of polyacrylamide was adjusted to 10% for proteins with molecular weight higher than 40 kDa, and to 12% for proteins with lower molecular weight. Vertical electrophoresis was performed using Mini-Protean II (Bio-Rad) with 1XTris/Glycin electrophoresis buffer (Bio-Rad; ref. 161-0771) in distilled water containing 0.1% SDS. Proteins were then transferred to a PROTAN^R nitrocellulose membrane (GE healthcare; ref. 10600002) for 2 hours and 15 minutes at 260 mA/cm², or for 30 minutes at

400 mA/cm² in the case of proteins with molecular weight lower than 40 kDa. Transference was performed using Mini-Protein II with 1X Tris/Glycin transfer buffer in distilled water containing 10% MeOH and 0.01% SDS. After transference, the membrane was stained with Ponceau red [0.1% Ponceau red (Sigma-Aldrich; ref. P3504), 5% acetic acid (ITW; ref. 141008) in distilled water] for protein detection. The membrane was then washed first with NaOH 0.1 M (Sigma-Aldrich; ref. S8045) and finally with distilled water. For blocking non-specific binding, the membrane was incubated for 1 hour at room temperature in TTBS containing 5% milk (TTBS: 120 mM NaCl, 20 mM Tris 1M pH 7.5, 0.1% Tween-20 in distilled water). The membrane was then incubated with primary antibody at 4°C over-night. Primary antibodies used are listed in Table 2.

Table III Secondary antibodies used by flow cytometry (FACS), immunofluorescence (IF) and western blot (WB).

Secondary antibodies						
Antibody	Host	Company	Reference	Dilution		
				FACS	IF	WB
Alexa Fluor [®] 488- conjugated	Mouse	Jackson ImmunoResearch	115-547- 003	1:100	1:100	-
Alexa Fluor [®] 488- conjugated	Rabbit	Jackson ImmunoResearch	111-547- 003	1:100	1:100	-
Dylight [™] 594- conjugated	Mouse	Jackson ImmunoResearch	115-517- 003	-	1:100	-
Dylight [™] 594- conjugated	Mouse	Jackson ImmunoResearch	111-517- 003	-	1:100	-
Dylight [™] 800- conjugated	Mouse	Thermo-Fisher	35521	-	-	1:100000

Dylight™ 800- conjugated	Rabbit	Thermo-Fisher	35521	-	-	1:100000
H+L horseradish peroxidase conjugated	Mouse	Biorad	170-6516	-	-	1:100000
H+L horseradish peroxidase conjugated	Rabbit	Biorad	170-6516	-	-	1:100000

The membrane was washed twice with TTBS for 15 minutes and incubated with the corresponding anti-mouse or anti-rabbit secondary antibody for 1 hour at room temperature (Table 3). Protein exposure was performed by the Odyssey Infrared Imaging System (Li-cor), specifically for the detection of γ H2AX, or by the Chemiluminescence Imaging System Fusion Solo (VilberLourmat).

8. mRNA analysis by Quantitative Real-Time PCR (Q-RT-PCR)

Cells were harvested and centrifuged as for western blotting. Cell pellets were stored at -20°C until the moment of RNA extraction. The RNA isolation NucleoSpin^R kit (Macherey-nagel; ref. 740955) was used, according to the instructions of the manufacturer. RNA quantification was performed by spectrophotometry by Gen 5™ with the accessory for RNA Take 3 micro-volume (Biotek) or by fluorometry using Qubit 4.0. For assessing RNA integrity, an electrophoresis gel was performed. 1 μ g of each sample stained with loading buffer (Sigma-Aldrich; ref. G2526-5ML) was applied onto a 1% agarose gel in distilled water containing 0.05% Tris-borate-EDTA buffer (TBE, Thermo-Fisher; ref. T/P050/15). Electrophoresis was performed with ENDURO™ Gel XL Electrophoresis System (Labnet) at 100V for 15 minutes. The RNA obtained was stored at -80°C.

Given the instability of RNA, it is necessary an intermediate step before quantification where complementary DNA (cDNA) is generated by retro-transcription. For this aim, the iScript™ cDNA Synthesis Kit (Bio-Rad) was used. Retro-transcription was performed using 1µg of RNA in the presence of deoxynucleotides and reverse transcriptase RNase H+. Oligonucleotides random hexamers were used as primers. The thermocycler (Mj mini Bio-Rad) was programmed for a first incubation of 5 minutes at 25°C, a second incubation of 30 minutes at 42°C, a third incubation of 5 minutes at 85°C and a final incubation of 10 minutes at 25°C. The cDNA obtained was stored at -20°C.

9. Comet assay

Alkaline comet assay for detection of DNA strand breaks was performed as described (Ritchie et al., 2009). Glass slides must be previously treated to ensure optimal adhesion of agarose. Slides were first immersed in ether-ethanol (1:2) for 1 hour and then in ethanol 70% for 30 minutes. They were dried and covered with 0.5% normal melting agarose (CondaLab; ref. 8016) in distilled water. Slides were then dried at 65°C for 5 minutes.

Cells were harvested by PBS-EDTA and trypsin in darkness. 50,000 cells were resuspended in 20 µl of PBS and 75µl of 0.5% low-melting agarose (LMA, Thermo-Fisher; ref: 15517-014) in distilled water previously melted and maintained at 37°C. 90µl of this mix were pipetted on the slide and covered with a coverslip. Slides were incubated for 10 minutes at 4°C. The coverslip was then removed. 75 µl of LMA 0.5% were added to the slide and this was covered with a new coverslip. Slides were incubated for 10 minutes at 4°C. The coverslip was removed and samples were incubated for

1 hour at 4°C in darkness in cold lysis solution containing 10% DMSO, 1% Triton X-100 and 89% lysis buffer pH=10 (NaCl 2.5M, EDTA 100 mM, Tris 10 mM, NaOH 200 mM). Samples were then incubated in cold electrophoresis buffer (83% EDTA 0.1 M, 17% NaOH 300 mM) for 20 minutes in darkness. Electrophoresis was performed at 25V for 20 minutes in electrophoresis buffer at 4°C in darkness. Samples were washed twice with neutralizing buffer (Tris 400 mM; pH = 7.5) and fixed with pure ethanol. Once dried, samples were stained with RedSafe 1:500 (JHSience; ref. 21141).

10. Transcriptome analysis

Total RNA was isolated from keratinocytes collected 30 hours after infection with shp53-427 or the corresponding empty vector, or 16h after treatment with Doxorubicin, ZM 447439 or BI 2536. In the case of shp53-427 experiments, the RNA isolation NucleoSpin^R kit was used and RNA samples were sent to the Centro Nacional de Análisis Genómico (CNAG) for their quantification and quality control. DNA libraries were prepared and sequenced by CNAG procedures. Each library was sequenced in paired-end mode with a read length of 2x76bp. At least, 40 million paired-end reads were generated. RNA from the remaining samples (Doxorubicin, ZM and BI) was isolated using DNA/RNA Mini Kit (Quiagen). These samples were sent to the Sequencing core of the University of Michigan for library preparation and sequencing. Each library was sequenced in single-end mode with a read length of 2x76bp. At least, 400 million single-end reads were generated.

Reads were mapped using STAR (Dobin et al., 2013) and gene expression levels were measured and normalized by HTSeq (Anders et al., 2015) and DESeq2 (Love et al., 2014). This was done in collaboration with the Group

of JT Elder at the University of Michigan (laboratory of Genetics of psoriasis and psoriatic arthritis, Department of Dermatology) where I spent an EMBO short-term stay. Differentially expressed genes (DEGs) were identified based on their p value < 0.05 . The Database for Annotation, Visualization, and Integrated Discovery (DAVID, <http://david.abcc.ncifcrf.gov/>) was used to classify the DEGs according to their biological functions by using the Gene Ontology (GO) Consortium Reference [<http://www.geneontology.org/>; (Ashburner et al., 2000, Huang da et al., 2009)].

RESULTS

ROLE OF p53 IN THE DIFFERENTIATION-MITOSIS CHECKPOINT OF HUMAN KERATINOCYTES.

In our aim to elucidate the mechanism that activates the DMC in human keratinocytes, we focused on the tumor suppressor protein p53. p53, also known as “the guardian of the genome”, is a transcription factor with an important role in the regulation of the cell cycle (Lane, 1992). It responds to DNA damage by activating the G1 and G2 cell cycle checkpoints via its transcriptional targets (Giono and Manfredi, 2006). In addition, it also activates the apoptotic pathway in case DNA damage cannot be repaired (Canman et al., 1994). Hence, we hypothesized that p53 might be mediating the differentiation response of primary keratinocytes. This work constituted in part my Master project and continued during the first year of my Thesis. The results obtained were published in *Cell Reports* (Freije et al., 2014) and the publication is included in this Thesis as an annex.

1. Inactivation of a temperature-sensitive p53 mutant protein promotes differentiation, whereas its inactivation attenuates it.

My participation in this work consisted in the overexpression of a retroviral construct carrying a conditional mutant form of p53 (p53ts), whose conformation state can be regulated by temperature (Michalovitz et al., 1990). At 32°C, p53ts displays the wild-type conformation, whereas at 39°C it adopts an inactive conformation and behaves as a dominant-negative mutant. Primary human keratinocytes were efficiently infected with the p53ts construct and the protein was overexpressed, as detected by western blot and immunofluorescence 48h after the temperature switch to 32°C or 39°C (Figure 13.A and B). Interestingly, we found that p53 accumulated in binucleated differentiating keratinocytes when cultured at 39°C (Figure 13.B, white arrow). In addition, by western blotting we observed that p53ts failed

to transactivate its target p21^{Cip} in response to Doxorubicin (DOXO) when keratinocytes were cultured at 39°C (Figure 13.C). Doxorubicin is a molecule that produces severe DNA damage during DNA replication by intercalation and inhibition of the progression of topoisomerase II (Fornari et al., 1994, Momparler et al., 1976). In keratinocytes DOXO induces terminal differentiation within 48h (Freije et al., 2012). This indicated that the conformational change to the inactive p53ts form was efficiently induced by temperature.

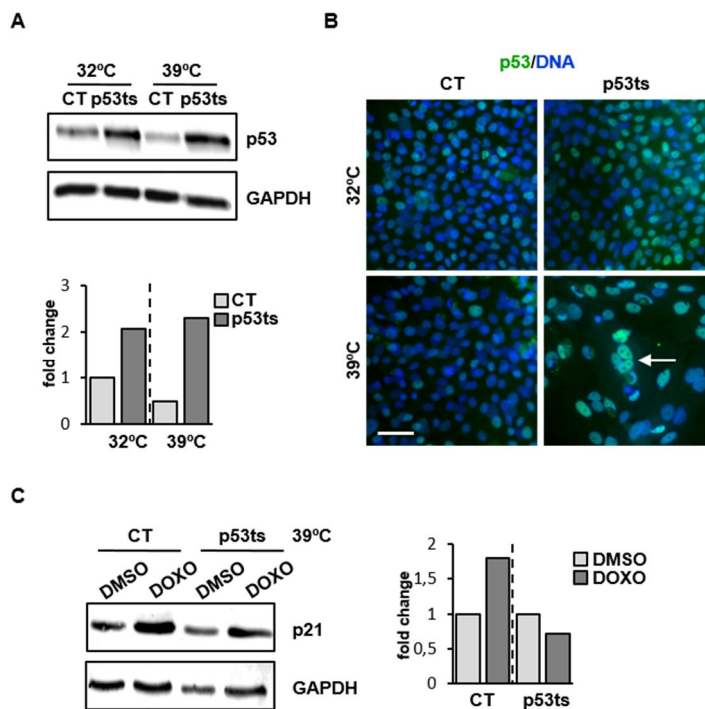


Figure 13 | p53ts is efficiently overexpressed and inactivated in primary keratinocytes at 39°C. **A)** Detection of p53 by western blotting in keratinocytes expressing control vector (CT) or the thermosensitive mutant p53 (p53ts) 48h after the temperature switch to 32°C or 39°C. Bottom histogram shows quantification of p53 western blot normalized to the loading control GAPDH. **B)** Immunofluorescence for p53 (green) on p53ts expressing keratinocytes as in A. White arrow: p53 accumulates in binucleated differentiating keratinocytes when cultured at 39°C. Nuclear DNA by DAPI. Scale bar: 50 μ m. **C)** Detection of p21^{Cip} (p21) by western blot in CT and p53ts keratinocytes cultured at 39°C, treated for 24h with

Doxorubicin (DOXO) or DMSO. Bottom histogram shows quantification of p21 western blot normalized to the loading control GAPDH.

Once we confirmed that the inactivation of p53 was efficiently achieved, we analysed its effect in the differentiation response of keratinocytes. Proliferative and differentiating keratinocytes can be distinguished by flow cytometry based on their light scatter parameters (Jones and Watt, 1993). As they differentiate, keratinocytes increase in size (forward scatter) and complexity (side scatter). As measured by flow cytometry, induction of the active p53 conformation at 32°C increased the proportion of cells with basal-like low-scatter parameters and diminished the proportion of cells expressing the differentiation markers Involucrin and Keratin K16 (K16; Figure 14.A), suggesting that wild type p53 retains keratinocytes in the proliferative compartment. Conversely, inactivation of p53 by the 39°C temperature switch resulted in increased differentiation, as measured by the increase in the light scatter parameters typical of differentiation and the expression of Involucrin and K16 (Figure 14.B). By immunofluorescence, we observed that while p53 was absent from suprabasal keratinocytes at 32°C, it accumulated in suprabasal Involucrin-positive cells at 39°C (Figure 15.A). It is well established that active p53 is degraded when terminal differentiation initiates, probably by an auto-regulatory feedback loop with MDM2 (Dazard et al., 2000, Haupt et al., 1997). Most p53 mutations avoid its degradation and result in protein accumulation (Lane, 1992, Aylon and Oren, 2011). Hence, accumulation of p53 in differentiating keratinocytes further indicated that the protein was inactive at 39°C. Consistently with the induction of differentiation, the inactive p53 form decreased the proliferative colony forming potential of keratinocytes at 39°C (Figure 15.B, top). The loss of clonogenic capacity was not rescued once cells were returned to 37°C (Figure 15.B, bottom), confirming that inactivation of p53 irreversibly triggers squamous differentiation (Freije et al., 2014).

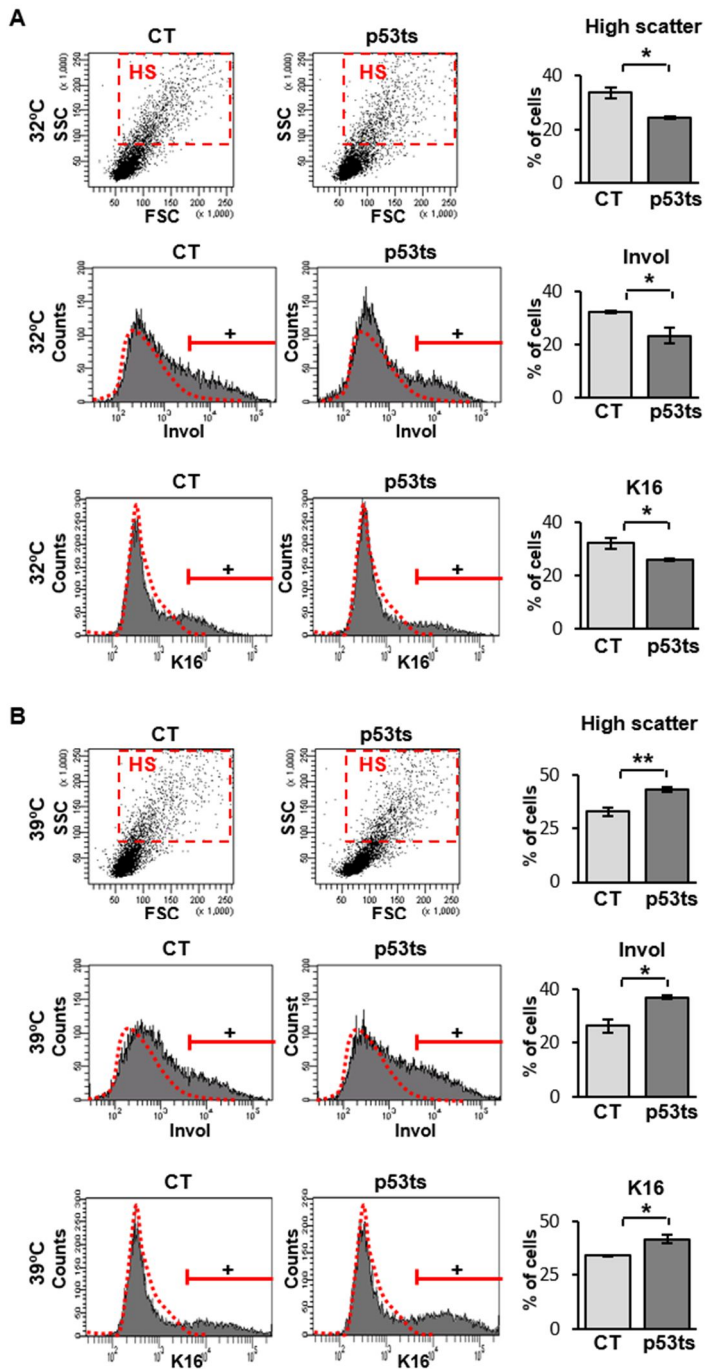


Figure 14 | Inactivation of p53ts induces terminal differentiation of primary keratinocytes. **A**) Left: analyses of light scatter parameters (top; SSC: side scatter, FCS:

forward scatter), Involucrin (middle; Involucrin: Invol) or Keratin K16 expression (bottom; K16: Keratin 16) of CT and p53ts keratinocytes cultured at 32°C for 6 days, detected by flow cytometry (+, positive cells according to negative isotype antibody control, red broken line). Red broken line in top dot plot histogram represents cells with high scatter parameter (HS). Bar histograms (right) represent the percent of cells with HS parameters, Involucrin or K16 expression (top, middle and bottom, respectively). **B)** Left: analyses of light scatter parameters (top), Involucrin (middle) or K16 expression (bottom) of CT and p53ts keratinocytes cultured at 39°C for 6 days, detected by flow cytometry. Bar histograms (right) represent the percent of cells with HS parameters, Involucrin or K16 expression (top, middle and bottom, respectively). p value: * <0.05 , ** <0.01 .

2. The differentiation response induced by loss of p53 is unaffected by ectopic AREG expression.

NTERT is an immortalized epidermal cell line that ectopically expresses the human telomerase (hTERT) catalytic subunit and is deficient in p16^{INK4A} expression (Dickson et al., 2000). p16^{INK4A} negative cells appeared stochastically from the hTERT cultures and are likely to have a clonal origin. NTERT escape from senescence but retain the expression of normal keratinocytes differentiation markers in organotypic cultures. AREG is an EGF-related factor whose silencing has been shown to inhibit NTERT keratinocyte proliferation by inducing differentiation through mitotic failure. As results, cells accumulated in the polyploid compartment of the cell cycle (Stoll et al., 2016). This effect was rescued by the ectopic expression of FOXM1 (Stoll et al., 2016), suggesting that AREG controls keratinocytes cell division. It has been reported that AREG is directly activated by p53 in response to DNA damage (Taira et al., 2014). Thus, we wondered whether the activation of the DMC by p53 loss could be rescued by overexpression of AREG. To elucidate this question we first inhibited AREG expression in primary human keratinocytes and analysed the effect. Keratinocytes were infected with a lentiviral construct expressing tetracycline (TET)-inducible short-hairpin RNA (shRNA) against AREG or EGFP (CT). By quantitative

RT-PCR we checked that AREG expression was efficiently silenced after addition of TET (1 $\mu\text{g}/\text{ml}$) to the culture medium (Figure 16.A). As expected, AREG silencing inhibited cell proliferation and increased cell size (Figure 16.B and C). Notably, we observed that keratinocytes became binucleated (Figure 16.B). By quantitative RT-PCR, we observed that AREG silencing increased the expression of the differentiation marker Keratin K1 (K1; Figure 16.D). Hence, our results confirmed that AREG silencing inhibited proliferation of primary keratinocytes by activating the squamous differentiation program.

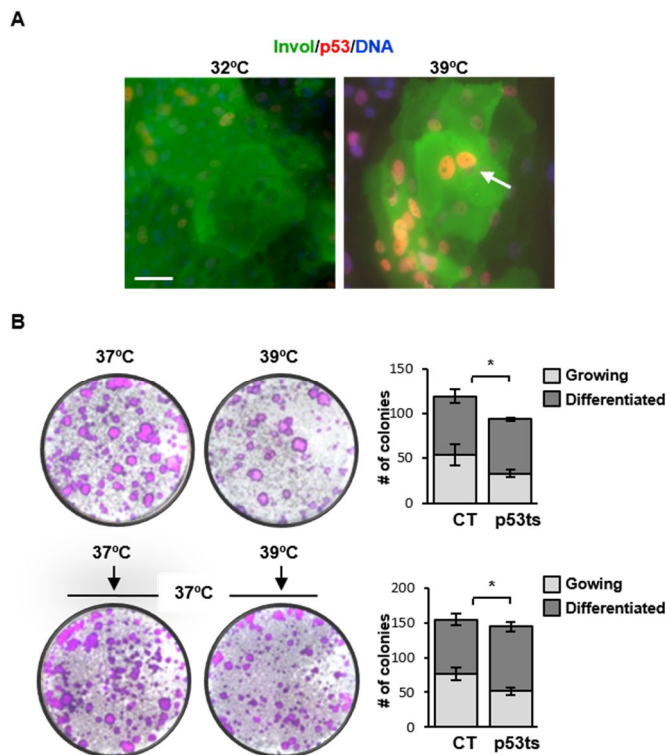


Figure 15 | Inactivation of p53ts irreversibly inhibits the colony forming potential of primary keratinocytes. A) Immunofluorescence for Involucrin (Invol; green) and p53 (red) on p53ts keratinocytes cultured at 32°C or 39°C for 4 days. White arrow: suprabasal involucrin-positive keratinocytes accumulate p53. Nuclear DNA by DAPI. Scale bar: 50 μm . **B)** Top: Clonogenic capacity of p53ts keratinocytes cultured at 37°C or 39°C. Bottom: Clonogenic capacity of p53ts keratinocytes cultured at 37°C or 39°C for 5 days and returned

to 37°C. Right histogram represents the number of growing or differentiated colonies after the temperature switch to 39°C (top) and after temperature release to 37°C (bottom). p value: * <0.05 .

We next ectopically expressed AREG in primary keratinocytes after silencing p53 and analysed its effect in the activation of the DMC. Keratinocytes were infected with a lentiviral construct carrying full length AREG (proAREG) or the corresponding empty vector (CT1). Cells stably expressing the construct were then selected with puromycin and subsequently infected with a lentiviral construct carrying shRNA against p53 (shp53), or the corresponding empty vector (CT2). p53 silencing inhibited keratinocyte proliferation and induced cell shedding as described [(Figure 17.A; (Freije et al., 2014)].

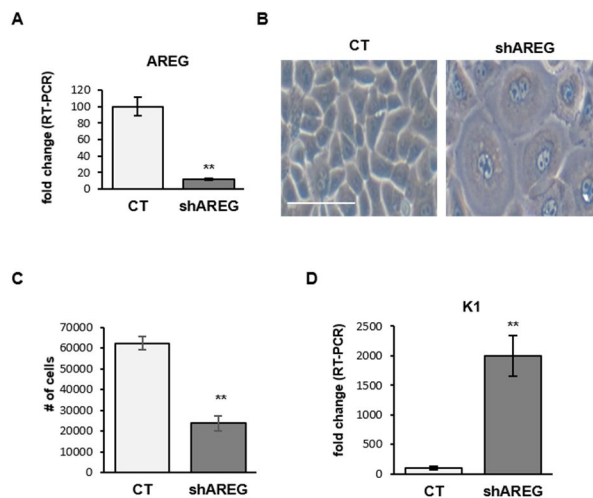


Figure 16 | AREG silencing induces terminal differentiation of primary keratinocytes. **A)** Detection of AREG expression in primary human keratinocytes infected with an shRNA against AREG (shAREG) or EGFP (CT), 5 days after addition of tetracyclin (+TET). **B)** Phase contrast images from primary keratinocytes infected with shAREG or CT, 5 days after addition of TET. Scale bar: 50 μ m. **C)** Bar histogram representing the number of primary keratinocytes infected with shAREG or CT that were collected 5 days after addition of TET.

D) Detection of Keratin 1 (K1) expression in primary keratinocytes infected with shAREG or CT, 5 days after addition of TET. p value $**<0.01$.

By flow cytometry we confirmed an increase in the expression of the differentiation marker K1 (Figure 17.B and C). Hence, as we expected, p53 silencing activated the DMC of keratinocytes. Overexpression of proAREG did not inhibit this response. Keratinocytes lacking p53 and expressing proAREG stopped proliferation, started shedding, and increased the expression of K1 even further than cells non-expressing proAREG (Figure 17). We concluded that forcing AREG expression was not sufficient for the inactivation of the DMC in the absence of p53.

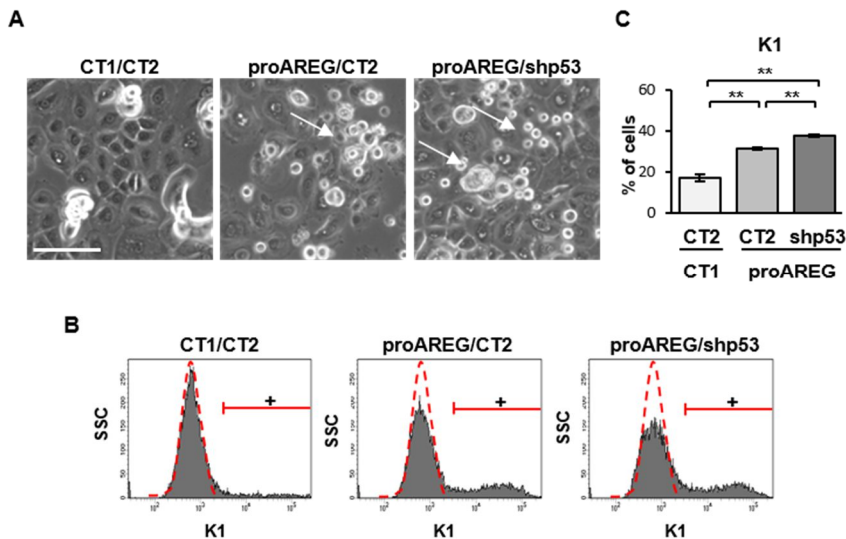


Figure 17 | AREG does not inhibit the DMC in the absence of p53. **A)** Phase contrast images from primary keratinocytes stably expressing full length AREG (proAREG) or the corresponding empty vector (CT1), 5 days after infection with shp53 or the corresponding empty vector (CT2). White arrows indicate cells shedding from the culture. **B)** Histograms representing the expression of Keratin 1(K1) as measured by flow cytometry (+, positive cells according to negative isotype antibody control, red broken line). **C)** Bar histogram representing the percent of cells expressing K1, as measured by flow cytometry. p value $**<0.01$.

ROLE OF FOXM1 OVEREXPRESSION IN THE DIFFERENTIATION-MITOSIS CHECKPOINT OF HUMAN KERATINOCYTES.

Cell cycle deregulation by MYC overexpression or p53 loss triggers squamous differentiation of primary keratinocytes by the activation of the mitotic checkpoints (Gandarillas and Watt, 1997, Freije et al., 2014). Activation of the DMC is part of an oncogene-induced differentiation response (OID) protecting the epidermis from oncogenic deregulation. We hypothesized that additional alterations directly involved in the mitosis control and promotion of cell division are need for epidermal carcinogenesis to occur (Freije et al., 2014). Based on this hypothesis, we decided to force mitosis after activating the DMC by MYC overexpression or p53 silencing. To promote mitosis, we overexpressed the transcription factor FOXM1. As explained in Introduction, FOXM1 plays a major role in the G2/M transition by the transactivation of mitosis and cytokinesis regulators (Laoukili et al., 2005). The results obtained from these experiments, described below, were published in 2017 in *Oncogene* (Molinuevo et al., 2017). The publication is included in this Thesis as an annex.

3. FOXM1 rescues the proliferative block and attenuates the squamous differentiation response caused by inactivation of p53.

We first investigated whether FOXM1 affected the loss of proliferation observed in primary keratinocytes when p53 was silenced. To this aim, we infected keratinocytes with a lentiviral construct carrying an shRNA against p53 (shp53) or the corresponding empty vector (CT1). These cells were also infected with a lentiviral construct that overexpressed FOXM1 or the corresponding empty vector (CT2). Gene delivery was efficiently performed

as detected by immunofluorescence, western blotting or quantitative RT-PCR (Figure 18). p53 silencing also inhibited p21^{Cip1} (Figure 18.B).

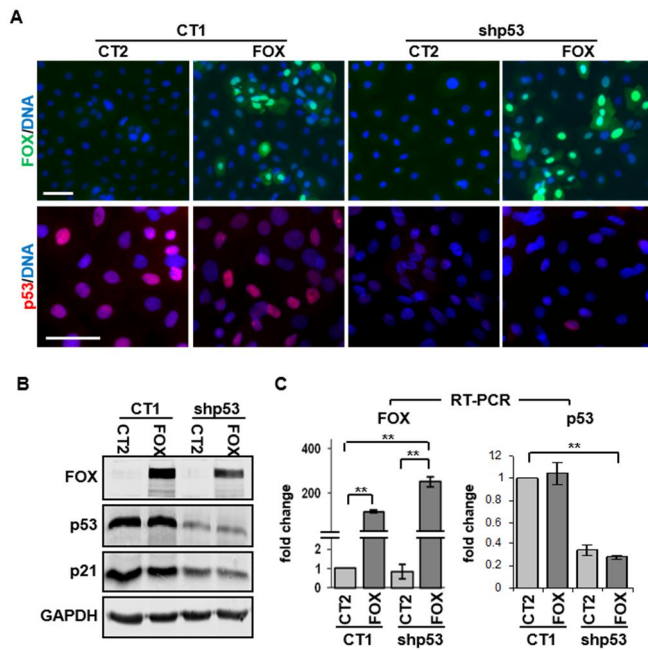


Figure 18 | Inhibition of p53 and overexpression of FOXM1 in primary keratinocytes. Detection of FOXM1 and p53 in primary keratinocytes infected with shRNA for p53 (shp53) or the corresponding empty control vector (CT1) and FOXM1 (FOX) or the corresponding empty control vector (CT2) by **A**) immunofluorescence (FOXM1: green; p53: red; Nuclear DNA by DAPI. Scale bar: 50 μ m), **B**) western blot and **C**) real-time (RT) PCR (fold change with respect to control CT1/CT2). Detection of the p53 target p21^{Cip} (p21) is also shown by western blot (B). GAPDH was used as loading control. p value: **<0.01.

As described previously (Freije et al., 2014), although cell number did not decrease due to an initial phase of fast proliferation permitted by the absence of p53, 5 days after gene delivery keratinocytes lacking p53 (Kshp53) stopped proliferation (Figure 19.A and B). However, keratinocytes overexpressing FOXM1 and lacking p53 (Kshp53/FOXM1) continue proliferating even further than control cells or cells overexpressing FOXM1 only. This observation was confirmed by the striking increase in cell count of keratinocyte cultures (Figure 19.B). We next investigated whether

FOXM1 affected the clonogenic capacity of keratinocytes by performing a clonogenicity assay 5 days after infection (Figure 19.C and D).

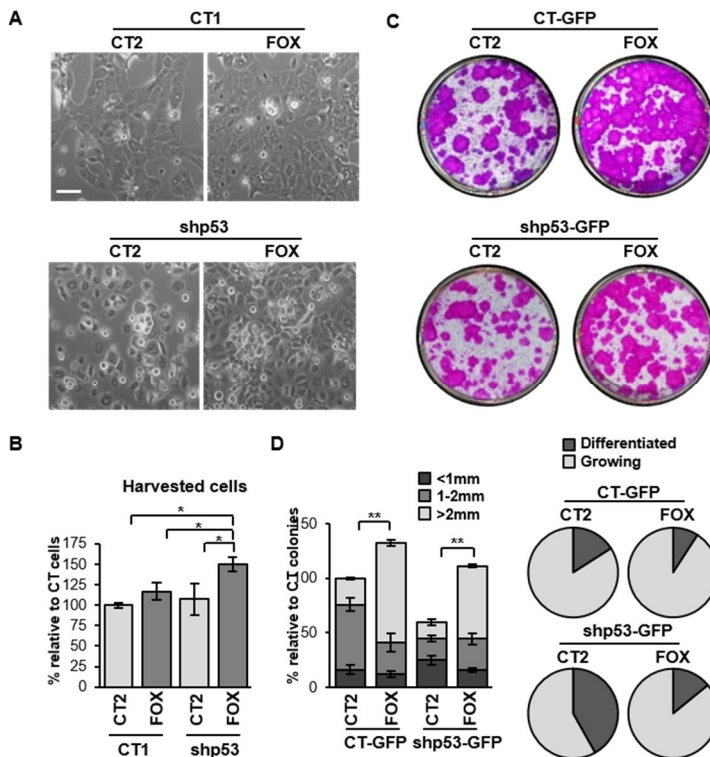


Figure 19 | FOXM1 rescues the proliferative capacity of human epidermal keratinocytes lacking p53. **A)** Phase contrast images of keratinocytes 5 days after infection as in Figure 18. Scale bar: 50 μ m. **B)** Bar histogram represents the differences in the number of cells collected relative to control (CT1/CT2=100%) 5 days after infection as indicated. **C)** Clonogenic capacity of cells plated 5 days after infections with CT-GFP or shp53-GFP and CT2 or FOXM1 (FOX). **D)** Bar histogram (left) represents the differences in large colonies, medium size colonies or small and differentiated colonies relative to control cells (CT-GFP/CT2=100%). Circle histograms (right) show the proportion of actively growing or differentiated colonies. p value: * <0.05 , ** <0.01 .

FOXM1 alone increased the clonogenic potential of keratinocytes, consistently with previous observations in keratinocytes from oral epithelium (Gemenetzidis et al., 2010). On the contrary, the number of total and proliferative colonies formed by Kshp53 cells was reduced, whereas the

number of abortive differentiated colonies was increased (Figure 19.C and D). In contrast, FOXM1 rescued and improved the potential of Kshp53 cells when compared to control (Figure 19.C-D). It is interesting that FOXM1 in combination with shp53 further increases the proliferative potential. This indicates that the mitosis checkpoints limit uncontrolled proliferation upon inactivation of p53. The size and the number of large colonies generated by putative stem cells were greatly increased in Kshp53/FOXM1 cells. Interestingly, the size of small colonies, formed by TACs, was also increased (Figure 19.D). Thus, FOXM1 rescues the proliferative and clonogenic capacity of primary Kshp53 cells.

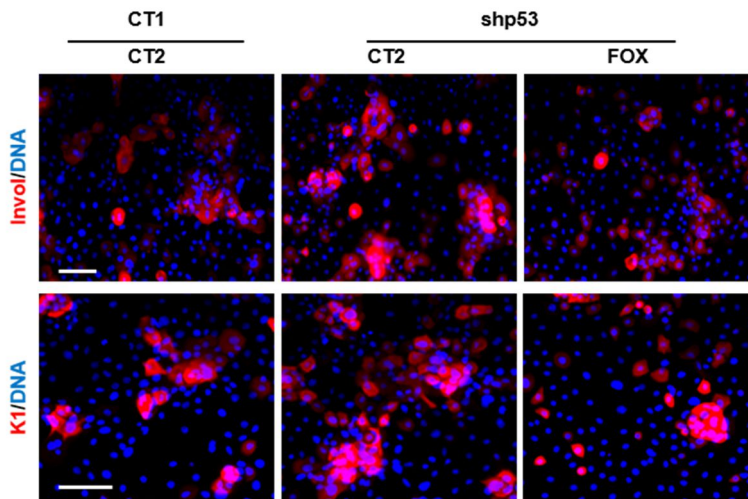


Figure 20 | FOXM1 inhibits the expression of differentiation markers induced by p53 loss. Immunodetection of the epidermal differentiation markers Involucrin (Invol; top panels) or Keratin 1 (K10; bottom panels) in keratinocytes 3 days after infection as indicated. DAPI for DNA in blue. Scale bar: 50 μ m.

Since FOXM1 improved the proliferative capacity of Kshp53 cells, we investigated whether it also affected their differentiation response. By immunofluorescence we observed a decrease in the expression of the differentiation markers Involucrin and K1 in Kshp53/FOXM1 cells 3 days after infection (Figure 20). By quantitative RT-PCR we confirmed the inhibition of Involucrin expression and detected a decrease in the

expression of the late differentiation marker Filaggrin (Figure 21.A). We also confirmed the inhibition of Involucrin and K1 expression by flow cytometry (Figure 21.B). In concordance, the percent of Kshp53/FOXM1 cells displaying high scatter parameters typical of differentiation was decreased (Figure 21.B).

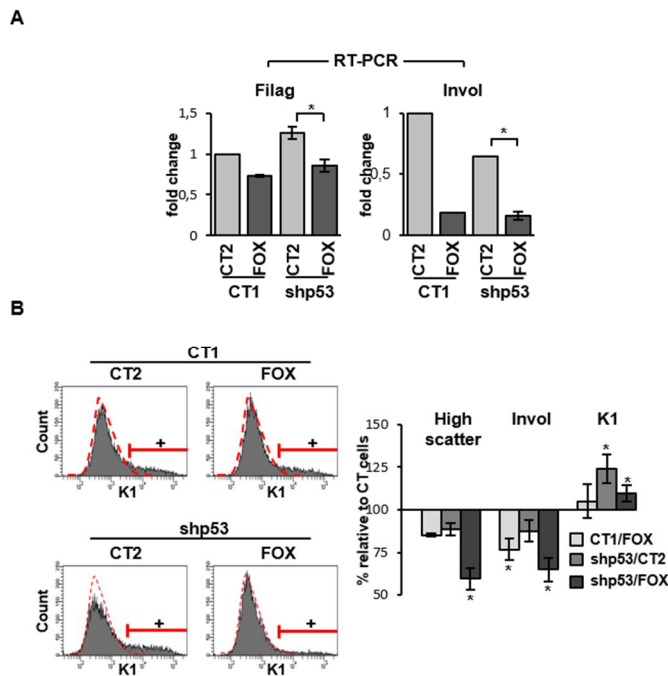


Figure 21 | FOXM1 inhibits the differentiation response to p53 loss. A) Real-time (RT)-PCR for the expression of the differentiation markers Filaggrin (Filag) and Involucrin (Invol), 2 days after infections as indicated (fold changes relative to control CT1/CT2). **B)** Left: Histograms representing the expression of K1 as measured by flow cytometry (+, positive cells according to negative isotype antibody control, red broken line). Right: Bar histogram shows cells with high scatter parameters, or positive for Invol or K1 relative to control cells (CT1/CT2=100%) as measured by flow cytometry. p value: $* < 0.05$.

It is important to mention that differentiation of primary keratinocytes increases at cell confluence (Borowiec et al., 2013), when keratinocytes are pushed to stratify and detach. Kshp53/FOXM1 cells reached confluence faster and stratified more than controls and certainly than Kshp53 cells (Figure 19.A). In spite of a higher cell density, FOXM1 inhibited the

initiation of differentiation at confluence as the proportion of cell shedding into the medium was attenuated (Figure 22.A). Increased confluence and decreased shedding in Kshp53/FOXM1 populations might be related to increased expression of β 1-integrins as detected by western blot (Figure 22.B). Therefore, although FOXM1 did not abolish stratification and differentiation of Kshp53 cells, it significantly rescued their proliferative potential.

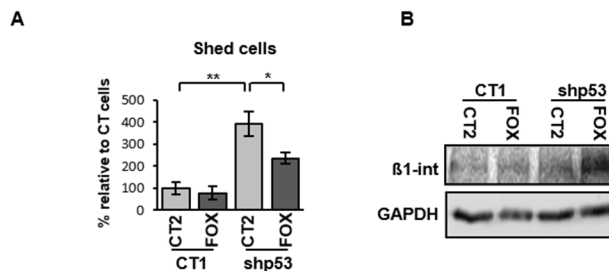


Figure 22 | FOXM1 inhibits cell shedding in the absence of p53. A) Shedding cells collected from the culture supernatant due to differentiation 5 days after infections as indicated, relative to control (CT1/CT2=100%). **B)** Detection by western blot of β 1-integrin 5 days after infections as indicated. GAPDH as loading control. p value: * <0.05 , ** <0.01 .

The expression of FOXM1 in normal human skin was unknown and we aimed to identify it. As shown in Figure 23, FOXM1 was found by immunofluorescence of frozen epidermis to strikingly accumulate in cells expressing mitotic cyclins A and B. This further suggests that the main function of FOXM1 in epidermal keratinocytes is related to mitosis.

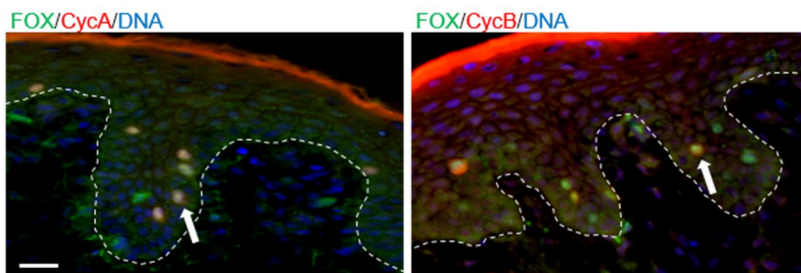


Figure 23 | FOXM1 is expressed in mitotic keratinocytes in the epidermis. Immunodetection of endogenous FOXM1 (FOX, green), CycA (red, left panel) and CycB

(red, right panel) in normal human epidermis by immunofluorescence. DAPI for DNA in blue. White arrows: cells coexpressing FOXM1 and CycA or CycB. Broken line for the basement membrane. Scale bars: 50 μ m.

4. FOXM1 allows keratinocytes to proliferate in spite of genomic instability.

Loss of p53 in epidermal keratinocytes induces early hyperactivation of the cell cycle that results in a G2/M block and endoreplication via mitotic bypass or slippage (Freije et al., 2014). The analysis of cell cycle regulators by western blotting suggested that Kshp53/FOXM1 cells did not accumulate as much in G2/M (Figure 24.A). Although the expression of the S/G2/M marker phospho-retinoblastoma (p-Rb) was increased in Kshp53 cells compared with controls, it was decreased upon FOXM1 overexpression indicating that this protein did not activate the cell cycle further. The expression of cyclin B, reduced when p53 was absent, increased upon FOXM1 overexpression. However, the expression of cyclin E and cyclin A remained unchanged, suggesting that the main action of FOXM1 in keratinocytes takes place in mitosis. We also observed changes in the cell cycle by analyzing keratinocytes DNA content 3 days after infection. The percent of Kshp53/FOXM1 cells in G2/M and in the polyploid compartment of the cell cycle decreased when comparing to Kshp53 cells (Figure 24.B and C). In concordance, the proportion of cells in G1 was increased. DNA synthesis was also measured in these cells by 5-bromodeoxyuridine (BrdU) incorporation (Figure 24.D). Similarly to the changes observed in the cell cycle, the percent of Kshp53/FOXM1 cells incorporating BrdU that bypassed mitosis and became polyploid decreased. Consistently, the percent of BrdU cells in G1/S phases increased as compared to Kshp53 cells. However, keratinocytes overexpressing FOXM1 only displayed an increase in the percent of BrdU-positive cells in G2/M (Figure 24.D). This suggested that FOXM1 with the loss of p53 accelerated the transition from G2/M to G1. Altogether, the results are consistent with

a role of FOXM1 in potentiating keratinocytes cell division downstream of p53. In addition, the number of binucleated cells within the Kshp53/FOXM1 polyploid population was increased, as scored by staining nuclei with DAPI (Figure 24.E). This suggested that FOXM1 pushes nuclei to divide even when the cell cannot divide anymore, consistent with the role of FOXM1 in mitotic spindle assembly, chromosome alignment and nuclear division (Laoukili et al., 2005, Costa, 2005).

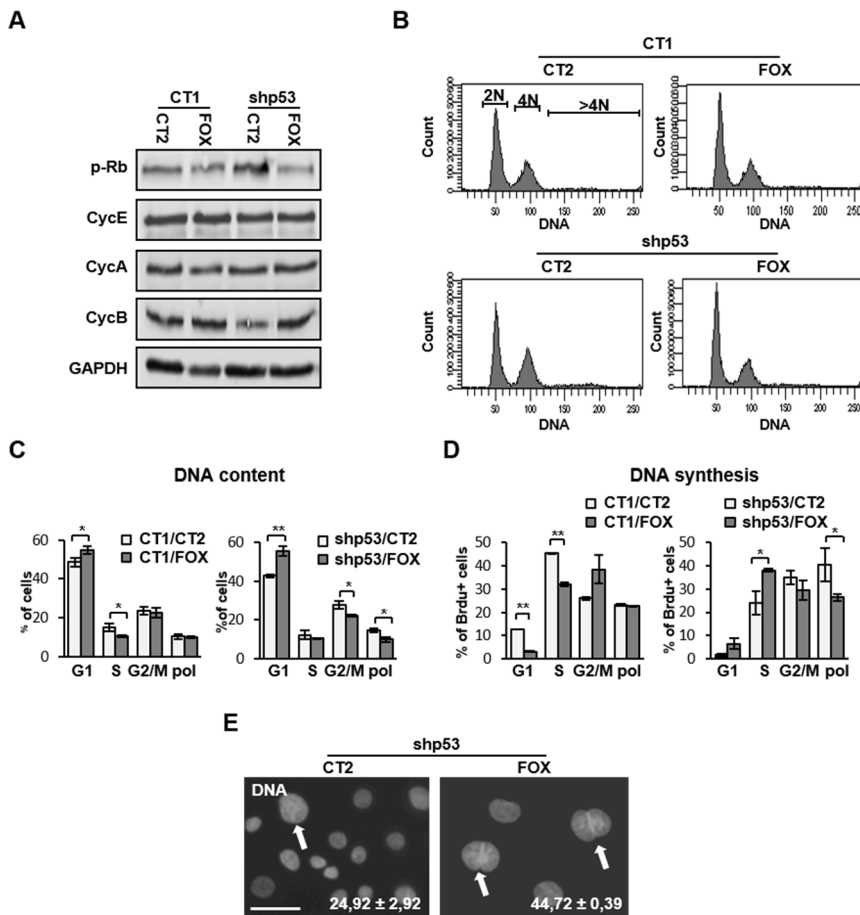


Figure 24 | FOXM1 suppresses the mitotic block caused by loss of p53 in primary keratinocytes. **A)** Expression of cell cycle regulators p-Rb, cyclin E (CycE), cyclin A (CycA) and cyclin B (CycB) by western blotting, 3 days after infections as indicated. GAPDH was used as loading control. **B)** Histograms representing the DNA content of keratinocytes 3 days after infection, as measured by flow cytometry. **C)** Percent of cells in the G1 (2N), S, G2/M (4N) or polyploid (pol; <4N) phases of the cell cycle, as determined by flow

cytometry. **D)** Percent of BrdU-positive cells in G1 (2N), S, G2/M (4N) or polyploid (pol; <4N) phases in the cell cycle. **E)** Binucleated keratinocytes (white arrows) bearing shp53 and CT2 or FOXM1 as indicated, stained with DAPI for DNA. White numbers are the percent of polyploid cells (nuclei <15 μ m) that are binucleated. Scale bar: 50 μ m. p value: *<0.05, **<0.01.

It is worth noting that ectopic expression of FOXM1 reduced the intensity of nascent RNA foci as measured by incorporation of 5'-fluorouridine (5'-Flu; Figure 25.A). This observation suggested that FOXM1 function might have a relationship with the inhibition of transcription required for the initiation of mitosis. Therefore, we performed double labeling for cyclin A, which accumulates mainly in G2/M. The analyses showed that, as expected, in control keratinocytes transcription was strong in cyclin A-negative cells and weak in mitotic cells. However, transcription was as weak in interphasic, nonmitotic FOXM1-overexpressing cells (Figure 25.B).

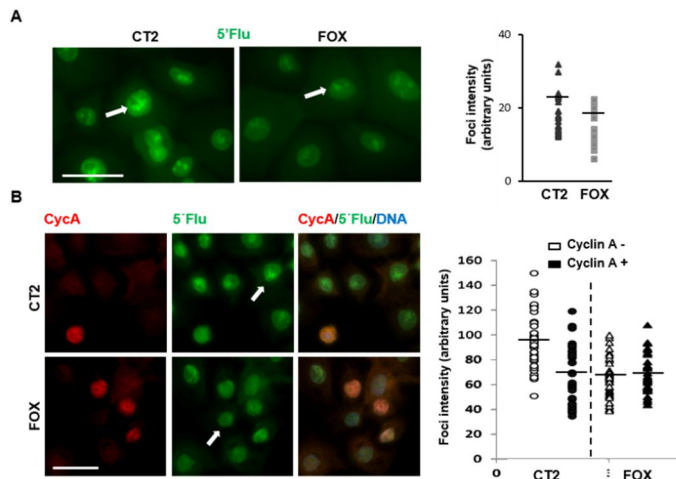


Figure 25 | FOXM1 might play a role in global transcription regulation. A) Detection of nascent transcription by 5'-fluorouridine (5'-Flu; green) incorporation 2 days after infections as indicated (nucleolar foci are indicated on representative photographs by white arrows). Dot plot on the right represents quantitation of the fluorescence intensity of 5'-Flu incorporating single foci. Black bars represent the mean. **B)** Detection of 5'-Flu incorporation (green) and CycA expression (red) by immunofluorescence, 2 days after infections as indicated. Dot plot on the right represents quantitation of the fluorescence intensity of 5'-Flu incorporating single foci in CycA negative (white) and positive (black) cells. Black bars represent the mean. Scale bars: 50 μ m.

The role of FOXM1 in the inhibition of transcription has not been studied. FOXM1 gene encodes three different protein isoforms by alternative splicing: FOXM1a, FOXM1b and FOXM1c (Wierstra and Alves, 2007). Although we have made use of a DNA construct bearing the FOXM1b isoform, it has been shown that this protein can induce the expression of the other two variants (Halasi and Gartel, 2009) and we confirmed by western blotting that this was the case in FOXM1 infected keratinocytes (Figure 26.A). Whereas FOXM1b and FOXM1c are considered transcriptionally active, FOXM1a lacks the transactivation domain and has a negative regulatory function on transcription (Kong et al., 2013). The expression of the three isoforms might be important for the correct regulation of mitosis.

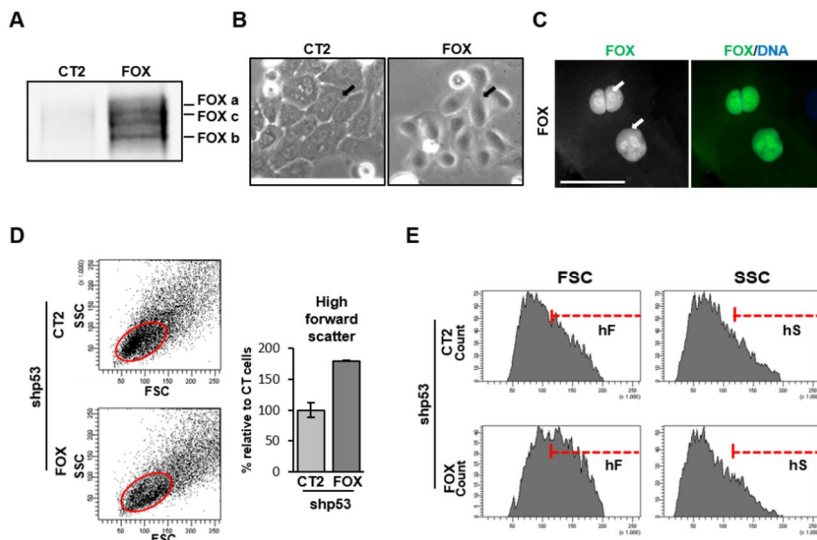


Figure 26 | Keratinocytes overexpressing FOXM1 displayed a lower optical density. **A)** Western blot for FOXM1 isoforms a, b and c in keratinocytes infected with CT2 or FOXM1 (FOX). **B)** Phase contrast images of keratinocytes infected with CT2 or FOX. Note that the cytoplasm of keratinocytes displays a lighter optical density (black arrows). **C):** Immunodetection of FOX (green) in keratinocytes infected with FOX. DAPI in blue for DNA. Note that exogenous FOXM1 accumulates in the nucleolus (white arrows). **D)** Dot plots show side and forward scatter parameters (SSC and FSC, respectively) for cell complexity and size by flow cytometry of keratinocytes infected as indicated. Red oval represents the basal proliferative population. Bar histogram indicates basal cells (red oval) with high FSC (according to gate in E, hF) relative to cells infected with shp53 and CT2

(shp53/CT2 = 100%). **E)** Forward (FSC; left) or side (SSC, right) scatter profiles of basal keratinocytes infected as indicated and gated by red oval in D (hF: high forward scatter; hS: high side scatter). Analyses by flow cytometry. Scale bars: 50 μ m.

Consistent with a global transcription decrease, we found that keratinocytes overexpressing FOXM1 displayed a lighter optical density (Figure 26.B). In addition, by immunofluorescence we observed FOXM1 in the nucleolus, centre of ribosomal RNA transcription (Figure 26.C). Nucleolar localization has been previously proposed to have a FOXM1 inhibitory role (Costa, 2005). By flow cytometry we detected that proliferative Kshp53/FOXM1 cells increased in size (measured by their forward scatter parameter), in spite of reduced cellular complexity (Figure 26.D and E). Cells enlarge in G2 in order to produce two daughters of the same size before cell division, and therefore the mitosis block provokes differentiating keratinocytes to increase in size. This process is stimulated by p53 loss (Freije et al., 2014). The higher size of proliferative Kshp53/FOXM1 cells suggested that this protein pushed cell division even though the mitosis arrest had initiated.

The deregulation of the cell cycle by p53 inhibition in keratinocytes leads to the accumulation of DNA damage because of replication stress (Freije et al., 2014). We studied whether FOXM1, by alleviating the mitosis block, allowed keratinocytes to divide in spite of irreparable damage. Expression of the DNA damage marker γ H2AX was evaluated by western blotting and flow cytometry in Kshp53/FOXM1 cells 5 days after gene delivery. We found a significant increase of γ H2AX with respect to control cells (Figure 27.A). In Kshp53 cells the increase in γ H2AX was detected both in basal and differentiating keratinocytes, according to light scatter parameters (Figure 27.B). However, in Kshp53/FOXM1 cells the accumulation of γ H2AX signal was mainly detected in the basal low scatter cell population (Figure 27.B). To assess for actual DNA breaks typical of replication stress

we performed comet assays. This technique consists on a single cell electrophoresis that allows quantification of DNA fragmentation. As shown in Figure 27.C, inactivation of p53 caused a striking increase of DNA breaks that augmented even further in combination with FOXM1. Interestingly, Kshp53/FOXM1 cells augmented significantly the DNA breaks in smaller nuclei (<15 μm), typical of proliferative cells. These results suggested that ectopic expression of FOXM1 allowed damaged cells lacking p53 to keep dividing and amplifying.

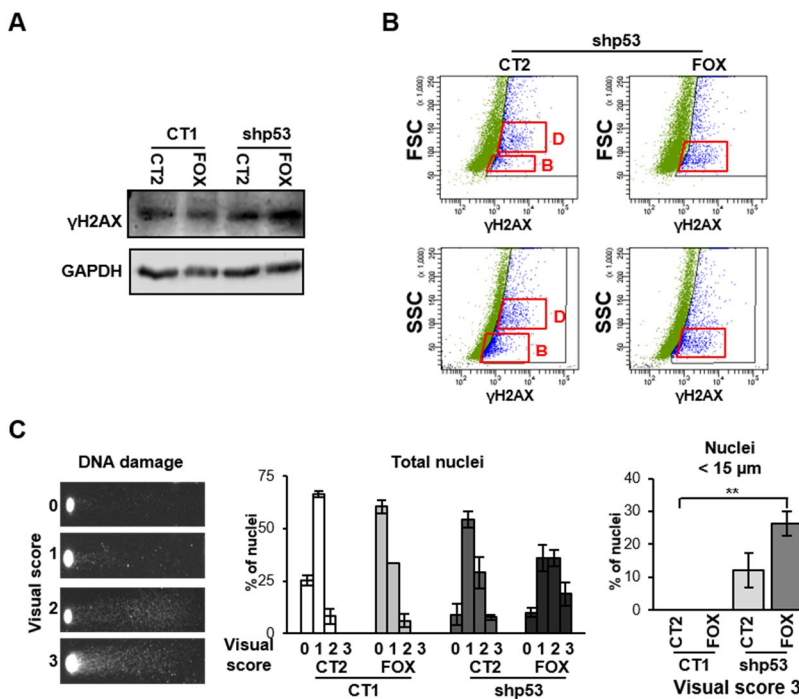


Figure 27 FOXM1 allows accumulation of DNA damage in proliferative keratinocytes upon p53 inactivation. **A)** Western blot for γ H2AX in keratinocytes 5 days after infections as indicated. GAPDH was used as loading control. **B)** Dot plots for FSC (top) or SSC (bottom; y axis) and γ H2AX (x axis) 3 days after infections as indicated, measured by flow cytometry. Red squares represent the main γ H2AX-positive populations (blue, according to negative isotype antibody control) of differentiating (D) or basal (B) cells. **C)** DNA damage monitored by comet assays. Left: scoring assigned for damage according to the size and intensity of the nuclear tails of keratinocytes (0–3) 5 days after infections. Centre: bar histogram showing the quantitation of DNA damage according to the 4 levels of intensity. Right: bar histogram represents only the percent of small nuclei (<15 μm) with maximum DNA damage intensity level 3. p value: **<0.01

5. Overexpression of FOXM1 drives MYC-induced differentiation into proliferation.

As explained in Introduction, the proto-oncogene MYC drives the cell cycle and subsequently epidermal differentiation due to activation of the DMC (Gandarillas et al., 2000, Gandarillas and Watt, 1997, Freije et al., 2014). We hypothesized that activation of the DMC by MYC could be inhibited by forcing cell division, as in the case of *shp53*. We investigated the effect of overexpressing FOXM1 in keratinocytes carrying a retroviral conditional form of human MYC (MYCER) whose protein product is regulated by 4-hydroxytamoxifen [OHT], (Littlewood et al., 1995)]. Keratinocytes efficiently expressed exogenous FOXM1 and MYCER as detected by western blot (Figure 28.A).

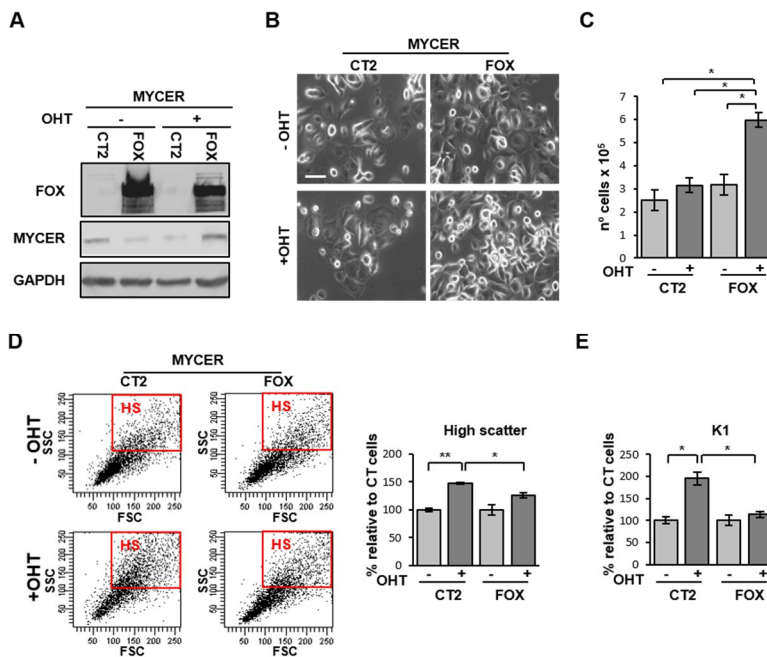


Figure 28 | increases the proliferative capacity of MYCER keratinocytes and inhibits squamous differentiation. **A**) Detection of FOXM1 (FOX) and MYCER by western blot in MYCER keratinocytes infected with CT2 or FOX and in the presence (+) or absence (-) of OHT as indicated. GAPDH used as loading control. **B**) Phase contrast images of MYCER

keratinocytes infected as indicated and cultured in the presence or absence of OHT for 3 days. Scale bar: 50 μ m. **C)** Bar histograms represent the number of harvested MYCER cells infected as indicated and after 5 days in the presence or absence of OHT. **D)** Dot plots showing light scatter parameters of MYCER keratinocytes infected as indicated and cultured for 5 days in the presence or absence of OHT. Red represents cells with high scatter parameter (HS). Right histogram represents the percent of cells with HS relative to control (MYCER cells infected with CT2, non-treated with OHT; -OHT/CT2=100%). **E)** Histogram represents the percent of cells positive for K1 expression as measured by flow cytometry, relative to control (MYCER cells infected with CT2, non-treated with OHT; -OHT/CT2=100%). p value: *<0.05, **<0.01.

As expected, cells expressing MYCER differentiated when treated with 100mM OHT for 5 days (Figure 28.B). However, the number of MYCER cells collected was doubled in the presence of FOXM1 (Figure 28.B and C). As in the case of p53 loss, flow cytometry showed that FOXM1 significantly suppressed MYC-induced differentiation as monitored by the decrease in light scattering parameters and the expression of the post-mitotic squamous terminal marker K1 (Figure 28.D and E).

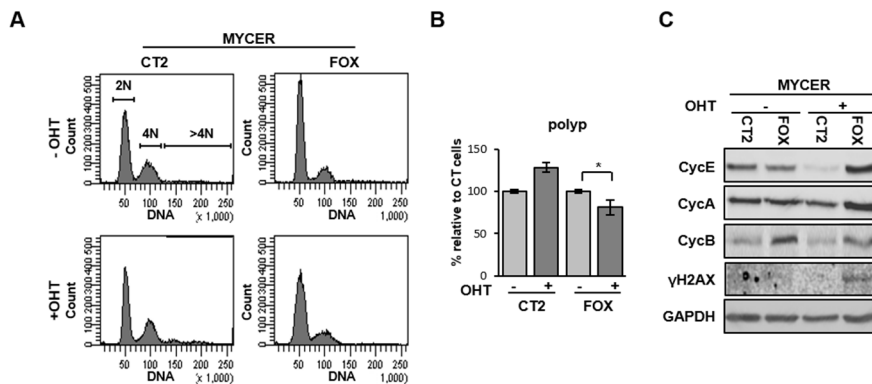
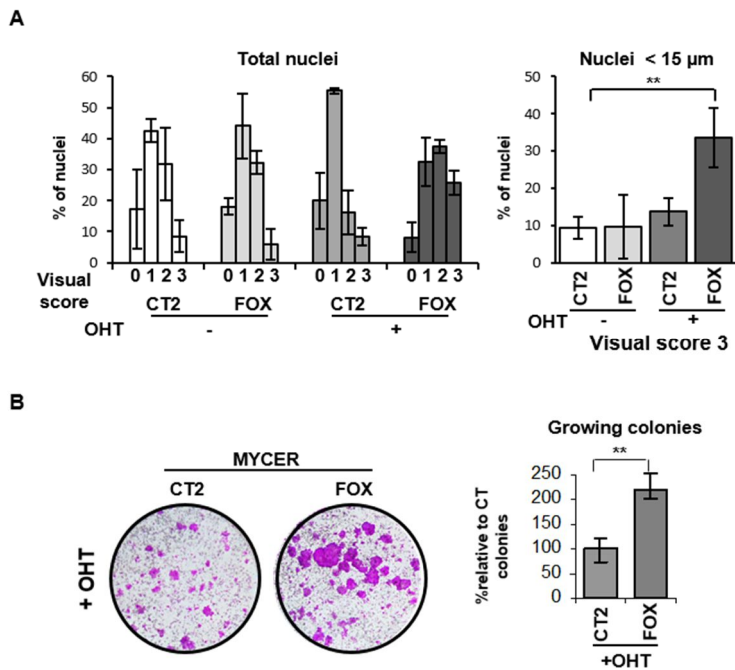


Figure 29 | FOXM1 alleviates the mitotic arrest induced by MYC. **A)** Histograms representing the DNA content of MYCER keratinocytes infected with CT2 or FOXM1 cultured for 5 days in the presence (+) or absence (-) of OHT. **B)** Bar histograms represent the proportion of cells in the polyploid compartment of the cell cycle relative to control (cells infected with CT2, non treated with OHT; CT2/-OHT =100%). **C)** Western blotting for p-Rb (a, activated; i, inactivated), cyclin E (CycE), cyclin A (CycA), cyclin B (CycB) and γ HA2X

in MYCER keratinocytes infected as indicated and in the presence or absence of OHT. GAPDH used as loading control. p value: * <0.05 , ** <0.01 .

We also observed that FOXM1 influenced the cell cycle parameters of MYCER cells. Analysis of DNA content showed that induction of MYCER with OHT drove keratinocytes into the polyploid compartment, whereas ectopic expression of FOXM1 significantly decreased the polyploid population (Figure 29.A and B). As detected by western blot, the expression of the cell cycle regulators cyclin E, cyclin A and cyclin B detected by western blots was reduced in the presence of MYCER, consistent with mitotic arrest [Figure 29.C; (Freije et al., 2012)]. However, ectopic expression of FOXM1 in MYCER cells recovered the expression of cyclin E and the mitotic cyclins A and B (Figure 29.C).



infected with CT2 or FOXM1 after 5 days in the presence or absence of OHT as indicated. Left bar histogram shows the quantitation of DNA damage according to the 4 levels of DNA damage intensity described in Figure 27.C. Right bar histogram shows the percent of small nuclei (<15 μm) with maximum DNA damage intensity level 3. **B)** Clonogenicity assays of MYCER keratinocytes infected as indicated and cultured in the presence of OHT for 10 days. Right bar histograms represent large growing colonies when FOX is ectopically expressed relative to control (CT2/+OHT=100%). p value: *<0.05, **<0.01.

MYC deregulation causes replication stress and DNA damage (Freije et al., 2014). We observed by western blotting a stronger accumulation of the DNA damage marker γH2AX when FOXM1 was overexpressed (Figure 29.C). Consistently, MYCER small nuclei typical of proliferative cells contained strikingly more damage in comet assays in the presence of FOXM1 (Figure 30.A). FOXM1 also recovered the colony-forming potential of keratinocytes that was lost by MYC activation (Figure 30.B). Altogether, the results strongly indicate that FOXM1 switched the activation of the cell cycle by MYC from differentiation to proliferation in spite of increased replication stress and DNA damage.

CHARACTERIZATION OF THE DIFFERENTIATION-MITOSIS CHECKPOINT IN IMMORTALIZED NTERT KERATINOCYTES.

Most of the immortalized cell lines present defects in the cell cycle control pathways. We hypothesized that the DMC might be a limiting factor in keratinocyte self-renewal. For this reason, we considered studying the DMC in the human immortalized epidermal cell line NTERT (Dickson et al., 2000). Given that inhibition of G2/M progression is sufficient to activate the differentiation response in primary human keratinocytes (Freije et al., 2012, Zanet et al., 2010, Gandarillas et al., 2000), we decided to treat NTERT with different mitotic drugs and analyse the effect in differentiation.

6. The immortalized cell line NTERT presents defects in the differentiation-mitosis checkpoint.

We treated NTERT with nocodazol (NOCO) with the aim of blocking mitosis progression. NOCO induces a G2/M arrest by inhibiting the polymerization of microtubules and is known to activate the DMC of primary keratinocytes (Gandarillas et al., 2000). Treatment with NOCO for 3 days increased in cell size (Figure 31.A). The analysis by flow cytometry confirmed a striking increase in the light scatters parameters (Figure 31.B and D), typically presented by differentiated cells. The analysis of DNA content showed that cells underwent mitotic slippage, becoming polyploid, mostly octaploid (8N; Figure 31.C and D).

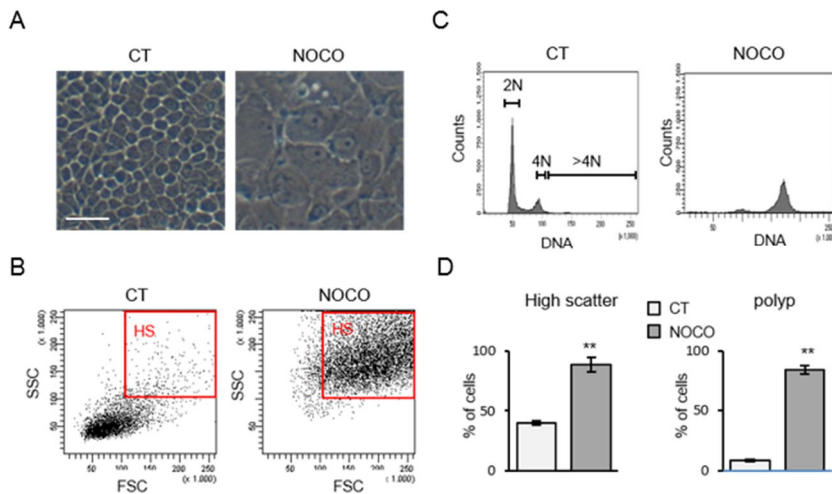


Figure 31 | NTERT increase cell size and become polyploid in response to Nocodazol. **A)** Phase contrast images of NTERT treated with DMSO (CT) or Nocodazol (NOCO) for 3 days. Scale bar: 20 μm. **B)** Dot plots representing the light scatter parameters of NTERT treated as indicated. Red box represents cell displaying high scatter parameters (HS). **C)** Histograms representing the DNA content of NTERT treated as indicated, as measured by flow cytometry. **D)** Bar histograms represent the proportion of NTERT with high scatter parameters (HS in B, left histogram) or in the polyploid (<4N, right histogram) compartment of the cell cycle. p value **<0.01.

Although this response is consistent with the activation of the DMC, analyses by flow cytometry showed that NOCO did not induced the expression of the differentiation marker Involucrin (Figure 32.A). In addition, clonogenicity assays confirmed that NOCO failed to activate the DMC in NTERT (Figure 32.B). While NOCO completely abolished the colony forming potential of primary keratinocytes when returned to normal growing conditions, colony forming potential of NTERT was barely affected.

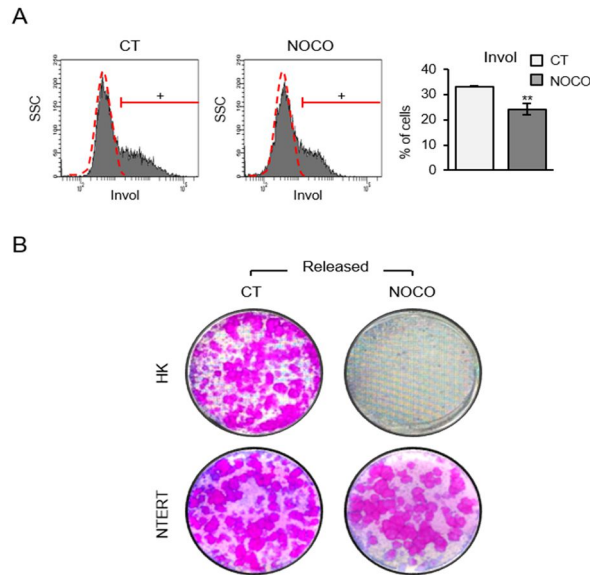


Figure 32 | NTERT continue proliferating after Nocodazol treatment. A) Histograms representing the expression of Involucrin (Invol) in NTERT treated with DMSO (CT) or Nocodazol (NOCO) for 3 days, as measured by flow cytometry (+, positive NTERT according to negative isotype antibody control). Right: Bar histogram shows the percentage of NTERT expressing Involucrin, as measured by flow cytometry. **B)** Clonogenicity assays of human keratinocytes (HK) or NTERT treated as indicated in A and returned to normal conditions (released). p value $** < 0.01$.

After these observations we decided to analyse NTERT cells growing after the release from NOCO treatment (NTERT-R1 from now on). Proliferating NTERT-R1 increased cell size comparing to CT (Figure 33.A). Flow cytometry analyses of light scatter parameters confirmed this observation (Figure 33.B and C). However, NTERT-R1 displayed lower light scatter parameters than NTERT collected just after NOCO treatment and before the release (Figure 33.B and C). Despite the changes in cell size and complexity typical of epidermal differentiation, we did not detect induction of Involucrin expression in NTERT-R1 when comparing to control (Figure 34.A and C). By analyzing their DNA content, we observed that NTERT-R1 accumulated at G2/M more than control (Figure 34.B and C). In addition, NERT-R1 presented a higher proportion of polyploid, but

not as many as cells just after the NOCO treatment. Taken together, the results demonstrated that NTERT did not respond to the G2/M arrest induced by NOCO in the same way that primary keratinocytes did. NTERT were able to continue dividing in spite of becoming polyploid, hence avoiding the activation of the DMC and the terminal differentiation program.

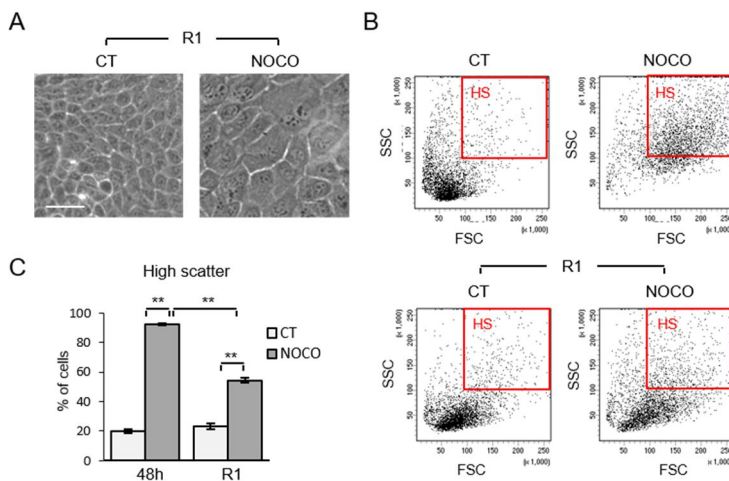


Figure 33 | Proliferating NTERT-R1 undergo morphological changes. A) Phase contrast images of NTERT released (R1) after treatment with DMSO (CT) or Nocodazol (NOCO) for 3 days. Scale bar: 20 μ m. **B)** Dot plots representing the light scatter parameters of NTERT collected after treatment with DMSO (CT) or NOCO (top panels) or after the release (R1, bottom panels). Red box represents cell displaying high scatter parameters (HS). **C)** Bar histograms represent the proportion of NTERT with HS after treatment or release (R1) as indicated in B. p value $** < 0.01$.

After observing the effect of NOCO we wanted to assess whether NTERT completely lacked the DMC. To this aim, we treated NTERT with chemical inhibitors specific for the mitotic kinases Polo-like (Plk) and Aurora B (AurB). Both Plk and AurB regulate chromosome segregation and entry into anaphase. While Plk contributes to the control of the APC activity (Hansen et al., 2004), AurB regulates chromosome segregation by associating with

microtubules at the centromeric region during metaphase (Ditchfield et al., 2003).

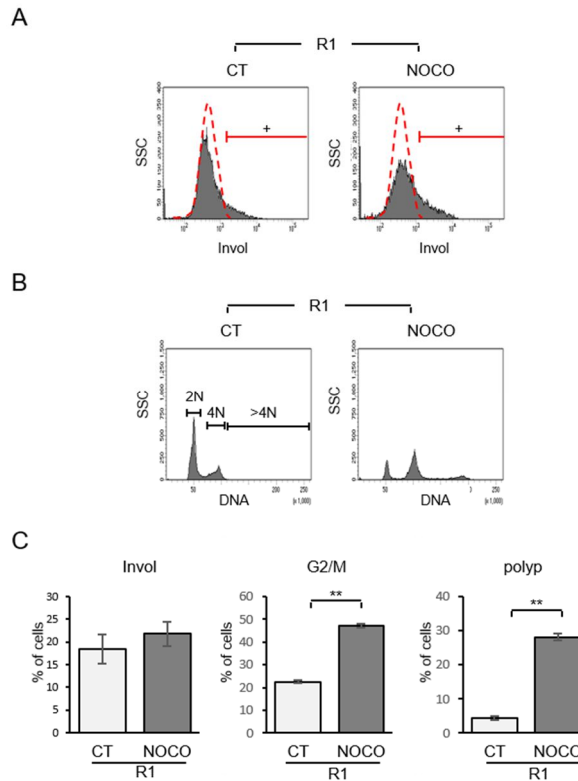


Figure 34 | NTERT-R1 proliferate in spite of becoming polyploid. A) Histograms representing the expression of Involutin (Invol) in NTERT released (R1) after treated with DMSO (CT) or Nocodazol (NOCO) for 3 days, as measured by flow cytometry (+, positive NTERT according to negative isotype antibody control). **B)** Histograms representing the DNA content of NTERT R1, as measured by flow cytometry. **C)** Bar histograms represent the proportion of NTERT R1 expressing Involutin (left histogram) or in the G2/M (4N, middle histogram) or polyploid (<4N, right histogram) compartments of the cell cycle. p value **<0.01.

Chemical inhibition of AurB kinase activity with ZM 447439 (ZM) for 3 days increased the light scatter parameters of NTERT, as detected by flow cytometry (Figure 35.A and C). The same effect was observed when we Plk

kinase activity was inhibited by BI 2536 (BI; Figure 35 A and C). Analyses of DNA content revealed that both treatments increased the proportion of cells arrested at G2/M and slipping into the polyploid compartment of the cell cycle (Figure 35.B and C).

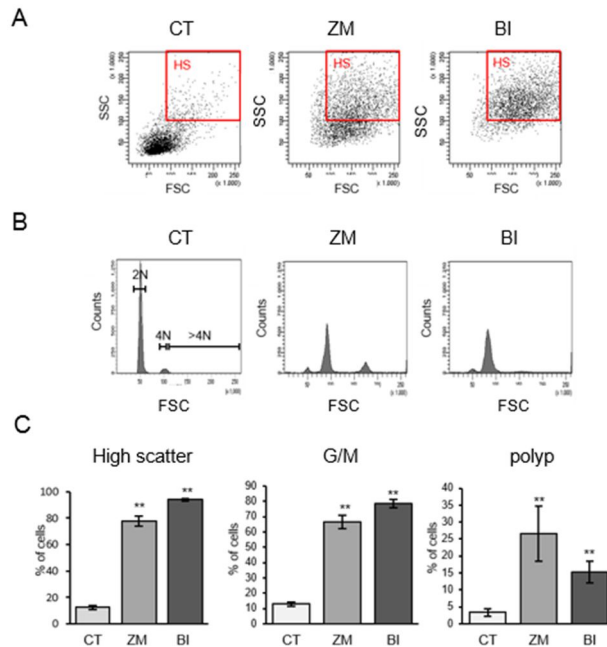


Figure 35 | Inhibition of Aurora B or Polo-like kinases induce morphological changes in NTERT. A) Dot plots representing the light scatter parameters of NTERT after treatment with DMSO (CT), AurB (ZM) or Plk (BI) inhibitors for 3 days. Red box represents cell displaying high scatter parameters (HS). **B)** Histograms representing the DNA content of NTERT treated as indicated in A. **C)** Bar histograms represent the proportion of NTERT presenting HS (left panel) or in the G2/M (4N, middle histogram) or polyploid (<4N, right histogram) compartments of the cell cycle, after treated as indicated in A. p value **<0.01.

So far, the results obtained after treating NTERT with ZM or BI were consistent with those obtained after NOCO treatment. However, by flow cytometry we detected that the expression of the differentiation marker Involucrin was strongly induced by ZM or BI (Figure 36.A and B). In addition, NTERT completely loss their colony forming potential when

returned to normal growing conditions (Figure 36.C). Hence, our results demonstrate that NTERT present defects in the activation of the DMC.

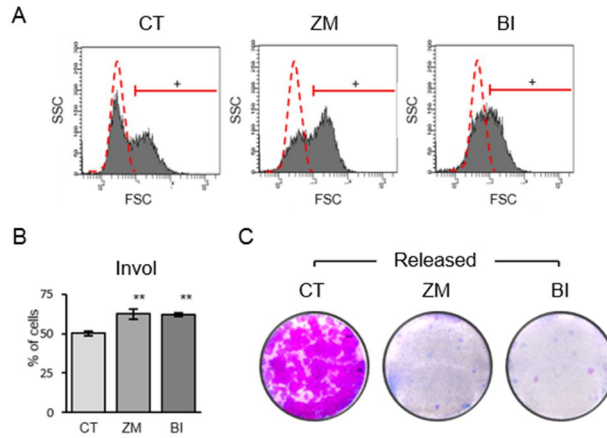


Figure 36 | Inhibition of anaphase progression induces terminal differentiation of NTERT. A) Histograms representing the expression of Involucrin (Invol) in NTERT treated with DMSO (CT) AurB (ZM) or Plk (BI) inhibitors for 3 days, as measured by flow cytometry (+, positive NTERT according to negative isotype antibody control). **B)** Bar histograms representing the percent of NTERT expressing Involucrin after treatment with DMSO, ZM or BI for 48h. p value $** < 0.01$. **C)** Clonogenicity assays of NTERT treated as indicated in A and released.

DNA DAMAGE AS PART OF THE NATURAL SQUAMOUS DIFFERENTIATION PROGRAM OF KERATINOCYTES.

The epidermis is a tissue that presents high self-renewal capacity and is continuously exposed to mutagenic hazard. These characteristics imply the existence of powerful mechanisms that regulate the balance between proliferation and differentiation, and ensure skin homeostasis. Despite its relevance, these mechanisms remain obscure. Given that keratinocytes under normal conditions undergo a phase of rapid proliferation prior to differentiation, we questioned whether accumulation of DNA damage due to RS might be a signal that activates the squamous pathway in normal healthy epidermis. To elucidate this question, we performed functional experiments to study the role of the DDR in the activation of the differentiation program of keratinocytes.

7. DNA damage signaling is detected in normal keratinocytes.

Several observations demonstrated that DNA damage occurs in keratinocytes. By immunofluorescence we detected the DNA damage marker γ H2AX in the proliferative border of keratinocyte colonies *in vitro* (Figure 37.A). Strongly positive γ H2AX keratinocytes were found stratifying into the differentiated layer of the colonies (Freije et al., 2014). In addition to γ H2AX, 53BP1 was also detected by immunofluorescence in keratinocytes growing *in vitro* (Figure 37.B). Nuclear spots of 53BP1 are known to be associated with persistent DNA damage foci (PDDF), which are kept silenced in order to avoid aberrant transcription (Mata-Garrido et al., 2016, Fernandez-Vidal et al., 2017). Interestingly, 53BP1 foci were present in keratinocytes expressing high levels of cyclin E, but not cyclin A or cyclin B (Figure 37.B). Accumulation of cyclin E is detected in keratinocytes that have already started terminal differentiation and

endoreplication (Zanet et al., 2010). However, although coincident, 53BP1 and cyclin E did not co-localize within the nucleus (Figure 37.B), further suggesting that PDDF were excluded from replication.

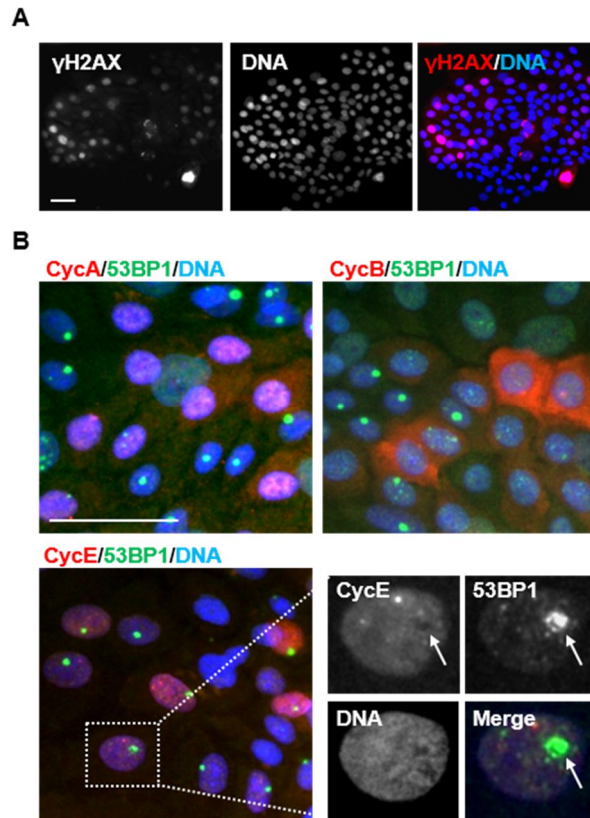


Figure 37 | DNA damage signaling is detected in primary keratinocytes *in vitro*. **A)** Detection of γ H2AX (red) in primary keratinocytes by immunofluorescence. Note that γ H2AX is present in the proliferative border of the colony. **B)** Detection of 53BP1 (green) and cyclin A (CycA, red; top left), cyclin B (CycB, red; top right) or cyclin E (CycE, red; bottom left) by immunofluorescence. Bottom right panels: augmentation from bottom left panel (white box). Note that CycE and 53BP1 do not co-localize (white arrow). Nuclear DNA by DAPI. Scale bar: 50 μ m.

By using an antibody that recognized substrates phosphorylated by ATM and/or ATR, we could confirm that the DDR is activated in normal

keratinocytes (Figure 38). A strong nuclear staining was found in cells expressing the differentiation marker Involucrin (Figure 38.A, left panel, white arrows). However, proliferating keratinocytes negative for Involucrin expression presented substrates phosphorylated by ATM and/or ATR in single foci (Figure 38.A, right panel). By performing a double immunofluorescence we observed that these foci co-localized with the expression of γ tubulin in interphasic and mitotic cells (Figure 38.B and C). Given that γ tubulin is a main component of the centrosomes this result suggests that the DDR might have a function on centrosome and therefore, somehow regulate cell division in proliferating keratinocytes.

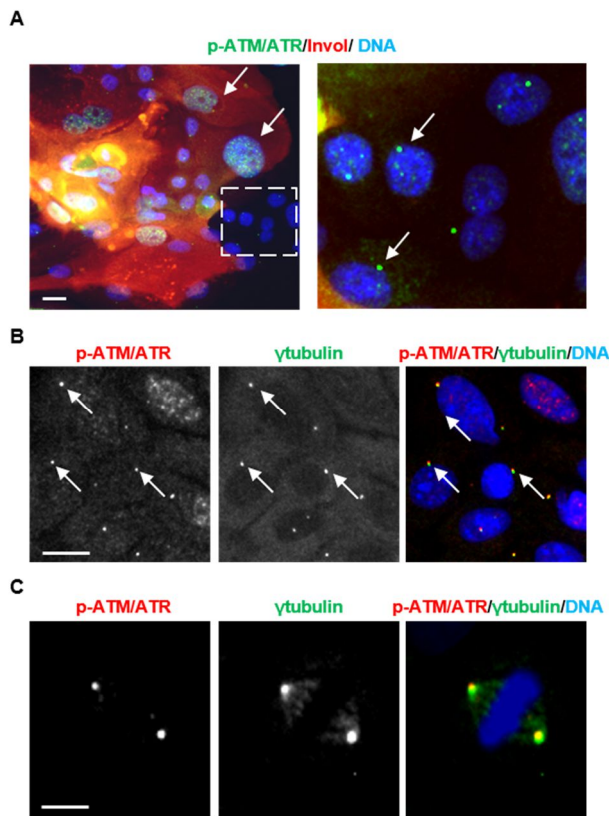


Figure 38 | The DDR is active in primary keratinocytes *in vitro*. **A)** Left: Detection of substrates phosphorylated by ATM and/or ATR (p-ATM/ATR, green) and Involucrin (Invol, red) by immunofluorescence. White arrows indicate big nuclei positive for Involucrin that accumulate substrates phosphorylated by ATM and/or ATR. Scale bar: 50 μ m. Right:

Augmentation from left panel (white box). White arrows point to cells negative for Involucrin with foci of substrates phosphorylated by ATM and/or ATR. Scale bar: 20 μm . **B)** Detection of substrates phosphorylated by ATM and/or ATR (red) and γ tubulin (green) by immunofluorescence. White arrows show the co-localization of γ tubulin expression and the presence of substrates phosphorylated by ATM and/or ATR. Scale bar: 20 μm . **C)** Detection of substrates phosphorylated by ATM and/or ATR (red) and γ tubulin (green) by immunofluorescence in a metaphasic cell. Scale bar: 20 μm . Nuclear DNA by DAPI.

8. ATR signaling activates the squamous differentiation program of primary keratinocytes.

To further study the role of DNA damage in keratinocyte physiology we chose to ectopically activate the DDR ATR pathway. These experiments were performed in collaboration with Ana Freije. ATR activation has been shown to be sufficient to induce senescence even in the absence of DNA damage (Toledo et al., 2008). Hence, we hypothesized that ATR signaling could be mediating the activation of the squamous differentiation program in keratinocytes. To test this hypothesis, we infected primary keratinocytes with a retroviral construct carrying the domain of TopBP1 that is able to stimulate the kinase activity of ATR in the absence of DNA damage, and which intracellular localization can be controlled by 4-hydroxytamoxifen [OHT; (Toledo et al., 2008)].

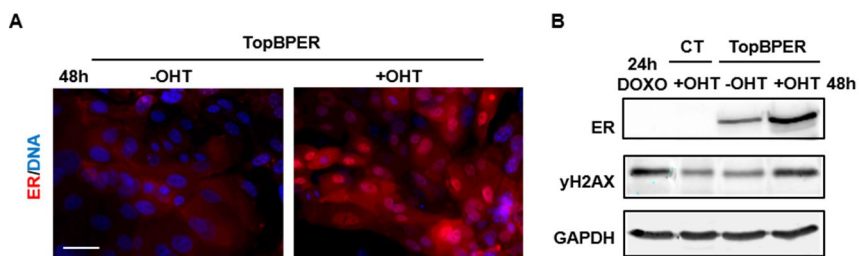


Figure 39 | TopBPER translocates to the nucleus in response to OHT. A) Detection of TopBPER (ER, red) by immunofluorescence in keratinocytes infected with TopBPER, 48h in the presence or absence of OHT as indicated. Nuclear DNA by DAPI. Scale bar: 50 μm . **B)** Detection of TopBPER (ER) and γ H2AX by western blotting in keratinocytes infected with CT or TopBPER vectors, 48h in the presence or absence of OHT as indicated. Keratinocytes treated for 24h with doxorubicin (DOXO) were used as positive control for γ H2AX detection. GAPDH was used as loading control.

As detected by immunofluorescence, the chimeric protein (TopBPER from now on) was mainly cytoplasmatic until the addition of 500nM OHT to the culture medium (Figure 39.A). 48 hours after OHT addition, the protein translocated to the nucleus (Figure 39.A). By performing western blot, we also detected that OHT increased TopBPER protein levels (Figure 39.B), possibly by preventing its degradation in the cytoplasm.

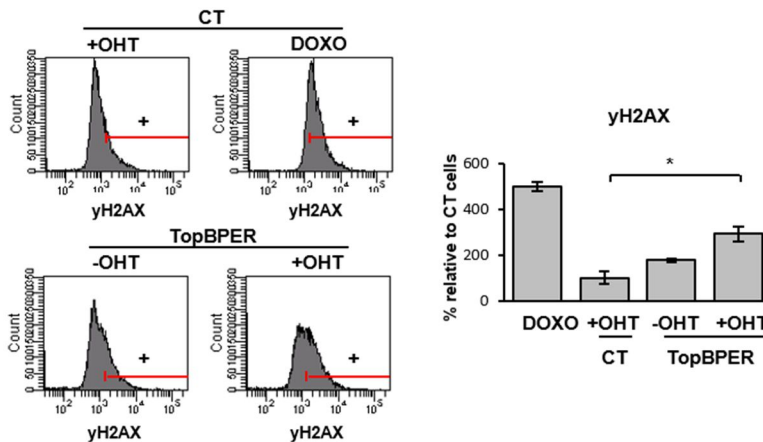


Figure 40 | TopBPER nuclear translocation increases γ H2AX signal. Left: Histograms representing the expression of γ H2AX in keratinocytes infected with control vector (CT) or TopBPER, 48h in the presence or absence of OHT, as measured by flow cytometry (+, positive keratinocytes according to negative isotype antibody control). Right: Bar histogram shows the percentage of keratinocytes positive for γ H2AX relative to CT (CT +OHT = 100%), as measured by flow cytometry. Treatment with doxorubicin (DOXO) for 24h was used as positive control for γ H2AX detection. p value: $* < 0.05$.

We determined that TopBPER translocation to the nucleus was sufficient for ATR activation. H2AX is an ATR substrate that is rapidly phosphorylated (γ H2AX) in response to RS and, therefore, we used it as a read-out (Fernandez-Capetillo et al., 2004, Ward and Chen, 2001). In response to OHT treatment, we observed an increase in the γ H2AX signal by western blot and flow cytometry (Figures 39.B and 40). The increase in γ H2AX signal after OHT treatment was commensurable to the signal detected after treating cells with DOXO for 24h. In addition to its well

known role in ATR activation, TopBP1 participates in the regulation of DNA replication (Makiniemi et al., 2001, Kumagai et al., 2010). Hence, in order to check that increased γ H2AX signal was specifically induced by ATR and not by any perturbation during DNA replication by TopBPER, we performed cometassays to detect actual DNA breaks. We did not detect any increase in DNA fragmentation 48 hours after OHT treatment, as measured by comets tail length (Figure 41). However, DOXO greatly increased DNA breaks and was used as a positive control. The results demonstrate that γ H2AX increase upon TopBPER was directly produced by ATR activation and not by real DNA damage.

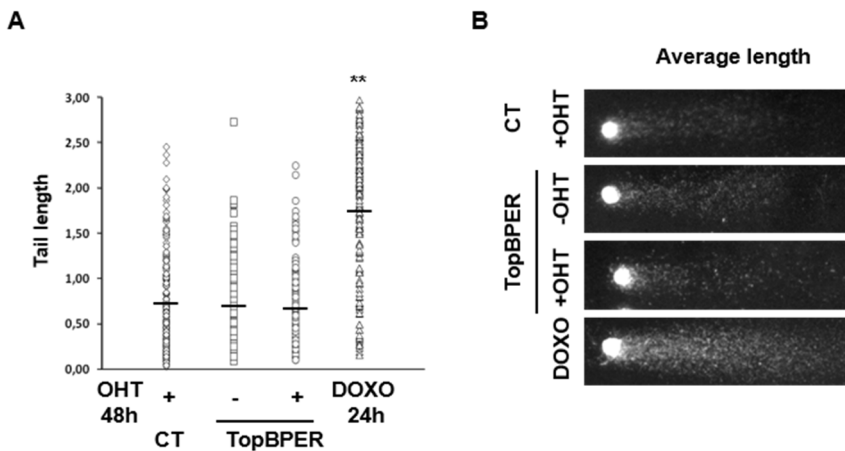


Figure 41 | TopBPER activates ATR in the absence of DNA damage. A) Quantification of comets tail length of keratinocytes infected with control vector (CT) or TopBPER, 48h in the presence or absence of OHT as indicated. Treatment with doxorubicin (DOXO) for 24h was used as positive control. Black lines represent the tail length average in each case. p value: **<0.01. **B)** Illustration of comets average length for each condition.

Finally, we studied the effect of activating ATR signaling in the differentiation of keratinocytes. First, we observed that 4 days after OHT treatment keratinocytes stopped proliferating and increased in cell size (Figure 42.A and B), as measured by light scatter parameters by flow cytometry. In addition, we observed an increase in the expression of the

differentiation marker Involucrin (Figure 42.B). Clonogenicity assays demonstrated that ATR induces terminal differentiation irreversibly (Figure 42.C). Induction of TopBPER with OHT for 4 days dramatically decreased the clonogenicity potential of keratinocytes when returned to normal conditions. Taken together, the results show that ATR signaling was sufficient for the activation of the squamous differentiation program of keratinocytes, even in the absence of actual DNA damage. However, it remains unclear whether ATR was directly responsible for triggering differentiation.

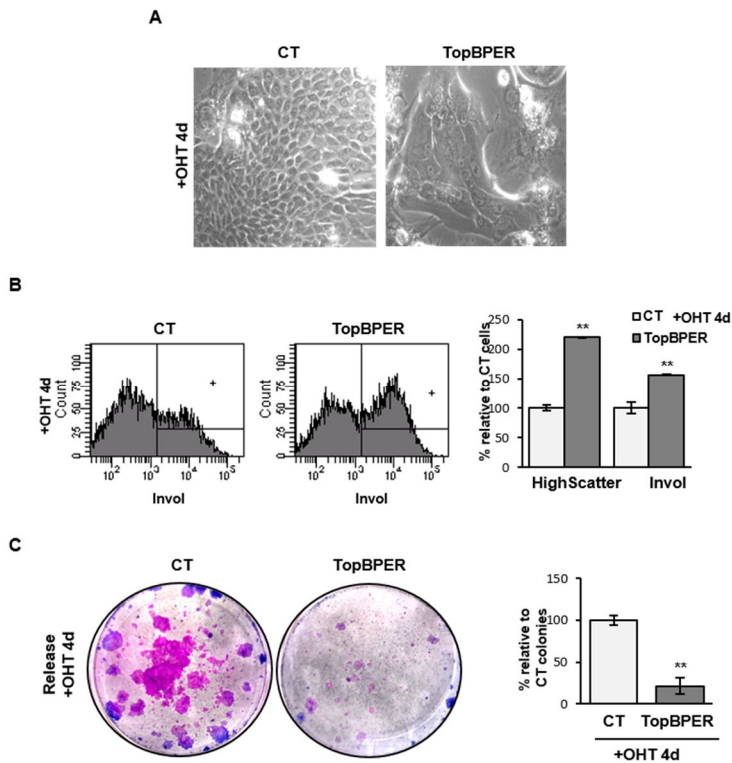


Figure 42 | ATR promotes squamous differentiation in primary keratinocytes. A) Phase contrast images of keratinocytes infected with control vector (CT) or TopBPER, 4 days in the presence of OHT. **B)** Histograms representing the expression of Involucrin (Invol) in keratinocytes infected with CT or TopBPER, 4 days in the presence of OHT, as measured by flow cytometry (+, positive keratinocytes according to negative isotype antibody control). Right: Bar histogram shows the percentage of keratinocytes with high scatter

parameters or Involucrin (Invol) expression relative to CT (CT +OHT = 100%), as measured by flow cytometry. **C)** Clonogenicity assays of keratinocytes infected with CT or TopBPER and released after 4 days cultured in the presence of OHT. Right bar histograms represent the percent of large growing colonies, relative to CT (CT +OHT = 100%).p value: **<0.01.

9. ATR inactivation leads to DNA damage accumulation and differentiation.

Given that hyperactivation of ATR signaling triggered squamous differentiation, we decided to assess whether its silencing would inhibit this response. To this aim we infected keratinocytes with a lentiviral construct carrying an shRNA against ATR (shATR), or with the corresponding empty vector. By quantitative RT-PCR we confirmed that ATR expression was efficiently silenced 4 days after infection (Figure 43.A). At that time, we observed by immunofluorescence that ATR silencing induced an increase in the γ H2AX signal (Figure 43.B), blocked G2/M progression and increased the percent of cells entering the polyploid compartment of the cell cycle, as measured by flow cytometry (Figure 44.A). In addition, we detected an increase in the percent of cells displaying high scatter parameters (Figure 44.B). Consistently with the increase in cell size, we observed by immunofluorescence and flow cytometry an increase in the expression of the differentiation marker K1 (Figures 43.B and 44.C).

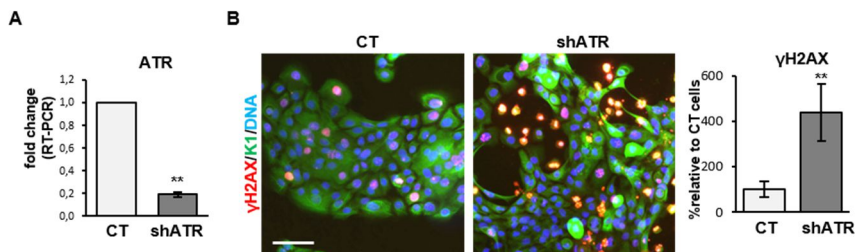


Figure 43 | shATR induces the accumulation of γ H2AX. **A)** Detection of ATR expression in keratinocytes infected with shRNA against ATR (shATR) or corresponding empty control vector (CT), by quantitative (Q) real-time (RT) PCR (fold change with respect

to control empty vector, CT). **B)** Detection of Keratin 1 (K1; green) and γ H2AX (red) by immunofluorescence in keratinocytes, 4 days after infection with shATR or CT. Right bar histogram represents the percent of keratinocytes positive for γ H2AX detected by immunofluorescence, relative to CT (CT = 100%). Nuclear DNA by DAPI. Scale bar: 50 μ m. p value: **<0.01.

Contrary to our initial hypothesis, inhibition of ATR activated the squamous differentiation response of keratinocytes. This apparent contradiction could be explained by the main role that ATR plays in DNA repair during replication: its silencing might led to the accumulation of DNA damage due to RS and in turn activate alternative DDR via ATM or DNA-PK. Activation of DDR might trigger squamous differentiation. The results point to a direct relationship between the DDR and the terminal differentiation response activation, and suggest that this relation is not ATR specific.

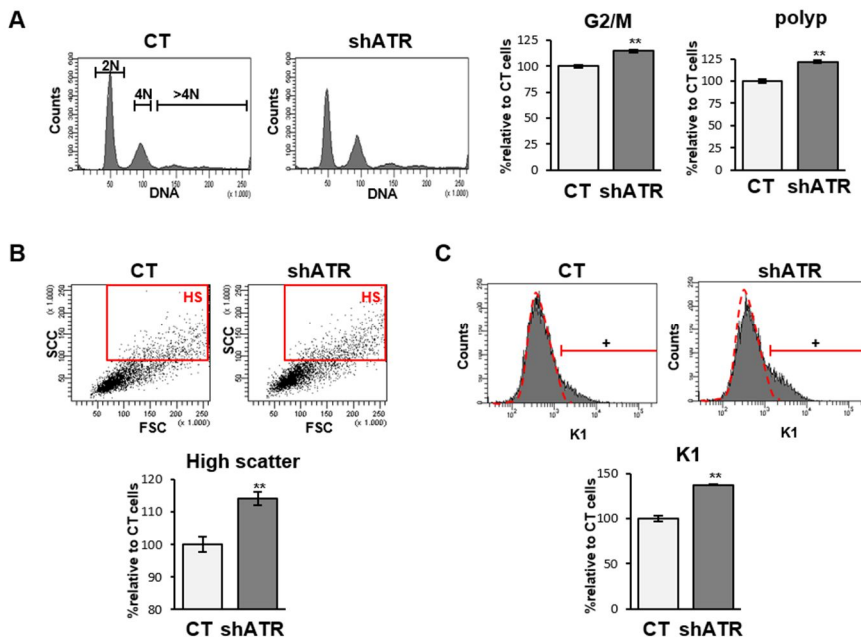


Figure 44 | shATR triggers squamous differentiation of primary keratinocytes. A) Histograms representing the DNA content of keratinocytes infected with shATR or CT for 4 days, as measured by flow cytometry. Right bar histograms represent the proportion of

keratinocytes in G2/M (4N) or the polyploid (<4N) compartment of the cell cycle relative to CT (CT = 100%). **B)** Dot plots representing the light scatter parameters of keratinocytes 4 days after infection with shATR or CT. Red box represents cell displaying high scatter parameters (HS). Bottom bar histogram represents the percent of keratinocytes with HS relative to CT (CT = 100%). **C)** Histograms representing the expression of Keratin 1 (K1) in keratinocytes 4 days after infection with shATR or CT, as measured by flow cytometry (+, positive keratinocytes according to negative isotype antibody control: red broken line). Bottom bar histogram represents the percent of keratinocytes expressing K1 relative to CT (CT = 100%). p value: **<0.01.

10. Inhibition of the DDR impairs terminal differentiation of keratinocytes.

As explained previously, although ATR, ATM and DNA-PK respond primarily to different types of DNA damage they cooperate actively in the phosphorylation of common substrates and in the activation of the DDR (Lopez-Contreras and Fernandez-Capetillo, 2012). We decided to inhibit ATR, ATM and DNA-PK simultaneously to impede the activation of the DDR. Given the difficulty to perform triple lentiviral infections with shRNAs against each of these proteins; we decided to use commercially available chemical inhibitors.

To assess the effect of the inhibitors in the activation of the DDR we checked again H2AX phosphorylation, a common substrate of ATR, ATM and DNA-PK in response to DNA damage (Fernandez-Capetillo et al., 2004). We measured γ H2AX signal by flow cytometry. Treatment with ATM (ATMi) or DNA-PK inhibitors (DNA-PKi) did not display any effect on γ H2AX signal (Figure 45.A and B, left panels). In addition, ATMi and DNA-PKi did not affect γ H2AX signal or the differentiation response of keratinocytes, as measured by Involucrin expression by flow cytometry (Figure 45, A and B, right panels). Interestingly, a 5 hours short treatment with ATR inhibitor (ATRi) decreased the γ H2AX signal in keratinocytes (Figure 46.A). Unfortunately 5h is too early to measure differentiation and a

3 days inhibition of ATR drastically induced H2AX phosphorylation (Figure 46.A). As expected, ATRi induced terminal differentiation of keratinocytes measured by light scatter parameters and Involucrin expression as detected by flow cytometry (Figure 46.B and C). This was in concordance with the results previously obtained by silencing ATR.

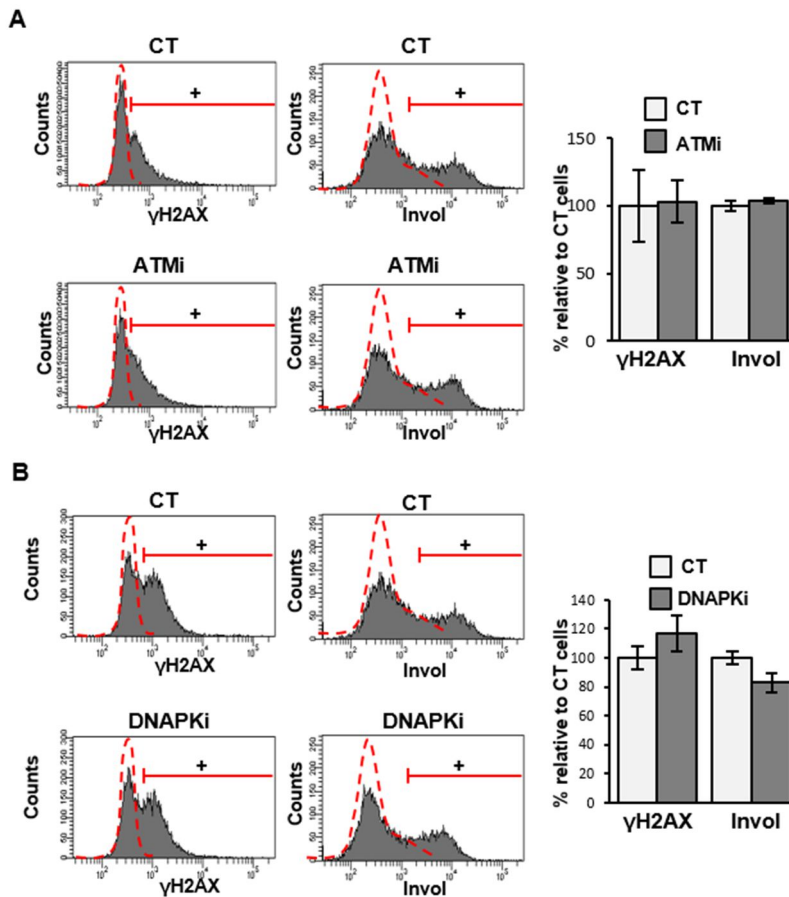


Figure 45 | ATM or DNA-PK inhibition does not affect the differentiation response of primary keratinocytes. Detection of γ H2AX signal (left) or Involucrin expression (Invol; right) in keratinocytes treated with **A**) ATM inhibitor (ATMi) or **B**) DNA-PK inhibitor (DNA-PKi) for 3 or 5 days as indicated, measured by flow cytometry (+, positive keratinocytes according to negative isotype antibody control: red broken line). DMSO was used as control (CT). Right bar histograms represent the percent of keratinocytes expressing γ H2AX (left) or Invol (right) relative to CT (CT = 100%).

We conclude that ATR inhibition early impaired H2AX phosphorylation at the sites of DNA lesions generated by RS and γ H2AX signal decreased. Later, inactivation of ATR brought as a consequence the accumulation of DNA damage due to insufficient DNA repair. Finally, accumulated DNA damage was detected by ATM and DNA-PK, which activated the DDR and compensated ATR lost by phosphorylating H2AX. As a result, γ H2AX signal drastically increased and terminal differentiation was induced.

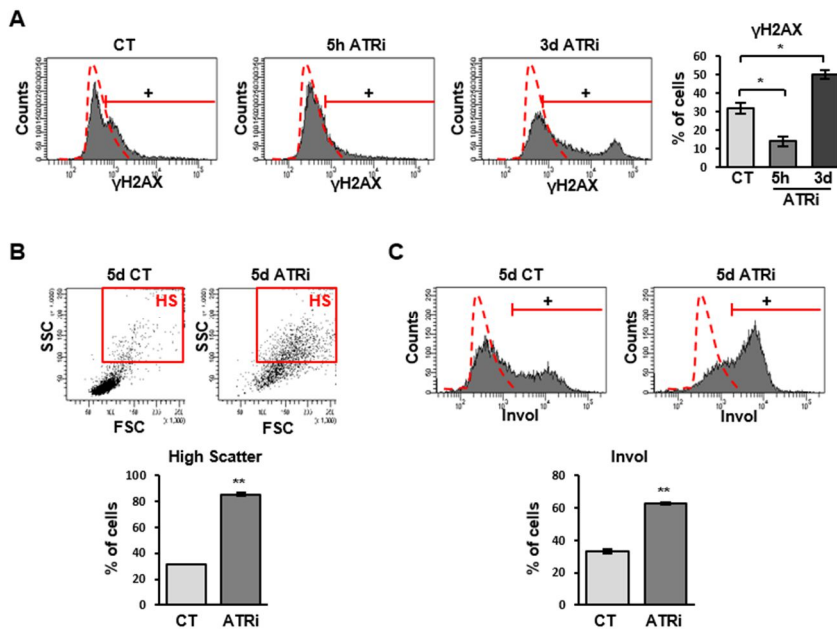


Figure 46 | ATR inhibition drastically induces H2AX phosphorylation. A) Detection of γ H2AX signal in keratinocytes treated with DMSO as control (CT) or with ATR inhibitor (ATRi) for 5 hours or 3 days as indicated, measured by flow cytometry (+, positive keratinocytes according to negative isotype antibody control: red broken line). Right bar histogram represents the percent of keratinocytes positive for γ H2AX relative to CT (CT = 100%). **B)** Dot plots representing the light scatter parameters of keratinocytes treated as indicated for 3 days. Red box represents cell displaying high scatter parameters (HS). Bottom bar histogram represents the percent of keratinocytes with HS relative to CT (CT = 100%). **C)** Histograms representing the expression of Involucrin (Invol) in keratinocytes 5 days after treatment as indicated, measured by flow cytometry (+, positive keratinocytes according to negative isotype antibody control: red broken line). Bottom bar histogram represents the percent of keratinocytes expressing Invol relative to CT (CT = 100%). p value: * <0.05 , ** <0.01 .

With the aim of successfully inhibit DDR activation we treated keratinocytes simultaneously with ATRi and ATMi (ATRi+ATMi) and observed by immunofluorescence and flow cytometry that the γ H2AX signal increased even further than when only ATRi was used (Figure 47.A and B). This suggested that ATM partially compensated for the lack of ATR repair activity. However, when we performed a triple inhibition by adding DNA-PK inhibitor to the mix (ATRi+ATMi+DNA-PKi) H2AX phosphorylation decreased (Figure 47.A and B). Triple inhibition also impaired γ H2AX signal in metaphasic chromosomes, at the point of the cell cycle at which this signal is known to peak [Figure 47.C; (McManus and Hendzel, 2005)]. The results indicate that treatment with ATRi+ATMi+DNA-PKi inhibited DDR at least partially.

Next, we examined the effect of inhibiting the DDR in the squamous differentiation response. By flow cytometry, we detected that treatment with ATRi+ATMi induced a dramatic increase in keratinocyte light scatter parameters, typical of terminal differentiation (Figure 48.A), which was accompanied by an increase in the expression of the terminal differentiation marker Involucrin (Figure 48.B and C), as detected by flow cytometry and immunofluorescence. Treatment with ATRi+ATMi+DNA-PKi did not display any effect on light scatter parameters (Figure 48.A) but inhibited the expression of Involucrin with respect to the double inhibition (Figure 48.B and C). This was consistent with the decrease observed above in γ H2AX. In addition, clonogenicity assays showed that while ATRi+ATMi drastically abolished the colony forming potential of keratinocytes returned to normal conditions 5 days after treatment, it was partially rescued by ATRi+ATMi+DNA-PKi (Figure 48.D). Taken together, the results suggest that inhibition of DDR activation and γ H2AX signaling impaired the differentiation response of keratinocytes.

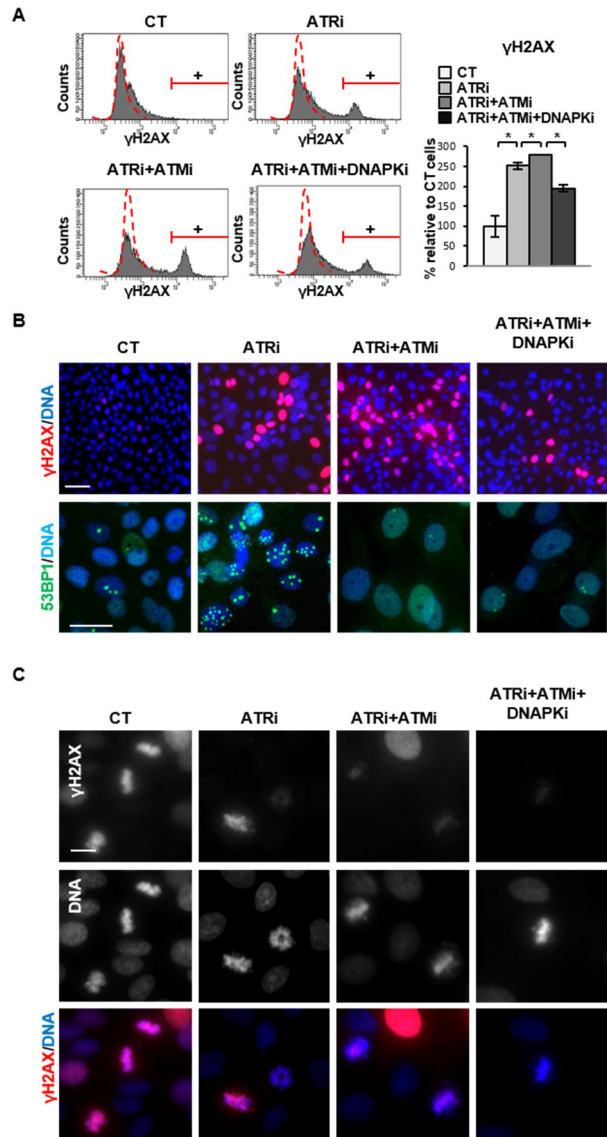


Figure 47 | Effect of ATR, ATM and DNA-PK inhibition in the DNA damage response. A) Detection of γ H2AX signal in keratinocytes treated with DMSO as control (CT), ATR inhibitor (ATRi), ATR and ATM inhibitors (ATRi+ATMi) or ATR, ATM and DNA-PK i (ATRi+ATMi+DNAPKi) for 3 days, measured by flow cytometry (+, positive keratinocytes according to negative isotype antibody control: red broken line). Right bar histogram represents the percent of keratinocytes positive for γ H2AX relative to CT (CT = 100%). p value: * <0.05 . **B)** Detection of γ H2AX (top; red. Scale bar: 50 μm) or 53BP1 (bottom; green. Scale bar: 25 μm) by immunofluorescence in keratinocytes treated as indicated. **C)** Detection of γ H2AX (red) in metaphasic keratinocytes treated as indicated. Scale bar: 25 μm . Nuclear DNA by DAPI.

To elucidate whether the decrease in the DNA damage signaling was due to DDR inhibition and not to an increase in DNA repair produced by an unknown compensatory mechanism, we performed cometassays (Figure 49). The results showed that DNA fragmentation was increased when keratinocytes were treated with ATRi+ATMi and that this level of fragmentation was maintained when treated with ATRi+ATMi+DNA-PKi (Figure 49), supporting the idea that simultaneous inhibition of ATR, ATM and DNA-PK impaired γ H2AX signal in the presence of DNA damage.

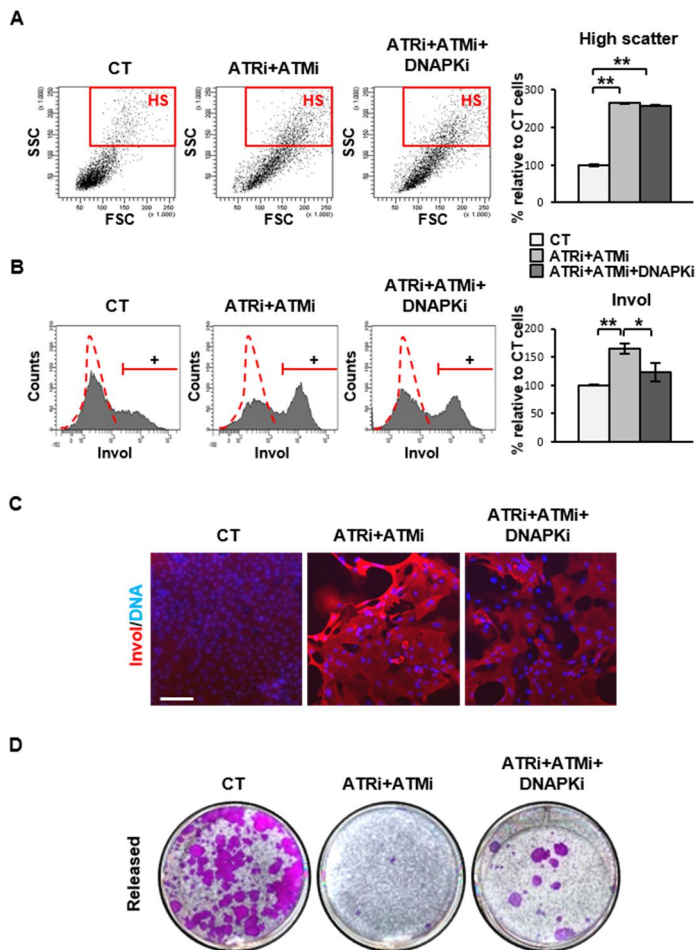


Figure 48 | Inhibition of the DNA damage response impairs the squamous differentiation program. A) Dot plots representing the light scatter parameters of keratinocytes 5 days after treatment with DMSO as control (CT), ATR and ATM inhibitors

(ATRi+ATMi) or with ATR, ATM and DNA-PK inhibitors (ATRi+ATMi+DNA-PKi), measured by flow cytometry. Red box represents cell displaying high scatter parameters (HS). Right bar histogram represents the percent of keratinocytes with HS relative to CT (CT = 100%). **B)** Histograms representing the expression of Involucrin (Invol) of keratinocytes treated for 5 days as indicated, measured by flow cytometry (+, positive keratinocytes according to negative isotype antibody control: red broken line). Right bar histogram represents the percent of keratinocytes expressing Involucrin relative to CT (CT = 100%). **C)** Detection of Involucrin (Invol, red) in keratinocytes treated for 5 days as indicated, by immunofluorescence. Nuclear DNA by DAPI. Scale bar: 50 μ m. **D)** Clonogenicity assays of keratinocytes released after 5 days as of treatment as indicated. p value: * <0.05 ; ** <0.01 .

Immunofluorescence also showed an interesting result. ATRi induced the formation of 53BP1 foci as detected by immunofluorescence, whereas ATRi+ATMi impaired it (Figure 47.B). This effect can be explained by the fact that 53BP1 recruitment to DNA lesions is dependent on ATM kinase activity (Lee et al., 2009, Schmidt et al., 2014). Adding DNA-PKi to the mix did not display any effect in the capability of 53BP1 foci formation in the absence of ATM (Figure 47.B).

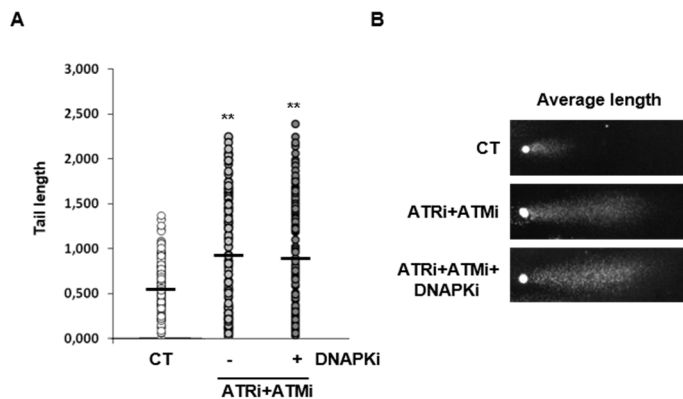


Figure 49 | Inhibition of ATR, ATM and DNA-PK impairs DDR in the presence of increased DNA damage. A) Quantification of comets tail length of keratinocytes treated with DMSO (CT) or ATR and ATM inhibitors (ATRi+ATMi) in the presence or absence of DNA-PK inhibitor (DNAPKi). Black lines represent the tail length average in each case. p value: ** <0.01 . **B)** Illustration of comets average length for each condition.

In summary, these results suggest that although ATR is the main kinase involved in activation of the DDR to RS, ATM and DNA-PK can also compensate for genome stability maintenance in proliferative keratinocytes. Consistently, when keratinocytes were treated with ATRi+ATMi+DNA-PKi γ H2AX signaling decreased in the presence of high damage. Finally, we found that γ H2AX signaling correlates with the differentiation response of keratinocytes, independently from actual DNA damage.

11. Inhibition of the γ H2AX signal impairs squamous differentiation and induces an epidermal to mesenchymal transition.

Although a role of the DDR in squamous differentiation was strongly supported by our results, the exact molecular signal implicated in the activation of differentiation remained unknown. The three DNA damage pathways converge on phosphorylation of H2AX. Given that we found a direct correlation between DDR signaling and differentiation, we decided to silence the expression of H2AX altogether. To this aim we infected keratinocytes with a lentiviral construct carrying a specific shRNA against H2AX (shH2AX) or the corresponding empty vector. Infection with the construct efficiently silenced the expression of H2AX, as observed by immunofluorescence, quantitative RT-PCR and western blotting (Figure 50.A, B and C). Consistently, western blot and flow cytometry showed that γ H2AX levels were also reduced even when global DNA damage was induced with DOXO (Figure 50.C and D). By immunofluorescence, we observed that H2AX silencing affected the DDR. γ H2AX signal is known to be necessary for the formation of the so called ionizing radiation-induced foci (IRIF) by the recruitment of repair factors such as 53BP1 (Ward et al., 2003). Accordingly, H2AX silencing impaired the formation of 53BP1 foci (Figure 51.A).

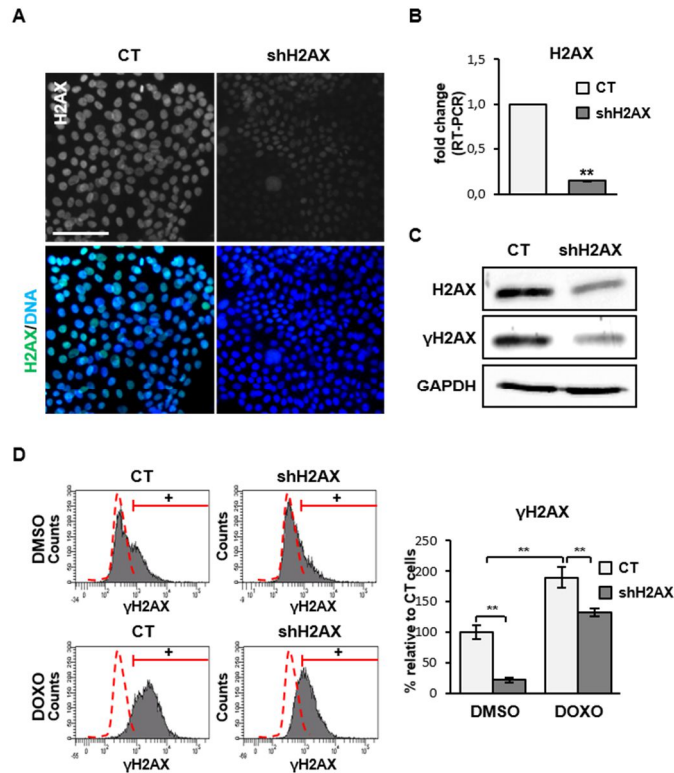


Figure 50 | Inhibition of H2AX expression in primary keratinocytes. Detection of H2AX expression in keratinocytes infected with an shRNA against H2AX (shH2AX) or the corresponding empty control vector (CT) by **A**) immunofluorescence (green), **B**) RT-PCR and **C**) western blotting. γ H2AX is also detected by western blot. GAPDH was used as loading control. **D**) Detection of γ H2AX in CT or shH2AX keratinocytes treated for 48h with DMSO or Doxorubicin (DOXO), measured by flow cytometry (+, positive keratinocytes according to negative isotype antibody control: red broken line). Right bar histogram represents the percent of keratinocytes positive for γ H2AX relative to CT keratinocytes (CT/DMSO = 100%). Nuclear DNA by DAPI. Scale bar: 50 μ m p value: **<0.01.

Inefficient DNA repair due to H2AX silencing likely induced ATM and/or ATR and the phosphorylation of their substrates (Figure 51.B). In addition, higher levels of DNA fragmentation were detected by the comet assay in cells lacking H2AX (Figure 51.C). Hence, H2AX silencing brought as a consequence the accumulation of DNA damage. By western blot we detected that the expression of several cell cycle regulators changed (Figure

52.A). Depletion of H2AX decreased the expression of the S phase regulator cyclin E and increased expression of mitotic cyclin A and cyclin B. In addition, we observed an increase in the phosphorylation of the histone H3, which is a marker of metaphase. These results suggest that loss of H2AX impairs the activation of the G2/M checkpoints in response to DNA damage.

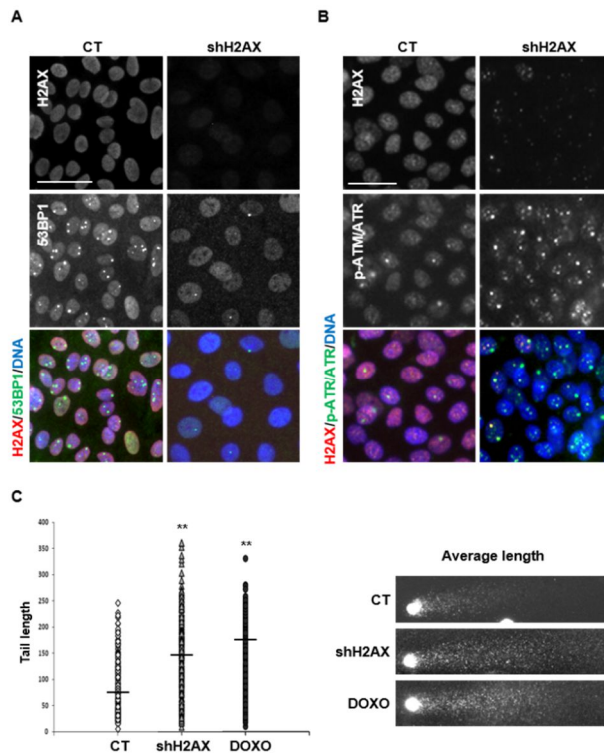


Figure 51 | shH2AX induces DNA damage. **A)** Immunofluorescence for the detection of H2AX (red) and 53BP1 (green) in keratinocytes infected with an shRNA against H2AX (shH2AX) or the corresponding empty control vector (CT). **B)** Detection of H2AX (red) and substrates phosphorylated by ATM and/or ATR (p-ATM/ATR; green) in control or shH2AX keratinocytes. Nuclear DNA by DAPI. Scale bar: 10 μ m. **C)** Left: Quantification of comets tail length in control or shH2AX keratinocytes. Treatment with Doxorubicin (DOXO) was used as positive control. Black lines represent the tail length average in each case. Right: Illustration of comets average length for each condition. p value: $** < 0.01$.

Finally, we examined the effect of H2AX silencing in the squamous differentiation program of keratinocytes. By flow cytometry we analysed the

light scatter parameters of keratinocytes and the expression of Involucrin. We observed that H2AX silencing did not affect keratinocytes size or complexity, but inhibited the expression of Involucrin (Figure 52.B and C, top). Inhibition of Involucrin expression was also confirmed by western blot (Figure 53.A). In addition, H2AX silencing decreased cell size and Involucrin expression of keratinocytes after treatment with DOXO (Figure 52.B and C, bottom). This is important because it shows that the keratinocyte differentiation response to DNA damage is mediated by γ H2AX. The inhibition of differentiation produced by H2AX loss was also confirmed by the decrease in the expression of K1 as measured by quantitative RT-PCR (Figure 53.B). Taken together, the results suggest that γ H2AX signal activates the differentiation response of keratinocytes.

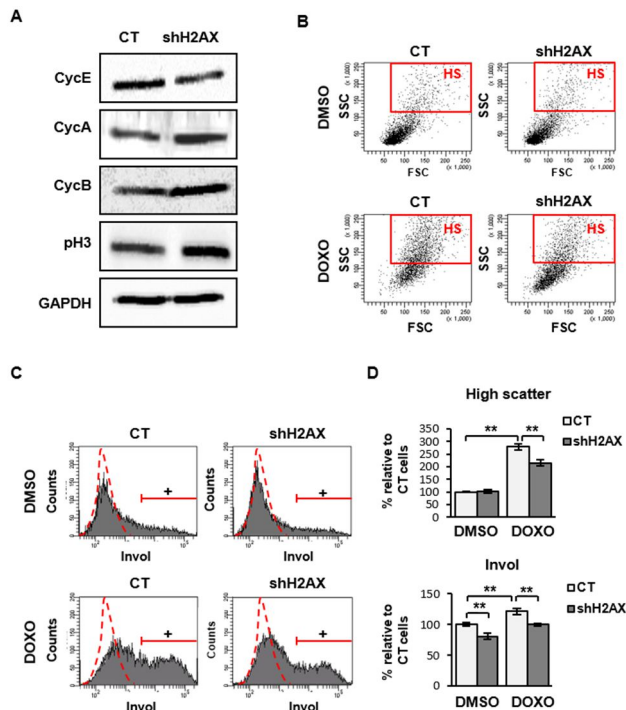


Figure 52 | shH2AX impairs the differentiation response of keratinocytes. A) Detection of cyclin E (CycE), cyclin A (CycA), cyclin B (CycB) and phosphor-H3 (pH3) in control (CT) or shH2AX keratinocytes by western blot. GAPDH was used as loading control. **B)** Dot plots representing the light scatter parameters of keratinocytes infected with

shH2AX or the control vector (CT) and treated for 48h with DMSO or Doxorubicin (DOXO), measured by flow cytometry. Red box represents cell displaying high scatter parameters (HS). **C)** Histograms representing the expression of Involucrin (Invol) in control CT or shH2AX keratinocytes treated for 48h with DMSO or DOXO, measured by flow cytometry (+, positive keratinocytes according to negative isotype antibody control: red broken line). **D)** Bar histogram represents the percent of keratinocytes with HS (top) or expressing Involucrin (Invol; bottom) relative to CT keratinocytes (CT/DMSO = 100%). p value: **<0.01.

H2AX depletion did not only inhibit in the expression of squamous differentiation markers. Very interestingly, we also observed an increase in the expression of molecular markers that are considered characteristic from an epithelia-to mesenchyma-transition (EMT). Western blotting, quantitative RT-PCR and immunofluorescence showed an increase in the expression of Keratin K8 (K8, Figure 53.A- B and Figure 54.B), which is a keratin typically expressed in simple epithelia and is gained in epidermoid carcinoma (Caulin et al., 1993, Tiwari et al., 2017). Accordingly, quantitative RT-PCR and immunofluorescence showed a decrease in the expression of Keratin 5 (K5, Figures 53.B and 54.A), which is expressed in the basal layer of stratified epithelia and is typically lost in epidermoid carcinoma (Caulin et al., 1993).

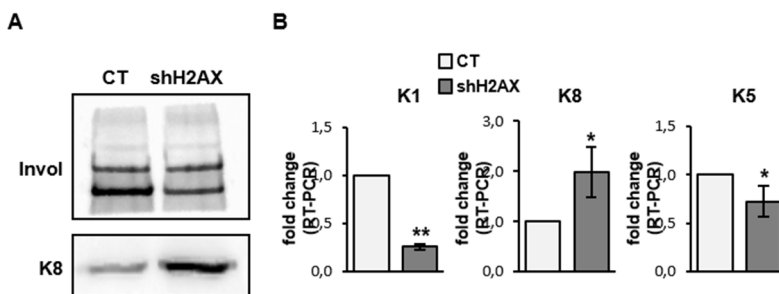


Figure 53 | shH2AX inhibits the squamous phenotype. A) Detection of Involucrin (Invol) and Keratin 8 (K8) in keratinocytes infected an shRNA against H2AX (shH2AX) or the corresponding empty vector (CT), by western blot. **B)** Detection of Keratin 1 (K1), Keratin 8 (K8) and Keratin 5 (K5) in CT or shH2AX keratinocytes, by real-time (RT) PCR (fold change with respect to control empty vector, CT). p value: *< 0.05, **<0.01.

12. DNA damage signaling is detected in the epidermis *in situ*.

Keratinocytes growing *in vitro* are stimulated by growth factors driving the cell cycle and this might cause RS. Indeed, lower concentrations of serum reduced the DNA damage marker γ H2AX *in vitro* (not shown). It was important to determine whether proliferative keratinocytes in the skin accumulate DNA damage. This encountered strong technical difficulties likely due to difficult access of antibodies to the histone within the formalin fixed tissue. Finally we could find a method by which we could detect cells accumulating γ H2AX by immunofluorescence in the epidermis *in situ* (see Material and Methods).

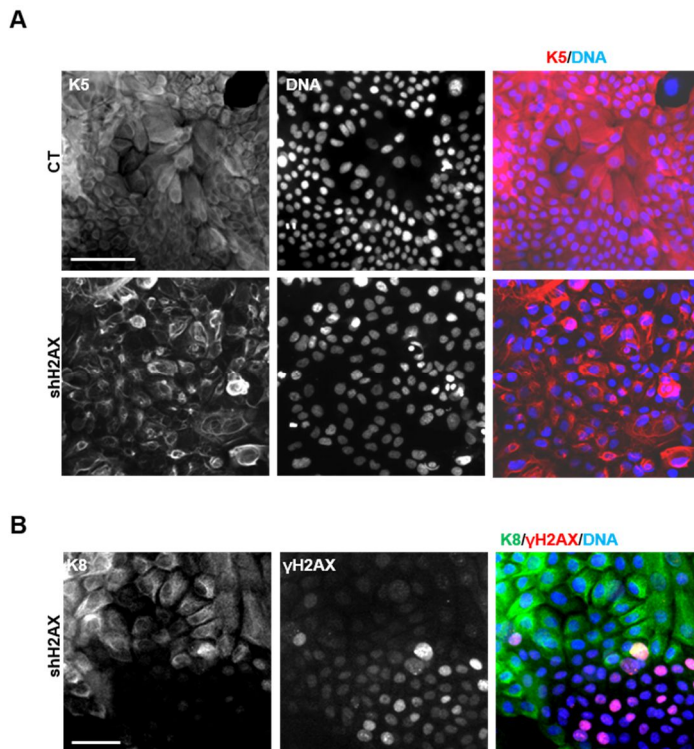


Figure 54 | shH2AX induces an epithelia to mesenchyma transition. A) Detection of Keratin 5 (K5, red) in keratinocytes infected with an shRNA against H2AX (shH2AX) or the corresponding empty control vector (CT) by immunofluorescence. **B)** Detection of Keratin 8 (K8, green) and γ H2AX (red) in CT or shH2AX keratinocytes by immunofluorescence. Note that K8 and γ H2AX are excluding. Nuclear DNA by DAPI. Scale bar: 50 μ m.

Positive cells were found as basal proliferative clones (Figure 55.A, left panel). Interestingly, γ H2AX was also detected in peribasal cells that had started stratification and expressed the differentiation marker K1 (Figure 55.A, right panel). It has been described that maximum γ H2AX signal is detected during mitosis (McManus and Hendzel, 2005) and, accordingly, we detected a strong γ H2AX signal in suprabasal metaphasic keratinocytes expressing K1 (Figure 55.B). Expression of K1 implies the incapability of cell division (Kartasova et al., 1992), and hence these cells might have undergone endoreplication. Hence, the results suggest that γ H2AX signaling plays a role in both proliferation and differentiation of keratinocytes.

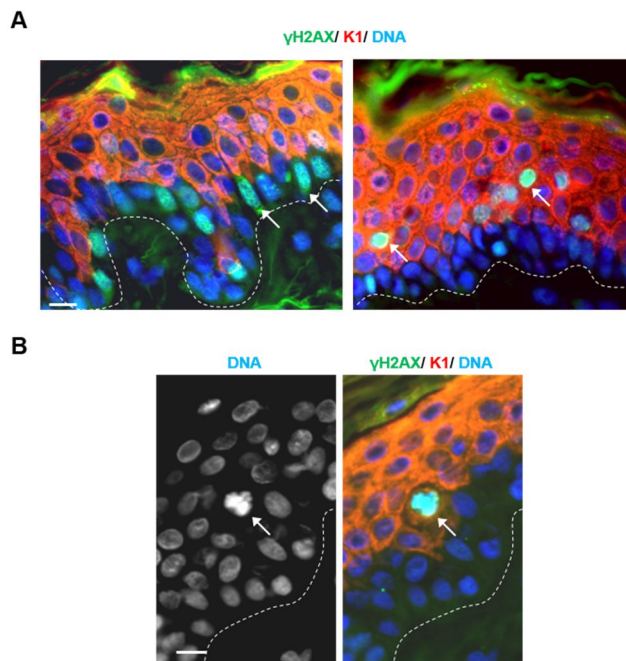


Figure 55 | DNA damage signaling is detected in the epidermis *in situ*. **A)** Detection of γ H2AX (green) and Keratin 1 (K1; red) immunofluorescence. Note that γ H2AX is detected in basal proliferative keratinocytes (left panel, white arrows) and suprabasal differentiating keratinocytes (right panel; white arrows). **B)** Detection of γ H2AX (green) in a mitotic cell expressing K1 (red). White broken line indicates the basement membrane. Nuclear DNA by DAPI. Scale bar: 50 μ m.

SEARCH FOR NOVEL MOLECULES POTENTIALLY INVOLVED IN THE DIFFERENTIATION RESPONSE TO DNA DAMAGE.

Our experiments demonstrating the role of DNA damage in the natural differentiation program of epidermal keratinocytes have provided new insight into the mechanisms that regulate skin homeostasis under normal healthy conditions. Activation of the DDR drove keratinocytes into differentiation in a γ H2AX signal-dependent manner. Although inhibition of γ H2AX signaling partially inhibited squamous differentiation, this response was not completely abolished. Hence, we concluded that, in addition to γ H2AX, other molecules downstream of, or alternative to the DDR might control squamous differentiation and we aimed to identify them. To accomplish this objective, we performed RNA sequencing (RNA-seq) to identify genes from the DDR whose expression is specifically up- or downregulated during DMC activation.

The DMC is activated by a series of events comprising cell cycle deregulation, accumulation of DNA damage and mitosis arrest. Thus, we decided to use different treatments that activate the DMC by affecting the process at different stages. To determine the duration of each treatment, we performed time course experiments. The molecular signal that activates the differentiation response might be subsequent to the G2/M arrest. For this reason, we searched for the moment at which most cells were accumulating the cyclin A protein. In addition, the G2/M arrest must occur in the absence of differentiation markers expression, given that the signal might precede the response. Based on these hypotheses, the cells were collected at the moment at which cyclin A protein was accumulated but K1 mRNA was not expressed yet.

We first performed a set of experiments in which we inhibited the expression of p53 in keratinocytes by using an shRNA against the protein (shp53). By inhibiting p53 we induced the deregulation of cell cycle and the activation of the DMC as a response to RS. Control cells were infected with a construct carrying an empty vector. Cells were collected 30 hours post-infection based on the premises previously exposed. Then, total RNA was isolated and sent to the Centro Nacional de Análisis Genómico (CNAG) in Barcelona for libraries preparation and sequencing. Next, we performed a second set of experiments treating keratinocytes with DOXO or commercially available chemical inhibitors against AurB or Plk kinases (ZM 44739 and BI 2536, respectively). These experiments were performed during my EMBO short-term fellowship at the University of Michigan in collaboration with Dr. JT Elder. Control cells were treated with DMSO. Treatment with DOXO directly produces severe DNA damage and in turn activates the DMC. The effect produced by DOXO is more rapid and direct than shp53. Treatment with AurB or Plk inhibitors activates the DMC by directly blocking mitosis progression and thus, their effect must be downstream of shp53 and DOXO. It is worth noting that although ZM and BI act at a similar stage during mitosis, their effect are slightly different. While AurB inhibition (ZM) induces very high levels of polyploidy, this effect is more moderate when Plk is inhibited (BI). For this set of experiments cells were collected 16 hours after treatment, based on the premises explained previously. Total RNA was isolated and sent to the Sequencing Core of the University for libraries preparation and sequencing. Measurement and normalization of gene expression levels obtained from these experiments and from the experiment with shp53 was performed in collaboration with Dr. Alex Tsoi from the University of Michigan.

All these treatments trigger squamous differentiation. Gene changes in every experiment was the first goal. In addition, by combining the differentially

expressing genes (DEGs) obtained from each treatment we could exclude genes involved in processes such as DDR, mitosis arrest, and identify common changes specific of the signal for differentiation.

13. Transcriptome analyses reveal a list of genes potentially involved in the activation of the differentiation-mitosis checkpoint of keratinocytes.

For each treatment, DEGs presenting a pvalue < 0.05 were selected. When we infected keratinocytes with shp53, 3,754 DEGs were identified. Among these, 1,957 genes were up-regulated and 1,797 were down-regulated. In the case of DOXO 8,392 DEGs were identified. From these, 4,240 were up-regulated and 4,152 genes were down-regulated. In the case of AurB inhibition, we identified 1,280 DEGs. From these, 507 genes were up-regulated and 773 were down regulated. Finally, when we inhibited Plk we identified 4,418 DEGs. From these, 2,300 were up-regulated and 2,118 were down-regulated (Figure 56).

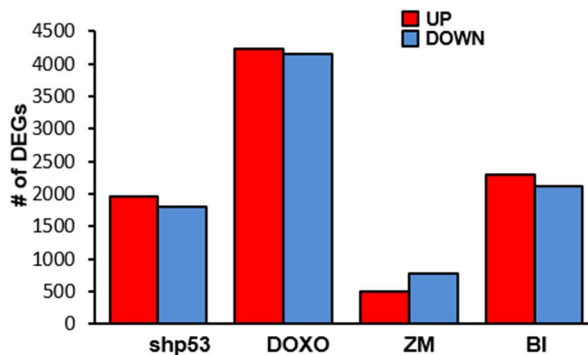


Figure 56 | Identification of differentially expressed genes. Bar histogram representing the number of DEGs identified in primary keratinocytes collected 30h after infection with shRNA against p53 (shp53) or after treated for 16h with Doxorubicin (DOXO), AurB inhibitor (ZM) or Plk inhibitor (BI). Red bars represent DEGs up-regulated. Blue bars represent DEGs down-regulated.

We next performed Gene Ontology (GO) enrichment analyses, focused on biological processes, of the sets of DEGs found in each treatment. Up- and down-regulated DEGs were analysed independently (Figures 57-60). GO analyses revealed an over-representation of DEGs involved in mitosis and cell division. These changes were interpreted as an internal control of the generalized mitotic arrest induced in response to the treatments. However, while DEGs involved in mitosis and cell division are up-regulated after p53 silencing or Plk inhibition (Figures 57 and 58), DEGs involved in these processes were down-regulated in DOXO and AurB inhibition (Figures 59 and 60).

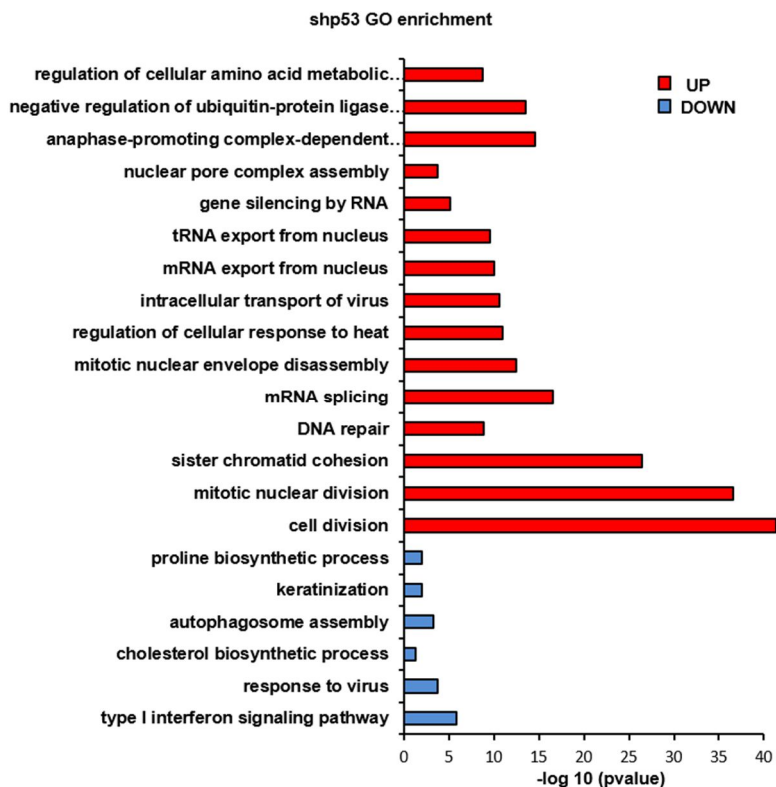


Figure 57 | GO enrichment analysis of DEGs identified after p53 silencing. Bar histogram representing p values ($-\log_{10}$) of the most significant GO terms enriched by up- (red bars) or down-regulated (blue bars) DEGs identified in primary keratinocytes 30h post-infection with shp53.

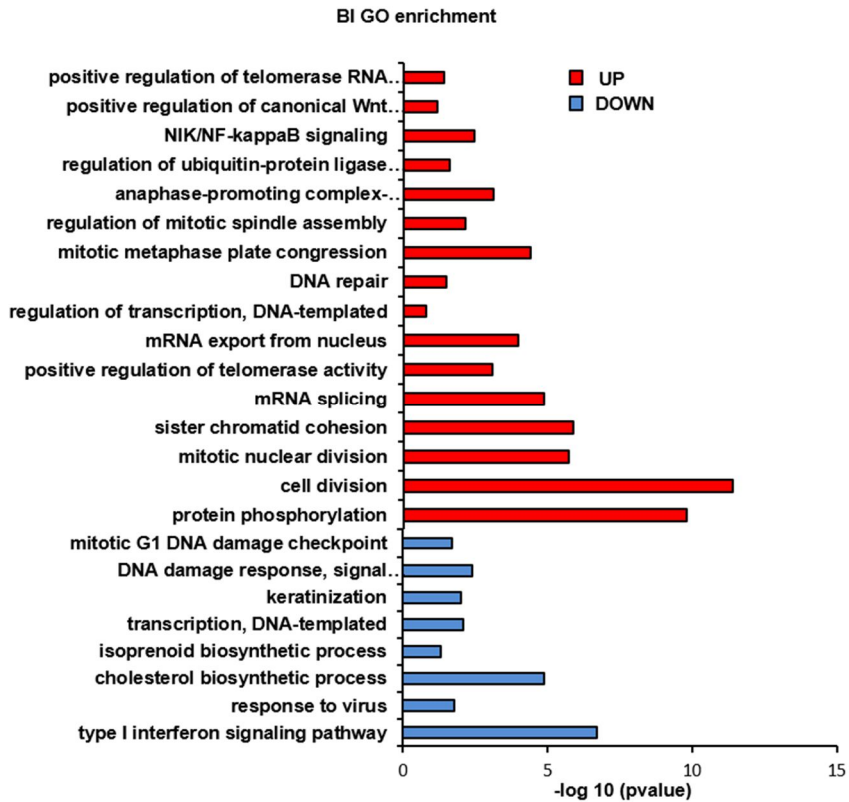


Figure 58 | GO enrichment analysis of DEGs identified after Polo-like kinase inhibition. Bar histogram representing p values ($-\log_{10}$) of the most significant GO terms enriched by up- (red bars) or down-regulated (blue bars) DEGs identified in primary keratinocytes treated with Polo-like kinase inhibitor (BI) for 16h.

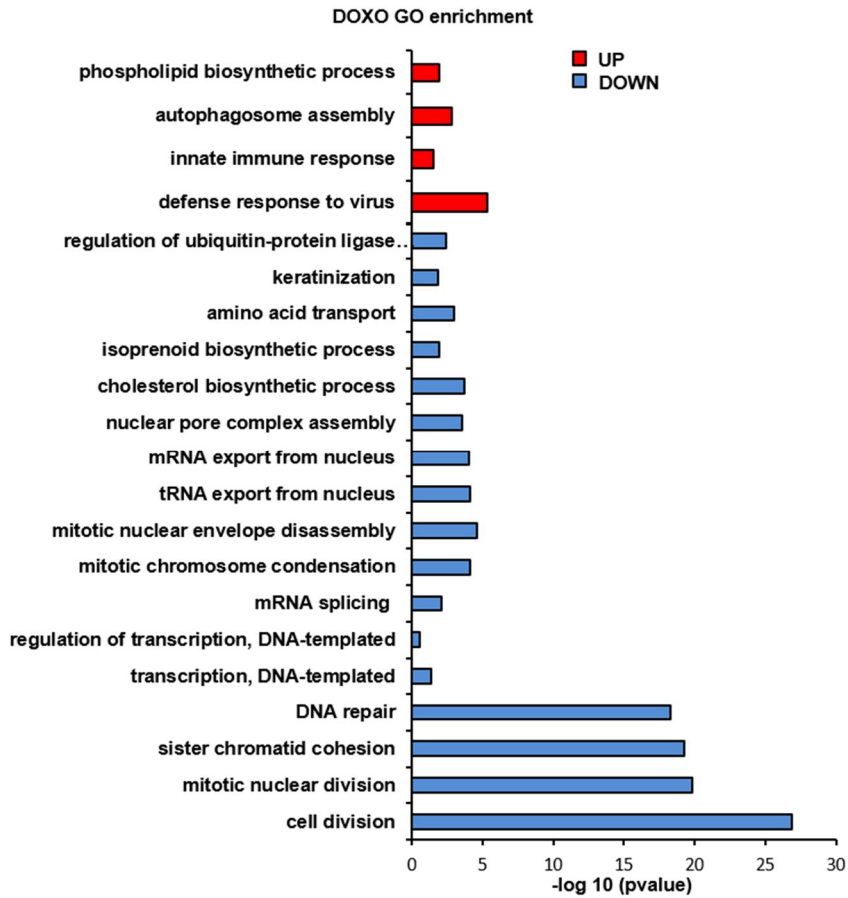


Figure 59 | GO enrichment analysis of DEGs identified after DOXO treatment. Bar histogram representing p values ($-\log_{10}$) of the most significant GO terms enriched by up- (red bars) or down-regulated (blue bars) DEGs identified in primary keratinocytes treated with doxorubicin (DOXO) for 16h.

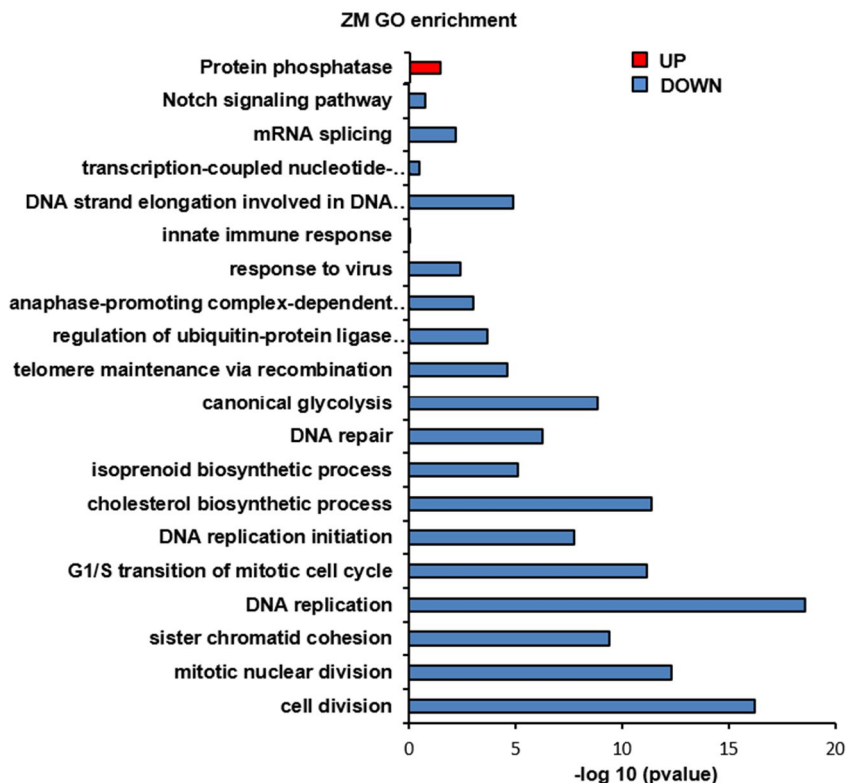


Figure 60 | GO enrichment analysis of DEGs identified after Aurora B inhibition. Bar histogram representing p values ($-\log_{10}$) of the most significant GO terms enriched by up- (red bars) or down-regulated (blue bars) DEGs identified in primary keratinocytes treated with Aurora B kinase inhibitor (ZM) for 16h.

At a glance, we detected gene expression changes involved in cell cycle regulation and mitosis, protein ubiquitination, neuronal development and Notch signaling. Venn analyses of the DEGs identified in all treatments were performed next. Up- and down-regulated DEGs were analysed independently. We found that 15 DEGs were commonly up-regulated (Figure 61.A, a). After performing GO enrichment analyses of these 15 DEGs, we found that biological processes involved in cell cycle regulation were significantly enriched ($\text{pvalue} < 0.01$; Figure 61.B). We also found that 40 DEGs were commonly down-regulated in all the treatments (Figure 61.A, b). After performing GO enrichment analyses of these 40 DEGs, we

found that biological processes involved in lipid metabolism were significantly enriched (p value <0.01 ; Figure 61.B).

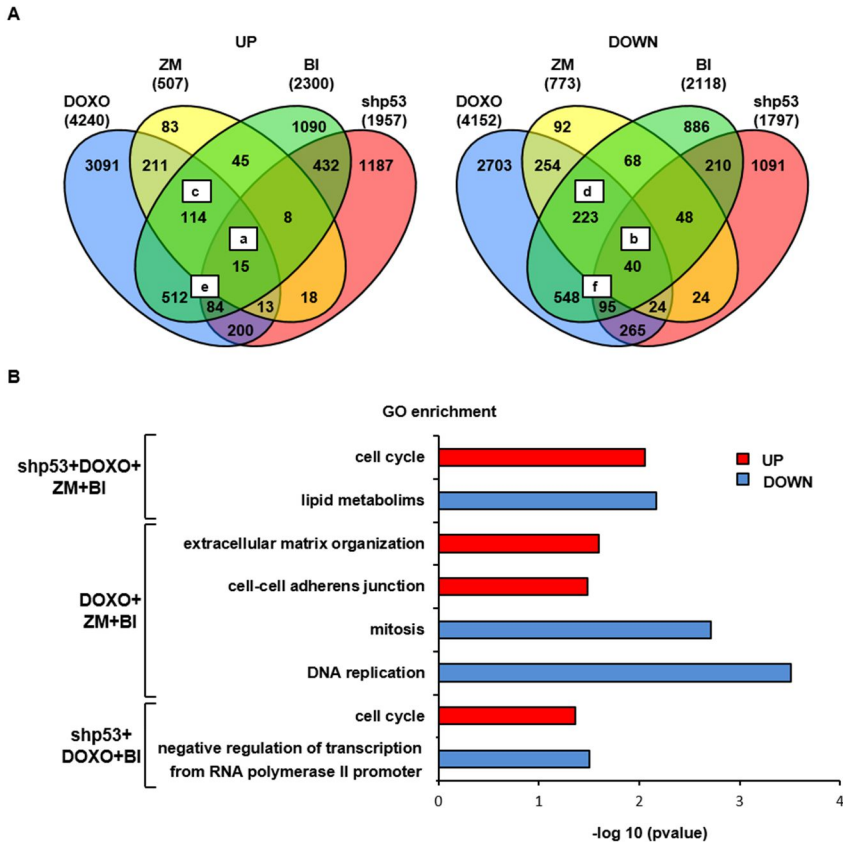


Figure 61 | GO enrichment analysis of common DEGs. A) Venn analyses of up- (left) or down-regulated (right) DEGs in the four treatments: infection with shRNA against p53 (shp53, red), doxorubicin (DOXO, blue), AurB inhibition (ZM, yellow) and Plk inhibition (BI, green). Numbers indicate DEGs in each case. Letters in white boxes represent DEGs selected for Gene Ontology (GO) enrichment analysis in B. **B)** Bar histogram representing p values ($-\log_{10}$) of the most significant GO terms enriched by commonly up- (red bars) or down-regulated (blue bars) DEGs in the treatments indicated.

These 55 DEGs were considered potentially involved in the DMC and its role in this response will be analysed in future studies. In addition to this set, we also identified potentially interesting genes by performing GO

enrichment analyses of DEGs commonly up- or down-regulated in different combinations of treatments. By combining the 114 DEGs commonly up-regulated in DOXO, AurB inhibitor and Plk inhibitor (Figure 61.A, c) we obtained an enrichment in biological processes involved in extracellular matrix organization and cell-cell adherent junctions (Figure 61.B). In the other hand, combination of the 223 commonly down-regulated in these treatments (Figure 61.A, d) resulted in enrichment in biological processes involved in mitosis and DNA replication (Figure 61.B). Combination of the 84 DEGs commonly up-regulated when keratinocytes were treated with shp53, DOXO or Plk inhibitor (Figure 61.A, e) resulted in an enrichment in biological processes involved in cell cycle regulation (Figure 61.B), whereas the 95 DEGs commonly down-regulated with these treatments (Figure 61.A, d) showed enrichment in processes involved in the negative regulation of transcription from RNA polymerase II promoter (Figure 59.B).

In our laboratory the results continue to be analysed in collaboration with the Group of JT Elder in Michigan. Validation studies will be subsequently run in order to select genes with role in the initiation of squamous differentiation in response to DNA damage. Some of these genes might be squamous master genes that are currently unknown

DISCUSSION

p53 PLAYS A DUAL ROLE IN EPIDERMAL HOMEOSTASIS.

The role of p53 protein as a tumor suppressor has been extensively described. p53 is known to induce apoptosis in the epidermis in response to severe DNA damage produced by UV radiation (Ziegler et al., 1994). However keratinocytes have not been reported to undergo apoptosis in a steady-state situation (Gandarillas et al., 1999). The role of p53 in normal epidermis is still unclear. Its overexpression has been shown to reduced keratinocyte proliferation and altered the normal differentiation program in cell-reconstituted epidermis (Woodworth et al., 1993). In carcinoma cells it induces the expression of epidermal markers (Brenner et al., 1993). In addition, p53 expression has been reported to be downregulated in differentiating keratinocytes, concomitantly with an increase in the activity (Weinberg et al., 1995, Kallassy et al., 1998). The skin of mice knockout for p53 or overexpressing of a mutant p53 form appears unaffected (Donehower et al., 1992, Lavigueur et al., 1989, Harvey et al., 1995).

We propose that p53 might play a dual role in the maintenance of epidermal homeostasis. On the one hand, p53 might protect the proliferative capacity of epidermal stem cells by activating the cell cycle checkpoints to allow time for DNA repair (Figure 62). In agreement, p53 is downregulated at the onset of epidermal differentiation (Dazard et al., 2000). On the other hand, p53 might induce apoptosis in the event of acute DNA damage.

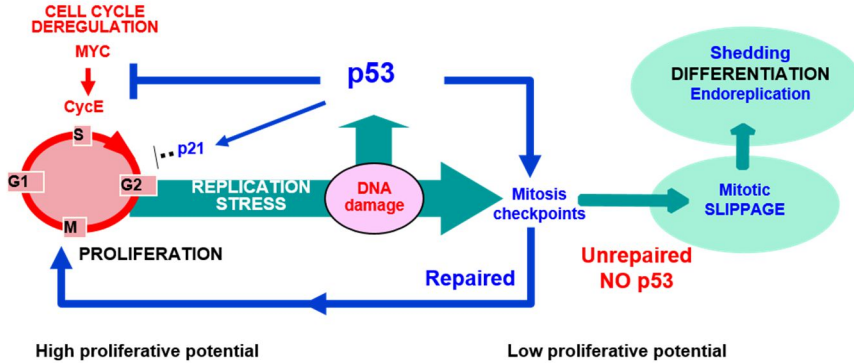


Figure 62 | Model for the role of p53 in proliferation and differentiation of human epidermal keratinocytes. In response to cell cycle deregulation and DNA damage accumulation due to replication stress p53 activates the mitosis checkpoints to allow DNA damage repair. Cells with successful repair would re-enter the proliferative compartment, and cells with irreparable levels of DNA damage would undergo mitotic slippage, terminal differentiation, stratification and shedding. Loss of p53 avoids efficient activation of the DNA damage checkpoints and results in the impairment of proliferative potential (Freije et al., 2014).

A DIFFERENTIATION-MITOSIS CHECKPOINT MIGHT MAINTAIN THE BALANCE BETWEEN PROLIFERATION AND DIFFERENTIATION OF EPIDERMAL KERATINOCYTES.

For a long time, epidermal keratinocytes have been thought to differentiate from a G1 arrest, also known as G0 or quiescence. However, previous results in our laboratory showed that keratinocytes differentiate from an active cell cycle (Zanet et al., 2010, Freije et al., 2012). They also suggested that; the limit to keratinocyte proliferation imposed by differentiation is established by mitotic checkpoints (Freije et al., 2014). The results presented in this Thesis functionally demonstrate this model.

By overexpressing FOXM1, primary keratinocytes overcame the differentiation-mitosis checkpoint (DMC) that is activated by oncogenic alterations (overexpression of MYC, loss of p53). FOXM1 enforces the mitosis machinery by promoting the transcription of genes involved in cell division (Costa, 2005), what imbalanced the keratinocyte decision making towards proliferation. This demonstrates that mitosis checkpoints control terminal differentiation. The results are in concordance with the role of FOXM1 in driving proliferation of keratinocytes from oral epithelium (Gemenetzidis et al., 2010). Also noteworthy is the fact that FOXM1 rescues the proliferative capacity of keratinocytes after the depletion of the EGF-related factor AREG (Stoll et al., 2016). The results obtained with the epidermal cell line NTERT point in the same direction. We showed that NTERT presents defects in the DMC that might contribute to immortalization. Interestingly, we have reported that the squamous cell carcinoma cell line SCC12F also presents defects in the activation of the DMC (Alonso-Lecue et al., 2017).

Altogether, the results support a key role of the DMC in coordinating keratinocyte proliferation with differentiation through mitosis checkpoints by limiting the keratinocyte lifespan. This mitotic checkpoint might also be relevant in the homeostasis of other developing self-renewal tissues, allowing proliferating cells to differentiate in the presence of an active cell cycle.

IMPLICATIONS OF THE DIFFERENTIATION-MITOSIS CHECKPOINT INTO EPIDERMAL CARCINOGENESIS

p53 is the most mutated gene in human cancers (Petitjean et al., 2007). Mutations in this gene are present in 80-90% of skin squamous carcinomas (Brash, 2006). However, loss of p53 in primary keratinocytes led to squamous differentiation, what is consistent with an oncogene-induced differentiation response (OID). The same phenomenon was observed in the presence of oncogenic alterations such as MYC or Cyclin E overexpression (Gandarillas and Watt, 1997, Waikel et al., 2001, Freije et al., 2012). These results would explain why (1) p53 is not an initiating event of epidermal carcinogenesis; and (2) the DMC acts as a protective barrier against oncogenic alterations. Several observations support the first statement. Mice lacking p53 die of thymic lymphoma and do not develop early skin tumors (Donehower et al., 1992). Indeed, epidermal-specific p53 knockout mice develop spontaneous tumors only from 5 months onward (Martinez-Cruz et al., 2008) and are not more susceptible to chemically induced skin carcinogenesis (Donehower et al., 1992, Kemp et al., 1993). In human skin, frequent clones of p53 mutant cells that do not seem to lead to cancer are frequently found (Jonason et al., 1996, Ren et al., 1997, le Pelletier et al., 2001). Consistently, Li-Fraumeni patients having one mutant p53 allele do not display a higher rate of skin carcinoma (Malkin et al., 1990, Srivastava et al., 1990). This apparent paradox can be explained by our second statement. We propose that the epidermis presents a powerful protective mechanism, the DMC that activates the squamous differentiation program in the event of cell cycle deregulation.

This model also explains why keratinocyte hyperproliferation results in benign hyperkeratosis, such as psoriasis. Activation of the DMC renders the mitotic arrest irreversible and prevents proliferation of mutated cells

(Figure 62). Indeed, we have shown that basal cell carcinoma cells (BCCs) presented an effective G2 arrest that allows DNA repair and genome stability maintenance (Alonso-Lecue et al., 2017). However, well differentiated SCC12F displayed a loose mitotic control that renders it more genomically unstable and aggressive than BCC.

Although loss of p53 does not have a role in early tumorigenesis in the skin, it accelerates cancer progression (Kemp et al., 1993, Bornachea et al., 2012). In addition, it seems to stimulate the development of skin tumors in mouse after UV radiation (Li et al., 1995, Jiang et al., 1999). Interestingly, genomic instability appears to contribute to the spontaneous tumors developed in p53 knockout mouse epidermis (Martinez-Cruz et al., 2009). Our results showed that terminal differentiation induced by p53 loss was preceded by DNA damage accumulation, activation of the mitotic checkpoints and endoreplication. This suggests that additional alterations stimulating cell division are needed for the development of skin cancer. By pushing mitosis, FOXM1 overexpression allowed p53 mutated cells to continue proliferating in spite of increasing DNA damage. The same result was obtained in the presence of MYC. In concordance, ectopic FOXM1 increased genomic instability of oral keratinocytes after exposure to nicotine (Gemenetzidis et al., 2009). Hence, the results suggest that impairment of the DMC by forcing cell division in the presence of oncogenic alterations might collaborate in the creation of a pool of genomically unstable cells with the capacity to divide (Figure 63). This might fix precancerous mutations such as MYC amplification or p53 inactivation, and give rise to cell clones with malignant potential [Figure 63; (Molinuevo et al., 2017)]. The model would explain why p53 and FOXM1 are frequently deregulated in epithelial cancer.

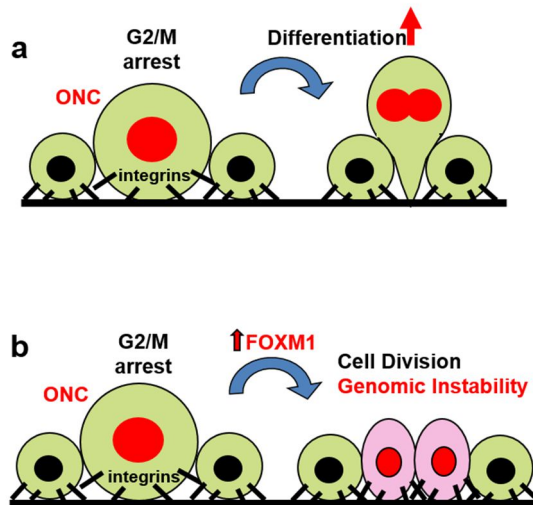


Figure 63 | Model of the action of mitotic FOXM1 in p53- or MYC- mutant keratinocytes. (a) Cells upon oncogenic alterations causing cell cycle deregulation and replication stress (ONC) and accumulation of irreparable DNA damage (red nuclei) block in mitosis unable to divide. Prolonged G2/M block allows cell size increase and triggers terminal epidermal differentiation, resulting in downregulation of integrins, irreversible suppression of cytokinesis and stratification. **(b)** Ectopic expression of FOXM1 pushes damaged keratinocytes to progress in mitosis and achieve cytokinesis in spite of an initial mitosis pause, giving rise to two slightly larger daughter cells that do not downregulate integrins. This leads to expansion of cells bearing genetic damage and to genomic instability (Molinuevo et al., 2017).

Our results suggest two novel functions of FOXM1 that might further contribute to tumorigenesis. The possibility that this factor inhibits global RNA transcription in order to allow mitosis adds insight into the key function in cell multiplication. It is well established that keratinocyte differentiate terminally when they lose adhesion to the extracellular matrix (Adams and Watt, 1989). The rise of integrin cell adhesion molecules caused by overexpression of FOXM1 that we have observed, would allow keratinocytes to maintain their proliferative capacity.

DISCUSSION

DNA DAMAGE AS PART OF THE NATURAL DIFFERENTIATION PROGRAM OF EPIDERMAL KERATINOCYTES.

The DMC in response to DNA damage might play an essential protective role in the epidermis, a tissue continuously renewed and exposed to the mutagenic effects of UV irradiation. We have shown that normal keratinocytes *in vitro* displayed expression of proteins involved in the DDR. These samples were obtained from asymptomatic human foreskin non-exposed to UV irradiation, suggesting that DDR activation was induced by an endogenous source. ATR is responsible for the repair of DNA lesions produced by RS (Lopez-Contreras and Fernandez-Capetillo, 2012). Consequently, its inhibition impedes the repair of this type of damage. Hence, the increase in γ H2AX (DNA damage signal) detected after ATR inhibition (repair) suggests that RS might be an important source of endogenous DNA damage in proliferative keratinocytes.

In addition, DDR signaling was detected in human epidermis *in situ* by means of γ H2AX. Although keratinocytes *in vitro* are highly proliferative due to the stimulation of growth factors, SCs in the epidermis are mainly quiescent (Watt et al., 2006). Initiation of terminal differentiation is accompanied by the downregulation of p53 expression, the inactivation of cell cycle inhibitor Rb and the induction of Cyclin E. These changes are concomitant with the transition from SCs to active proliferating TACs (Zanet et al., 2010, Freije et al., 2012, Dazard et al., 2000). It is not unreasonable to suggest that loss of cell cycle control in TACs, by inducing RS, might in turn induce the activation of the DDR in the epidermis under normal conditions. In spite of their active proliferative state, TACs are committed to differentiate by unknown mechanisms (Watt et al., 2006). We have shown that inhibition of the DNA damage marker γ H2AX impaired

squamous differentiation and induced an epithelial-mesenchymal transition. Loss of γ H2AX in the squamous cell carcinoma cell line SCC1F has been shown to be related to inhibition of the squamous phenotype and aggressiveness (Alonso-Lecue et al., 2017). Hence, the γ H2AX signal seems to be mediating a DNA damage-induced differentiation response (DDDR; Figure 64). Our observations suggest that accumulation of DNA damage due to naturally programmed cell cycle deregulation might act as a clock and commit proliferative cells to differentiation.

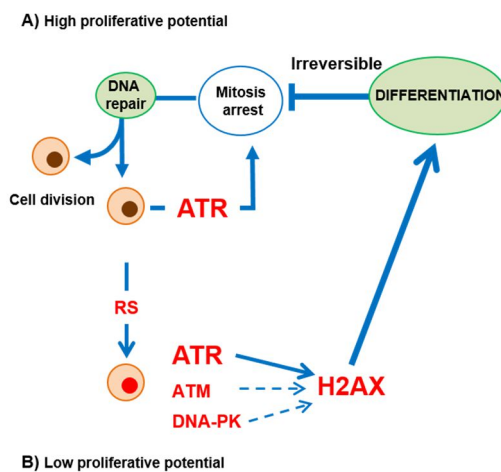


Figure 64 | Model for the role of the DDR in the natural differentiation program of epidermal keratinocytes. (A) In keratinocytes presenting high proliferative capacity ATR activates the mitosis checkpoint, allowing DNA repair and cell division. After a phase of rapid clonal expansion, keratinocytes with low proliferative potential (B) accumulate DNA damage due to replication stress (RS). RS activates the DDR and results in terminal differentiation, in a γ H2AX-specific manner.

Although we have found a strong correlation between γ H2AX signaling and the epidermal differentiation response, H2AX depletion does not completely abolish squamous differentiation. By studying the role of the DNA damage pathways in the initiation of keratinocyte differentiation, we were aiming to identify molecules controlling the DMC. An alternative approach is to run gene searches. This strategy might identify squamous master genes that are currently unknown.

THE DNA DAMAGE-INDUCED DIFFERENTIATION RESPONSE AS AN AUTOMATIC CELL-AUTONOMOUS LIMIT TO PROLIFERATION IN MORPHOGENESIS.

The molecular mechanisms that coordinate proliferation and differentiation in developing tissues remain largely obscure. By studying the epidermis, we have identified the DDR, which might be a cell-autonomous self-limiting mechanism linking proliferation with differentiation (Gandarillas et al., 2018).

In addition to its demonstrated relevance in epidermal homeostasis, it is tempting to speculate that the DDR plays a role in the regulation of other developing tissues. Although it has been scarcely studied, there exists a bunch of other evidence supporting DDR. It has been proposed the existence of a differentiation checkpoint induced by genotoxic stress inhibiting myogenesis in instable cells (Puri et al., 2002). On the contrary, loss of genome integrity has been shown to promote maturation of lymphoid and myeloid lineages (Mandal and Rossi, 2012, Wang et al., 2012, Santos et al., 2014). Other evidence for this response has been documented in neuron and hematopoietic differentiation (Sherman et al., 2011). Programmed induction of DSBs is required for the differentiation of B lymphoid lineage cells during the development of vertebrate immune system. In neurons, several observations suggest a link between DSBs-dependent activation of the DDR and differentiation of neural precursor stem cells. In addition, ionizing radiation has been shown to promote terminal differentiation of mouse melanocytes and astrocytes (Inomata et al., 2009, Schneider et al., 2013). Recent reports have shown that DNA damage can limit hematopoietic self-renewal and leukemic cancer via differentiation (Wang et al., 2012, Santos et al., 2014). We have obtained

evidence for a dual role of that RS-induced differentiation in squamous cells carcinoma (Alonso-Lecue et al., 2017). It limited uncontrolled proliferation when irreversible and contributed to malignancy when reversible, likely by promoting genomic instability.

As extensively explained in this work, keratinocytes differentiate from a mitotic arrest resulting in mitotic slippage and endoreplication (Gandarillas, 2012, Zanet et al., 2010). Based greatly on the results described in this Thesis, we are proposing that the DMC might be part of a key automatic control of homeostasis coordinating proliferation with differentiation in developing or regenerating tissues. The keratinocyte DMC results in endoreplication. A growing body of evidence is boosting the potential importance of endoreplication in mammalian tissues. In human, endoreplication is known to occur in megakaryocytes (Ravid et al., 2002), hepatocytes (Gentric and Desdouets, 2014) and endometrium (Das, 2009). In last years, heart (Meckert et al., 2005, Senyo et al., 2013) and mammary gland (Rios et al., 2016) have been incorporated to the list. Endoreplication is emerging as a common mechanism in developing, and regenerating tissues, situations that require sustained and rapid proliferation (Gandarillas et al., 2018). Under these conditions the level of RS should be high. We propose that the DDDR might link cell multiplication with terminal differentiation in developing or expanding tissues, thereby controlling cell number and organ size and function (Figure 65).

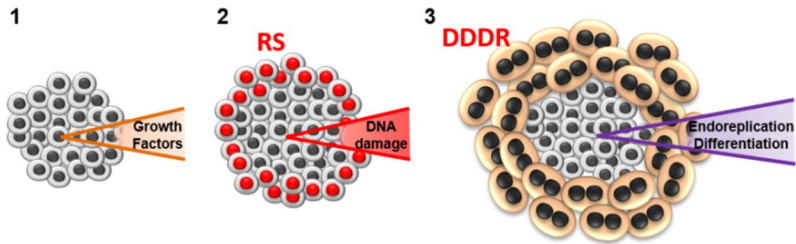


Figure 65 | The DNA damage differentiation response (DDDR) might link proliferation with differentiation in endoreplicating tissues. Cell cycle is hyperactivated by growth factors and cells undergo proliferation (1). Active proliferating cells accumulate DNA damage due to replication stress (RS; red nuclei). (2). The DDR pathway is activated upon a prolonged G2/M arrest and irreparable damage. Finally, cells undergo differentiation and endoreplication (3). (Gandarillas et al., 2018).

The limit to cell proliferation would be imposed by proliferation itself due to RS caused during hyperactivation of the cell cycle. Cells not having robust mitosis checkpoints, not undergoing apoptosis, would terminally differentiate, endoreplicate and start massive protein production. Cancer cells with defects in the DDR would continue to proliferate in spite of accumulating unrepaired DNA damage, thus leading to genomic instability and malignant progression.

CONCLUSIONS

CONCLUSIONS

1. p53 protects the proliferative potential of epidermal keratinocytes.
2. p53 is dispensable for the activation of the differentiation-mitosis checkpoint.
3. AREG does not suppress the differentiation-mitosis checkpoint (DMC) induced by p53 loss.
4. FOXM1 increases the proliferative capacity and inhibits the DMC of human keratinocytes in the presence of oncogenic alterations, such as p53 loss or MYC overexpression
5. FOXM1 allows proliferation of keratinocytes accumulating oncogene-induced DNA damage thus resulting in genome instability.
6. The immortalized cell line NTERT present defects in the DMC.
7. DNA damage signaling is detected in normally proliferating epidermal keratinocytes.
8. The DNA damage response (DDR) controls keratinocyte differentiation via γ H2AX signaling.
9. Loss of H2AX favors an epithelial- mesenchymal phenotypic conversion.

REFERENCES

REFERENCES

- ABUD, H. E. 2004. Shaping developing tissues by apoptosis. *Cell Death Differ*, 11, 797-9.
- ADAMS, J. C. & WATT, F. M. 1989. Fibronectin inhibits the terminal differentiation of human keratinocytes. *Nature*, 340, 307-9.
- ALBERTS B., LEWIS J., RAFF M., ROBERTS K. & WALTER P. 2007. *Molecular biology of the cell*, Garland Science.
- ALONSO-LECUE, P., DE PEDRO, I., COULON, V., MOLINUEVO, R., LORZ, C., SEGRELLES, C., CEBALLOS, L., LOPEZ-AVENTIN, D., GARCIA-VALTUILLE, A., BERNAL, J. M., MAZORRA, F., PUJOL, R. M., PARAMIO, J., RAMON SANZ, J., FREIJE, A., TOLL, A. & GANDARILLAS, A. 2017. Inefficient differentiation response to cell cycle stress leads to genomic instability and malignant progression of squamous carcinoma cells. *Cell Death Dis*, 8, e2901.
- ANDERS, S., PYL, P. T. & HUBER, W. 2015. HTSeq--a Python framework to work with high-throughput sequencing data. *Bioinformatics*, 31, 166-9.
- ANDREASSEN, P. R. & MARGOLIS, R. L. 1994. Microtubule dependency of p34cdc2 inactivation and mitotic exit in mammalian cells. *J Cell Biol*, 127, 789-802.
- ARELLANO, M. & MORENO, S. 1997. Regulation of CDK/cyclin complexes during the cell cycle. *Int J Biochem Cell Biol*, 29, 559-73.
- ARESSY, B. & DUCOMMUN, B. 2008. Cell cycle control by the CDC25 phosphatases. *Anticancer Agents Med Chem*, 8, 818-24.
- ASHBURNER, M., BALL, C. A., BLAKE, J. A., BOTSTEIN, D., BUTLER, H., CHERRY, J. M., DAVIS, A. P., DOLINSKI, K., DWIGHT, S. S., EPPIG, J. T., HARRIS, M. A., HILL, D. P., ISSEL-TARVER, L., KASARSKIS, A., LEWIS, S., MATESE, J. C., RICHARDSON, J. E., RINGWALD, M., RUBIN, G. M. & SHERLOCK, G. 2000. Gene ontology: tool for the unification of biology. The Gene Ontology Consortium. *Nat Genet*, 25, 25-9.
- AYLON, Y. & OREN, M. 2011. p53: guardian of ploidy. *Mol Oncol*, 5, 315-23.
- BAKER, D. J., WIJSHAKE, T., TCHKONIA, T., LEBRASSEUR, N. K., CHILDS, B. G., VAN DE SLUIS, B., KIRKLAND, J. L. & VAN DEURSEN, J. M. 2011. Clearance of p16Ink4a-positive senescent cells delays ageing-associated disorders. *Nature*, 479, 232-6.

- BAKKENIST, C. J. & KASTAN, M. B. 2003. DNA damage activates ATM through intermolecular autophosphorylation and dimer dissociation. *Nature*, 421, 499-506.
- BARNUM, K. J. & O'CONNELL, M. J. 2014. Cell cycle regulation by checkpoints. *Methods Mol Biol*, 1170, 29-40.
- BARTKOVA, J., REZAEI, N., LIONTOS, M., KARAKAIDOS, P., KLETSAS, D., ISSAEVA, N., VASSILIOU, L. V., KOLETTAS, E., NIFOROU, K., ZOUMPOURLIS, V. C., TAKAOKA, M., NAKAGAWA, H., TORT, F., FUGGER, K., JOHANSSON, F., SEHESTED, M., ANDERSEN, C. L., DYRSKJOT, L., ORNTOFT, T., LUKAS, J., KITTAS, C., HELLEDAY, T., HALAZONETIS, T. D., BARTEK, J. & GORGOLIS, V. G. 2006. Oncogene-induced senescence is part of the tumorigenesis barrier imposed by DNA damage checkpoints. *Nature*, 444, 633-7.
- BEKKER-JENSEN, S., LUKAS, C., MELANDER, F., BARTEK, J. & LUKAS, J. 2005. Dynamic assembly and sustained retention of 53BP1 at the sites of DNA damage are controlled by Mdc1/NFBD1. *J Cell Biol*, 170, 201-11.
- BEKKER-JENSEN, S. & MAILAND, N. 2010. Assembly and function of DNA double-strand break repair foci in mammalian cells. *DNA Repair (Amst)*, 9, 1219-28.
- BESSON, A., DOWDY, S. F. & ROBERTS, J. M. 2008. CDK inhibitors: cell cycle regulators and beyond. *Dev Cell*, 14, 159-69.
- BESTER, A. C., RONIGER, M., OREN, Y. S., IM, M. M., SARNI, D., CHAOAT, M., BENSIMON, A., ZAMIR, G., SHEWACH, D. S. & KEREM, B. 2011. Nucleotide deficiency promotes genomic instability in early stages of cancer development. *Cell*, 145, 435-46.
- BLACKFORD, A. N. & JACKSON, S. P. 2017. ATM, ATR, and DNA-PK: The Trinity at the Heart of the DNA Damage Response. *Mol Cell*, 66, 801-817.
- BLAGOSKLONNY, M. V. 2007. Mitotic arrest and cell fate: why and how mitotic inhibition of transcription drives mutually exclusive events. *Cell Cycle*, 6, 70-4.
- BORNACHEA, O., SANTOS, M., MARTINEZ-CRUZ, A. B., GARCIA-ESCUADERO, R., DUENAS, M., COSTA, C., SEGRELLES, C., LORZ, C., BUITRAGO, A., SAIZ-LADERA, C., AGIRRE, X., GRANDE, T., PARADELA, B., MARAVER, A., ARIZA, J. M., PROSPER, F., SERRANO, M., SANCHEZ-CEPESDES, M. & PARAMIO, J. M. 2012. EMT and induction of miR-21 mediate metastasis development in Trp53-deficient tumours. *Sci Rep*, 2, 434.

- BOROWIEC, A. S., DELCOURT, P., DEWAILLY, E. & BIDAUX, G. 2013. Optimal differentiation of in vitro keratinocytes requires multifactorial external control. *PLoS One*, 8, e77507.
- BRASH, D. E. 2006. Roles of the transcription factor p53 in keratinocyte carcinomas. *Br J Dermatol*, 154 Suppl 1, 8-10.
- BREITKREUTZ, D., MIRANCEA, N. & NISCHT, R. 2009. Basement membranes in skin: unique matrix structures with diverse functions? *Histochem Cell Biol*, 132, 1-10.
- BRENNER, L., MUNOZ-ANTONIA, T., VELLUCCI, V. F., ZHOU, Z. L. & REISS, M. 1993. Wild-type p53 tumor suppressor gene restores differentiation of human squamous carcinoma cells but not the response to transforming growth factor beta. *Cell Growth Differ*, 4, 993-1004.
- BRETONES, G., DELGADO, M. D. & LEON, J. 2015. Myc and cell cycle control. *Biochim Biophys Acta*, 1849, 506-16.
- BRITO, D. A. & RIEDER, C. L. 2006. Mitotic checkpoint slippage in humans occurs via cyclin B destruction in the presence of an active checkpoint. *Curr Biol*, 16, 1194-200.
- BROWN, E. J. & BALTIMORE, D. 2000. ATR disruption leads to chromosomal fragmentation and early embryonic lethality. *Genes Dev*, 14, 397-402.
- BYUN, T. S., PACEK, M., YEE, M. C., WALTER, J. C. & CIMPRICH, K. A. 2005. Functional uncoupling of MCM helicase and DNA polymerase activities activates the ATR-dependent checkpoint. *Genes Dev*, 19, 1040-52.
- CALLEGARI, A. J. & KELLY, T. J. 2006. UV irradiation induces a postreplication DNA damage checkpoint. *Proc Natl Acad Sci U S A*, 103, 15877-82.
- CALLEN, E., JANKOVIC, M., WONG, N., ZHA, S., CHEN, H. T., DIFILIPPANTONIO, S., DI VIRGILIO, M., HEIDKAMP, G., ALT, F. W., NUSSENZWEIG, A. & NUSSENZWEIG, M. 2009. Essential role for DNA-PKcs in DNA double-strand break repair and apoptosis in ATM-deficient lymphocytes. *Mol Cell*, 34, 285-97.
- CANMAN, C. E., CHEN, C. Y., LEE, M. H. & KASTAN, M. B. 1994. DNA damage responses: p53 induction, cell cycle perturbations, and apoptosis. *Cold Spring Harbor Symposia on Quantitative Biology*, 59, 277-86.
- CAO, L., CHEN, F., YANG, X., XU, W., XIE, J. & YU, L. 2014. Phylogenetic analysis of CDK and cyclin proteins in premetazoan lineages. *BMC Evol Biol*, 14, 10.

- CAULIN, C., BAULUZ, C., GANDARILLAS, A., CANO, A. & QUINTANILLA, M. 1993. Changes in keratin expression during malignant progression of transformed mouse epidermal keratinocytes. *Experimental Cell Research*, 204, 11-21.
- CICCIA, A. & ELLEDGE, S. J. 2010. The DNA damage response: making it safe to play with knives. *Mol Cell*, 40, 179-204.
- CLAASSEN, G. F. & HANN, S. R. 2000. A role for transcriptional repression of p21CIP1 by c-Myc in overcoming transforming growth factor beta -induced cell-cycle arrest. *Proc Natl Acad Sci U S A*, 97, 9498-503.
- COATS, S., FLANAGAN, W. M., NOURSE, J. & ROBERTS, J. M. 1996. Requirement of p27Kip1 for restriction point control of the fibroblast cell cycle. *Science*, 272, 877-80.
- COOKE, M. S., EVANS, M. D., DIZDAROGLU, M. & LUNEC, J. 2003. Oxidative DNA damage: mechanisms, mutation, and disease. *FASEB J*, 17, 1195-214.
- COSTA, R. H. 2005. FoxM1 dances with mitosis. *Nat Cell Biol*, 7, 108-10.
- COVERLEY, D., PELIZON, C., TREWICK, S. & LASKEY, R. A. 2000. Chromatin-bound Cdc6 persists in S and G2 phases in human cells, while soluble Cdc6 is destroyed in a cyclin A-cdk2 dependent process. *J Cell Sci*, 113 (Pt 11), 1929-38.
- CUADRADO, M., MARTINEZ-PASTOR, B., MURGA, M., TOLEDO, L. I., GUTIERREZ-MARTINEZ, P., LOPEZ, E. & FERNANDEZ-CAPETILLO, O. 2006. ATM regulates ATR chromatin loading in response to DNA double-strand breaks. *J Exp Med*, 203, 297-303.
- CHANG, L. F., ZHANG, Z., YANG, J., MCLAUGHLIN, S. H. & BARFORD, D. 2014. Molecular architecture and mechanism of the anaphase-promoting complex. *Nature*, 513, 388-393.
- CHEN, Y. & ZHAO, X. 1998. Shaping limbs by apoptosis. *J Exp Zool*, 282, 691-702.
- CHINNAIYAN, A. M. 1999. The apoptosome: heart and soul of the cell death machine. *Neoplasia*, 1, 5-15.
- DALEY, J. M. & WILSON, T. E. 2005. Rejoining of DNA double-strand breaks as a function of overhang length. *Mol Cell Biol*, 25, 896-906.
- DAS, S. K. 2009. Cell cycle regulatory control for uterine stromal cell decidualization in implantation. *Reproduction*, 137, 889-99.
- DAZARD, J. E., PIETTE, J., BASSET-SEGUIN, N., BLANCHARD, J. M. & GANDARILLAS, A. 2000. Switch from p53 to MDM2 as

- differentiating human keratinocytes lose their proliferative potential and increase in cellular size. *Oncogene*, 19, 3693-705.
- DE ANTONI, A., PEARSON, C. G., CIMINI, D., CANMAN, J. C., SALA, V., NEZI, L., MAPELLI, M., SIRONI, L., FARETTA, M., SALMON, E. D. & MUSACCHIO, A. 2005. The Mad1/Mad2 complex as a template for Mad2 activation in the spindle assembly checkpoint. *Curr Biol*, 15, 214-25.
- DEGREGORI, J., LEONE, G., OHTANI, K., MIRON, A. & NEVINS, J. R. 1995. E2F-1 accumulation bypasses a G1 arrest resulting from the inhibition of G1 cyclin-dependent kinase activity. *Genes Dev*, 9, 2873-87.
- DELACROIX, S., WAGNER, J. M., KOBAYASHI, M., YAMAMOTO, K. & KARNITZ, L. M. 2007. The Rad9-Hus1-Rad1 (9-1-1) clamp activates checkpoint signaling via TopBP1. *Genes Dev*, 21, 1472-7.
- DICKSON, M. A., HAHN, W. C., INO, Y., RONFARD, V., WU, J. Y., WEINBERG, R. A., LOUIS, D. N., LI, F. P. & RHEINWALD, J. G. 2000. Human keratinocytes that express hTERT and also bypass a p16(INK4a)-enforced mechanism that limits life span become immortal yet retain normal growth and differentiation characteristics. *Mol Cell Biol*, 20, 1436-47.
- DITCHFIELD, C., JOHNSON, V. L., TIGHE, A., ELLSTON, R., HAWORTH, C., JOHNSON, T., MORTLOCK, A., KEEN, N. & TAYLOR, S. S. 2003. Aurora B couples chromosome alignment with anaphase by targeting BubR1, Mad2, and Cenp-E to kinetochores. *Journal of Cell Biology*, 161, 267-80.
- DOBIN, A., DAVIS, C. A., SCHLESINGER, F., DRENKOW, J., ZALESKI, C., JHA, S., BATUT, P., CHAISSON, M. & GINGERAS, T. R. 2013. STAR: ultrafast universal RNA-seq aligner. *Bioinformatics*, 29, 15-21.
- DONEHOWER, L. A., HARVEY, M., SLAGLE, B. L., MCARTHUR, M. J., MONTGOMERY, C. A., JR., BUTEL, J. S. & BRADLEY, A. 1992. Mice deficient for p53 are developmentally normal but susceptible to spontaneous tumours. *Nature*, 356, 215-21.
- DURKIN, S. G. & GLOVER, T. W. 2007. Chromosome fragile sites. *Annu Rev Genet*, 41, 169-92.
- EDGAR, B. A. & ORR-WEAVER, T. L. 2001. Endoreplication cell cycles: more for less. *Cell*, 105, 297-306.
- EL-DEIRY, W. S., TOKINO, T., VELCULESCU, V. E., LEVY, D. B., PARSONS, R., TRENT, J. M., LIN, D., MERCER, W. E., KINZLER, K. W. & VOGELSTEIN, B. 1993. WAF1, a potential mediator of p53 tumor suppression. *Cell*, 75, 817-25.

- ELIEZER, Y., ARGAMAN, L., KORNOWSKI, M., RONIGER, M. & GOLDBERG, M. 2014. Interplay between the DNA damage proteins MDC1 and ATM in the regulation of the spindle assembly checkpoint. *J Biol Chem*, 289, 8182-93.
- EVAN, G. & LITTLEWOOD, T. 1998. A matter of life and cell death. *Science*, 281, 1317-22.
- FENG, W. & JASIN, M. 2017. BRCA2 suppresses replication stress-induced mitotic and G1 abnormalities through homologous recombination. *Nat Commun*, 8, 525.
- FERNANDEZ-CAPETILLO, O., LEE, A., NUSSENZWEIG, M. & NUSSENZWEIG, A. 2004. H2AX: the histone guardian of the genome. *DNA Repair (Amst)*, 3, 959-67.
- FERNANDEZ-VIDAL, A., VIGNARD, J. & MIREY, G. 2017. Around and beyond 53BP1 Nuclear Bodies. *Int J Mol Sci*, 18.
- FORNARI, F. A., RANDOLPH, J. K., YALOWICH, J. C., RITKE, M. K. & GEWIRTZ, D. A. 1994. Interference by doxorubicin with DNA unwinding in MCF-7 breast tumor cells. *Molecular Pharmacology*, 45, 649-56.
- FOX, D. T. & DURONIO, R. J. 2013. Endoreplication and polyploidy: insights into development and disease. *Development*, 140, 3-12.
- FREIJE, A., CEBALLOS, L., COISY, M., BARNES, L., ROSA, M., DE DIEGO, E., BLANCHARD, J. M. & GANDARILLAS, A. 2012. Cyclin E drives human keratinocyte growth into differentiation. *Oncogene*, 31, 5180-92.
- FREIJE, A., MOLINUEVO, R., CEBALLOS, L., CAGIGAS, M., ALONSO-LECUE, P., RODRIGUEZ, R., MENENDEZ, P., ABERDAM, D., DE DIEGO, E. & GANDARILLAS, A. 2014. Inactivation of p53 in Human Keratinocytes Leads to Squamous Differentiation and Shedding via Replication Stress and Mitotic Slippage. *Cell Rep*, 9, 1349-60.
- FU, Z., MALUREANU, L., HUANG, J., WANG, W., LI, H., VAN DEURSEN, J. M., TINDALL, D. J. & CHEN, J. 2008. Plk1-dependent phosphorylation of FoxM1 regulates a transcriptional programme required for mitotic progression. *Nat Cell Biol*, 10, 1076-82.
- FUCHS, E. & GREEN, H. 1980. Changes in keratin gene expression during terminal differentiation of the keratinocyte. *Cell*, 19, 1033-42.
- FUNG, T. K., YAM, C. H. & POON, R. Y. 2005. The N-terminal regulatory domain of cyclin A contains redundant ubiquitination targeting sequences and acceptor sites. *Cell Cycle*, 4, 1411-20.

- GADEA, B. B. & RUDERMAN, J. V. 2005. Aurora kinase inhibitor ZM447439 blocks chromosome-induced spindle assembly, the completion of chromosome condensation, and the establishment of the spindle integrity checkpoint in *Xenopus* egg extracts. *Mol Biol Cell*, 16, 1305-18.
- GANDARILLAS, A. 2000. Epidermal differentiation, apoptosis, and senescence: common pathways? *Exp Gerontol*, 35, 53-62.
- GANDARILLAS, A. 2012. The mysterious human epidermal cell cycle, or an oncogene-induced differentiation checkpoint. *Cell Cycle*, 11, 4507-16.
- GANDARILLAS, A., DAVIES, D. & BLANCHARD, J. M. 2000. Normal and c-Myc-promoted human keratinocyte differentiation both occur via a novel cell cycle involving cellular growth and endoreplication. *Oncogene*, 19, 3278-89.
- GANDARILLAS, A. & FREIJE, A. 2014. Cycling up the epidermis: reconciling 100 years of debate. *Exp Dermatol*, 23, 87-91.
- GANDARILLAS, A., GOLDSMITH, L. A., GSCHMEISSNER, S., LEIGH, I. M. & WATT, F. M. 1999. Evidence that apoptosis and terminal differentiation of epidermal keratinocytes are distinct processes. *Exp Dermatol*, 8, 71-9.
- GANDARILLAS, A., MOLINUEVO, R. & SANZ-GOMEZ, N. 2018. Mammalian endoreplication emerges to reveal a potential developmental timer. *Cell Death Differ*.
- GANDARILLAS, A. & WATT, F. M. 1997. c-Myc promotes differentiation of human epidermal stem cells. *Genes Dev*, 11, 2869-82.
- GARTEL, A. L. & TYNER, A. L. 1999. Transcriptional regulation of the p21((WAF1/CIP1)) gene. *Exp Cell Res*, 246, 280-9.
- GAY, S., LACHAGES, A. M., MILLOT, G. A., COURBET, S., LETESSIER, A., DEBATISSE, M. & BRISON, O. 2010. Nucleotide supply, not local histone acetylation, sets replication origin usage in transcribed regions. *EMBO Rep*, 11, 698-704.
- GELL, D. & JACKSON, S. P. 1999. Mapping of protein-protein interactions within the DNA-dependent protein kinase complex. *Nucleic Acids Res*, 27, 3494-502.
- GEMENET'ZIDIS, E., BOSE, A., RIAZ, A. M., CHAPLIN, T., YOUNG, B. D., ALI, M., SUGDEN, D., THURLOW, J. K., CHEONG, S. C., TEO, S. H., WAN, H., WASEEM, A., PARKINSON, E. K., FORTUNE, F. & TEH, M. T. 2009. FOXM1 upregulation is an early event in human squamous cell carcinoma and it is enhanced by nicotine during malignant transformation. *PLoS One*, 4, e4849.

- GEMENETZIDIS, E., ELENA-COSTEA, D., PARKINSON, E. K., WASEEM, A., WAN, H. & TEH, M. T. 2010a. Induction of human epithelial stem/progenitor expansion by FOXM1. *Cancer Research*, 70, 9515-26.
- GEMENETZIDIS, E., ELENA-COSTEA, D., PARKINSON, E. K., WASEEM, A., WAN, H. & TEH, M. T. 2010b. Induction of human epithelial stem/progenitor expansion by FOXM1. *Cancer Res*, 70, 9515-26.
- GENG, Y., EATON, E. N., PICON, M., ROBERTS, J. M., LUNDBERG, A. S., GIFFORD, A., SARDET, C. & WEINBERG, R. A. 1996. Regulation of cyclin E transcription by E2Fs and retinoblastoma protein. *Oncogene*, 12, 1173-80.
- GENTRIC, G. & DESDOUETS, C. 2014. Polyploidization in liver tissue. *Am J Pathol*, 184, 322-31.
- GIONO, L. E. & MANFREDI, J. J. 2006. The p53 tumor suppressor participates in multiple cell cycle checkpoints. *Journal of Cellular Physiology*, 209, 13-20.
- GLUCKSMANN, A. 1965. Cell death in normal development. *Arch Biol (Liege)*, 76, 419-37.
- GONG, D. & FERRELL, J. E., JR. 2010. The roles of cyclin A2, B1, and B2 in early and late mitotic events. *Mol Biol Cell*, 21, 3149-61.
- GORGOULIS, V. G., VASSILIOU, L. V., KARAKAIDOS, P., ZACHARATOS, P., KOTSINAS, A., LILOGLOU, T., VENERE, M., DITULLIO, R. A., JR., KASTRINAKIS, N. G., LEVY, B., KLETSAS, D., YONETA, A., HERLYN, M., KITTAS, C. & HALAZONETIS, T. D. 2005. Activation of the DNA damage checkpoint and genomic instability in human precancerous lesions. *Nature*, 434, 907-13.
- GUSAROVA, G. A., WANG, I. C., MAJOR, M. L., KALINICHENKO, V. V., ACKERSON, T., PETROVIC, V. & COSTA, R. H. 2007. A cell-penetrating ARF peptide inhibitor of FoxM1 in mouse hepatocellular carcinoma treatment. *J Clin Invest*, 117, 99-111.
- HAAHR, P., HOFFMANN, S., TOLLENAERE, M. A., HO, T., TOLEDO, L. I., MANN, M., BEKKER-JENSEN, S., RASCHLE, M. & MAILAND, N. 2016. Activation of the ATR kinase by the RPA-binding protein ETAA1. *Nat Cell Biol*, 18, 1196-1207.
- HALASI, M. & GARTEL, A. L. 2009. A novel mode of FoxM1 regulation: positive auto-regulatory loop. *Cell Cycle*, 8, 1966-7.
- HALAZONETIS, T. D., GORGOULIS, V. G. & BARTEK, J. 2008. An oncogene-induced DNA damage model for cancer development. *Science*, 319, 1352-5.

- HALLIDAY, G. M. 2005. Inflammation, gene mutation and photoimmunosuppression in response to UVR-induced oxidative damage contributes to photocarcinogenesis. *Mutat Res*, 571, 107-20.
- HANAWALT, P. C. & SPIVAK, G. 2008. Transcription-coupled DNA repair: two decades of progress and surprises. *Nat Rev Mol Cell Biol*, 9, 958-70.
- HANSEN, D. V., LOKTEV, A. V., BAN, K. H. & JACKSON, P. K. 2004. Plk1 regulates activation of the anaphase promoting complex by phosphorylating and triggering SCFbetaTrCP-dependent destruction of the APC Inhibitor Emi1. *Molecular Biology of the Cell*, 15, 5623-34.
- HARLEY, C. B., FUTCHER, A. B. & GREIDER, C. W. 1990. Telomeres shorten during ageing of human fibroblasts. *Nature*, 345, 458-60.
- HARPER, J. W., BURTON, J. L. & SOLOMON, M. J. 2002. The anaphase-promoting complex: it's not just for mitosis any more. *Genes Dev*, 16, 2179-206.
- HARVEY, M., VOGEL, H., MORRIS, D., BRADLEY, A., BERNSTEIN, A. & DONEHOWER, L. A. 1995. A mutant p53 transgene accelerates tumour development in heterozygous but not nullizygous p53-deficient mice. *Nat Genet*, 9, 305-11.
- HAUPT, Y., MAYA, R., KAZAZ, A. & OREN, M. 1997. Mdm2 promotes the rapid degradation of p53. *Nature*, 387, 296-9.
- HELMRICH, A., BALLARINO, M. & TORA, L. 2011. Collisions between replication and transcription complexes cause common fragile site instability at the longest human genes. *Mol Cell*, 44, 966-77.
- HERMEKING, H., LENGAUER, C., POLYAK, K., HE, T. C., ZHANG, L., THIAGALINGAM, S., KINZLER, K. W. & VOGELSTEIN, B. 1997. 14-3-3sigma is a p53-regulated inhibitor of G2/M progression. *Mol Cell*, 1, 3-11.
- HILLS, S. A. & DIFFLEY, J. F. 2014. DNA replication and oncogene-induced replicative stress. *Curr Biol*, 24, R435-44.
- HINDS, P. W., MITTNACHT, S., DULIC, V., ARNOLD, A., REED, S. I. & WEINBERG, R. A. 1992. Regulation of retinoblastoma protein functions by ectopic expression of human cyclins. *Cell*, 70, 993-1006.
- HUANG DA, W., SHERMAN, B. T., ZHENG, X., YANG, J., IMAMICHI, T., STEPHENS, R. & LEMPICKI, R. A. 2009. Extracting biological meaning from large gene lists with DAVID. *Curr Protoc Bioinformatics*, Chapter 13, Unit 13 11.

- INOMATA, K., AOTO, T., BINH, N. T., OKAMOTO, N., TANIMURA, S., WAKAYAMA, T., ISEKI, S., HARA, E., MASUNAGA, T., SHIMIZU, H. & NISHIMURA, E. K. 2009. Genotoxic stress abrogates renewal of melanocyte stem cells by triggering their differentiation. *Cell*, 137, 1088-99.
- JIANG, W., ANANTHASWAMY, H. N., MULLER, H. K. & KRIPKE, M. L. 1999. p53 protects against skin cancer induction by UV-B radiation. *Oncogene*, 18, 4247-53.
- JIRICNY, J. 2013. Postreplicative mismatch repair. *Cold Spring Harb Perspect Biol*, 5, a012633.
- JOHNSON, D. G. & SCHNEIDER-BROUSSARD, R. 1998. Role of E2F in cell cycle control and cancer. *Front Biosci*, 3, d447-8.
- JONASON, A. S., KUNALA, S., PRICE, G. J., RESTIFO, R. J., SPINELLI, H. M., PERSING, J. A., LEFFELL, D. J., TARONE, R. E. & BRASH, D. E. 1996. Frequent clones of p53-mutated keratinocytes in normal human skin. *Proc Natl Acad Sci U S A*, 93, 14025-9.
- JONES, P. H. & WATT, F. M. 1993. Separation of human epidermal stem cells from transit amplifying cells on the basis of differences in integrin function and expression. *Cell*, 73, 713-24.
- KALIN, T. V., USTIYAN, V. & KALINICHENKO, V. V. 2011. Multiple faces of FoxM1 transcription factor: lessons from transgenic mouse models. *Cell Cycle*, 10, 396-405.
- KALINICHENKO, V. V., MAJOR, M. L., WANG, X., PETROVIC, V., KUECHLE, J., YODER, H. M., DENNEWITZ, M. B., SHIN, B., DATTA, A., RAYCHAUDHURI, P. & COSTA, R. H. 2004. Foxm1b transcription factor is essential for development of hepatocellular carcinomas and is negatively regulated by the p19ARF tumor suppressor. *Genes Dev*, 18, 830-50.
- KALLASSY, M., MARTEL, N., DAMOUR, O., YAMASAKI, H. & NAKAZAWA, H. 1998. Growth arrest of immortalized human keratinocytes and suppression of telomerase activity by p21WAF1 gene expression. *Mol Carcinog*, 21, 26-36.
- KANUNGO, J. 2013. DNA-dependent protein kinase and DNA repair: relevance to Alzheimer's disease. *Alzheimers Res Ther*, 5, 13.
- KARTASOVA, T., ROOP, D. R. & YUSPA, S. H. 1992. Relationship between the expression of differentiation-specific keratins 1 and 10 and cell proliferation in epidermal tumors. *Mol Carcinog*, 6, 18-25.
- KEMP, C. J., DONEHOWER, L. A., BRADLEY, A. & BALMAIN, A. 1993. Reduction of p53 gene dosage does not increase initiation or

- promotion but enhances malignant progression of chemically induced skin tumors. *Cell*, 74, 813-22.
- KHORRAMI, A., SHARIF BAGHERI, M., TAVALLAEI, M. & GHARECHAHI, J. 2017. The functional significance of 14-3-3 proteins in cancer: focus on lung cancer. *Horm Mol Biol Clin Investig*, 32.
- KIM, J. A., LEE, J., MARGOLIS, R. L. & FOTEDAR, R. 2010. SP600125 suppresses Cdk1 and induces endoreplication directly from G2 phase, independent of JNK inhibition. *Oncogene*, 29, 1702-16.
- KOHCHI, C., INAGAWA, H., NISHIZAWA, T. & SOMA, G. 2009. ROS and innate immunity. *Anticancer Res*, 29, 817-21.
- KONG, X., LI, L., LI, Z., LE, X., HUANG, C., JIA, Z., CUI, J., HUANG, S., WANG, L. & XIE, K. 2013. Dysregulated expression of FOXM1 isoforms drives progression of pancreatic cancer. *Cancer Res*, 73, 3987-96.
- KORVER, W., ROOSE, J. & CLEVERS, H. 1997a. The winged-helix transcription factor Trident is expressed in cycling cells. *Nucleic Acids Res*, 25, 1715-9.
- KORVER, W., ROOSE, J., WILSON, A. & CLEVERS, H. 1997b. The winged-helix transcription factor Trident is expressed in actively dividing lymphocytes. *Immunobiology*, 198, 157-61.
- KOZLOV, S. V., GRAHAM, M. E., PENG, C., CHEN, P., ROBINSON, P. J. & LAVIN, M. F. 2006. Involvement of novel autophosphorylation sites in ATM activation. *EMBO J*, 25, 3504-14.
- KROKAN, H. E. & BJORAS, M. 2013. Base excision repair. *Cold Spring Harb Perspect Biol*, 5, a012583.
- KRTOLICA, A., PARRINELLO, S., LOCKETT, S., DESPREZ, P. Y. & CAMPISI, J. 2001. Senescent fibroblasts promote epithelial cell growth and tumorigenesis: a link between cancer and aging. *Proc Natl Acad Sci U S A*, 98, 12072-7.
- KUMAGAI, A., LEE, J., YOO, H. Y. & DUNPHY, W. G. 2006. TopBP1 activates the ATR-ATRIP complex. *Cell*, 124, 943-55.
- KUMAGAI, A., SHEVCHENKO, A. & DUNPHY, W. G. 2010. Treslin collaborates with TopBP1 in triggering the initiation of DNA replication. *Cell*, 140, 349-59.
- LANE, D. P. 1992. Cancer. p53, guardian of the genome. *Nature*, 358, 15-6.
- LAOUKILI, J., KOOISTRA, M. R., BRAS, A., KAUW, J., KERKHOVEN, R. M., MORRISON, A., CLEVERS, H. & MEDEMA, R. H. 2005. FoxM1 is required for execution of the

- mitotic programme and chromosome stability. *Nat Cell Biol*, 7, 126-36.
- LAOUKILI, J., STAHL, M. & MEDEMA, R. H. 2007a. FoxM1: at the crossroads of ageing and cancer. *Biochim Biophys Acta*, 1775, 92-102.
- LAOUKILI, J., STAHL, M. & MEDEMA, R. H. 2007b. FoxM1: at the crossroads of ageing and cancer. *Biochimica et Biophysica Acta*, 1775, 92-102.
- LAVIGUEUR, A., MALTBY, V., MOCK, D., ROSSANT, J., PAWSON, T. & BERNSTEIN, A. 1989. High incidence of lung, bone, and lymphoid tumors in transgenic mice overexpressing mutant alleles of the p53 oncogene. *Mol Cell Biol*, 9, 3982-91.
- LAVKER, R. M. & SUN, T. T. 1983. Epidermal stem cells. *J Invest Dermatol*, 81, 121s-7s.
- LE PELLETIER, F., SOUFIR, N., DE LA SALMONIERE, P., JANIN, A. & BASSET-SEGUIN, N. 2001. p53 Patches are not increased in patients with multiple nonmelanoma skin cancers. *J Invest Dermatol*, 117, 1324-5.
- LEE, H., KWAK, H. J., CHO, I. T., PARK, S. H. & LEE, C. H. 2009. S1219 residue of 53BP1 is phosphorylated by ATM kinase upon DNA damage and required for proper execution of DNA damage response. *Biochemical and Biophysical Research Communications*, 378, 32-6.
- LEE, H. S., PARK, J. H., KIM, S. J., KWON, S. J. & KWON, J. 2010. A cooperative activation loop among SWI/SNF, gamma-H2AX and H3 acetylation for DNA double-strand break repair. *EMBO J*, 29, 1434-45.
- LEE, J., KUMAGAI, A. & DUNPHY, W. G. 2007. The Rad9-Hus1-Rad1 checkpoint clamp regulates interaction of TopBP1 with ATR. *J Biol Chem*, 282, 28036-44.
- LEE, J. H. & PAULL, T. T. 2005. ATM activation by DNA double-strand breaks through the Mre11-Rad50-Nbs1 complex. *Science*, 308, 551-4.
- LEHNER, C. F. & O'FARRELL, P. H. 1989. Expression and function of *Drosophila* cyclin A during embryonic cell cycle progression. *Cell*, 56, 957-68.
- LEIGH, I. M., LANE, E. B. & WATT, F. M. 1994. *The keratinocyte handbook*, Press Syndicate of the University of Cambridge.
- LEUNG, T. W., LIN, S. S., TSANG, A. C., TONG, C. S., CHING, J. C., LEUNG, W. Y., GIMLICH, R., WONG, G. G. & YAO, K. M.

2001. Over-expression of FoxM1 stimulates cyclin B1 expression. *FEBS Lett*, 507, 59-66.
- LI, X., HO, S. N., LUNA, J., GIACALONE, J., THOMAS, D. J., TIMMERMAN, L. A., CRABTREE, G. R. & FRANCKE, U. 1995. Cloning and chromosomal localization of the human and murine genes for the T-cell transcription factors NFATc and NFATp. *Cytogenet Cell Genet*, 68, 185-91.
- LIM, S. & KALDIS, P. 2013. Cdks, cyclins and CKIs: roles beyond cell cycle regulation. *Development*, 140, 3079-93.
- LITTLEWOOD, T. D., HANCOCK, D. C., DANIELIAN, P. S., PARKER, M. G. & EVAN, G. I. 1995. A modified oestrogen receptor ligand-binding domain as an improved switch for the regulation of heterologous proteins. *Nucleic Acids Res*, 23, 1686-90.
- LIU, D. & HORNSBY, P. J. 2007. Senescent human fibroblasts increase the early growth of xenograft tumors via matrix metalloproteinase secretion. *Cancer Res*, 67, 3117-26.
- LOPEZ-CONTRERAS, A. J. & FERNANDEZ-CAPETILLO, O. 2012. Signalling DNA damage. In: HUANG, C. (ed.) *Protein phosphorylation in human health*. InTech.
- LOVE, M. I., HUBER, W. & ANDERS, S. 2014. Moderated estimation of fold change and dispersion for RNA-seq data with DESeq2. *Genome Biol*, 15, 550.
- MA, R. Y., TONG, T. H., CHEUNG, A. M., TSANG, A. C., LEUNG, W. Y. & YAO, K. M. 2005. Raf/MEK/MAPK signaling stimulates the nuclear translocation and transactivating activity of FOXM1c. *J Cell Sci*, 118, 795-806.
- MA, Y., PANNICKE, U., SCHWARZ, K. & LIEBER, M. R. 2002. Hairpin opening and overhang processing by an Artemis/DNA-dependent protein kinase complex in nonhomologous end joining and V(D)J recombination. *Cell*, 108, 781-94.
- MACHERET, M. & HALAZONETIS, T. D. 2015. DNA replication stress as a hallmark of cancer. *Annu Rev Pathol*, 10, 425-48.
- MAHANEY, B. L., MEEK, K. & LEES-MILLER, S. P. 2009. Repair of ionizing radiation-induced DNA double-strand breaks by non-homologous end-joining. *Biochem J*, 417, 639-50.
- MAKINIEMI, M., HILLUKKALA, T., TUUSA, J., REINI, K., VAARA, M., HUANG, D., POSPIECH, H., MAJURI, I., WESTERLING, T., MAKELA, T. P. & SYVAOJA, J. E. 2001. BRCT domain-containing protein TopBP1 functions in DNA replication and damage response. *Journal of Biological Chemistry*, 276, 30399-406.

- MALKIN, D., LI, F. P., STRONG, L. C., FRAUMENI, J. F., JR., NELSON, C. E., KIM, D. H., KASSEL, J., GRYKA, M. A., BISCHOFF, F. Z., TAINSKY, M. A. & ET AL. 1990. Germ line p53 mutations in a familial syndrome of breast cancer, sarcomas, and other neoplasms. *Science*, 250, 1233-8.
- MALUMBRES, M. & BARBACID, M. 2009. Cell cycle, CDKs and cancer: a changing paradigm. *Nat Rev Cancer*, 9, 153-66.
- MANCHADO, E., EGUREN, M. & MALUMBRES, M. 2010. The anaphase-promoting complex/cyclosome (APC/C): cell-cycle-dependent and -independent functions. *Biochem Soc Trans*, 38, 65-71.
- MANDAL, P. K. & ROSSI, D. J. 2012. DNA-damage-induced differentiation in hematopoietic stem cells. *Cell*, 148, 847-8.
- MANTEL, C., GUO, Y., LEE, M. R., HAN, M. K., RHORABOUGH, S., KIM, K. S. & BROXMEYER, H. E. 2008. Cells enter a unique intermediate 4N stage, not 4N-G1, after aborted mitosis. *Cell Cycle*, 7, 484-92.
- MARTIN-OLIVA, D., MARTIN-GUERRERO, S. M., MATTIA-GONZALEZ, A. M., FERRER-MARTIN, R. M., MARTIN-ESTEBANE, M., CARRASCO, M. C., SIERRA, A., MARIN-TEVA, J. L., CALVENTE, R., NAVASCUES, J. & CUADROS, M. A. 2015. DNA damage, poly(ADP-Ribose) polymerase activation, and phosphorylated histone H2AX expression during postnatal retina development in C57BL/6 mouse. *Invest Ophthalmol Vis Sci*, 56, 1301-9.
- MARTINEZ-CRUZ, A. B., SANTOS, M., GARCIA-ESCUADERO, R., MORAL, M., SEGRELLES, C., LORZ, C., SAIZ, C., BUITRAGO-PEREZ, A., COSTA, C. & PARAMIO, J. M. 2009. Spontaneous tumor formation in Trp53-deficient epidermis mediated by chromosomal instability and inflammation. *Anticancer Res*, 29, 3035-42.
- MARTINEZ-CRUZ, A. B., SANTOS, M., LARA, M. F., SEGRELLES, C., RUIZ, S., MORAL, M., LORZ, C., GARCIA-ESCUADERO, R. & PARAMIO, J. M. 2008. Spontaneous squamous cell carcinoma induced by the somatic inactivation of retinoblastoma and Trp53 tumor suppressors. *Cancer Res*, 68, 683-92.
- MATA-GARRIDO, J., CASAFONT, I., TAPIA, O., BERCIANO, M. T. & LAFARGA, M. 2016. Neuronal accumulation of unrepaired DNA in a novel specific chromatin domain: structural, molecular and transcriptional characterization. *Acta Neuropathol Commun*, 4, 41.
- MATSUSHIME, H., ROUSSEL, M. F., ASHMUN, R. A. & SHERR, C. J. 1991. Colony-stimulating factor 1 regulates novel cyclins during the G1 phase of the cell cycle. *Cell*, 65, 701-13.

- MATT, S. & HOFMANN, T. G. 2016. The DNA damage-induced cell death response: a roadmap to kill cancer cells. *Cell Mol Life Sci*, 73, 2829-50.
- MCMANUS, K. J. & HENDZEL, M. J. 2005a. ATM-dependent DNA damage-independent mitotic phosphorylation of H2AX in normally growing mammalian cells. *Mol Biol Cell*, 16, 5013-25.
- MCMANUS, K. J. & HENDZEL, M. J. 2005b. ATM-dependent DNA damage-independent mitotic phosphorylation of H2AX in normally growing mammalian cells. *Molecular Biology of the Cell*, 16, 5013-25.
- MCHUGH, D. & GIL, J. 2018. Senescence and aging: Causes, consequences, and therapeutic avenues. *J Cell Biol*, 217, 65-77.
- MECKERT, P. C., RIVELLO, H. G., VIGLIANO, C., GONZALEZ, P., FAVALORO, R. & LAGUENS, R. 2005. Endomitosis and polyploidization of myocardial cells in the periphery of human acute myocardial infarction. *Cardiovasc Res*, 67, 116-23.
- MEEK, K., DANG, V. & LEES-MILLER, S. P. 2008. DNA-PK: the means to justify the ends? *Adv Immunol*, 99, 33-58.
- MERTZ, T. M., BARANOVSKIY, A. G., WANG, J., TAHIROV, T. H. & SHCHERBAKOVA, P. V. 2017. Nucleotide selectivity defect and mutator phenotype conferred by a colon cancer-associated DNA polymerase delta mutation in human cells. *Oncogene*, 36, 4427-4433.
- MICHALOVITZ, D., HALEVY, O. & OREN, M. 1990. Conditional inhibition of transformation and of cell proliferation by a temperature-sensitive mutant of p53. *Cell*, 62, 671-80.
- MITCHELL, D. L., ALLISON, J. P. & NAIRN, R. S. 1990. Immunoprecipitation of pyrimidine(6-4)pyrimidone photoproducts and cyclobutane pyrimidine dimers in uv-irradiated DNA. *Radiat Res*, 123, 299-303.
- MIYASHITA, T. & REED, J. C. 1995. Tumor suppressor p53 is a direct transcriptional activator of the human bax gene. *Cell*, 80, 293-9.
- MOLINUEVO, R., FREIJE, A., DE PEDRO, I., STOLL, S. W., ELDER, J. T. & GANDARILLAS, A. 2017. FOXM1 allows human keratinocytes to bypass the oncogene-induced differentiation checkpoint in response to gain of MYC or loss of p53. *Oncogene*, 36, 956-965.
- MOLL, R., DIVO, M. & LANGBEIN, L. 2008. The human keratins: biology and pathology. *Histochem Cell Biol*, 129, 705-33.
- MOMPARLER, R. L., KARON, M., SIEGEL, S. E. & AVILA, F. 1976. Effect of adriamycin on DNA, RNA, and protein synthesis in cell-free systems and intact cells. *Cancer Research*, 36, 2891-5.

- MONTERO, J. A., SANCHEZ-FERNANDEZ, C., LORDA-DIEZ, C. I., GARCIA-PORRERO, J. A. & HURLE, J. M. 2016. DNA damage precedes apoptosis during the regression of the interdigital tissue in vertebrate embryos. *Sci Rep*, 6, 35478.
- MORGAN, D. O. 2007. *The cell cycle: Principles of Control*, Lonson, New Science Press.
- MUNOZ-ESPIN, D., CANAMERO, M., MARAVER, A., GOMEZ-LOPEZ, G., CONTRERAS, J., MURILLO-CUESTA, S., RODRIGUEZ-BAEZA, A., VARELA-NIETO, I., RUBERTE, J., COLLADO, M. & SERRANO, M. 2013. Programmed cell senescence during mammalian embryonic development. *Cell*, 155, 1104-18.
- MURRAY, A. W. 2004. Recycling the cell cycle: cyclins revisited. *Cell*, 116, 221-34.
- NAKANO, K. & VOUSDEN, K. H. 2001. PUMA, a novel proapoptotic gene, is induced by p53. *Mol Cell*, 7, 683-94.
- NAKAYAMA, K. I., HATAKEYAMA, S. & NAKAYAMA, K. 2001. Regulation of the cell cycle at the G1-S transition by proteolysis of cyclin E and p27Kip1. *Biochem Biophys Res Commun*, 282, 853-60.
- NARITA, M., NUNEZ, S., HEARD, E., LIN, A. W., HEARN, S. A., SPECTOR, D. L., HANNON, G. J. & LOWE, S. W. 2003. Rb-mediated heterochromatin formation and silencing of E2F target genes during cellular senescence. *Cell*, 113, 703-16.
- NIEMANN, C. & WATT, F. M. 2002. Designer skin: lineage commitment in postnatal epidermis. *Trends Cell Biol*, 12, 185-92.
- NYBERG, K. A., MICHELSON, R. J., PUTNAM, C. W. & WEINERT, T. A. 2002. Toward maintaining the genome: DNA damage and replication checkpoints. *Annu Rev Genet*, 36, 617-56.
- ODA, E., OHKI, R., MURASAWA, H., NEMOTO, J., SHIBUE, T., YAMASHITA, T., TOKINO, T., TANIGUCHI, T. & TANAKA, N. 2000. Noxa, a BH3-only member of the Bcl-2 family and candidate mediator of p53-induced apoptosis. *Science*, 288, 1053-8.
- OHTANI, K., DEGREGORI, J. & NEVINS, J. R. 1995. Regulation of the cyclin E gene by transcription factor E2F1. *Proc Natl Acad Sci U S A*, 92, 12146-50.
- OPENSTAX. 2016. *Anatomy & Physiology* [Online]. OpenStax CNX. Available: <http://cnx.org/contents/14fb4ad7-39a1-4cee-ab6e-3ef2482e3e22@8.24>.
- PAMPFER, S. & DONNAY, I. 1999. Apoptosis at the time of embryo implantation in mouse and rat. *Cell Death Differ*, 6, 533-45.

- PARRINELLO, S., SAMPER, E., KRTOLICA, A., GOLDSTEIN, J., MELOV, S. & CAMPISI, J. 2003. Oxygen sensitivity severely limits the replicative lifespan of murine fibroblasts. *Nat Cell Biol*, 5, 741-7.
- PENNEYS, N. S., FULTON, J. E., JR., WEINSTEIN, G. D. & FROST, P. 1970. Location of proliferating cells in human epidermis. *Arch Dermatol*, 101, 323-7.
- PERRIGUE, P. M., NAJBAUER, J., JOZWIAK, A. A., BARCISZEWSKI, J., ABOODY, K. S. & BARISH, M. E. 2015. Planarians as a model of aging to study the interaction between stem cells and senescent cells in vivo. *Pathobiol Aging Age Relat Dis*, 5, 30052.
- PETERMANN, E. & HELLEDAY, T. 2010. Pathways of mammalian replication fork restart. *Nat Rev Mol Cell Biol*, 11, 683-7.
- PETERS, J. M. 2006. The anaphase promoting complex/cyclosome: a machine designed to destroy. *Nat Rev Mol Cell Biol*, 7, 644-56.
- PETERSEN, B. O., LUKAS, J., SORENSEN, C. S., BARTEK, J. & HELIN, K. 1999. Phosphorylation of mammalian CDC6 by cyclin A/CDK2 regulates its subcellular localization. *EMBO J*, 18, 396-410.
- PETTIJEAN, A., MATHE, E., KATO, S., ISHIOKA, C., TAVTIGIAN, S. V., HAINAUT, P. & OLIVIER, M. 2007. Impact of mutant p53 functional properties on TP53 mutation patterns and tumor phenotype: lessons from recent developments in the IARC TP53 database. *Hum Mutat*, 28, 622-9.
- PIERARD-FRANCHIMONT, C. & PIERARD, G. E. 1989. Stereotyped distribution of proliferating keratinocytes in disorders affecting the epidermis. *Am J Dermatopathol*, 11, 233-7.
- PINES, J. & HUNTER, T. 1991. Human cell division: the involvement of cyclins A and B1, and multiple cdc2s. *Cold Spring Harb Symp Quant Biol*, 56, 449-63.
- PURI, P. L., BHAKTA, K., WOOD, L. D., COSTANZO, A., ZHU, J. & WANG, J. Y. 2002. A myogenic differentiation checkpoint activated by genotoxic stress. *Nat Genet*, 32, 585-93.
- RADERSCHALL, E., GOLUB, E. I. & HAAF, T. 1999. Nuclear foci of mammalian recombination proteins are located at single-stranded DNA regions formed after DNA damage. *Proc Natl Acad Sci U S A*, 96, 1921-6.
- RAVID, K., LU, J., ZIMMET, J. M. & JONES, M. R. 2002. Roads to polyploidy: the megakaryocyte example. *J Cell Physiol*, 190, 7-20.
- REN, Z. P., AHMADIAN, A., PONTEN, F., NISTER, M., BERG, C., LUNDEBERG, J., UHLEN, M. & PONTEN, J. 1997. Benign

- clonal keratinocyte patches with p53 mutations show no genetic link to synchronous squamous cell precancer or cancer in human skin. *Am J Pathol*, 150, 1791-803.
- RHEINWALD, J. G. 1989. Human epidermal keratinocyte cell culture and xenograft systems: applications in the detection of potential chemical carcinogens and the study of epidermal transformation. *Prog Clin Biol Res*, 298, 113-25.
- RHEINWALD, J. G. & BECKETT, M. A. 1980. Defective terminal differentiation in culture as a consistent and selectable character of malignant human keratinocytes. *Cell*, 22, 629-32.
- RIOS, A. C., FU, N. Y., JAMIESON, P. R., PAL, B., WHITEHEAD, L., NICHOLAS, K. R., LINDEMAN, G. J. & VISVADER, J. E. 2016. Essential role for a novel population of binucleated mammary epithelial cells in lactation. *Nat Commun*, 7, 11400.
- RITCHIE, A., GUTIERREZ, O. & FERNANDEZ-LUNA, J. L. 2009. PAR bZIP-bik is a novel transcriptional pathway that mediates oxidative stress-induced apoptosis in fibroblasts. *Cell Death Differ*, 16, 838-46.
- ROGAKOU, E. P., PILCH, D. R., ORR, A. H., IVANOVA, V. S. & BONNER, W. M. 1998. DNA double-stranded breaks induce histone H2AX phosphorylation on serine 139. *J Biol Chem*, 273, 5858-68.
- ROHBAN, S. & CAMPANER, S. 2015. Myc induced replicative stress response: How to cope with it and exploit it. *Biochim Biophys Acta*, 1849, 517-24.
- SANTOS, M. A., FARYABI, R. B., ERGEN, A. V., DAY, A. M., MALHOWSKI, A., CANELA, A., ONOZAWA, M., LEE, J. E., CALLEN, E., GUTIERREZ-MARTINEZ, P., CHEN, H. T., WONG, N., FINKEL, N., DESHPANDE, A., SHARROW, S., ROSSI, D. J., ITO, K., GE, K., APLAN, P. D., ARMSTRONG, S. A. & NUSSENZWEIG, A. 2014. DNA-damage-induced differentiation of leukaemic cells as an anti-cancer barrier. *Nature*, 514, 107-11.
- SCHARER, O. D. 2013. Nucleotide excision repair in eukaryotes. *Cold Spring Harb Perspect Biol*, 5, a012609.
- SCHMIDT, L., WIEDNER, M., VELIMEZI, G., PROCHAZKOVA, J., OWUSU, M., BAUER, S. & LOIZOU, J. I. 2014. ATM is required for the ATM-mediated signaling and recruitment of 53BP1 to DNA damage sites upon replication stress. *DNA Repair (Amst)*, 24, 122-130.

- SCHMIDT, M., ROHE, A., PLATZER, C., NAJJAR, A., ERDMANN, F. & SIPPL, W. 2017. Regulation of G2/M Transition by Inhibition of WEE1 and PKMYT1 Kinases. *Molecules*, 22.
- SCHNEIDER, L., PELLEGGATTA, S., FAVARO, R., PISATI, F., RONCAGLIA, P., TESTA, G., NICOLIS, S. K., FINOCCHIARO, G. & D'ADDA DI FAGAGNA, F. 2013. DNA damage in mammalian neural stem cells leads to astrocytic differentiation mediated by BMP2 signaling through JAK-STAT. *Stem Cell Reports*, 1, 123-38.
- SCHULZE, A., ZERFASS, K., SPITKOVSKY, D., MIDDENDORP, S., BERGES, J., HELIN, K., JANSEN-DURR, P. & HENGLEIN, B. 1995. Cell cycle regulation of the cyclin A gene promoter is mediated by a variant E2F site. *Proc Natl Acad Sci U S A*, 92, 11264-8.
- SENYO, S. E., STEINHAUSER, M. L., PIZZIMENTI, C. L., YANG, V. K., CAI, L., WANG, M., WU, T. D., GUERQUIN-KERN, J. L., LECHENE, C. P. & LEE, R. T. 2013. Mammalian heart renewal by pre-existing cardiomyocytes. *Nature*, 493, 433-6.
- SERRANO, M., LIN, A. W., MCCURRACH, M. E., BEACH, D. & LOWE, S. W. 1997. Oncogenic ras provokes premature cell senescence associated with accumulation of p53 and p16INK4a. *Cell*, 88, 593-602.
- SHECHTER, D., COSTANZO, V. & GAUTIER, J. 2004. Regulation of DNA replication by ATR: signaling in response to DNA intermediates. *DNA Repair (Amst)*, 3, 901-8.
- SHERMAN, M. H., BASSING, C. H. & TEITTELL, M. A. 2011. Regulation of cell differentiation by the DNA damage response. *Trends Cell Biol*, 21, 312-9.
- SHERR, C. J. 1995. D-type cyclins. *Trends Biochem Sci*, 20, 187-90.
- SHERR, C. J. & ROBERTS, J. M. 1995. Inhibitors of mammalian G1 cyclin-dependent kinases. *Genes Dev*, 9, 1149-63.
- SHERR, C. J. & ROBERTS, J. M. 1999. CDK inhibitors: positive and negative regulators of G1-phase progression. *Genes Dev*, 13, 1501-12.
- SHERR, C. J. & ROBERTS, J. M. 2004. Living with or without cyclins and cyclin-dependent kinases. *Genes Dev*, 18, 2699-711.
- SHIBATA, A. 2017. Regulation of repair pathway choice at two-ended DNA double-strand breaks. *Mutat Res*, 803-805, 51-55.
- SINGLETON, B. K., TORRES-ARZAYUS, M. I., ROTTINGHAUS, S. T., TACCIOLI, G. E. & JEGGO, P. A. 1999. The C terminus of

- Ku80 activates the DNA-dependent protein kinase catalytic subunit. *Mol Cell Biol*, 19, 3267-77.
- SLACK, J. M. W. 2013. *Essential developmental biology*, Oxford.
- SOBHIAN, B., SHAO, G., LILLI, D. R., CULHANE, A. C., MOREAU, L. A., XIA, B., LIVINGSTON, D. M. & GREENBERG, R. A. 2007. RAP80 targets BRCA1 to specific ubiquitin structures at DNA damage sites. *Science*, 316, 1198-202.
- SONG, X., FIATI KENSTON, S. S., ZHAO, J., YANG, D. & GU, Y. 2017. Roles of FoxM1 in cell regulation and breast cancer targeting therapy. *Med Oncol*, 34, 41.
- SORENSEN, C. S., SYLJUASEN, R. G., FALCK, J., SCHROEDER, T., RONNSTRAND, L., KHANNA, K. K., ZHOU, B. B., BARTEK, J. & LUKAS, J. 2003. Chk1 regulates the S phase checkpoint by coupling the physiological turnover and ionizing radiation-induced accelerated proteolysis of Cdc25A. *Cancer Cell*, 3, 247-58.
- SORENSEN, C. S., SYLJUASEN, R. G., LUKAS, J. & BARTEK, J. 2004. ATR, Claspin and the Rad9-Rad1-Hus1 complex regulate Chk1 and Cdc25A in the absence of DNA damage. *Cell Cycle*, 3, 941-5.
- SPYCHER, C., MILLER, E. S., TOWNSEND, K., PAVIC, L., MORRICE, N. A., JANSČAK, P., STEWART, G. S. & STUCKI, M. 2008. Constitutive phosphorylation of MDC1 physically links the MRE11-RAD50-NBS1 complex to damaged chromatin. *J Cell Biol*, 181, 227-40.
- SRIVASTAVA, S., ZOU, Z. Q., PIROLLO, K., BLATTNER, W. & CHANG, E. H. 1990. Germ-line transmission of a mutated p53 gene in a cancer-prone family with Li-Fraumeni syndrome. *Nature*, 348, 747-9.
- STOLL, S. W., STUART, P. E., SWINDELL, W. R., TSOI, L. C., LI, B., GANDARILLAS, A., LAMBERT, S., JOHNSTON, A., NAIR, R. P. & ELDER, J. T. 2016. The EGF receptor ligand amphiregulin controls cell division via FoxM1. *Oncogene*, 35, 2075-86.
- STORER, M., MAS, A., ROBERT-MORENO, A., PECORARO, M., ORTELLS, M. C., DI GIACOMO, V., YOSEF, R., PILPEL, N., KRIZHANOVSKY, V., SHARPE, J. & KEYES, W. M. 2013. Senescence is a developmental mechanism that contributes to embryonic growth and patterning. *Cell*, 155, 1119-30.
- STUCKI, M., CLAPPERTON, J. A., MOHAMMAD, D., YAFFE, M. B., SMERDON, S. J. & JACKSON, S. P. 2005. MDC1 directly binds phosphorylated histone H2AX to regulate cellular responses to DNA double-strand breaks. *Cell*, 123, 1213-26.

- STUCKI, M. & JACKSON, S. P. 2006. gammaH2AX and MDC1: anchoring the DNA-damage-response machinery to broken chromosomes. *DNA Repair (Amst)*, 5, 534-43.
- SULLIVAN, C., LIU, Y., SHEN, J., CURTIS, A., NEWMAN, C., HOCK, J. M. & LI, X. 2012. Novel interactions between FOXM1 and CDC25A regulate the cell cycle. *PLoS One*, 7, e51277.
- SUN, T. T. & GREEN, H. 1976. Differentiation of the epidermal keratinocyte in cell culture: formation of the cornified envelope. *Cell*, 9, 511-21.
- SYMINGTON, L. S. 2014. End resection at double-strand breaks: mechanism and regulation. *Cold Spring Harb Perspect Biol*, 6.
- TAIRA, N., YAMAGUCHI, T., KIMURA, J., LU, Z. G., FUKUDA, S., HIGASHIYAMA, S., ONO, M. & YOSHIDA, K. 2014. Induction of amphiregulin by p53 promotes apoptosis via control of microRNA biogenesis in response to DNA damage. *Proceedings of the National Academy of Sciences of the United States of America*, 111, 717-22.
- TEDESCHI, A. & DI GIOVANNI, S. 2009. The non-apoptotic role of p53 in neuronal biology: enlightening the dark side of the moon. *EMBO Rep*, 10, 576-83.
- TIWARI, R., SAHU, I., SONI, B. L., SATHE, G. J., DATTA, K. K., THAPA, P., SINHA, S., VADIVEL, C. K., DHAKA, B., GOWDA, H. & VAIDYA, M. M. 2017. Quantitative phosphoproteomic analysis reveals system-wide signaling pathways regulated by site-specific phosphorylation of Keratin-8 in skin squamous cell carcinoma derived cell line. *Proteomics*, 17.
- TOLEDO, L. I., MURGA, M., GUTIERREZ-MARTINEZ, P., SORIA, R. & FERNANDEZ-CAPETILLO, O. 2008. ATR signaling can drive cells into senescence in the absence of DNA breaks. *Genes Dev*, 22, 297-302.
- TOMINAGA, K. 2015. The emerging role of senescent cells in tissue homeostasis and pathophysiology. *Pathobiol Aging Age Relat Dis*, 5, 27743.
- TONNESSEN-MURRAY, C. A., LOZANO, G. & JACKSON, J. G. 2017. The Regulation of Cellular Functions by the p53 Protein: Cellular Senescence. *Cold Spring Harb Perspect Med*, 7.
- VAN ATTIKUM, H. & GASSER, S. M. 2009. Crosstalk between histone modifications during the DNA damage response. *Trends Cell Biol*, 19, 207-17.
- WAIKEL, R. L., KAWACHI, Y., WAIKEL, P. A., WANG, X. J. & ROOP, D. R. 2001. Deregulated expression of c-Myc depletes epidermal stem cells. *Nat Genet*, 28, 165-8.

- WANG, I. C., CHEN, Y. J., HUGHES, D., PETROVIC, V., MAJOR, M. L., PARK, H. J., TAN, Y., ACKERSON, T. & COSTA, R. H. 2005. Forkhead box M1 regulates the transcriptional network of genes essential for mitotic progression and genes encoding the SCF (Skp2-Cks1) ubiquitin ligase. *Mol Cell Biol*, 25, 10875-94.
- WANG, J., SUN, Q., MORITA, Y., JIANG, H., GROSS, A., LECHER, A., HILDNER, K., GUACHALLA, L. M., GOMPF, A., HARTMANN, D., SCHAMBACH, A., WUESTEFELD, T., DAUCH, D., SCHREZENMEIER, H., HOFMANN, W. K., NAKAUCHI, H., JU, Z., KESTLER, H. A., ZENDER, L. & RUDOLPH, K. L. 2012. A differentiation checkpoint limits hematopoietic stem cell self-renewal in response to DNA damage. *Cell*, 148, 1001-14.
- WANG, X., KRUPCZAK-HOLLIS, K., TAN, Y., DENNEWITZ, M. B., ADAMI, G. R. & COSTA, R. H. 2002. Increased hepatic Forkhead Box M1B (FoxM1B) levels in old-aged mice stimulated liver regeneration through diminished p27Kip1 protein levels and increased Cdc25B expression. *J Biol Chem*, 277, 44310-6.
- WARD, I. M. & CHEN, J. 2001a. Histone H2AX is phosphorylated in an ATR-dependent manner in response to replicational stress. *J Biol Chem*, 276, 47759-62.
- WARD, I. M. & CHEN, J. 2001b. Histone H2AX is phosphorylated in an ATR-dependent manner in response to replicational stress. *Journal of Biological Chemistry*, 276, 47759-62.
- WARD, I. M., MINN, K., JORDA, K. G. & CHEN, J. 2003. Accumulation of checkpoint protein 53BP1 at DNA breaks involves its binding to phosphorylated histone H2AX. *J Biol Chem*, 278, 19579-82.
- WATT, F. M. 2014. Mammalian skin cell biology: at the interface between laboratory and clinic. *Science*, 346, 937-40.
- WATT, F. M. & GREEN, H. 1981. Involucrin synthesis is correlated with cell size in human epidermal cultures. *J Cell Biol*, 90, 738-42.
- WATT, F. M. & JONES, P. H. 1993. Expression and function of the keratinocyte integrins. *Dev Suppl*, 185-92.
- WATT, F. M., KUBLER, M. D., HOTCHIN, N. A., NICHOLSON, L. J. & ADAMS, J. C. 1993. Regulation of keratinocyte terminal differentiation by integrin-extracellular matrix interactions. *J Cell Sci*, 106 (Pt 1), 175-82.
- WATT, F. M., LO CELSO, C. & SILVA-VARGAS, V. 2006. Epidermal stem cells: an update. *Curr Opin Genet Dev*, 16, 518-24.
- WEINBERG, W. C., AZZOLI, C. G., CHAPMAN, K., LEVINE, A. J. & YUSPA, S. H. 1995. p53-mediated transcriptional activity increases

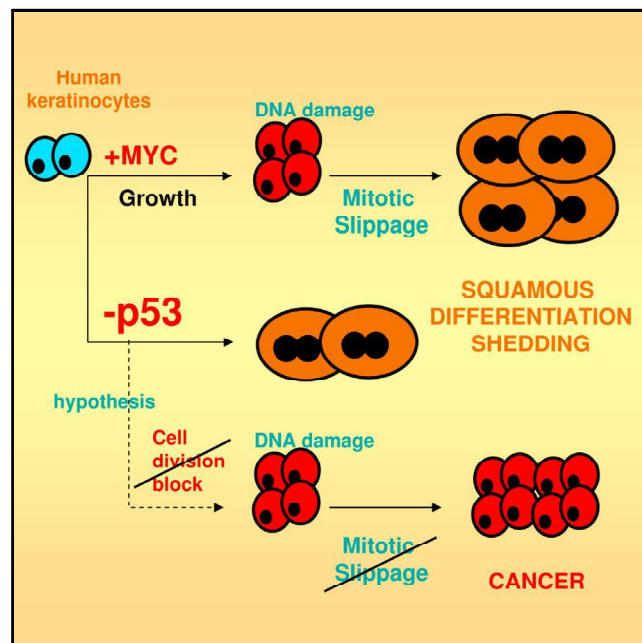
- in differentiating epidermal keratinocytes in association with decreased p53 protein. *Oncogene*, 10, 2271-9.
- WEINSTEIN, G. D., MCCULLOUGH, J. L. & ROSS, P. 1984. Cell proliferation in normal epidermis. *J Invest Dermatol*, 82, 623-8.
- WIERSTRA, I. & ALVES, J. 2006. FOXM1c transactivates the human c-myc promoter directly via the two TATA boxes P1 and P2. *FEBS J*, 273, 4645-67.
- WIERSTRA, I. & ALVES, J. 2007a. FOXM1, a typical proliferation-associated transcription factor. *Biol Chem*, 388, 1257-74.
- WIERSTRA, I. & ALVES, J. 2007b. FOXM1, a typical proliferation-associated transcription factor. *Biological Chemistry*, 388, 1257-74.
- WON, K. A., XIONG, Y., BEACH, D. & GILMAN, M. Z. 1992. Growth-regulated expression of D-type cyclin genes in human diploid fibroblasts. *Proc Natl Acad Sci U S A*, 89, 9910-4.
- WOO, R. A. & POON, R. Y. 2003. Cyclin-dependent kinases and S phase control in mammalian cells. *Cell Cycle*, 2, 316-24.
- WOODWORTH, C. D., WANG, H., SIMPSON, S., ALVAREZ-SALAS, L. M. & NOTARIO, V. 1993. Overexpression of wild-type p53 alters growth and differentiation of normal human keratinocytes but not human papillomavirus-expressing cell lines. *Cell Growth Differ*, 4, 367-76.
- YANG, W., SHEN, J., WU, M., ARSURA, M., FITZGERALD, M., SULDAN, Z., KIM, D. W., HOFMANN, C. S., PIANETTI, S., ROMIEU-MOUREZ, R., FREEDMAN, L. P. & SONENSHEIN, G. E. 2001. Repression of transcription of the p27(Kip1) cyclin-dependent kinase inhibitor gene by c-Myc. *Oncogene*, 20, 1688-702.
- YE, H., KELLY, T. F., SAMADANI, U., LIM, L., RUBIO, S., OVERDIER, D. G., ROEBUCK, K. A. & COSTA, R. H. 1997. Hepatocyte nuclear factor 3/fork head homolog 11 is expressed in proliferating epithelial and mesenchymal cells of embryonic and adult tissues. *Mol Cell Biol*, 17, 1626-41.
- YEKEZARE, M., GOMEZ-GONZALEZ, B. & DIFFLEY, J. F. 2013. Controlling DNA replication origins in response to DNA damage - inhibit globally, activate locally. *J Cell Sci*, 126, 1297-306.
- ZANET, J., FREIJE, A., RUIZ, M., COULON, V., SANZ, J. R., CHIESA, J. & GANDARILLAS, A. 2010. A mitosis block links active cell cycle with human epidermal differentiation and results in endoreplication. *PLoS One*, 5, e15701.

- ZENG, Y. & PIWNICA-WORMS, H. 1999. DNA damage and replication checkpoints in fission yeast require nuclear exclusion of the Cdc25 phosphatase via 14-3-3 binding. *Mol Cell Biol*, 19, 7410-9.
- ZIEGLER, A., JONASON, A. S., LEFFELL, D. J., SIMON, J. A., SHARMA, H. W., KIMMELMAN, J., REMINGTON, L., JACKS, T. & BRASH, D. E. 1994. Sunburn and p53 in the onset of skin cancer. *Nature*, 372, 773-6.
- ZOU, L. & ELLEDGE, S. J. 2003. Sensing DNA damage through ATRIP recognition of RPA-ssDNA complexes. *Science*, 300, 1542-8.
- ZOU, L. & STILLMAN, B. 1998. Formation of a preinitiation complex by S-phase cyclin CDK-dependent loading of Cdc45p onto chromatin. *Science*, 280, 593-6.

ANNEX

Inactivation of p53 in Human Keratinocytes Leads to Squamous Differentiation and Shedding via Replication Stress and Mitotic Slippage

Graphical Abstract



Authors

Ana Freije, Rut Molinuevo, ..., Ernesto De Diego, Alberto Gandarillas

Correspondence

agandarillas@idival.org

In Brief

The p53 tumor suppressor is frequently inactivated in squamous cell carcinoma, yet loss of p53 does not initiate nonmelanoma skin cancer, suggesting that epithelial skin cells have self-protective mechanisms. Freije et al. show that p53 enhances proliferation and inhibits differentiation in keratinocytes by preventing endoreplication. p53 loss leads to squamous differentiation and expulsion of mutant cells, which may confer the epidermis with a molecular protective response.

Highlights

p53 limits the power of the proto-oncogene MYC to drive epidermal differentiation

Loss of p53 causes replication stress and mitotic slippage in human keratinocytes

p53 protects the proliferative potential of the keratinocyte stem cell compartment

Loss or mutation of p53 promotes human squamous differentiation and shedding



Freije et al., 2014, Cell Reports 9, 1349–1360
November 20, 2014 ©2014 The Authors
<http://dx.doi.org/10.1016/j.celrep.2014.10.012>

CellPress

Inactivation of p53 in Human Keratinocytes Leads to Squamous Differentiation and Shedding via Replication Stress and Mitotic Slippage

Ana Freije,¹ Rut Molinuevo,¹ Laura Ceballos,¹ Marta Cagigas,¹ Pilar Alonso-Lecue,¹ René Rodriguez,² Pablo Menendez,^{3,4} Daniel Aberdam,⁵ Ernesto De Diego,^{1,6} and Alberto Gandarillas^{1,7,*}

¹Cell Cycle, Stem Cell Fate and Cancer Laboratory, Fundación Instituto de Investigación Marqués de Valdecilla (IDIVAL), Santander 39011, Spain

²Lab 2-ORL, Instituto Universitario de Oncología de Asturias (IUOPA) Hospital Universitario Central de Asturias (HUCA), Oviedo 33006, Spain

³Josep Carreras Leukaemia Research Institute, School of Medicine, University of Barcelona, Barcelona 08036, Spain

⁴Institució Catalana de Recerca i Estudis Avançats (ICREA), Avenida Lluís Companys, Barcelona 08010, Spain

⁵INSERM UMR-S976, University Paris Diderot, Hôpital Saint-Louis, Equerre Bazin, Paris 75475, France

⁶Paediatric Surgery, Hospital Universitario Marqués de Valdecilla (HUMV), Santander 39011, Spain

⁷INSERM, Languedoc-Roussillon, Montpellier 34394, France

*Correspondence: agandarillas@idival.org

<http://dx.doi.org/10.1016/j.celrep.2014.10.012>

This is an open access article under the CC BY-NC-ND license (<http://creativecommons.org/licenses/by-nc-nd/3.0/>).

SUMMARY

Tumor suppressor p53 is a major cellular guardian of genome integrity, and its inactivation is the most frequent genetic alteration in cancer, rising up to 80% in squamous cell carcinoma (SCC). By adapting the small hairpin RNA (shRNA) technology, we inactivated endogenous p53 in primary epithelial cells from the epidermis of human skin. We show that either loss of endogenous p53 or overexpression of a temperature-sensitive dominant-negative conformation triggers a self-protective differentiation response, resulting in cell stratification and expulsion. These effects follow DNA damage and exit from mitosis without cell division. p53 preserves the proliferative potential of the stem cell compartment and limits the power of proto-oncogene MYC to drive cell cycle stress and differentiation. The results provide insight into the role of p53 in self-renewal homeostasis and help explain why p53 mutations do not initiate skin cancer but increase the likelihood that cancer cells will appear.

INTRODUCTION

Mutations of tumor suppressor p53 are detected in 50% of human cancer and are associated with poor prognosis (<http://p53.free.fr>; Petitjean et al., 2007). p53 is a transcription factor with a major role in halting the cell cycle upon DNA damage, allowing DNA repair and chromosomal integrity, its loss of function often causing genomic instability (Di Leonardo et al., 1997; Taylor and Stark, 2001; Aylon and Oren, 2011; Carvajal and Manfredi, 2013). For these reasons, it has been referred to as the “guardian of the genome” (Lane, 1992). p53 upregulates diverse cell cycle inhibitors such as p21CIP1 or the 14-3-3 family.

Concomitantly, it induces MDM2, which by a negative loop promotes p53 degradation. Most p53 mutations render it inactive, avoiding degradation and resulting in protein accumulation (Lane, 1992; Aylon and Oren, 2011). Insufficient DNA repair in the presence of p53 can result in cell death via apoptosis (Yonish-Rouach et al., 1991; Roos and Kaina, 2006; Aylon and Oren, 2011).

Squamous cell carcinoma (SCC) is the most frequent human malignancy. SCC of the skin is rapidly increasing worldwide, especially in fair individuals (Rogers et al., 2010; <http://seer.cancer.gov>). SCC tends to be aggressive and develop metastasis, also in the skin (4%–5%; Karia et al., 2013), and due to its high incidence, the associated mortality is reaching significant numbers. In the United States, SCC of the skin caused 4,000 to 8,000 deaths in 2012 (Karia et al., 2013). The frequency of p53 inactivation is strikingly high in skin SCC (over 80%; Shea et al., 1992; Brash, 2006; <http://p53.free.fr>). This is mostly due to the mutagenic effects of UV light (Jonason et al., 1996). Understanding the function of p53 in human epidermis provides insight into its role in malignancy.

p53 has been reported to accumulate and mediate apoptosis in the epidermis in response to sunburn (Hall et al., 1993; Ziegler et al., 1994). However, the role of p53 in epidermal homeostasis is not well understood, although it is detected in proliferative cells and downregulated during differentiation (Woodworth et al., 1993; Kallassy et al., 1998; Dazard et al., 2000). Studying this issue has in part been hampered because the skin of p53 knockout mice appears unaffected (Donehower et al., 1992). These mice develop spontaneous tumors and die mainly of thymic lymphoma by 4–6 months of age. Intriguingly, during this time, they do not develop skin carcinomas. The skin must have powerful self-protective mechanisms, since patches or “columns” of cells containing mutated p53 have been frequently reported in otherwise asymptomatic skin (Jonason et al., 1996; Ren et al., 1997; le Pelletier et al., 2001). These mutations are UV associated and do not lead to SCC, further indicating that disruption of p53 in mouse skin alone is insufficient to drive



skin epithelial cancer. Consistently, the absence of p53 does not increase the number or growth rate of chemically induced benign tumors but accelerates their progression to carcinoma (Kemp et al., 1993). Accordingly, the rare human Li-Fraumeni inherited syndrome, caused by heterozygous autosomal p53 mutation, involves spontaneous cancer excluding cutaneous carcinomas (Malkin et al., 1990; Srivastava et al., 1990). Similarly, mice over-expressing mutant p53 do not display higher rates of spontaneous skin carcinomas (Lavigne et al., 1989; Harvey et al., 1995). The mechanisms protecting the skin from loss of p53 remain intriguing (Kemp et al., 1993).

We have previously identified an epidermal checkpoint that responds to deregulated S phase of the cell cycle and DNA damage by triggering terminal squamous differentiation (Gandarillas, 2012). This response involves mitotic bypass or slippage (failure to maintain G2/M arrest, leading to defective exit of mitosis and re-replication in the absence of cell division; Andreassen and Margolis, 1994; Blagosklonny, 2007; Gandarillas, 2012). During mitotic slippage, the nuclei can divide and return to G1 or not, but cells stay in a special G2/M, unable to achieve cytokinesis (Mantel et al., 2008; Zanet et al., 2010; Freije et al., 2012). Over-expression of MYC or cyclin E triggers this mitosis-differentiation checkpoint in human keratinocytes as an oncogene-induced differentiation response (OID; Freije et al., 2012; Gandarillas, 2012).

It has been shown that overfunction of MYC and other oncogenes can cause DNA damage (DNA strand breaks), and this in turn induces p53-mediated apoptosis (Pusapati et al., 2006; Halazonetis et al., 2008). Ectopic cyclin E in human keratinocytes mediates MYC-induced differentiation and causes accumulation of DNA damage (Freije et al., 2012). In addition, MYC induces p53 in keratinocytes as they commit to differentiation (Dazard et al., 2000). Altogether, these results raise the possibility that MYC might promote epidermal differentiation by causing DNA damage, and this response might be mediated by p53. We aimed to investigate this issue by suppressing p53 function in human primary keratinocytes from different individuals, with or without overactivation of MYC, by making use of three different well-characterized small hairpin RNA (shRNA) constructs, a temperature-sensitive mutant, and stratifying organotypic cultures. The results reveal a human squamous differentiation mechanism protecting self-renewal homeostasis against genetic damage.

RESULTS

Replication Stress Initiates MYC-Induced Differentiation of Human Epidermal Keratinocytes

In order to determine whether MYC-induced keratinocyte differentiation is mediated by DNA damage, we generated primary keratinocytes isolated from human skin expressing a conditional MYCER (HKMYCER). This fusion protein renders MYC activatable by 4-OH-tamoxifen (OHT; Littlewood et al., 1995). Activation of MYC by OHT in keratinocytes for 2 days induces the cell cycle (Freije et al., 2012) and for 5 days promotes terminal differentiation and polyploidy (Gandarillas and Watt, 1997; Gandarillas et al., 2000).

We compared the dynamics of DNA replication, p53 induction, and DNA damage after activation of MYCER by OHT. We studied this by measure of bromodeoxyuridine (BrdU) incorporation

(DNA synthesis) and phosphorylation on serine 139 of histone H2AX (γ H2AX, a marker of DNA strand breaks; Rogakou et al., 1998). Activation of MYC rapidly caused an increase of the proportion of cells undergoing DNA replication (Figure 1A, BrdU 12h). This induced the p53/p21 pathway (Figures 1B, 1C, and S1A), as reported previously (Dazard et al., 2000; Pusapati et al., 2006), accumulation of cells in the G2/M phase of the cell cycle (Figure 1A), and expression of cyclin A and metaphasic phosphohistone H3 (P-H3, strong at condensed chromosomes; Figures 1C and S1B). The rapid activation of the cell cycle shortly preceded an increase of the DNA damage marker γ H2AX peaking by 24 hr (Figures 1A and S1A). These changes are consistent with cell cycle deregulation and replication stress leading to DNA strand breaks (Bartkova et al., 2006). By 2 days, a striking increase of nuclear and nucleolar size and binucleation followed (Gandarillas et al., 2000; Figures 1B and S1A). These results show that MYC causes DNA damage prior to increased differentiation in human keratinocytes.

In keratinocytes, a mitosis block by genotoxic agents triggers squamous differentiation (Gandarillas, 2012). To test whether MYC at least in part might enhance differentiation by causing irreparable DNA damage, we treated HKMYCER cells with KU55933 (KU), a specific inhibitor of the DNA-break repair ataxia telangiectasia mutated (ATM) pathway (Hickson et al., 2004). Interestingly, treatment with KU augmented the power of MYC to induce differentiation by 6 days, as measured by involucrin expression (Figure 1D), suggesting that unrepaired DNA damage contributes to MYC-induced keratinocyte differentiation. In order to further test whether accumulation of DNA damage and failure to complete DNA repair triggers a differentiation response, we treated human keratinocytes with NU1025 (NU) a specific inhibitor of the DNA repair poly(ADP-ribose)polymerase (PARP; Griffin et al., 1995). Interestingly, treating keratinocytes with NU caused accumulation of DNA damage and subsequently induced terminal differentiation as monitored by involucrin expression and cell stratification (Figures 1E and S1C). These results provide evidence suggesting that a DNA damage-induced differentiation response might be part of the normal program of keratinocytes. Consistently, keratinocytes heavily labeled for γ H2AX were found stratifying into the differentiated layer (Figure S1D; Movie S1).

Inactivation of p53 Potentiates MYC-Induced Differentiation

We aimed to investigate whether p53 mediates MYC-induced keratinocyte differentiation as a response to replication stress. To this end, we adapted shRNA technology for primary keratinocytes and knocked down endogenous p53 in the presence of conditional MYC (MYCER). We have made use of three well-characterized lentiviral constructs bearing p53 shRNA (see Experimental Procedures; Kim et al., 2007; Rodriguez et al., 2011; Sandler et al., 2011; from hereon shP53), one of which (as its vector control) carries a gene for GFP. Figures 2A–2C show the inhibition of endogenous p53 by immunofluorescence, western blotting (protein), and RT-PCR (mRNA). Immunofluorescence analyses showed undetectable levels of p53 in individual GFP-expressing cells shortly after infections (Figure 2A and not shown). shP53 suppressed MYC induction of p53 and its

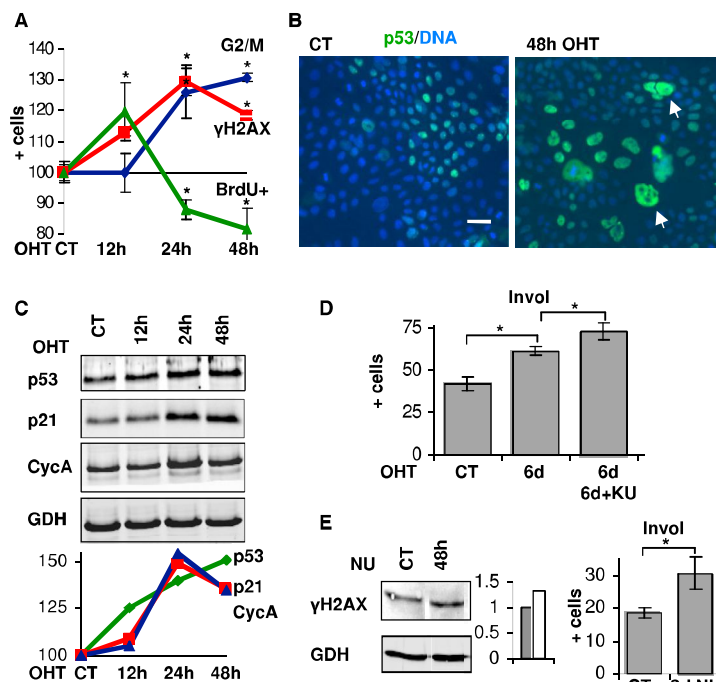


Figure 1. DNA Damage Initiates MYC-Induced Differentiation of Human Epidermal Keratinocytes

(A) Flow-cytometry quantitation of human keratinocytes (HK) expressing conditional MYCER after activation of MYC by OHT for the periods of time indicated with respect to controls with no OHT (CT); percent of cells undergoing DNA synthesis (BrdU+, green), in G2/M (4N, DNA content, blue), or expressing the DNA damage marker γ H2AX (red). (B) Immunostaining for p53 (green) in CT or after activation of MYC for 48 hr. Nuclear DNA by DAPI (blue). Arrows: large nuclei positive for p53. Scale bar, 50 μ M. See also Figure S1A.

(C) Expression of the cell cycle regulators indicated in MYCER cells after activation of MYC as indicated. Plots: quantitation of the western blots normalized to the loading control housekeeping protein GAPDH (GDH); CycA, cyclin A. See also Figure S1B.

(D) Flow-cytometry quantitation of the epidermal differentiation marker involucrin (Invol) in MYCER cells untreated or treated with the ATM inhibitor KU55933 (KU) for 6 days, as indicated.

(E) Effects of the inhibition of PARP repair polymerase in HK by treatment with NU1025 (NU) as analyzed by western blot for γ H2AX (left) or by flow cytometry for Invol (large bar histogram, right), for the periods indicated. Small bar histogram is a quantitation of the γ H2AX western blots normalized to GDH. The Invol positive region was determined by a negative isotype antibody control (CD8). See also Figure S1C.

Error bars are SEM. Data are average of duplicate samples of representative experiments. * $p < 0.05$.

transcriptional target protein, p21CIP1 (p21; Figures 2A–2C). Unexpectedly, the induction of differentiation 5 days after activation of MYC was not attenuated but augmented in the presence of shP53, as this provoked a higher rate of stratification, morphological changes, and expression of the terminal differentiation markers involucrin and keratin K1 (Figures 2D–2G). Activation of MYC and inactivation of p53 therefore cooperated in driving cells toward differentiation. This indicates that in keratinocytes, endogenous p53 does not mediate MYC-induced differentiation but rather restrains it.

Inactivation of p53 in Human Normal Keratinocytes Causes Replication Stress

Enhanced differentiation in HKMYCER after inhibition of p53 suggested that endogenous p53 opposes the action of MYC. To explore the cell cycle mechanisms by which p53 functions, we infected normal primary keratinocytes freshly isolated from human skin with the three shP53 constructs. The shP53 constructs efficiently downregulated p53 even upon treatment with the genotoxic drug doxorubicin (DOXO), which causes acute DNA damage and strongly induces p53 (Figures 3A–3C and S2A). In the absence of DOXO, western blotting and immunofluorescence staining or RT-PCR showed barely detectable levels of the endogenous protein or mRNA, respectively, 2 or 3 days after delivery of the shP53s (Figures 3B–3D and S2A). p53 target p21CIP1 was also downregulated (Figures 3A, 3B, and S2A), indi-

cating that both p53 protein and function were suppressed. We first tested whether the loss of p53/p21 in human keratinocytes might cause cell cycle deregulation and failure to repair DNA breaks. Inhibition of p53 did not alter significantly the expression of its related factor, p63 (Figure 3A), but provoked a rapid induction of cell cycle markers phospho-Rb, premitotic cyclin A, and mitotic phosphohistone p3 (Figures 3B, S3A, and S3B). Given the reported capacity of p63 to induce cell cycle and epidermal differentiation molecules (Koster, 2010), it might contribute to the observed effects.

Interestingly, the cell cycle changes caused by shP53 resulted in increased DNA damage as measured by γ H2AX foci (Figure 3B, 3D, and 3E). The induction of phospho-Rb and γ H2AX after inactivation of p53 was transient (Figures 3B and S5B). Inactivation of p53 in keratinocytes therefore caused cell cycle and replication stress as identified by S phase deregulation and accumulation of DNA strand breaks.

Loss of p53 Provokes Mitotic Slippage and Loss of Proliferative Potential

The early cell cycle activation upon suppression of p53 led to a transient increase of DNA replication (BrdU incorporation; Figures 4A and S2B, 48 hr). Subsequently, the peak of BrdU-positive cells shifted from the diploid to the polyploid range (Figures 4A and S2B), thus indicating that some replicating cells lost the capacity to divide. As a result, the cell cycle profile of the whole

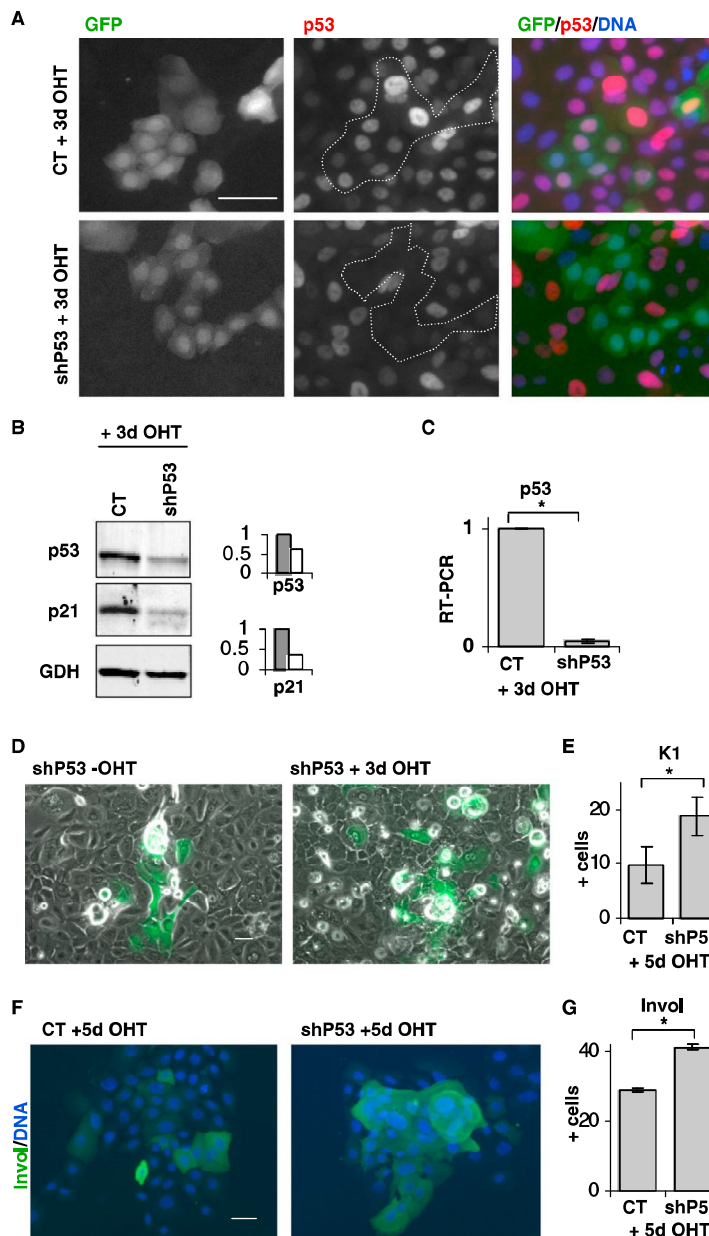


Figure 2. p53 Restrains MYC-Induced Epidermal Differentiation

(A) Expression of GFP (green) and p53 (red) by immunofluorescence of HKMYCER cells infected with control vector CTGFP (CT) or with shP53 as indicated after activation of MYC by addition of OHT for 3 days. Note that within the mixed cultures, p53 is undetected in cells expressing shP53 (green cells, broken line).

(B) Detection of p53 and its target p21 by western blot in CT or shP53 cells treated with OHT for 3 days as indicated. Bar histograms represent quantitation of the western blots normalized to GAPDH (GDH).

(C) Expression of p53 as measured by RT-PCR in CT or shP53 cells after activation of MYC by OHT for 3 days.

(D) Typical phase contrast and green fluorescence (GFP) of live shP53 cells 4 days postinfection with or without OHT as indicated.

(E) Percent of CT or shP53 GFP cells expressing the terminal differentiation marker keratin K1 after addition of OHT for 5 days, as determined by immunofluorescence.

(F) Immunofluorescence for involucrin (green) of CT or shP53 cells, 5 days after addition of OHT. Nuclear DNA by DAPI (blue).

(G) Percent of CT or shP53 cells expressing involucrin (Invol) after addition of OHT for 5 days, as determined by flow-cytometry. Error bars are SEM of duplicate samples of representative experiments. * $p < 0.05$. Scale bar, 50 μm .

population decreased in G1/diploidy and increased in polyploidy (with frequent multinucleation), while the G2/M fraction remained basically unchanged (Figures 4B, S2B, and S2C). All in all, we found no great increase of S phase or proliferative mitosis 3 days after inhibition of p53, but a cell cycle shift toward

polyploidy as a result of mitotic bypass or mitotic slippage shP53 (re-replication or endoreplication in the absence of cell division; Andreassen and Margolis, 1994; red arrow in Figure 4B and Figure S2B). Consistently, there was a transient accumulation of mitotic markers cyclin A and cyclin B and the metaphase marker P-H3 (Figures 3B, 4C, S3A, and S3B; Movies S2, S4, S5, and S6), an increase of cells expressing postmitotic keratin K1 (Figure 4C), and an accumulation of cyclin E that typically associates with keratinocyte mitotic slippage (Figures 3B and S3C; Zanet et al., 2010; Freije et al., 2012). Concomitantly, a high frequency of cells displayed striking accumulation of cytoplasmic cyclin A or B (Figures 4C and S3A; Movie S2). Inhibition of shP53 induced a shorter form of cyclin A (Figure 3B), likely inactive (Kaufmann et al., 2001; Wang et al., 2012), even more upon overactivation of MYC (Figure S3D). Timely degradation of cyclins A and B is required for exit from mitosis, and their cytoplasmic accumulation is likely to associate with defective mitosis (Murray, 2004; Zanet et al., 2010; Rosa-Garrido et al., 2012).

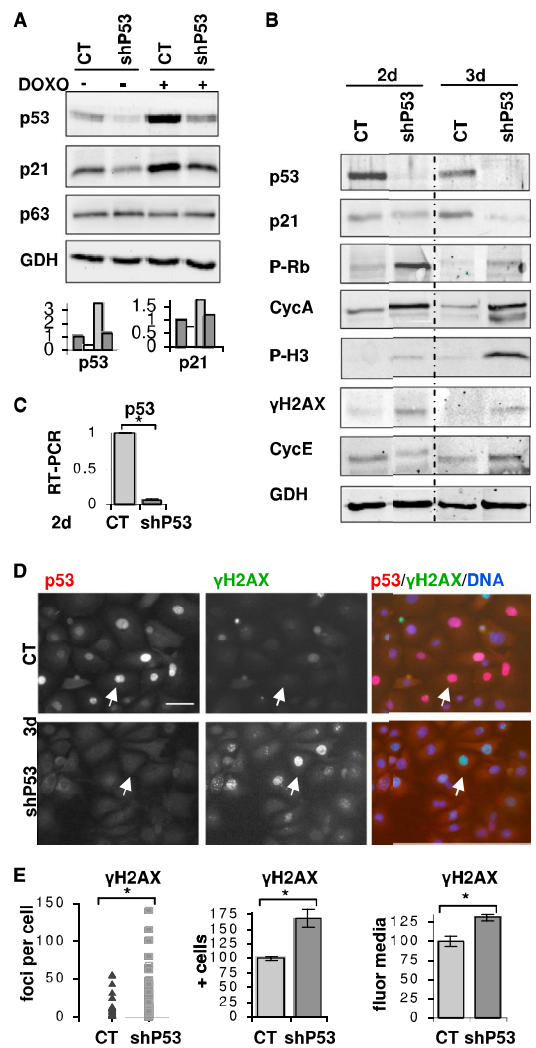


Figure 3. Disruption of Endogenous p53 in Human Keratinocytes Causes Replication Stress

(A) Expression of p53, its target p21, and p63 in HK infected with CTGFP (CT) or with shP53 as indicated, untreated or treated with the genotoxic drug doxorubicin (DOXO) for 24 hr. Bar histogram represents quantitation of western blots normalized to GAPDH (GDH).

(B) Western blot for the cell cycle regulators indicated in CT or shP53 cells, 2 or 3 days postinfection; Cyc, cyclin. See also Figure S2A.

(C) Bar histogram shows expression of p53 in CT or shP53 cells as measured by RT-PCR 2 days postinfection. See also Figure S2A.

(D) Double immunostaining for p53 (red) and γ H2AX (green) 3 days postinfection. Note that cells with low p53 tend to accumulate DNA damage (arrows) and vice versa. Nuclear DNA by DAPI (blue). See also Figure S5. Scale bar, 50 μ m.

(E) Distribution histogram shows number of foci of γ H2AX per nucleus, as scored by immunofluorescence as in Figure 3D and image analyses. Left bar

As a consequence of failure to exit cytokinetic mitosis, loss of p53 did not result in increased proliferation but did result in a significant loss of clonogenic potential (Figure 4D). Cells expressing shP53 were impaired especially in the generation of large colonies that are founded by the great potential of stem cells (Jones and Watt, 1993). The loss of clonogenic potential by inactivating p53 did not involve detectable apoptosis (absence of a sub-G1 DNA peak; Figure S2B). Accumulation of mitotic markers and metaphase figures, loss of the capacity to divide, polyploidy, BrdU incorporation by polyploid cells, and multinucleation altogether indicate that loss of p53 in keratinocytes leads to mitotic slippage, by which cells enter mitosis but fail to divide (see also below).

Loss of p53 Promotes Squamous Differentiation

Mitosis failure in keratinocytes triggers terminal differentiation, and cell cycle stress triggers this mitosis-differentiation checkpoint (Zanet et al., 2010; Freije et al., 2012; Gandarillas, 2012). We explored whether loss of p53 triggered this response, thus explaining the observed loss of clonogenic potential. As shown in Figures 5A–5C and S4, inhibition of p53 strikingly induced the squamous differentiation markers involucrin, keratin K1 (see also Figure 4C), keratin K10, and flaggrin as well as cell-size increase and morphological changes typical of terminal differentiation. As a consequence, cells with low levels of p53 were found to stratify and detach at a higher rate than control cells in confocal analyses (Figure S5A; Movie S3). The time-lapse videos also showed that HKshP53 stressed and accumulated in mitosis attempting to divide (Movies S4, S5, and S6). To better study the effect on differentiation, we placed cells in a high-calcium medium that allows stratification closely resembling the process in human epidermis (Rheinwald, 1989). Cells expressing the GFP marker displayed very low levels of p53, stratified, and detached (Movies S3 and S7). Shed cells were counted in the culture medium showing that inactivation of p53 produced a higher rate of desquamation (Figure 5D). Consistently, within unselected mixed cultures, 5–6 days after delivery of shP53, cells with detectable levels of p53 and low levels of γ H2AX had repopulated the basal proliferative layer (Figure S5B). This further indicates that cells expressing p53 are more proliferative. Maintaining the proliferative potential might be a keratinocyte stem cell p53 function, since in parallel experiments, inhibition of p53 led to increased proliferation and impaired senescence in pluripotent mesenchymal stem cells (Figure S6).

Inactivation of a Temperature-Sensitive p53 Mutant Protein Promotes Differentiation, whereas Its Activation Attenuates It

Often, in skin tumors and in patients with Li-Fraumeni syndrome, mutated p53 coexists with the normal allele. In this context, inactive p53 mutants can have a dominant-negative effect by disrupting the function of the endogenous protein (Hann and

histogram shows percentage of positive γ H2AX cells as quantitated by flow cytometry. Right bar histogram shows the mean γ H2AX intensity per cell as measured by flow cytometry in the whole population.

Error bars are SEM of duplicate samples of representative experiments. *p < 0.05.

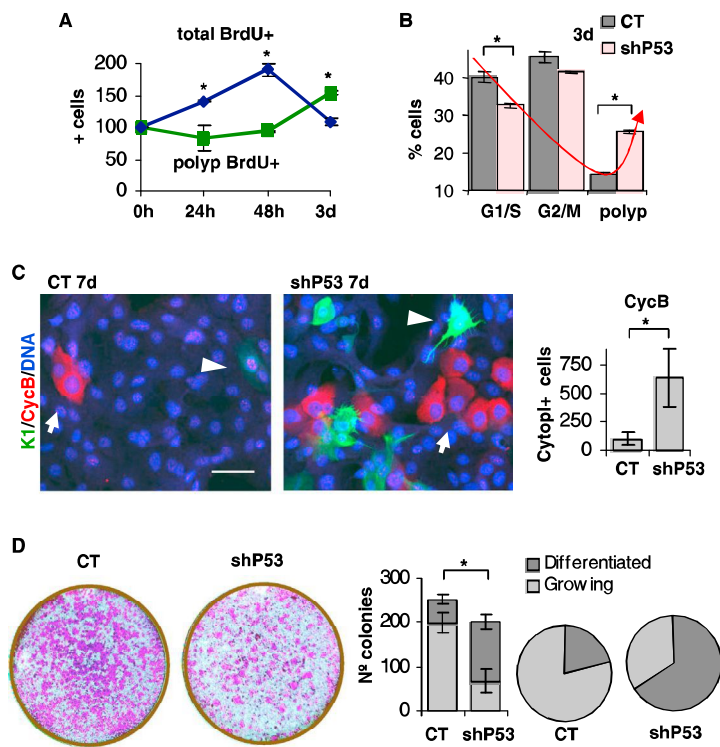


Figure 4. Disruption of Endogenous p53 in Human Keratinocytes Causes Mitotic Slippage and Loss of Clonogenic Potential

(A) Percent of total or polyploid (polyp) HK infected with shP53 undergoing DNA synthesis (BrdU+) for the periods of time postinfection indicated, as quantitated by flow cytometry and normalized to HK infected with CTGFP (CT). See also [Figure S2B](#). (B) Percent of cells in the G1/S (2N), G2/M (4N), or polyp phases of the cell cycle in CT (gray) or shP53 (light red) cells 3 days postinfection, as determined by flow cytometry. Red arrow shows the shift of shP53 cells toward polyploidy, a consequence of mitotic slippage. See also [Figures S2B](#) and [S2C](#).

(C) Double immunostaining for K1 (green, arrow heads) and mitotic cyclin B (CycB, red; arrows). Nuclear DNA by DAPI (blue). shP53 cells displayed frequent accumulation of cytoplasmic cyclin B (cytop+), and scoring is shown in the bar histogram. See also [Movie S2](#).

(D) Clonogenic capacity of CT or shP53 cells (10,000 cells plated 3 days postinfection). Bar and circle histograms show the number (bars) and percent (circles) of actively shP53 growing colonies (light gray) versus small abortive, differentiated colonies (dark gray).

Error bars are SEM of duplicate (A–C) or triplicate (D) samples of representative experiments. * $p < 0.05$.

Lane, 1995; Blagosklonny, 2000; Sigal and Rotter, 2000; Lee et al., 2012). To mimic this condition, we have overexpressed in epidermal keratinocytes (HKp53ts) a well-characterized mutant form of p53 (p53ts), whose conformation state can be regulated by temperature (Michalovitz et al., 1990). At 32°C, p53ts displays the wild-type conformation, whereas at 39°C, it adopts an inactive conformation and can thus behave as a dominant-negative mutant. It is well established that active p53 is rapidly degraded due to an autoregulatory feedback loop with MDM2, whereas the inactive protein stabilizes and accumulates (Haupt et al., 1997). Consistently, HKp53ts expressed higher levels of p53 at 32°C than control cells, but the protein accumulated further at 39°C as it adopted the inactive conformation (antigen pab240 positive; [Figures 6A](#), [6B](#), and [S7A](#); [Gannon et al., 1990](#); [Michalovitz et al., 1990](#)). In addition, while p53 was absent from suprabasal HKp53ts at 32°C, as the endogenous protein, it accumulated in suprabasal involucrin-positive cells at 39°C ([Figure 6B](#) and [S7A](#)). This further indicated that the protein was inactivated at 39°C.

Inactivation of p53ts in human keratinocytes by the 39°C temperature switch resulted in increased differentiation monitored as high light scatter and expression of the suprabasal markers involucrin and keratin K16 ([Figures 6B](#), [6C](#), and [S7B](#), and [S7C](#)). Conversely, inducing the active conformation of p53ts at 32°C retained keratinocytes in the proliferative compartment as deter-

mined by an increased proportion of cells with basal-like low-scatter parameters and decreased expression of the suprabasal markers ([Figures 6B](#), [6C](#), [S7B](#), and [S7C](#)). Loss or gain of cell cycle control by inactivation or activation of p53 was reflected in the increase or decrease of hyperproliferative suprabasal K16 at 39°C or 32°C, respectively. As observed after suppressing endogenous p53 by shRNA, the inactive form of p53ts caused binucleation, increased nuclear size and γ H2AX-associated DNA damage ([Figures 6B](#) and [S7A](#), [S7D](#), and [S7E](#); arrows), and reduced the clonogenic potential of the stem cell compartment once cells were returned to 37°C ([Figure 6D](#)). No additional gains of function were observed.

DISCUSSION

Role of p53 in Human Keratinocytes

Altogether, our results demonstrate a human epidermal cell response to loss of p53 function consistent with an oncogene-induced differentiation checkpoint (OID). Keratinocytes lacking p53 differentiated, as determined by the expression of various differentiation markers, morphological changes, and loss of proliferative capacity. This process was preceded by mitosis defects, suggesting that endogenous p53 interferes with the initiation of epidermal differentiation by retaining cells within the proliferative compartment. p53 might cause this by two mechanisms ([Figure 7](#)): (1) by holding cells in the G1 and G2/M phases of the cell cycle and ensuring efficient DNA repair, or (2) by opposing cyclin E function. Interestingly, p53 has been proposed

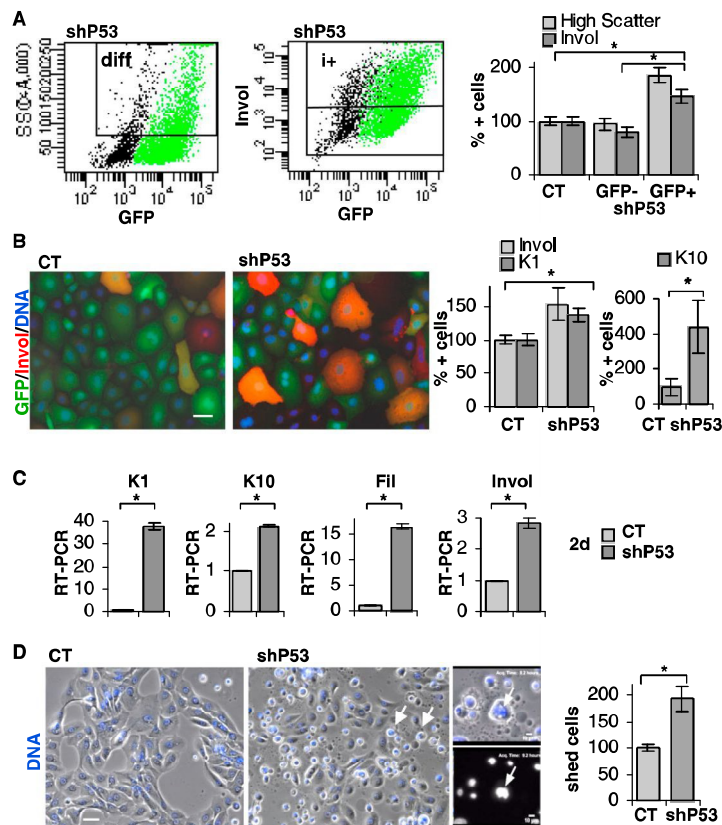


Figure 5. Loss of Endogenous p53 in Human Keratinocytes Triggers Terminal Differentiation, Stratification, and Shedding

(A) Dot plots show flow-cytometry analyses for GFP (green) versus light scatter (SSC-A; left) or involucrin (Invol, right) of HK infected with shP53. Bar histograms show percent of differentiating (high light scatter; diff. in dot plot) or Invol positive (+ in dot plot) cells in the GFP (+) or non-GFP (–) populations, as indicated. CT, cells infected with control vector. See also Figure S4A.

(B) Double immunostaining for GFP (green) and Invol (red) 5 days postinfection of HK with CTGFP (CT) or shP53 as indicated; nuclear DNA by DAPI (blue). Bar histograms show percentage of cells positive for Invol and K1 (flow cytometry), or K10 (immunofluorescence) in shP53 cells relative to CT cells. Scale bar, 50 μ m. See also Figure S4.

(C) Expression of differentiation markers K1, keratin K10, filaggrin (Fil), and *Invol*, as determined by RT-PCR in shP53 cells relative to CT cells 2 days postinfections.

(D) Snap frames from Movies S4 and S6 showing the accumulation of shP53 cells in mitosis (arrows) 5 days postinfection. Nuclear DNA by NucBlue (blue). Amplified insets show a cell blocked in metaphase (bottom panel: DNA only). See also Movies S4, S5, and S6. Bar histogram shows percent of shP53 cells shed into the medium, relative to control cells.

Error bars are SEM of duplicate samples of representative experiments. * $p < 0.05$. Scale bars represent 50 μ m (B and D) or 10 μ m (small insets in D).

to constitute a barrier against hyperactivation of cyclin E/cdk2 (Minella et al., 2002), and cyclin E mediates MYC-induced keratinocyte cell cycle stress and differentiation (Freije et al., 2012). Loss of p53 may thus allow cyclin E/cdk2 (ergo MYC) full power to trigger the differentiation response. This would mitigate the cell cycle stress/OID response and the cell division block that triggers squamous differentiation (Zanet et al., 2010; Freije et al., 2012; Gandarillas, 2012).

The results provide insight into the enigmatic role of p53 in epidermal homeostasis with implications in stem cell regulation. First, they show that p53 is dispensable for the epidermal differentiation signal. Second, by promoting the correct timing of the cell cycle checkpoints and avoiding mitotic slippage, p53 appears to protect the proliferative capacity of epidermal stem cells (Figure 7). Consistent with this model, p53 is downregulated as epidermal differentiation initiates (see Dazard et al., 2000 and references therein), and its overexpression inhibited growth and squamous differentiation markers in cell-reconstituted epidermis (Woodworth et al., 1993). p53 was also dispensable for the differentiation signal caused by overactivation of MYC. This signal might be triggered in cells accumulating irreparable DNA damage (strand breaks) and escaping the protective role

of p53 (Figure 7), since it was enhanced by inhibition of the DNA repair ATM pathway. Interestingly, the differentiation signal was also enhanced in normal keratinocytes by inhibition of the DNA repair poly-(ADP-ribose)-polymerase.

Protecting the proliferative potential of stem cells from differentiation might be a keratinocyte function of p53, since in other cell types, it promotes apoptosis, senescence, or even differentiation. In this study, shP53 prolonged the lifespan of human pluripotent mesenchymal stem cells. As mentioned above, we have shown that MYC in keratinocytes promotes differentiation, while in other cells it promotes proliferation. As we have suggested for MYC (Gandarillas, 2012; Muñoz-Alonso et al., 2012), the cell-growth deregulation that follows p53 loss might trigger differentiation in cells where this process is associated with cellular growth. Paradoxical inhibition of senescence by p53 has also been reported (Demidenko et al., 2010). Conversely, p53 has been shown to induce apoptosis in keratinocytes after acute damage caused by sunburn (Ziegler et al., 1994). p53 might thus play a dual role in epidermal survival by keeping proliferative cells “healthy” and inducing cell death of severely damaged cells.

Implications into Skin Homeostasis and Cancer

Our fluorescent confocal and video analyses on mixed (GFP and no-GFP cells) stratifying cultures showed that

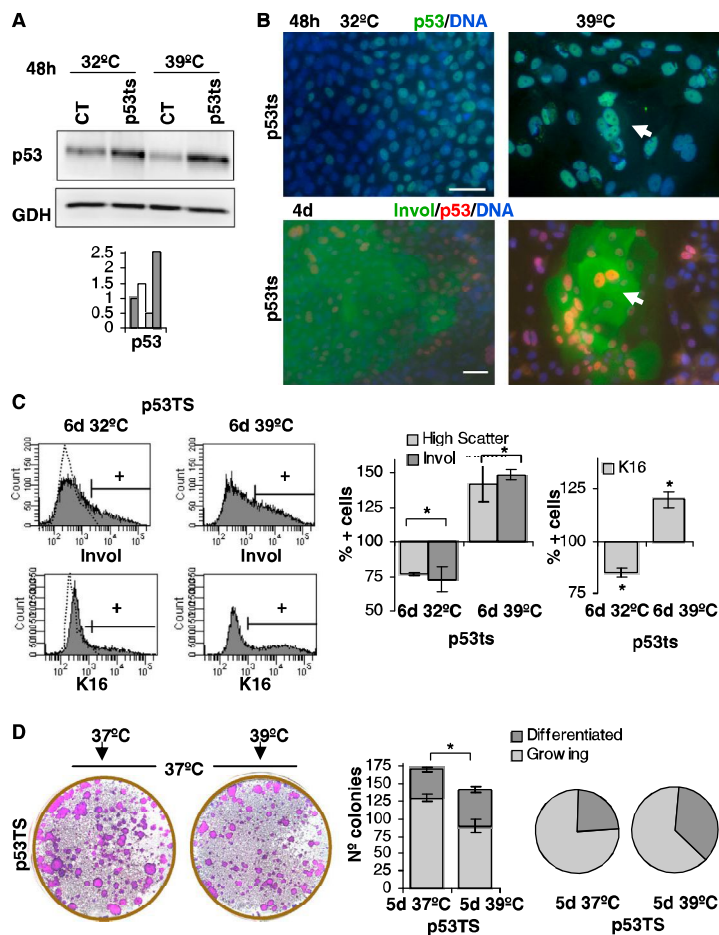


Figure 6. A Mutant Inactive Conformation of p53 Induces Keratinocyte Differentiation and Reduces the Great Proliferative Potential Cell Compartment

(A) Detection of p53 by western blotting in keratinocytes expressing control vector (CT) or the temperature-sensitive mutant p53 (p53ts) 48 hr after the temperature switch to 32°C or 39°C as indicated. Bar histogram show quantitation of p53 western blots normalized to GAPDH (GDH). Note that p53 accumulates at 39°C (inactive conformation).

(B) Top: immunofluorescence for p53 (green) on p53ts cells as in (A); Bottom: double immunofluorescence for involucrin (Invol, green) and p53 (red) on p53ts cells 4 days after the temperature switch. Note the binucleate differentiating p53ts cells that accumulate p53 at 39°C (arrows). Nuclear DNA by DAPI (blue). See also Figure S7A. Scale bar, 50 μ m.

(C) Representative flow cytometry for the expression of Invol (top) or the hyperproliferative marker keratin K16 (bottom) in p53ts cells 6 days after the temperature switch, as indicated. Bar histograms show percent of morphologically differentiated (high scatterer) cells or cells positive for Invol or K16 as indicated, normalized to CT cells; quantitation of positive cells by the gates indicated on the histograms (+), as determined by a negative isotype antibody control (dotted line; CD8). See also Figure S7B.

(D) Clonogenic capacity of p53ts cells plated 5 days after the 39°C temperature switch. A total of 2,500 proliferative cells were plated. Bar and circle histogram show number (bars) or percent (circles) of actively shP53 growing colonies (light gray) versus small abortive, differentiated colonies (dark gray).

Error bars are SEM of duplicate (C) or triplicate (D) samples of representative experiments. * $p < 0.05$.

adjacent clones unless the skin is UV irradiated (Zhang et al., 2001).

Altogether, our results have implications into the mechanisms leading to epithelial skin cancer (mainly SCC), in which p53 is frequently mutated. Disruption of p53, however, does not seem to be an initiating event in this malignancy, since mice lacking p53 die around 4–6 months, mainly of thymic lymphoma, and do not develop early skin tumors (Donehower et al., 1992). Consistently, epidermal-specific p53 knockout mice develop spontaneous tumors from 5 months onward (Martinez-Cruz et al., 2008). This is also consistent with humans usually developing skin carcinomas at an old age. In addition, p53 knockout mice are not more susceptible to chemically induced skin carcinogenesis (Donehower et al., 1992; Kemp et al., 1993). Within similar lines, Li-Fraumeni patients having one mutant p53 allele do not display a higher rate of skin carcinomas (Malkin et al., 1990; Srivastava et al., 1990). Altogether, these observations suggest that the epidermis has mechanisms to be protected from p53 mutations. This is further supported by the well-documented presence of frequent clones or “columns” of p53 mutant cells in

p53-defective keratinocytes had a higher tendency to stratify and detach than the normal cells. It is intriguing that the absence of p53 did not cause apparent physiological defects in mouse skin in vivo (Donehower et al., 1992; Martinez-Cruz et al., 2008). This, in part, might be due to compensatory mechanisms. Also, the in vivo niche might rescue the proliferative capacity of stem cells. For instance, lack of MYC renders mouse keratinocytes unable to proliferate in vitro, but they can form an epidermis in vivo (Zanet et al., 2005). Interestingly, however, the specific ablation of p53 in mouse epidermis caused mitotic defects (Martinez-Cruz et al., 2009). In addition, our model for mitosis-induced differentiation is that keratinocytes undergoing a prolonged arrest in mitosis are pushed to stratify and differentiate by other more proliferative and more adherent neighbor cells (Gandarillas, 2012). This might thus involve competition phenomena. Within these lines, it is interesting that in mouse epidermis, p53 mutant clones are growth limited by normal

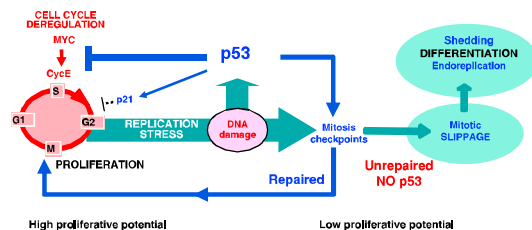


Figure 7. Model for the Role of p53 in Proliferation and Differentiation of Human Epidermal Keratinocytes

p53 would hold cells, allowing DNA repair. Cells with successful repair would re-enter the proliferative compartment, and cells with irreparable levels of DNA damage would undergo mitosis slippage, terminal differentiation, stratification, and shedding. p53 would protect the proliferative potential of stem cells (left), and its loss of function would lead to loss of proliferative potential (right).

sun-exposed asymptomatic skin that do not seem to lead to cancer (Jonason et al., 1996; Ren et al., 1997; le Pelletier et al., 2001). Our results herein provide a mechanism explaining these observations. Loss of cells with inactive p53, by stratification and shedding due to unrepaired DNA damage, may explain how the skin protects itself from mutations hitting this tumor suppressor. Precancerous keratinocytes would be removed via squamous differentiation, therefore avoiding clinical impact.

Although loss of p53 does not sensitize the skin to early tumorigenesis, it accelerates cancer progression (Kemp et al., 1993; Bomachea et al., 2012). Interestingly, genomic instability appears to contribute to the spontaneous tumors developed in p53 knockout mouse epidermis (Martínez-Cruz et al., 2009). In addition, mouse skin deficient in p53 or overexpressing a mutant form develops tumors more frequently when UV irradiated (Li et al., 1995; Jiang et al., 1999). UV causes keratinocytes to arrest in G2 (Pavey et al., 2001). Our results support a model that might reconcile these observations. In our experiments, inhibition of p53 impaired efficient G2 arrest, resulting in mitotic slippage and terminal differentiation, thereby suppressing cell division (Figure 7). Additional alterations cooperating with inactivation of p53 might hit the control of mitosis and bypass the proliferative block. This would allow p53-mutated cells to escape terminal differentiation and expulsion and divide in spite of a high genomic instability context caused by genetic damage, thus promoting malignant clones to appear.

EXPERIMENTAL PROCEDURES

Cell Culture, Plasmids, Viral Infections, and Treatments

Ethical permission for this study was requested, approved, and obtained from the Ethical Committee for Clinical Research of Cantabria Council, Spain. In all cases, human tissue material discarded after surgery was obtained with written consent presented by clinicians to the patients, and it was treated anonymously.

Primary keratinocytes were isolated from neonatal human foreskin and cultured in the presence of a mouse fibroblast feeder layer (inactivated by mitomycin C) in Rheinwald FAD medium as described previously (10% serum and 1.2 mM Ca²⁺; Rheinwald, 1989; Gandarillas and Watt, 1997). Low passages (one to five) of keratinocytes from four different individuals were utilized.

For gene delivery in primary keratinocytes the following viral constructs driven by viral constitutive promoters were used. Retroviral constructs were pBabe empty vector, pBabe-MYCER (Littlewood et al., 1995; Gandarillas and Watt, 1997; MYC fusion protein with the ligand binding domain of a mutant estrogen receptor that responds to 4-OH-hydroxytamoxifen; OHT), or pBabe-p53Val135 (p53ts; kindly provided by M. Oren, Weizmann Institute, Rehovot, Israel) carrying a mutant p53 whose conformation can be regulated by a temperature shift (wild-type at 32°C, inactive at 39°C; Michalovitz et al., 1990). All pBabe constructs carried puromycin resistance and were delivered by cell infection, and cells were selected as described previously (Freije et al., 2012). Lentiviral constructs were control pLKO1 (CT; Sigma-Aldrich), control GFP pLVTHM (CTGFP), and three constructs expressing shRNA specific against p53: the GFP expressing vector pLVUH-shp53 (shP53) and two non-GFP constructs pLKO1-p53-shRNA-427 (shP53-427; Addgene; Kim et al., 2007) and pLKO1-p53-shRNA-941 (shP53-941; Addgene; Kim et al., 2007). More details can be found in Supplemental Experimental Procedures.

For delivery of shRNA expressing constructs in primary human keratinocytes, two alternative optimized methods of infection were used giving “low” (25%–35%) or “high” (80%–90%) efficiency. Cells were then placed on low calcium or high calcium media depending on the experiment. See Supplemental Experimental Procedures for method details.

MYCER was activated by addition of 100 nM OHT (Sigma-Aldrich) to the culture medium for the periods of time indicated. Keratinocytes were grown at 37°C and 5% CO₂ except for induction of active or inactive conformations of p53ts, when the temperature was shifted to 32°C and 39°C, respectively, for the periods of time indicated.

Primary keratinocytes were treated for 6 days with the ATM inhibitor KU55933 (10 μM; Tocris Bioscience) or with the PARP inhibitor NU1025 (200 μM; Millipore) for 24 or 72 hr. Parallel control cultures were always subjected to the DMSO vehicle only.

For clonogenicity assays, 15,000 keratinocytes grown in low-calcium medium or 2,500 grown in high-calcium FAD medium were plated per T6 well triplicates and cultured in FAD medium. About 10 days later, the cultures were stained with rhodanile blue as described previously (Jones and Watt, 1993). This dye colors keratinocytes pink (darker the more differentiated) and feeder fibroblasts purple.

Cell Shedding

Quantitation of cell shedding was measured by counting cells detached into the culture medium. Data were obtained from duplicate samples and normalized to controls.

Antibodies

Primary and secondary antibodies utilized in this study are listed in Supplemental Experimental Procedures.

Flow Cytometry

Keratinocytes were harvested, fixed, and stained for BrdU and DNA (propidium iodide [PI]) or for involucrin and analyzed by flow cytometry as described in Supplemental Experimental Procedures. All antibody stainings were controlled by the use of a similar concentration of isotype-negative immunoglobulins (mouse anti-CD8 or rabbit serum). A total of 10,000 events were gated and acquired in list mode for every sample except for some GFP-positive analyses, when 50,000 cells were acquired. In order to gate out cell aggregates, the area of the fluorescent pulse of PI (DNA content; PE-A) was plotted versus the width of the fluorescent pulse (PE-W).

Immunofluorescence and Confocal Microscopy

Keratinocytes were grown on glass coverslips, fixed and stained as previously described (Freije et al., 2012). After washing with PBS, coverslips were stained with 0.1 μg/ml DAPI, mounted with ProLong Gold Antifade Reagent (Life Technologies), and visualized and photographed under AxioVision Zeiss fluorescence microscopy. z stack 3D digital images were reconstructed after frame collection by confocal microscopy (Nikon A1R, 20× numerical aperture [NA] 0.75) and processed by NIS Elements software (AR, 3.2 64 bits; Nikon) as indicated in the supplemental movie legends.

Whole-Cell Extracts and Western Blotting

Cells were washed twice with PBS and incubated for 30 min on ice in lysis buffer as described previously (Freije et al., 2012). Supernatant concentrations were determined using the Qubit protein assay kit (Life Technologies). For western blot analysis, 80 μ g of cell extracts was separated by SDS-PAGE (10% or 12%) and transferred to nitrocellulose membranes. After blocking and incubating with the primary antibodies, the membranes were subjected to secondary antibodies and subjected to enhanced chemiluminescence substrate (SuperSignalTM West Femto, Pierce), following the supplier's protocol, and analyzed with an Odyssey scanner (Li-Cor) or C-Digit scanner (Li-Cor).

RT-PCR

Total RNA was isolated using NucleoSpin RNA (Macherey-Nagel) according to the manufacturer's instructions. A total of 1 μ g of total RNA was reverse transcribed with the iScript cDNA synthesis kit (Bio-Rad) in a 20 μ l reaction for 30 min at 42°C. The cDNAs (1 μ l) were amplified by real-time PCR (Bio-Rad iQ SYBR green supermix) and normalized to β -actin mRNA levels. Primers utilized in this study are listed in Supplemental Experimental Procedures.

Time-Lapse Videos

For Movies S4, S5, and S6, keratinocytes 4 days postinfection with a control (CT) or non-GFP-expressing shP53 construct (shP53-427) were treated with NucBlue Live ReadyProbes Reagent (Life Technologies) and filmed by time-lapse imaging for 24 hr, photographed every 7 min. For Movie S7, keratinocytes 5 days postinfection with shP53-GFP construct were filmed by time-lapse imaging for 11 hr, photographed every 10 min. In all cases, phase-contrast and green- or blue-fluorescence images were obtained by an epifluorescence microscope (NIKON Ti; 10 \times NA 0.30) by an ORCA R2 camera.

Statistical Analyses

Data sets were compared using an unpaired Student's t test. A p value of less than 0.05 was considered statistically significant.

SUPPLEMENTAL INFORMATION

Supplemental Information includes Supplemental Experimental Procedures, seven figures, and seven movies and can be found with this article online at <http://dx.doi.org/10.1016/j.celrep.2014.10.012>.

AUTHOR CONTRIBUTIONS

A.G. conceived the project. A.G. and A.F. designed the study and wrote the paper. A.F., R.M., L.C., M.C., and P.A. performed assays. P.M., R.R., D.A., and E.D.D. provided materials and technical input and made critical suggestions to the paper.

ACKNOWLEDGMENTS

We thank Moshe Oren and Javier León for reagents, Alicia Noriega, Fidel Madrazo, and Elida del Cerro for technical assistance, Todd Waldman for providing DNA constructs, M. Oren for helpful comments, and Talveen Purba for English proofreading of the manuscript. This work was funded by Instituto de Salud Carlos III FIS/FEDER grants PI11/02070 (A.G.), PI12/033112 (P.M.), and FEDER-CP11/00024 (R.R.).

Received: May 6, 2014

Revised: August 14, 2014

Accepted: October 3, 2014

Published: November 6, 2014

REFERENCES

Andreassen, P.R., and Margolis, R.L. (1994). Microtubule dependency of p34cdc2 inactivation and mitotic exit in mammalian cells. *J. Cell Biol.* 127, 789–802.

Aylon, Y., and Oren, M. (2011). p53: guardian of ploidy. *Mol. Oncol.* 5, 315–323.

Bartkova, J., Rezaei, N., Liontos, M., Karakaidos, P., Klatsas, D., Issaeva, N., Vassiliou, L.V., Kolettas, E., Niforou, K., Zoumpourlis, V.C., et al. (2006). Oncogene-induced senescence is part of the tumorigenesis barrier imposed by DNA damage checkpoints. *Nature* 444, 633–637.

Blagosklonny, M.V. (2000). p53 from complexity to simplicity: mutant p53 stabilization, gain-of-function, and dominant-negative effect. *FASEB J.* 14, 1901–1907.

Blagosklonny, M.V. (2007). Mitotic arrest and cell fate: why and how mitotic inhibition of transcription drives mutually exclusive events. *Cell Cycle* 6, 70–74.

Bornachea, O., Santos, M., Martínez-Cruz, A.B., García-Escudero, R., Dueñas, M., Costa, C., Segrelles, C., Lorz, C., Buitrago, A., Saiz-Ladera, C., et al. (2012). EMT and induction of miR-21 mediate metastasis development in Trp53-deficient tumours. *Sci. Rep.* 2, 434.

Brash, D.E. (2006). Roles of the transcription factor p53 in keratinocyte carcinomas. *Br. J. Dermatol.* 154 (Suppl 1), 8–10.

Carvajal, L.A., and Manfredi, J.J. (2013). Another fork in the road—life or death decisions by the tumour suppressor p53. *EMBO Rep.* 14, 414–421.

Dazard, J.E., Piette, J., Basset-Seguín, N., Blanchard, J.M., and Gandarillas, A. (2000). Switch from p53 to MDM2 as differentiating human keratinocytes lose their proliferative potential and increase in cellular size. *Oncogene* 19, 3693–3705.

Demidenko, Z.N., Korotchkina, L.G., Gudkov, A.V., and Blagosklonny, M.V. (2010). Paradoxical suppression of cellular senescence by p53. *Proc. Natl. Acad. Sci. USA* 107, 9660–9664.

Di Leonardo, A., Khan, S.H., Linke, S.P., Greco, V., Seidita, G., and Wahl, G.M. (1997). DNA rereplication in the presence of mitotic spindle inhibitors in human and mouse fibroblasts lacking either p53 or pRb function. *Cancer Res.* 57, 1013–1019.

Donehower, L.A., Harvey, M., Slagle, B.L., McArthur, M.J., Montgomery, C.A., Jr., Butel, J.S., and Bradley, A. (1992). Mice deficient for p53 are developmentally normal but susceptible to spontaneous tumours. *Nature* 356, 215–221.

Freije, A., Ceballos, L., Coisy, M., Barnes, L., Rosa, M., De Diego, E., Blanchard, J.M., and Gandarillas, A. (2012). Cyclin E drives human keratinocyte growth into differentiation. *Oncogene* 31, 5180–5192.

Gandarillas, A. (2012). The mysterious human epidermal cell cycle, or an oncogene-induced differentiation checkpoint. *Cell Cycle* 11, 4507–4516.

Gandarillas, A., and Watt, F.M. (1997). c-Myc promotes differentiation of human epidermal stem cells. *Genes Dev.* 11, 2869–2882.

Gandarillas, A., Davies, D., and Blanchard, J.M. (2000). Normal and c-Myc-promoted human keratinocyte differentiation both occur via a novel cell cycle involving cellular growth and endoreplication. *Oncogene* 19, 3278–3289.

Gannon, J.V., Greaves, R., Iggo, R., and Lane, D.P. (1990). Activating mutations in p53 produce a common conformational effect. A monoclonal antibody specific for the mutant form. *EMBO J.* 9, 1595–1602.

Griffin, R.J., Pemberton, L.C., Rhodes, D., Bleasdale, C., Bowman, K., Calvert, A.H., Curtin, N.J., Durkacz, B.W., Newell, D.R., Porteous, J.K., et al. (1995). Novel potent inhibitors of the DNA repair enzyme poly(ADP-ribose)polymerase (PARP). *Anticancer Drug Des.* 10, 507–514.

Halazonetis, T.D., Gorgoulis, V.G., and Bartek, J. (2008). An oncogene-induced DNA damage model for cancer development. *Science* 319, 1352–1355.

Hall, P.A., McKee, P.H., Menage, H.D., Dover, R., and Lane, D.P. (1993). High levels of p53 protein in UV-irradiated normal human skin. *Oncogene* 8, 203–207.

Hann, B.C., and Lane, D.P. (1995). The dominating effect of mutant p53. *Nat. Genet.* 9, 221–222.

Harvey, M., Vogel, H., Morris, D., Bradley, A., Bernstein, A., and Donehower, L.A. (1995). A mutant p53 transgene accelerates tumour development in heterozygous but not nullizygous p53-deficient mice. *Nat. Genet.* 9, 305–311.

Haupt, Y., Maya, R., Kazaz, A., and Oren, M. (1997). Mdm2 promotes the rapid degradation of p53. *Nature* 387, 296–299.

- Hickson, I., Zhao, Y., Richardson, C.J., Green, S.J., Martin, N.M., Orr, A.I., Reaper, P.M., Jackson, S.P., Curtin, N.J., and Smith, G.C. (2004). Identification and characterization of a novel and specific inhibitor of the ataxia-telangiectasia mutated kinase ATM. *Cancer Res.* **64**, 9152–9159.
- Jiang, W., Ananthaswamy, H.N., Muller, H.K., and Kripke, M.L. (1999). p53 protects against skin cancer induction by UV-B radiation. *Oncogene* **18**, 4247–4253.
- Jonason, A.S., Kunala, S., Price, G.J., Restifo, R.J., Spinelli, H.M., Persing, J.A., Leffell, D.J., Tarone, R.E., and Brash, D.E. (1996). Frequent clones of p53-mutated keratinocytes in normal human skin. *Proc. Natl. Acad. Sci. USA* **93**, 14025–14029.
- Jones, P.H., and Watt, F.M. (1993). Separation of human epidermal stem cells from transit amplifying cells on the basis of differences in integrin function and expression. *Cell* **73**, 713–724.
- Kallassy, M., Martel, N., Damour, O., Yamasaki, H., and Nakazawa, H. (1998). Growth arrest of immortalized human keratinocytes and suppression of telomerase activity by p21WAF1 gene expression. *Mol. Carcinog.* **21**, 26–36.
- Karia, P.S., Han, J., and Schmults, C.D. (2013). Cutaneous squamous cell carcinoma: estimated incidence of disease, nodal metastasis, and deaths from disease in the United States, 2012. *J. Am. Acad. Dermatol.* **68**, 957–966.
- Kaufmann, H., Marone, R., Olajoye, M.A., Bailey, J.E., and Fussenegger, M. (2001). Characterization of an N-terminally truncated cyclin A isoform in mammalian cells. *J. Biol. Chem.* **276**, 29987–29993.
- Kemp, C.J., Donehower, L.A., Bradley, A., and Balmain, A. (1993). Reduction of p53 gene dosage does not increase initiation or promotion but enhances malignant progression of chemically induced skin tumors. *Cell* **74**, 813–822.
- Kim, J.S., Lee, C., Bonifant, C.L., Ransom, H., and Waldman, T. (2007). Activation of p53-dependent growth suppression in human cells by mutations in PTEN or PIK3CA. *Mol. Cell. Biol.* **27**, 662–677.
- Koster, M.I. (2010). p63 in skin development and ectodermal dysplasias. *J. Invest. Dermatol.* **130**, 2352–2358.
- Lane, D.P. (1992). Cancer. p53, guardian of the genome. *Nature* **358**, 15–16.
- Lavigueur, A., Maltby, V., Mock, D., Rossant, J., Pawson, T., and Bernstein, A. (1989). High incidence of lung, bone, and lymphoid tumors in transgenic mice overexpressing mutant alleles of the p53 oncogene. *Mol. Cell. Biol.* **9**, 3982–3991.
- le Pelletier, F., Soufir, N., de La Salmoniere, P., Janin, A., and Basset-Seguin, N. (2001). p53 Patches are not increased in patients with multiple nonmelanoma skin cancers. *J. Invest. Dermatol.* **117**, 1324–1325.
- Lee, M.K., Teoh, W.W., Phang, B.H., Tong, W.M., Wang, Z.Q., and Sabapathy, K. (2012). Cell-type, dose, and mutation-type specificity dictate mutant p53 functions in vivo. *Cancer Cell* **22**, 751–764.
- Li, G., Ho, V.C., Berean, K., and Tron, V.A. (1995). Ultraviolet radiation induction of squamous cell carcinomas in p53 transgenic mice. *Cancer Res.* **55**, 2070–2074.
- Littlewood, T.D., Hancock, D.C., Daniellian, P.S., Parker, M.G., and Evan, G.I. (1995). A modified oestrogen receptor ligand-binding domain as an improved switch for the regulation of heterologous proteins. *Nucleic Acids Res.* **23**, 1686–1690.
- Malkin, D., Li, F.P., Strong, L.C., Fraumeni, J.F., Jr., Nelson, C.E., Kim, D.H., Kassel, J., Gryka, M.A., Bischoff, F.Z., Tainsky, M.A., et al. (1990). Germ line p53 mutations in a familial syndrome of breast cancer, sarcomas, and other neoplasms. *Science* **250**, 1233–1238.
- Mantel, C., Guo, Y., Lee, M.R., Han, M.K., Rhorabough, S., Kim, K.S., and Broxmeyer, H.E. (2008). Cells enter a unique intermediate 4N stage, not 4N-G1, after aborted mitosis. *Cell Cycle* **7**, 484–492.
- Martínez-Cruz, A.B., Santos, M., Lara, M.F., Segrelles, C., Ruiz, S., Moral, M., Lorz, C., García-Escudero, R., and Paramio, J.M. (2008). Spontaneous squamous cell carcinoma induced by the somatic inactivation of retinoblastoma and Trp53 tumor suppressors. *Cancer Res.* **68**, 683–692.
- Martínez-Cruz, A.B., Santos, M., García-Escudero, R., Moral, M., Segrelles, C., Lorz, C., Saiz, C., Buitrago-Pérez, A., Costa, C., and Paramio, J.M. (2009). Spontaneous tumor formation in Trp53-deficient epidermis mediated by chromosomal instability and inflammation. *Anticancer Res.* **29**, 3035–3042.
- Michalovitz, D., Halevy, O., and Oren, M. (1990). Conditional inhibition of transformation and of cell proliferation by a temperature-sensitive mutant of p53. *Cell* **62**, 671–680.
- Minella, A.C., Swanger, J., Bryant, E., Welcker, M., Hwang, H., and Clurman, B.E. (2002). p53 and p21 form an inducible barrier that protects cells against cyclin E-cdk2 deregulation. *Curr. Biol.* **12**, 1817–1827.
- Muñoz-Alonso, M.J., Ceballos, L., Bretones, G., Frade, P., León, J., and Gandarillas, A. (2012). MYC accelerates p21CIP-induced megakaryocytic differentiation involving early mitosis arrest in leukemia cells. *J. Cell. Physiol.* **227**, 2069–2078.
- Murray, A.W. (2004). Recycling the cell cycle: cyclins revisited. *Cell* **116**, 221–234.
- Pavey, S., Russell, T., and Gabrielli, B. (2001). G2 phase cell cycle arrest in human skin following UV irradiation. *Oncogene* **20**, 6103–6110.
- Petitjean, A., Achatz, M.I., Borresen-Dale, A.L., Hainaut, P., and Olivier, M. (2007). TP53 mutations in human cancers: functional selection and impact on cancer prognosis and outcomes. *Oncogene* **26**, 2157–2165.
- Pusapati, R.V., Rounbehler, R.J., Hong, S., Powers, J.T., Yan, M., Kiguchi, K., McArthur, M.J., Wong, P.K., and Johnson, D.G. (2006). ATM promotes apoptosis and suppresses tumorigenesis in response to Myc. *Proc. Natl. Acad. Sci. USA* **103**, 1446–1451.
- Ren, Z.P., Ahmadian, A., Pontén, F., Nistér, M., Berg, C., Lundeberg, J., Uhlén, M., and Pontén, J. (1997). Benign clonal keratinocyte patches with p53 mutations show no genetic link to synchronous squamous cell precancer or cancer in human skin. *Am. J. Pathol.* **150**, 1791–1803.
- Rheinwald, J.G. (1989). Methods for clonal growth and serial cultivation of normal human epidermal keratinocytes and mesothelial cells. In *Cell Growth and Division*, R. Baserga, ed. (Oxford: IRL Press), pp. 81–94.
- Rodríguez, R., Rubio, R., Gutierrez-Aranda, I., Melen, G.J., Elosua, C., García-Castro, J., and Menendez, P. (2011). FUS-CHOP fusion protein expression coupled to p53 deficiency induces liposarcoma in mouse but not in human adipose-derived mesenchymal stem/stromal cells. *Stem Cells* **29**, 179–192.
- Rogakou, E.P., Pilch, D.R., Orr, A.H., Ivanova, V.S., and Bonner, W.M. (1998). DNA double-stranded breaks induce histone H2AX phosphorylation on serine 139. *J. Biol. Chem.* **273**, 5858–5868.
- Rogers, H.W., Weinstock, M.A., Harris, A.R., Hinckley, M.R., Feldman, S.R., Fleischer, A.B., and Coldiron, B.M. (2010). Incidence estimate of nonmelanoma skin cancer in the United States, 2006. *Arch. Dermatol.* **146**, 283–287.
- Roos, W.P., and Kaina, B. (2006). DNA damage-induced cell death by apoptosis. *Trends Mol. Med.* **12**, 440–450.
- Rosa-Garrido, M., Ceballos, L., Alonso-Lecue, P., Abaira, C., Delgado, M.D., and Gandarillas, A. (2012). A cell cycle role for the epigenetic factor CTCF-L/BORIS. *PLoS ONE* **7**, e39371.
- Sandler, V.M., Lailier, N., and Bouhassira, E.E. (2011). Reprogramming of embryonic human fibroblasts into fetal hematopoietic progenitors by fusion with human fetal liver CD34+ cells. *PLoS ONE* **6**, e18265.
- Shea, C.R., McNutt, N.S., Volkenandt, M., Lugo, J., Prioleau, P.G., and Albino, A.P. (1992). Overexpression of p53 protein in basal cell carcinomas of human skin. *Am. J. Pathol.* **141**, 25–29.
- Sigal, A., and Rotter, V. (2000). Oncogenic mutations of the p53 tumor suppressor: the demons of the guardian of the genome. *Cancer Res.* **60**, 6788–6793.
- Srivastava, S., Zou, Z.Q., Pirolo, K., Blattner, W., and Chang, E.H. (1990). Germ-line transmission of a mutated p53 gene in a cancer-prone family with Li-Fraumeni syndrome. *Nature* **348**, 747–749.
- Taylor, W.R., and Stark, G.R. (2001). Regulation of the G2/M transition by p53. *Oncogene* **20**, 1803–1815.

- Wang, L.H., Huang, W., Lai, M.D., and Su, I.J. (2012). Aberrant cyclin A expression and centrosome overduplication induced by hepatitis B virus pre-S2 mutants and its implication in hepatocarcinogenesis. *Carcinogenesis* 33, 466–472.
- Woodworth, C.D., Wang, H., Simpson, S., Alvarez-Salas, L.M., and Notario, V. (1993). Overexpression of wild-type p53 alters growth and differentiation of normal human keratinocytes but not human papillomavirus-expressing cell lines. *Cell Growth Differ.* 4, 367–376.
- Yonish-Rouach, E., Resnitzky, D., Lotem, J., Sachs, L., Kimchi, A., and Oren, M. (1991). Wild-type p53 induces apoptosis of myeloid leukaemic cells that is inhibited by interleukin-6. *Nature* 352, 345–347.
- Zanet, J., Fíbre, S., Jacquet, C., Ramírez, A., de Alborán, I.M., and Gandarillas, A. (2005). Endogenous Myc controls mammalian epidermal cell size, hyperproliferation, endoreplication and stem cell amplification. *J. Cell Sci.* 118, 1693–1704.
- Zanet, J., Freije, A., Ruiz, M., Coulon, V., Sanz, J.R., Chiesa, J., and Gandarillas, A. (2010). A mitosis block links active cell cycle with human epidermal differentiation and results in endoreplication. *PLoS ONE* 5, e15701.
- Zhang, W., Remenyik, E., Zelterman, D., Brash, D.E., and Wikonkal, N.M. (2001). Escaping the stem cell compartment: sustained UVB exposure allows p53-mutant keratinocytes to colonize adjacent epidermal proliferating units without incurring additional mutations. *Proc. Natl. Acad. Sci. USA* 98, 13948–13953.
- Ziegler, A., Jonason, A.S., Leffell, D.J., Simon, J.A., Sharma, H.W., Kimmelman, J., Remington, L., Jacks, T., and Brash, D.E. (1994). Sunburn and p53 in the onset of skin cancer. *Nature* 372, 773–776.

ORIGINAL ARTICLE

FOXM1 allows human keratinocytes to bypass the oncogene-induced differentiation checkpoint in response to gain of MYC or loss of p53

R Molinuevo¹, A Freije¹, I de Pedro¹, SW Stoll², JT Elder^{2,3} and A Gandarillas^{1,4}

Tumour suppressor p53 or proto-oncogene MYC is frequently altered in squamous carcinomas, but this is insufficient to drive carcinogenesis. We have shown that overactivation of MYC or loss of p53 via DNA damage triggers an anti-oncogenic differentiation-mitosis checkpoint in human epidermal keratinocytes, resulting in impaired cell division and squamous differentiation. Forkhead box M1 (FOXM1) is a transcription factor recently proposed to govern the expression of a set of mitotic genes. Deregulation of FOXM1 occurs in a wide variety of epithelial malignancies. We have ectopically expressed FOXM1 in keratinocytes of the skin after overexpression of MYC or inactivation of endogenous p53. Ectopic FOXM1 rescues the proliferative capacity of MYC- or p53-mutant cells in spite of higher genetic damage and a larger cell size typical of differentiation. As a consequence, differentiation induced by loss of p53 or MYC is converted into increased proliferation and keratinocytes displaying genomic instability are maintained within the proliferative compartment. The results demonstrate that keratinocyte oncogene-induced differentiation is caused by mitosis control and provide new insight into the mechanisms driving malignant progression in squamous cancer.

Oncogene (2017) 36, 956–965; doi:10.1038/onc.2016.262; published online 25 July 2016

INTRODUCTION

Although squamous cell carcinomas (SCCs) in different locations such as skin, head and neck or oesophagus are heterogeneous in clinic and prognosis, they share a similar histology with cell morphology reminiscent of the differentiated layers of the epidermis. For this reason they are also referred to as epidermoid carcinomas. In addition, they share similar risk factors that cause genetic damage, including ultraviolet light, human papillomavirus, tobacco and alcohol. Therefore, they might share common or overlapping molecular mechanisms. SCCs are often aggressive and have poor prognosis. Finding common pathways to SCCs would provide a new basis for their diagnosis and treatment.

Human epidermis is a paradigm of self-renewal stratified squamous epithelium highly exposed to mutagenic hazard and frequently affected by cancer. The tumour suppressor protein p53, also known as the guardian of the genome, is mutated in most human skin SCCs (80%),^{1,2} although its alteration is not sufficient for the development of epithelial skin cancer.^{3,4} Within the same lines, it is well established that proto-oncogene MYC in keratinocytes promotes differentiation instead of proliferation.^{5–8} Similarly, overactivation of a variety of cell growth promoters including the DNA replication protein Cyclin E is not tumourigenic when overexpressed in epidermal cells^{9–12} (reviewed in Gandarillas¹³). The cell cycle regulation explaining this resistance of keratinocytes to transformation upon cell cycle deregulation remains intriguing but is critical to understand squamous carcinogenesis. Recently, we have reported that loss of p53 causes squamous differentiation in epidermal human keratinocytes.¹⁴ This might explain why inactivation of p53 does not drive skin carcinogenesis by itself and, notably, why sun-

exposed healthy skin often contains patches of cells with the mutated protein that cause no clinical impact.^{15–17} This finding points at a self-protective response of the epidermis against oncogenic transformation. We have shown that epidermal keratinocytes respond to a differentiation-mitosis checkpoint (DMC) that triggers squamous differentiation in the event of cell cycle deregulation.^{13,18} The DMC functions as an oncogene-induced differentiation response (OID).¹³ Upon hyperactivation of the cell cycle, keratinocytes block cell division and trigger terminal differentiation, although they fail to maintain G2/M arrest (mitotic slippage) and continue DNA replication (endoreplication), become polyploid and significantly increase their size. Differentiating keratinocytes migrate towards the surface of the epidermis and are finally eliminated from the skin by shedding. We have proposed that because of the DMC, precancerous alterations need additional modifications in the mitosis control for epidermal carcinogenesis to occur.¹⁴ We now have challenged this model by overexpressing forkhead box M1 (FOXM1) in human keratinocytes after overactivation of conditional MYC or inactivation of endogenous p53.

The FOXM1 transcription factor is a mammalian regulator of cell cycle progression and frequently upregulated in human cancer.¹⁹ Although FOXM1 can induce cell cycle progression into the DNA replication S phase (G1/S), it plays a major role in the G2/M transition by the transactivation of regulators of mitosis and cytokinesis such as Cyclin B, Aurora B, Polo-like kinase and CENP.²⁰ FOXM1 is frequently deregulated in SCCs of head and neck and the skin.^{21,22}

The results herein show that FOXM1, in combination with precancerous cell growth deregulation, allows human keratinocytes to proliferate in spite of accumulating DNA damage and therefore

¹Cell Cycle, Stem Cell Fate and Cancer Laboratory, Institute of Research Marqués de Valdecilla (IDIVAL), Santander, Spain; ²Department of Dermatology, University of Michigan, Ann Arbor, MI, USA; ³Department of Ann Arbor Veterans Affairs Health System, Ann Arbor, MI, USA and ⁴INSERM, Languedoc-Roussillon, Montpellier, France. Correspondence: Dr A Gandarillas, Cell Cycle, Stem Cell Fate and Cancer Laboratory, Institute of Research Marqués de Valdecilla (IDIVAL), Cardenal Herrera Oria s/n, Santander, Cantabria 39011, Spain. E-mail: agandarillas@idival.org

Received 28 October 2015; revised 2 June 2016; accepted 16 June 2016; published online 25 July 2016

promoting genomic instability. This may explain why mutated p53 and deregulated FOXM1 are both frequently selected in cancer.

RESULTS

FOXM1 rescues the proliferative block caused by inactivation of p53. We aimed to investigate whether FOXM1 affects the loss of proliferation potential observed in primary human keratinocytes when the expression of p53 is inhibited. To this end, we silenced p53 by means of a specific lentiviral construct carrying a short

hairpin RNA (shRNA; shp53)^{14,23} in human keratinocytes (Kshp53) and then overexpressed FOXM1 (Kshp53/FOXM1) by a lentiviral vector. Figures 1a–c and Supplementary Figure 1a show the downregulation of p53 or the overexpression of FOXM1 as determined by immunofluorescence, western blot or real-time PCR. shp53 was delivered into 90–95% of cells (Supplementary Figure 1a).¹⁴ Downregulation of p53 not only reduced the amount of protein but also its ability to induce its target gene p21Cip (Figure 1b). As described previously,¹⁴ although cell number did not decrease, by 5 days Kshp53 cells halted proliferation as

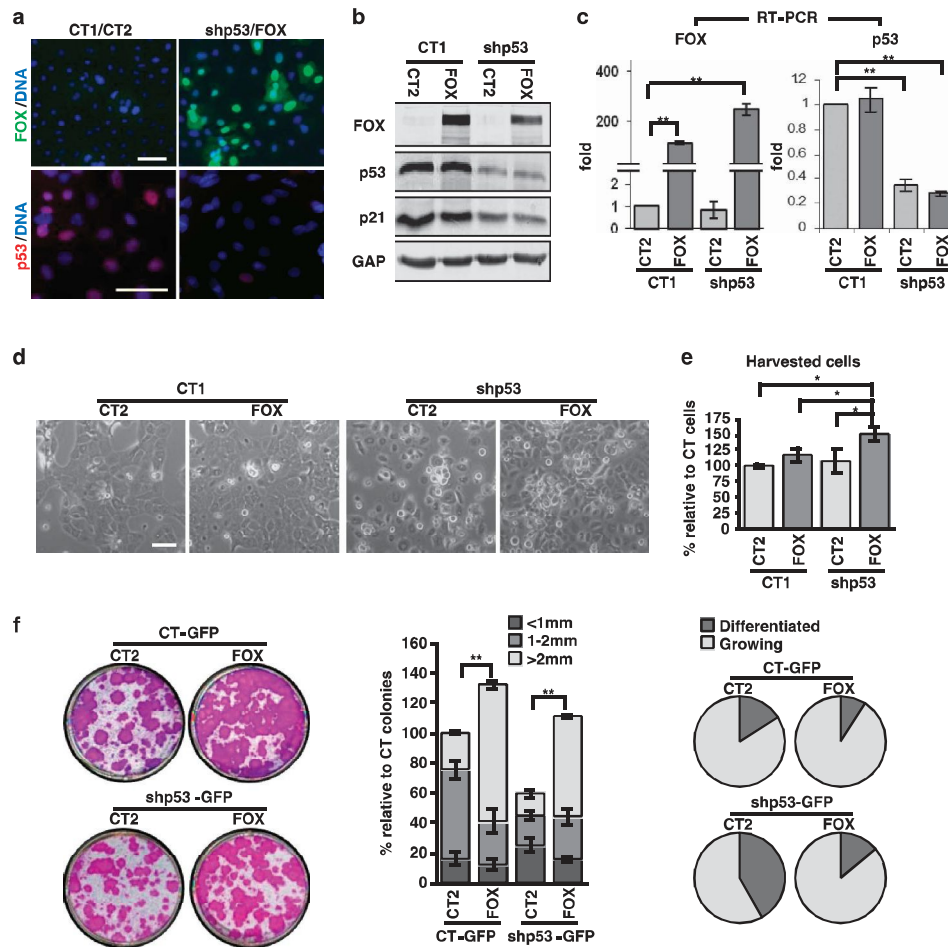


Figure 1. Ectopic expression of FOXM1 rescues the proliferative capacity of human epidermal keratinocytes lacking p53. (a–c) Detection of FOXM1 and p53 in primary keratinocytes infected with shRNA for p53 (shp53-1) or the corresponding empty control vector (pIK01, CT1) and FOXM1 (FOX) or the corresponding empty control vector (pIVX, CT2) by (a) immunofluorescence (also in Supplementary Figure 1a, DAPI for DNA in blue), (b) western blot and (c) real-time (RT)–PCR (fold differences with respect to control CT1/CT2). Detection of the p53 target p21Cip (p21) is also shown by western blot (b). GAPDH (GAP) was used as loading control. (d) Phase contrast images of keratinocytes 5 days after construct delivery, as indicated. (e) Bar histogram represents the differences in the number of cells collected relative to control (CT1/CT2 = 100%) 5 days after infections with the indicated constructs. Similar results were obtained when a different shRNA for p53 (shp53-2) was used. (f) Clonogenic capacity of cells plated 5 days after infections with CT-GFP or shp53-GFP and CT2 or FOX (2500 cells per well). Representative wells of triplicate samples are shown (left). Bar histogram represents the differences in large colonies (> 2 mm, light grey), medium size colonies (1–2 mm, intermediate grey) or small and differentiated colonies (< 1 mm, dark grey) relative to control cells (CT-GFP/CT2 = 100%). Circle histograms show the proportion of actively growing (light grey) or differentiated (dark grey) colonies. Scale bars: 50 μm; **P* < 0.05 and ***P* < 0.01. Data are mean ± s.e.m. of triplicate samples of representative experiments (*n* = 3). Results are representative of two different strains of keratinocytes from different individuals (*N* = 2).

compared with control cells carrying the empty vector (Figure 1d). However, Kshp53/FOXM1 cells continued to proliferate even further than control cells or cells overexpressing FOXM1 only. This observation was confirmed by the striking increase in the cell count of the Kshp53/FOXM1 cultures (Figure 1e). The effect on cell proliferation was confirmed by the inhibition of p53 with a second shRNA (shp53-2, data not shown).

To investigate whether FOXM1 affected the clonogenic capacity of Kshp53, we performed clonogenicity assays 5 days after introducing shp53-GFP and/or FOXM1 (Figure 1f). These assays allow to detect the effect on cell fate by estimating both the capacity to form colonies and the degree of cell expansion of the stem (large colonies, >2 mm) or the committed progenitor amplifying cells (small colonies, <1 mm).²⁴ Overexpression of FOXM1 in normal keratinocytes increased their clonogenic potential (Figure 1f), consistently with previous observations in cells from oral epithelium.²⁵ However, in the Kshp53 cultures the number of total and proliferative colonies was reduced compared with controls, whereas the number of abortive differentiated colonies was increased. In contrast, Kshp53/FOXM1 cells recovered and improved the potential of control cells. The size and the number of large colonies generated by putative stem cells were greatly increased in the Kshp53/FOXM1 cultures. Interestingly, the size of small colonies, formed by transit amplifying progenitors, was also increased. Thus, ectopic FOXM1 rescues the proliferative and clonogenic capacity of human epidermal keratinocytes that is lost by inactivation of p53. Although Kshp53/FOXM1 cells

proliferated more than FOXM1 cells 5 days after infection (Figure 1e), their clonogenicity potential was weaker as the loss of p53 had already driven cell differentiation (Figure 1f).

FOXM1 attenuates the squamous differentiation response caused by loss of p53

As the ectopic expression of FOXM1 improves the proliferative capacity of Kshp53, we aimed to investigate whether FOXM1 affects their differentiation response. At 3 days after gene delivery the proportion of Kshp53/FOXM1 cells expressing the epidermal differentiation markers involucrin, keratin K1 and filaggrin significantly decreased (Figures 2a–c and Supplementary Figures 1b and c). The inhibition of differentiation by FOXM1 was also observed when the shp53-2 was used (data not shown). Keratinocytes enlarge and become more complex as they differentiate and this can be monitored by flow cytometry by means of increased light scattering.^{24,26} Accordingly with the decrease in the expression of differentiation markers, we found that the percent of cells with high scatter parameters typical of differentiation was also decreased in Kshp53/FOXM1 with respect to Kshp53 (Figure 2b). It is important to mention that differentiation of human epidermal keratinocytes increases at cell confluence,²⁷ when keratinocytes are pushed to stratify and detach. Kshp53/FOXM1 cells reached confluence faster and stratified more than controls and certainly than Kshp53 cells (Figure 1d and Supplementary Videos 1 and 2). In addition, at

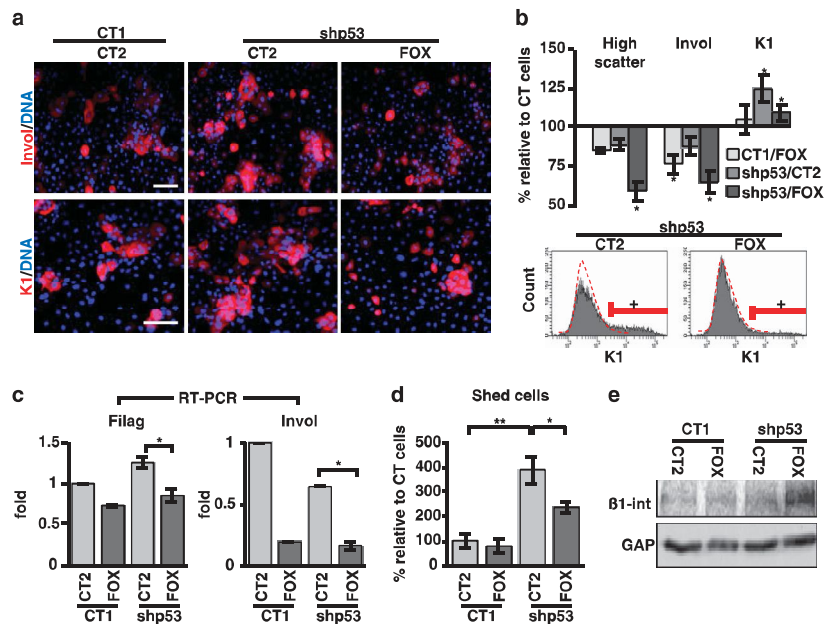


Figure 2. Ectopic expression of FOXM1 inhibits the differentiation response to loss of p53. **(a)** Immunodetection of the epidermal differentiation markers in red, involucrin (Invol) or keratin K1 (K1) in keratinocytes 3 days after infection with CT1 or shp53-1 and CT2 or FOX (as in Figure 1). DAPI for DNA in blue. **(b)** Bar histogram shows cells with high size and complexity (light scatter; differentiation), or positive for Invol or K1 relative to control cells (CT1/CT2 = 100%) as measured by flow cytometry. Bottom histograms show representative plots for the expression of K1 (+, positive cells according to negative isotype antibody control, red broken line). More details in Supplementary Figures 1b and c. **(c)** Real-time (RT)–PCR for expression of the differentiating markers Filaggrin (Filag) and Invol 2 days after infections as indicated (fold differences relative to control CT1/CT2). **(d)** Shedding cells collected from the culture supernatant due to differentiation 5 days after infections relative to control (CT1/CT2 = 100%). **(e)** Detection by western blot of $\beta 1$ integrin 5 days after infections as indicated. GAPDH (GAP) was used as loading control. Scale bar: 50 μ m; * $P < 0.05$ and ** $P < 0.01$. Data are mean \pm s.e.m. of triplicate samples of representative experiments ($n = 3$). Results are representative of two different strains from different individuals ($N = 2$).

confluence and in spite of a higher cell density, FOXM1 inhibited the initiation of differentiation as the proportion of cell shedding into the medium was attenuated (Figure 2d). Increased stratification and decreased shedding in Kshp53/FOXM1 populations might be related to increased expression of $\beta 1$ integrin (Figure 2e). The $\beta 1$ integrins are adhesion molecules that maintain keratinocytes attached to the basement membrane and thus their proliferative potential.²⁸ They are lost at differentiation. Therefore, although FOXM1 did not abolish stratification and differentiation of Kshp53 cells, it significantly rescued the proliferative potential lost by the absence of p53.

FOXM1 allows Kshp53 to proliferate in spite of genome instability. Loss of p53 induces early hyperactivation of the cell cycle that results in a G2/M block and endoreplication in human epidermal keratinocytes, subsequently increasing the population of differentiated polyploid cells.¹⁴ The analysis of cell cycle regulators suggested that Kshp53/FOXM1 cells did not accumulate as much in G2/M. Although the expression of the S/G2/M marker phospho-retinoblastoma (p-Rb) was increased in Kshp53 cells compared with controls, it was decreased upon FOXM1 overexpression (Figure 3a). Rb is hyperphosphorylated at entry in S phase and hypophosphorylated after cell division.²⁹ FOXM1 induces Cyclin B among other mitosis/cytokinesis regulators²⁰ to drive cell division. The expression of Cyclin B was reduced in Kshp53 cells and increased in Kshp53/FOXM1 (Figure 3a).¹⁴ However, the expression of Cyclin E and Cyclin A remained unchanged, suggesting that the main action of FOXM1 in keratinocytes takes place in mitosis. We also observed changes in the cell cycle 3 days after infection. Kshp53/FOXM1 cells showed a decrease in the percent of cells accumulated in G2/M and in the polyploid region (Figure 3b and Supplementary Figures 2a and b). Accordingly, the proportion of cells returning to G1 increased. DNA synthesis was also measured in these cells by 5-bromodeoxyuridine (BrdU) incorporation (Figure 3c and Supplementary Figure 2c). Similar to the changes observed in the cell cycle, the percent of Kshp53/FOXM1 cells bypassing mitosis into polyploidy was decreased and the percent of BrdU cells in G1/S phase increased as compared with Kshp53 cells. However, cultures carrying only the FOXM1 plasmid displayed an increase in the percent of BrdU-positive cells in G2/M (Supplementary Figure 2c). This suggests that FOXM1 and loss of p53 together accelerated the transition from G2/M to G1. Altogether, the results are consistent with a role of FOXM1 in potentiating keratinocyte cell division downstream of p53. Interestingly, although FOXM1 caused a decrease of polyploidy in Kshp53, yet the number of binucleated cells within the reduced polyploid population was increased (Figure 3d). This suggests that FOXM1 pushes nuclei to divide even when the cell cannot divide anymore, consistent with the role of FOXM1 in mitotic spindle assembly, chromosome alignment and nuclear division.^{20,30} The expression of FOXM1 in normal human skin is unknown and we aimed to identify it. As shown in Figure 3e, FOXM1 strikingly accumulated in cells expressing mitotic Cyclins A and B, suggesting that the main function of FOXM1 in keratinocytes in the epidermis is related to mitosis.

It is worth noting that ectopic expression of FOXM1 reduced the intensity of nascent RNA foci as measured by incorporation of 5'-fluorouridine (Figure 3f). This suggests that FOXM1 function may have a relationship with the inhibition of transcription required for the initiation of mitosis. Therefore, we performed double labelling for Cyclin A, which accumulates mainly in G2/M, and transcription in these cells. The analyses showed that, as expected, in controls transcription was strong in Cyclin A-negative cells and weak in mitotic cells. However, transcription was as weak in interphasic, nonmitotic FOXM1-overexpressing cells (Supplementary Figure 3a). The role of FOXM1 in the inhibition of transcription has not been studied. FOXM1 gene encodes three

different protein isoforms obtained by alternative splicing: FOXM1a, FOXM1b and FOXM1c.³¹ Although we have made use of a DNA construct bearing the FOXM1b isoform, involved in oncogenesis,^{32,33} it has been shown that this protein can induce the expression of the other two variants³⁴ (Supplementary Figure 3b). Whereas FOXM1b and FOXM1c are considered transcriptionally active, FOXM1a lacks the transactivation domain and has a negative regulatory function on transcription.³¹ The expression of the three isoforms might be important for the correct regulation of mitosis. Consistent with a global transcription decrease, we found that keratinocytes overexpressing FOXM1 displayed a lighter optical density (Supplementary Figure 3c). In addition, we observed FOXM1 in the nucleolus, centre of ribosomal RNA transcription (Supplementary Figure 3d). Nucleolar localisation has been previously proposed to have a FOXM1 inhibitory role.³⁵

Kshp53/FOXM1 proliferative keratinocytes increased in size (measured by their forward scatter parameter), in spite of reduced cellular complexity (side scatter parameter; Figure 4a and Supplementary Figure 3e). Cells enlarge in G2 in order to produce two daughters of the same size before cell division, and therefore the mitosis block provokes differentiating keratinocytes to increase in size and this process is stimulated by shp53.¹⁴ The higher size of proliferative Kshp53/FOXM1 cells suggests that this protein pushes cell division even though the mitosis block has initiated.

The deregulation of the cell cycle in Kshp53 leads to the accumulation of DNA damage because of replication stress. We studied whether FOXM1, by alleviating the mitosis block, allowed keratinocytes to divide in spite of irreparable damage. Expression of the canonical DNA damage marker γ H2AX^{36,37} was evaluated in Kshp53/FOXM1 cells 5 days after gene delivery and we found a significant increase with respect to control cells (Figure 4b). In Kshp53 cells the increase in γ H2AX was detected both in basal and differentiating keratinocytes according to light scatter parameters (Figure 4c and Supplementary Figure 4). However, in Kshp53/FOXM1 cells the accumulation of the γ H2AX signal was detected mainly in the basal low scatter population (Figure 4c and Supplementary Figure 4). This result was confirmed by using shp53-2 (data not shown). To assess for actual DNA breaks typical of replication stress³⁷ we performed comet assays. As shown in Figure 4d, inactivation of p53 caused a striking increase of DNA breaks that augmented even further in combination with FOXM1. Interestingly, Kshp53/FOXM1 cells augmented significantly the DNA breaks in smaller nuclei (< 15 μ m), typical of proliferative cells. These results suggest that ectopic expression of FOXM1 allowed damaged Kshp53 cells to keep dividing and amplifying.

Overexpression of FOXM1 drives MYC-induced differentiation into proliferation

In primary keratinocytes, the activation of MYC drives the cell cycle in 1–2 days and epidermal differentiation in 5–6 days.^{5,12,38} We infected human epidermal keratinocytes with a retroviral construct carrying a conditional form of human MYC (MYCER) whose protein product is regulated by 4-hydroxytamoxifen (OHT),³⁹ and then infected them with the lentiviral construct bearing FOXM1. Cells expressing MYCER (KMYCER) differentiated when treated with OHT for 5 days (Figure 5a). The number of KMYCER cells collected after 5 days of OHT treatment was doubled when FOXM1 was ectopically expressed (Figure 5a and Supplementary Figure 5a). FOXM1 also significantly suppressed MYC-induced differentiation as monitored by the reduced expression of the squamous terminal marker keratin K1 (Figure 5a) and the decrease in light scattering (Figure 5a and Supplementary Figure 5b). We also observed that FOXM1 influenced the cell cycle parameters of KMYCER cells. Induction of MYCER with OHT drove keratinocytes into the polyploid

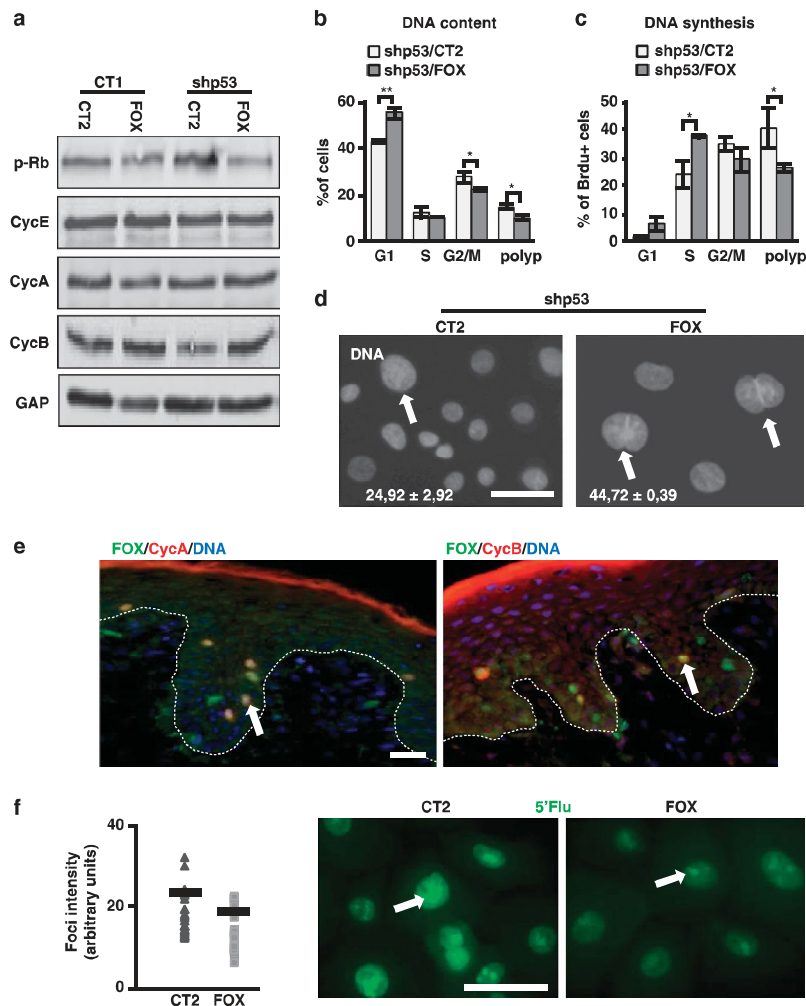


Figure 3. Ectopic expression of FOXM1 suppresses the mitotic block caused by loss of p53 in human epidermal keratinocytes. (a–d) Analyses 3 days after infections with CT1 or shp53-1 and CT2 or FOX (as in Figure 1). (a) Expression of cell cycle regulators p-Rb, Cyclin E (CycE), Cyclin A (CycA) and Cyclin B (CycB) by western blotting. GAPDH (GAP) was used as loading control. (b) Percent of cells in the G1 (2N), S, G2/M (4N) or polyploid (>4N) phases of the cell cycle as determined by flow cytometry. More details in Supplementary Figures 2a and b. (c) Percent of BrdU-positive cells in the G1, S (2N), G2/M (4N) and polyploid (>4N) phases as in (b). More details in Supplementary Figure 2c. (d) Binucleated keratinocytes (white arrows) bearing shp53 and CT2 or FOX as indicated, stained with DAPI for DNA. White numbers are the percent of polyploid cells (nuclei > 15 μm) that were binucleated. (e) Immunodetection of endogenous FOX (green), CycA (red, left panel) and CycB (red, right panel) in normal human epidermis by immunofluorescence. DAPI for DNA in blue. Red line is nonspecific staining of the superficial cornified layer. Arrows for cells coexpressing FOX and CycA or CycB. Broken line for the basement membrane. (f) Detection of nascent transcription by 5'-fluorouridine 5'-Flu; green incorporation 2 days after infections as indicated (nucleolar foci are indicated on representative photographs by white arrows). Dot plot on the left side represents quantitation of the fluorescence intensity of 5'-Flu incorporating single foci. Black bars represent the mean. Scale bars: 50 μm; *P < 0.05 and **P < 0.01. Data are mean ± s.e.m. of triplicate samples of representative experiment (n = 3).

compartment, whereas ectopic expression of FOXM1 significantly decreased the polyploid population (Figure 5a and Supplementary Figure 5c). The expression of cell cycle regulators Cyclin E, Cyclin A and Cyclin B was reduced in KMYCER treated with OHT 3 days, whereas phospho-Rb was inactivated (Figure 5b), consistent with mitotic block slippage.¹² However, ectopic expression of FOXM1 in KMYCER cells recovered the expression of Cyclin E and the mitotic Cyclins A and B (Figure 5b). In addition, MYC deregulation causes replication stress and DNA damage¹⁴ and we observed a stronger

accumulation of the DNA damage marker γH2AX when FOXM1 was overexpressed (Figure 5b and Supplementary Figure 5d). Consistently and as observed for shp53, in KMYCER small nuclei typical of proliferative cells contained strikingly more damage in comet assays when FOXM1 was overexpressed (Figure 5c and Supplementary Figure 5e).

FOXM1 also recovered the colony-forming potential of keratinocytes that is lost by MYC activation (Figure 5d).⁵ Overexpression of FOXM1 in KMYCER cells treated with OHT not

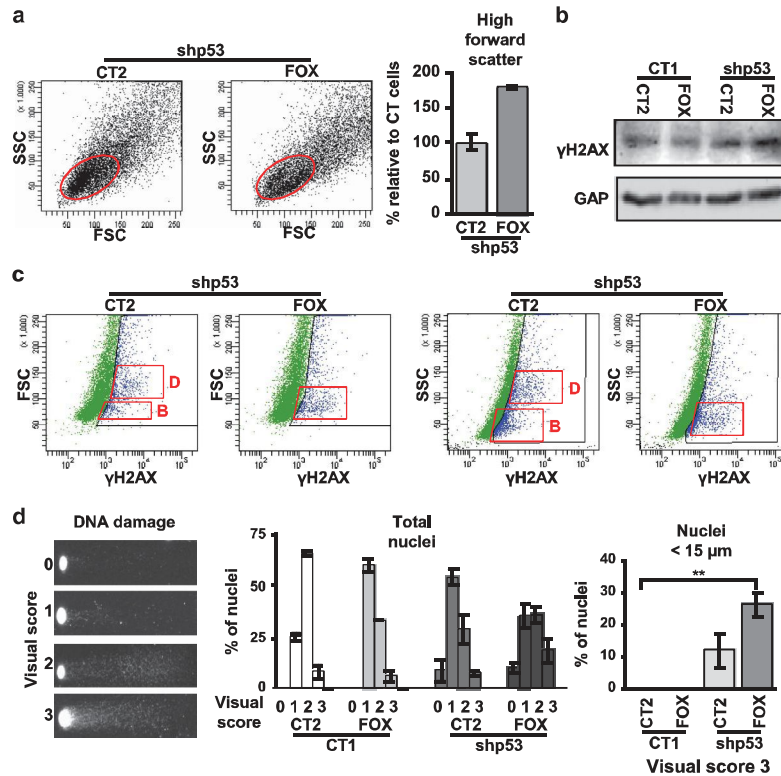


Figure 4. FOXM1 allows accumulation of DNA damage in proliferative keratinocytes upon p53 inactivation. (a) Dot plots show side and forward scatter parameters for cell complexity and size (side scatter parameter (SSC) and forward scatter parameter (FSC)) by flow cytometry of keratinocytes infected with shp53-1 and CT2 or FOX. Red oval represents the basal proliferative population. Histograms showing the SSC and FSC of proliferative cells (red oval) are shown in Supplementary Figure 3e. Bar histogram indicates basal cells (red oval) with high FSC (according to gate in Supplementary Figure 3e) relative to cells infected with shp53 and CT2 (shp53/CT2 = 100%) for γ H2AX in keratinocytes 5 days after infections as indicated. GAPDH (GAP) was used as loading control. (b) Western blot for γ H2AX. (c) Dot plots for FSC or SSC (y axis) and γ H2AX (x axis) 3 days after infections as indicated. Red squares represent the main γ H2AX-positive populations (blue) of differentiating (D) or basal (B) cells. Similar results were obtained when shp53-2 was used. More details in Supplementary Figure 4. (d) DNA damage monitored by comet assays (see Materials and methods). (d, left) Scoring assigned for damage according to the size and intensity of the nuclear tails of keratinocytes (0–3) 5 days after infections. (d, centre) Bar histogram showing the quantitation of DNA damage according to the 4 levels of intensity. (d, right) Bar histogram represents only the percent of small nuclei (< 15 μ m) with maximum DNA damage intensity level 3. Constructs as indicated. ** $P < 0.01$. Data are mean \pm s.e.m. of triplicate samples of representative experiment ($n = 3$).

only rescued the deleterious effect of MYC on colony growth, but also boosted this capacity beyond controls (Figure 5d and Supplementary Figure 5f).

Altogether, the results strongly indicate that FOXM1 switches the activation of the cell cycle by MYC from differentiation to proliferation in spite of increased replication stress and DNA damage.

DISCUSSION

Induction of squamous differentiation in the epidermis by proto-oncogene MYC and other oncogenic molecules is a long standing paradox^{5–8,13} in spite of the important implications to squamous cancer. Clearly, MYC does not promote sustained cell division in keratinocytes. The finding that replication stress in keratinocytes triggers the mitosis checkpoints and in turn squamous differentiation (DMC) suggests that mitosis control might be the limiting factor in epidermal carcinogenesis.¹⁴ Our hypothesis was therefore that reinforcement of the mitosis machinery might inhibit

differentiation and imbalance the keratinocyte decision making towards proliferation. Our present results upon ectopic expression of FOXM1 in keratinocytes strongly support this model.

FOXM1 controls a set of mitotic genes and has been proposed to be a mitosis master gene.³⁰ FOXM1 promotes the transcription of genes linked to execution of mitosis and proper chromosome segregation.^{20,30} Here we have shown that FOXM1 drives proliferation of keratinocytes, although cell cycle entry was barely affected. In contrast, the cell cycle shortened because of a shorter G2/M phase. In addition, we found FOXM1 to accumulate in mitotic keratinocytes in human epidermis.

Overexpression of FOXM1 in freshly isolated keratinocytes rescued the proliferative loss caused by inactivation of p53 or by hyperactivation of MYC. Keratinocytes overcame the DMC and continued to proliferate. Concomitantly, FOXM1 provoked a decrease in general transcription. Transcription is inactive during mitosis but very active during keratinocyte differentiation involving massive protein production. The lower level of nascent RNAs upon ectopic FOXM1 might be because of a transcription

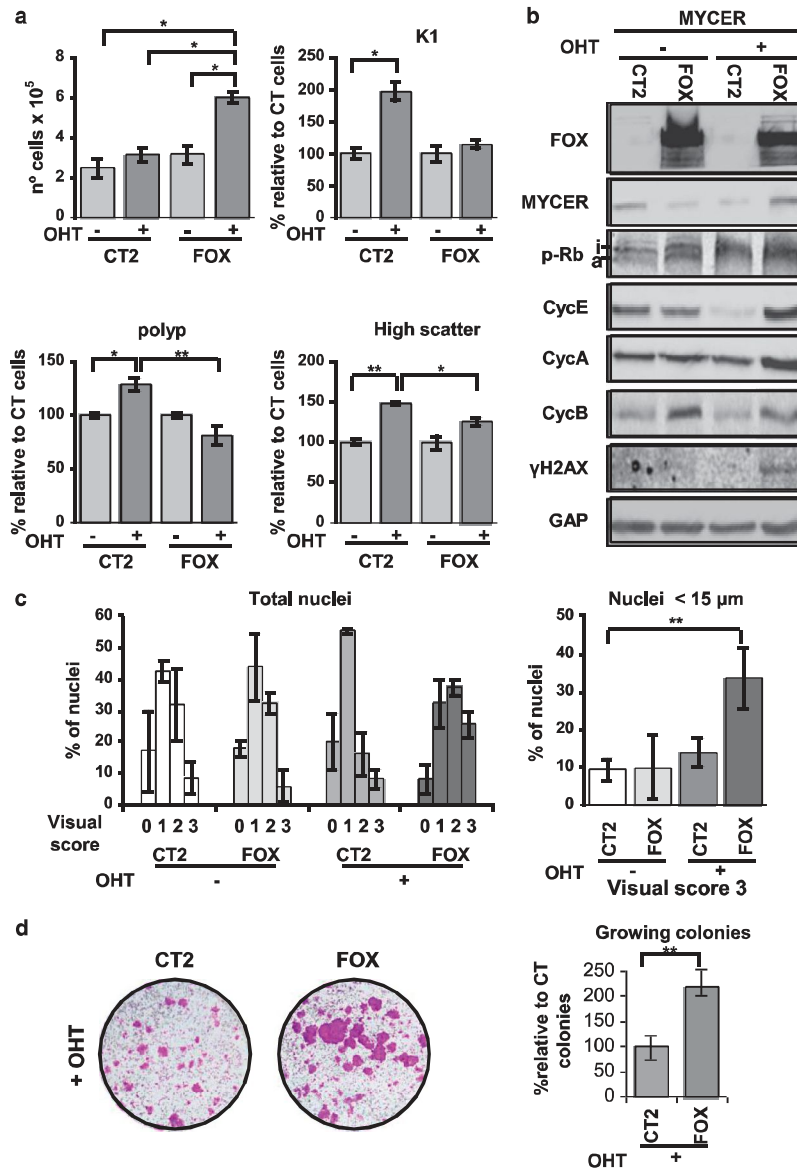


Figure 5. FOXM1 drives MYC-induced differentiation into increased proliferation. (a) MYCER keratinocyte cultures plated at high density (see Supplementary Materials and methods) and infected with CT2 or FOX for 5 days in the presence (+) or absence (-) of 4-hydroxytamoxifen (OHT) as indicated. Bar histograms represent: number of cells harvested (top left), percent of cells expressing keratin K1 (K1; top right), differences in the proportion of polyploid cells relative to control (bottom left; histograms in Supplementary Figure 5c) and differences in the proportion of cells with high scatter parameters relative to control (bottom right; dot plots in Supplementary Figure 5b). Controls are cells infected with CT2, nontreated with OHT; CT2/OHT = 100%. (b) Western blotting for FOX, MYCER, p-Rb (a, activated; i, inactivated), Cyclin E (CycE), Cyclin A (CycA), Cyclin B (CycB) and γH2AX in MYCER keratinocytes in the presence or absence of exogenous FOX and in the presence or absence of OHT as indicated. GAPDH (GAP) was used as loading control. (c) DNA damage monitored by comet assays after 5 days in the presence or absence of OHT as indicated. Left bar histogram shows the quantitation of DNA damage according to the 4 levels of DNA damage intensity described in Figure 4d. Right bar histogram shows the percent of small nuclei (< 15 μm) with maximum DNA damage intensity level 3. Representative pictures are shown in Supplementary Figure 5e. (d) Clonogenicity assays of keratinocytes plated at low density (see Supplementary Materials and methods), sequentially infected with MYCER and CT2 or FOX and cultured in the presence of OHT for 10 days. Bar histograms represent large growing colonies when FOX is ectopically expressed relative to MYCER+OHT cells infected with control vector (CT2/+OHT = 100%). Clonogenicity in the absence of OHT is shown in Supplementary Figure 5f. **P* < 0.05 and ***P* < 0.01. Data are mean ± s.e.m. of triplicate (*n* = 3) or duplicate (*n* = 2) samples of representative experiments. Results are representative of two different strains from different individuals (*N* = 2).

inhibitory function of a FOXM1 isoform³¹ contributing to coordinate the end of the S phase with mitosis. Possibly as a consequence of decreased global transcription, keratinocytes overexpressing FOXM1 displayed a clearer, less granulated and complex cytoplasm, reminiscent of 'clear cell carcinomas' of poor prognosis, some of which have been associated with FOXM1 overexpression.⁴⁰

Our results altogether support a key role of FOXM1 in driving epidermal cell division, consistent with observations in keratinocytes of oral epithelium.²⁵ To note, we have recently shown that FOXM1 mediates the function of the epidermal growth factor receptor in keratinocyte proliferation.⁴¹ In our present study, although FOXM1 did not abolish differentiation, it did increase the proportion of binucleated cells within the remaining polyploid population, indicating that it pushed nuclear division even when cytokinesis was irreversibly blocked by terminal differentiation.

The results have implications in cancer beyond the role of FOXM1 in keratinocytes. The inhibition of squamous differentiation by this key mitotic regulator and the resulting imbalance in cell decision making supports a model where mitosis control (DMC) is critical in squamous homeostasis. We have shown that gain of MYC or loss of p53 provokes mitosis slippage and differentiation via DNA damage.¹⁴ The results herein show that FOXM1 overexpressing proliferative keratinocytes accumulate DNA damage. Altogether, the results suggest that ectopic FOXM1 by driving entry in mitosis shortens the repair G2 phase and prevents cells with irreparable damage to undergo terminal differentiation (Figure 6). This supports a role for the DMC as a protective mechanism against irreparable genetic damage^{5,12-14} by which precancerous cells are eliminated by stratification and shedding.⁴² We have proposed that additional alterations in the DMC might render cells harbouring mutations in cell growth control (p53, MYC) capable to divide (Figure 6). As a consequence, precancerous cells would be selected for, leading to malignant transformation.¹⁴ This may explain why deregulation of p53 or MYC is frequently found in skin carcinomas, even though they are

not considered initiators of cancer and they trigger the mitosis checkpoints.

In summary, FOXM1 drove the cell cycle deregulation caused by MYC or loss of p53 from differentiation into increased proliferation. In part, this process might be mediated by cell adhesion. In steady-state epidermis keratinocyte proliferation within the basal layer is tightly maintained by cell adhesion $\beta 4$ or $\beta 1$ integrin complexes.²⁸ We found that ectopic FOXM1 in keratinocytes recovered the expression of $\beta 1$ integrins upon the loss of p53. Integrin recovery might be a direct effect of FOXM1 or an indirect effect because of sustained proliferation. However, it is interesting that FOXM1 knockout mice suffered from severe abnormalities in lung development because of the downregulation of $\beta 1$ integrins.⁴³ Keratinocytes arrested in mitosis because of irreparable DNA damage might stratify by lateral pressure from more adherent proliferative neighbour cells (Figure 6).¹⁴ FOXM1 cells with a basal-like morphology and high integrin expression displayed a higher size and a higher level of DNA damage typical of the onset of differentiation. These results suggest that FOXM1 might drive cells that were committed to initiate differentiation into cell division. FOXM1 might raise the threshold of genetic damage allowed for keratinocytes to divide even when the mitotic checkpoints delay mitosis (Figure 6). As a result, FOXM1 would extend the number of cell divisions in a high genomic instability context. Interestingly, most squamous carcinomas of the skin and head and neck still conserve a differentiated component and we have evidence that this paradox might respond to alterations in mitosis control.⁴⁴

In conclusion, in the context of overexpression of MYC or inactivation of p53, persistent expression of FOXM1 may result in the creation of a pool of genomically instable cells with the capacity to divide, even if they are committed to leave the basal layer of the epidermis. This may fix precancerous mutations and give rise to cell clones with malignant potential. These results support a model where the DMC is key in coordinating keratinocyte proliferation with differentiation. This novel checkpoint might exist in developmental tissues, particularly in those where mitotic slippage leads to polyploidy.¹³ A variety of mammalian tissues have been so far found to undergo endoreplication.⁴⁵ Very recently, the greatly expanding mammary epithelium has been shown to become binucleated at lactancy.⁴⁶ The challenge now is dissecting the DMC whose alterations might give rise to genome instability and cancer.

MATERIALS AND METHODS

Cell culture, plasmids and viral infections

Ethical permission for this study was requested, approved and obtained from the Ethical Committee for Clinical Research of Cantabria Council, Spain. In all cases, human tissue material discarded after surgery was obtained with written consent presented by clinicians to the patients, and it was treated anonymously.

Primary keratinocytes were isolated from neonatal human foreskin and cultured in the presence of a mouse fibroblast feeder layer (inactivated by mitomycin C) in Rheinwald FAD medium as described (10% serum and 1.2 mM Ca^{+2}).^{5,47} Low passages (1-4) of keratinocytes were utilised.

For gene delivery in primary keratinocytes the following constructs driven by constitutive promoters were used. (1) Retroviral: pBabe empty vector (CT-pb) and pBabe-MYCER,^{5,14,39} MYC fusion protein with the ligand binding domain of a mutant oestrogen receptor that responds to 4-OH-hydroxytamoxifen (OHT; Research Biochemicals International, Natick, MA, USA). (2) Lentiviral: empty pLKO1 (CT1; Sigma-Aldrich, Inc., St Louis, MO, USA), empty pLVTHM-GFP (CT-GFP) and three different constructs coding for shRNAs against p53 with different target sequences: pLVUH-shp53-GFP (shp53-GFP), pLKO1-p53-shRNA-427 (shp53-1) and pLKO1-p53-shRNA-941 (shp53-2), all from Addgene (Cambridge, MA, USA);⁴⁸ empty pLVX (CT2) and pLVX-FOXM1 (FOX).⁴⁹

Lentiviral production was performed by transient transfection of 293T cells as previously described¹⁴ (see Supplementary Materials and methods). For infections with CT-pb, MYCER, CT2 and FOX, keratinocytes

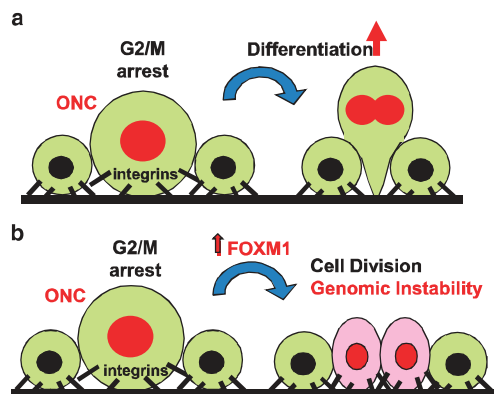


Figure 6. Model for the action of ectopic FOXM1 in p53- or MYC-mutant keratinocytes. (a) Cells upon potentially oncogenic alterations causing cell cycle deregulation and replication stress (ONC) and accumulation of irreparable DNA damage (red nuclei) block in mitosis unable to divide.¹⁴ Prolonged G2/M block allows cell size increase and triggers terminal epidermal differentiation, resulting in downregulation of integrins,⁵² irreversible suppression of cytokinesis and stratification.^{12,26} (b) Ectopic expression of FOXM1 pushes damaged keratinocytes to progress in mitosis and achieve cytokinesis in spite of an initial mitosis pause, giving rise to two slightly larger daughter cells that do not downregulate integrins. This leads to expansion of cells bearing genetic damage and to genomic instability.

were cultured in FAD medium. After cell selection (CT-pb and MYCER) or confluency (CT2 and FOX), cells were transferred to low-calcium concentration medium (<0.1 mM; Keratinocyte Media 2, Promocell, Heidelberg, Germany), following the manufacturer's instructions, and lentiviral infections with CT2 and FOX or CT1 and shp53 plasmids respectively were performed. MYCER was activated by addition of 100 nM OHT (Sigma-Aldrich, Inc.) to the culture medium 24 h after the infection with CT2 or FOX for the periods of time indicated. When necessary, MYCER cells were cultured in high calcium medium after infection with CT2 and FOX by adding CaCl₂ (1.2 mM) in order to allow stratification.

Clonogenicity assays were made as described previously²⁴ (see also Supplementary Materials and methods). Quantitation of cell shedding was measured by counting cells detached into the culture medium. Data were obtained from duplicate samples and normalised to controls.

Antibodies

Primary and secondary antibodies utilised in this study are listed in Supplementary Materials and methods.

Flow cytometry

Keratinocytes were harvested, fixed and stained for DNA synthesis, involucrin and keratin K1 as previously described.¹⁴ All antibody stainings were controlled by the use of similar concentration of isotype-negative immunoglobulins (mouse or rabbit serum). After staining, cells were firmly resuspended and filtered through a 70 µm mesh to minimise the presence of aggregates and then analysed on a Becton Dickinson FACSCanto (Franklin Lakes, NJ, USA). A total of 10 000 events were gated and acquired.

Immunodetection

For immunofluorescence, keratinocytes were grown on glass coverslips, fixed and stained as previously described.¹² For determination of protein expression, cells were washed with phosphate-buffered saline, lysed and subjected to SDS-PAGE electrophoresis and western blotting as previously described.¹²

Real-time PCR

Total RNA was isolated and reverse-transcribed using NucleoSpin RNA (Macherey-Nagel, Düren, Germany) and the iScript cDNA synthesis kit (Bio-Rad, Hercules, CA, USA) according to the manufacturer's instructions. The cDNAs (2 µl) were amplified by real-time PCR (Bio-Rad iQ SYBR Green supermix) and normalised to β-actin mRNA levels. Primers utilised in this study are listed in Supplementary Materials and methods.

Run-on transcription assay and comet assay

For immunodetection of nascent RNA, primary keratinocytes were cultured for 20' with 5'-fluorouridine (Sigma-Aldrich, Inc.), as described in Rosa-Garrido *et al.*⁵⁰ (see Supplementary Materials and Methods).

Alkaline comet assays were performed as described previously.⁵¹ A visual score related to the level of DNA damage observed was assigned to each tail. Scoring was performed by blind counting.

Confocal microscopy

For Supplementary Video 1, keratinocytes were grown on glass coverslips, fixed and stained as previously described.¹⁴ Z-stack 3D digital images were reconstructed after frame collection by confocal microscopy (Nikon A1R, Melville, NY, USA; 20× numerical aperture (NA) 0.75) and processed by NIS Elements software (AR, 3.2.64 bits; Nikon) as indicated in the legend of Supplementary Video 1.

Time-lapse videos

For Supplementary Video 2, keratinocytes 5 days after infection were treated with NucBlue Live ReadyProbes Reagent (Life Technologies, Carlsbad, CA, USA), filmed by time-lapse imaging for 12 h and photographed every 7 min.

Statistical analyses

Results were obtained with two different keratinocyte strains from different individuals (*N*=2). Data are average of triplicate samples of representative experiments (*n*=3). Exclusion of samples was carried out

based on the appearance of the negative control sample. Standard deviation and variance were calculated and served as estimates of variation within each group of data. For statistical comparison of groups with similar variance, a homoscedastic *t*-test was performed. For statistical comparison of groups with diverging variance, a heteroscedastic *t*-test was applied. A *P*-value of < 0.05 was considered statistically significant.

CONFLICT OF INTEREST

The authors declare no conflict of interest.

ACKNOWLEDGEMENTS

This work was funded by Instituto de Salud Carlos III ISCIII FIS/FEDER Grants P111/02070 and P114/00900 (to AG) and National Institutes of Health, NIH Awards R03 AR049420 (to SWS) and R01 AR052889 (to JTE).

REFERENCES

- 1 Shea CR, McNutt NS, Volkenandt M, Lugo J, Prioleau PG, Albino AP. Overexpression of p53 protein in basal cell carcinomas of human skin. *Am J Pathol* 1992; **141**: 25–29.
- 2 Brash DE. Roles of the transcription factor p53 in keratinocyte carcinomas. *Br J Dermatol* 2006; **154**(Suppl 1): 8–10.
- 3 Donehower LA, Harvey M, Slagle BL, McArthur MJ, Montgomery Jr CA, Butel JS *et al*. Mice deficient for p53 are developmentally normal but susceptible to spontaneous tumours. *Nature* 1992; **356**: 215–221.
- 4 Kemp CJ, Donehower LA, Bradley A, Balmain A. Reduction of p53 gene dosage does not increase initiation or promotion but enhances malignant progression of chemically induced skin tumors. *Cell* 1993; **74**: 813–822.
- 5 Gandarillas A, Watt FM. c-Myc promotes differentiation of human epidermal stem cells. *Genes Dev* 1997; **11**: 2869–2882.
- 6 Waikel RL, Wang XJ, Roop DR. Targeted expression of c-Myc in the epidermis alters normal proliferation, differentiation and UV-B induced apoptosis. *Oncogene* 1999; **18**: 4870–4878.
- 7 Watt FM, Frye M, Benitah SA. MYC in mammalian epidermis: how can an oncogene stimulate differentiation? *Nat Rev Cancer* 2008; **8**: 234–242.
- 8 Gebhardt A, Frye M, Herold S, Benitah SA, Braun K, Samans B *et al*. Myc regulates keratinocyte adhesion and differentiation via complex formation with Miz1. *J Cell Biol* 2006; **172**: 139–149.
- 9 Macias E, Miliani de Marval PL, Senderowicz A, Cullen J, Rodriguez-Puebla ML. Expression of CDK4 or CDK2 in mouse oral cavity is retained in adult pituitary with distinct effects on tumorigenesis. *Cancer Res* 2008; **68**: 162–171.
- 10 Pierce AM, Fisher SM, Conti CJ, Johnson DG. Deregulated expression of E2F1 induces hyperplasia and cooperates with ras in skin tumor development. *Oncogene* 1998; **16**: 1267–1276.
- 11 Ruiz S, Santos M, Segrelles C, Leis H, Jorcano JL, Berns A *et al*. Unique and overlapping functions of pRb and p107 in the control of proliferation and differentiation in epidermis. *Development* 2004; **131**: 2737–2748.
- 12 Freije A, Ceballos L, Coisy M, Barnes L, Rosa M, De Diego E *et al*. Cyclin E drives human keratinocyte growth into differentiation. *Oncogene* 2012; **31**: 5180–5192.
- 13 Gandarillas A. The mysterious human epidermal cell cycle, or an oncogene-induced differentiation checkpoint. *Cell Cycle* 2012; **11**: 4507–4516.
- 14 Freije A, Molinuevo R, Ceballos L, Cagigas M, Alonso-Lecue P, Rodriguez R *et al*. Inactivation of p53 in human keratinocytes leads to squamous differentiation and shedding via replication stress and mitotic slippage. *Cell Rep* 2014; **9**: 1349–1360.
- 15 Jonason AS, Kunala S, Price GJ, Restifo RJ, Spinelli HM, Persing JA *et al*. Frequent clones of p53-mutated keratinocytes in normal human skin. *Proc Natl Acad Sci USA* 1996; **93**: 14025–14029.
- 16 Ren ZP, Ahmadian A, Ponten F, Nister M, Berg C, Lundeberg J *et al*. Benign clonal keratinocyte patches with p53 mutations show no genetic link to synchronous squamous cell precancer or cancer in human skin. *Am J Pathol* 1997; **150**: 1791–1803.
- 17 le Pelletier F, Soufir N, de La Salmoniere P, Janin A, Basset-Seguin N. p53 Patches are not increased in patients with multiple nonmelanoma skin cancers. *J Invest Dermatol* 2001; **117**: 1324–1325.
- 18 Gandarillas A, Molinuevo R, Freije A, Alonso-Lecue P. The mitosis-differentiation checkpoint, another guardian of the epidermal genome. *Mol Cell Oncol* 2015; **2**: e997127.
- 19 Laoukili J, Stahl M, Medema RH. FoxM1: at the crossroads of ageing and cancer. *Biochim Biophys Acta* 2007; **1775**: 92–102.

- 20 Laoukili J, Kooistra MR, Bras A, Kaur J, Kerkhoven RM, Morrison A *et al*. FoxM1 is required for execution of the mitotic programme and chromosome stability. *Nat Cell Biol* 2005; **7**: 126–136.
- 21 Teh MT, Wong ST, Neill GW, Ghali LR, Philpott MP, Quinn AG. FOXM1 is a downstream target of Gli1 in basal cell carcinomas. *Cancer Res* 2002; **62**: 4773–4780.
- 22 Teh MT, Hutchison IL, Costea DE, Neppelberg E, Liavaag PG, Purdie K *et al*. Exploiting FOXM1-orchestrated molecular network for early squamous cell carcinoma diagnosis and prognosis. *Int J Cancer* 2013; **132**: 2095–2106.
- 23 Rodriguez R, Rubio R, Gutierrez-Aranda I, Melen GJ, Elosua C, Garcia-Castro J *et al*. FUS-CHOP fusion protein expression coupled to p53 deficiency induces liposarcoma in mouse but not in human adipose-derived mesenchymal stem/stromal cells. *Stem Cells* 2011; **29**: 179–192.
- 24 Jones PH, Watt FM. Separation of human epidermal stem cells from transit amplifying cells on the basis of differences in integrin function and expression. *Cell* 1993; **73**: 713–724.
- 25 Gemenetzidis E, Elena-Costea D, Parkinson EK, Waseem A, Wan H, Teh MT. Induction of human epithelial stem/progenitor expansion by FOXM1. *Cancer Res* 2010; **70**: 9515–9526.
- 26 Zanet J, Freije A, Ruiz M, Coulon V, Sanz JR, Chiesa J *et al*. A mitosis block links active cell cycle with human epidermal differentiation and results in endoreplication. *PLoS One* 2010; **5**: e15701.
- 27 Borowiec AS, Delcourt P, Dewailly E, Bidaux G. Optimal differentiation of in vitro keratinocytes requires multifactorial external control. *PLoS One* 2013; **8**: e77507.
- 28 Watt FM. Role of integrins in regulating epidermal adhesion, growth and differentiation. *EMBO J* 2002; **21**: 3919–3926.
- 29 van Deursen JM. Rb loss causes cancer by driving mitosis mad. *Cancer Cell* 2007; **11**: 1–3.
- 30 Costa RH. FoxM1 dances with mitosis. *Nat Cell Biol* 2005; **7**: 108–110.
- 31 Kong X, Li L, Li Z, Le X, Huang C, Jia Z *et al*. Dysregulated expression of FOXM1 isoforms drives progression of pancreatic cancer. *Cancer Res* 2013; **73**: 3987–3996.
- 32 Myatt SS, Lam EW. The emerging roles of forkhead box (Fox) proteins in cancer. *Nat Rev Cancer* 2007; **7**: 847–859.
- 33 Duarte B, Miselli F, Murillas R, Espinosa-Hevia L, Cigudosa JC, Recchia A *et al*. Long-term skin regeneration from a gene-targeted human epidermal stem cell clone. *Mol Ther* 2014; **22**: 1878–1880.
- 34 Halasi M, Gartel AL. A novel mode of FoxM1 regulation: positive autoregulatory loop. *Cell Cycle* 2009; **8**: 1966–1967.
- 35 Costa RH, Kalinichenko VV, Major ML, Raychaudhuri P. New and unexpected: forkhead meets ARF. *Curr Opin Genet Dev* 2005; **15**: 42–48.
- 36 Rogakou EP, Pilch DR, Orr AH, Ivanova VS, Bonner WM. DNA double-stranded breaks induce histone H2AX phosphorylation on serine 139. *J Biol Chem* 1998; **273**: 5858–5868.
- 37 Lecona E, Fernandez-Capetillo O. Replication stress and cancer: it takes two to tango. *Exp Cell Res* 2014; **329**: 26–34.
- 38 Gandarillas A, Davies D, Blanchard JM. Normal and c-Myc-promoted human keratinocyte differentiation both occur via a novel cell cycle involving cellular growth and endoreplication. *Oncogene* 2000; **19**: 3278–3289.
- 39 Littlewood TD, Hancock DC, Danielian PS, Parker MG, Evan GI. A modified oestrogen receptor ligand-binding domain as an improved switch for the regulation of heterologous proteins. *Nucleic Acids Res* 1995; **23**: 1686–1690.
- 40 Xue YJ, Xiao RH, Long DZ, Zou XF, Wang XN, Zhang GX *et al*. Overexpression of FoxM1 is associated with tumor progression in patients with clear cell renal cell carcinoma. *J Transl Med* 2012; **10**: 200.
- 41 Stoll SW, Stuart PE, Swindell WR, Tsol LC, Li B, Gandarillas A *et al*. The EGF receptor ligand amphiregulin controls cell division via FoxM1. *Oncogene* 2015; **35**: 2075–2086.
- 42 Gandarillas A, Molinuevo R, Freije A, Alonso-Lecue P. The mitosis-differentiation checkpoint, another guardian of the epidermal genome. *Mol Cell Oncol* 2015; **2**: e997127.
- 43 Kim JM, Ramakrishna S, Gusarova GA, Yoder HM, Costa RH, Kalinichenko VV. The forkhead box m1 transcription factor is essential for embryonic development of pulmonary vasculature. *J Biol Chem* 2005; **280**: 22278–22286.
- 44 Alonso-Lecue P, Coulon V, Ceballos L, Lopez-Aventin D, Molinuevo R, Garcia-Valtuille A *et al*. Bypass of mitotic block in response to cell cycle stress leads to genomic instability and malignant progression of squamous carcinoma cells of the skin (submitted).
- 45 Orr-Weaver TL. When bigger is better: the role of polyploidy in organogenesis. *Trends Genet* 2015; **31**: 307–315.
- 46 Rios AC, Fu NY, Jamieson PR, Pal B, Whitehead L, Nicholas KR *et al*. Essential role for a novel population of binucleated mammary epithelial cells in lactation. *Nat Commun* 2016; **7**: 11400.
- 47 Rheinwald JG. Methods for clonal growth and serial cultivation of normal human epidermal keratinocytes and mesothelial cells. In: Baserga R (ed) *Cell Growth and Division*. IRL Press: Oxford, 1989, pp 81–94.
- 48 Kim JS, Lee C, Bonifant CL, Ransom H, Waldman T. Activation of p53-dependent growth suppression in human cells by mutations in PTEN or PIK3CA. *Mol Cell Biol* 2007; **27**: 662–677.
- 49 Toll A, Real FX. Somatic oncogenic mutations, benign skin lesions and cancer progression: where to look next? *Cell Cycle* 2008; **7**: 2674–2681.
- 50 Rosa-Garrido M, Ceballos L, Alonso-Lecue P, Abreira C, Delgado MD, Gandarillas A. A cell cycle role for the epigenetic factor CTCF-L-BORIS. *PLoS One* 2012; **7**: e39371.
- 51 Ritchie A, Gutierrez O, Fernandez-Luna JL. PAR bZIP-bik is a novel transcriptional pathway that mediates oxidative stress-induced apoptosis in fibroblasts. *Cell Death Differ* 2009; **16**: 838–846.
- 52 Hotchin NA, Gandarillas A, Watt FM. Regulation of cell surface beta 1 integrin levels during keratinocyte terminal differentiation. *J Cell Biol* 1995; **128**: 1209–1219.



This work is licensed under a Creative Commons Attribution-NonCommercial-NoDerivs 4.0 International License. The images or other third party material in this article are included in the article's Creative Commons license, unless indicated otherwise in the credit line; if the material is not included under the Creative Commons license, users will need to obtain permission from the license holder to reproduce the material. To view a copy of this license, visit <http://creativecommons.org/licenses/by-nc-nd/4.0/>

© The Author(s) 2017

Supplementary Information accompanies this paper on the Oncogene website (<http://www.nature.com/onc>)